BMR JOURNAL
OF AUSTRALIAN GEOLOGY & GEOPHYSICS

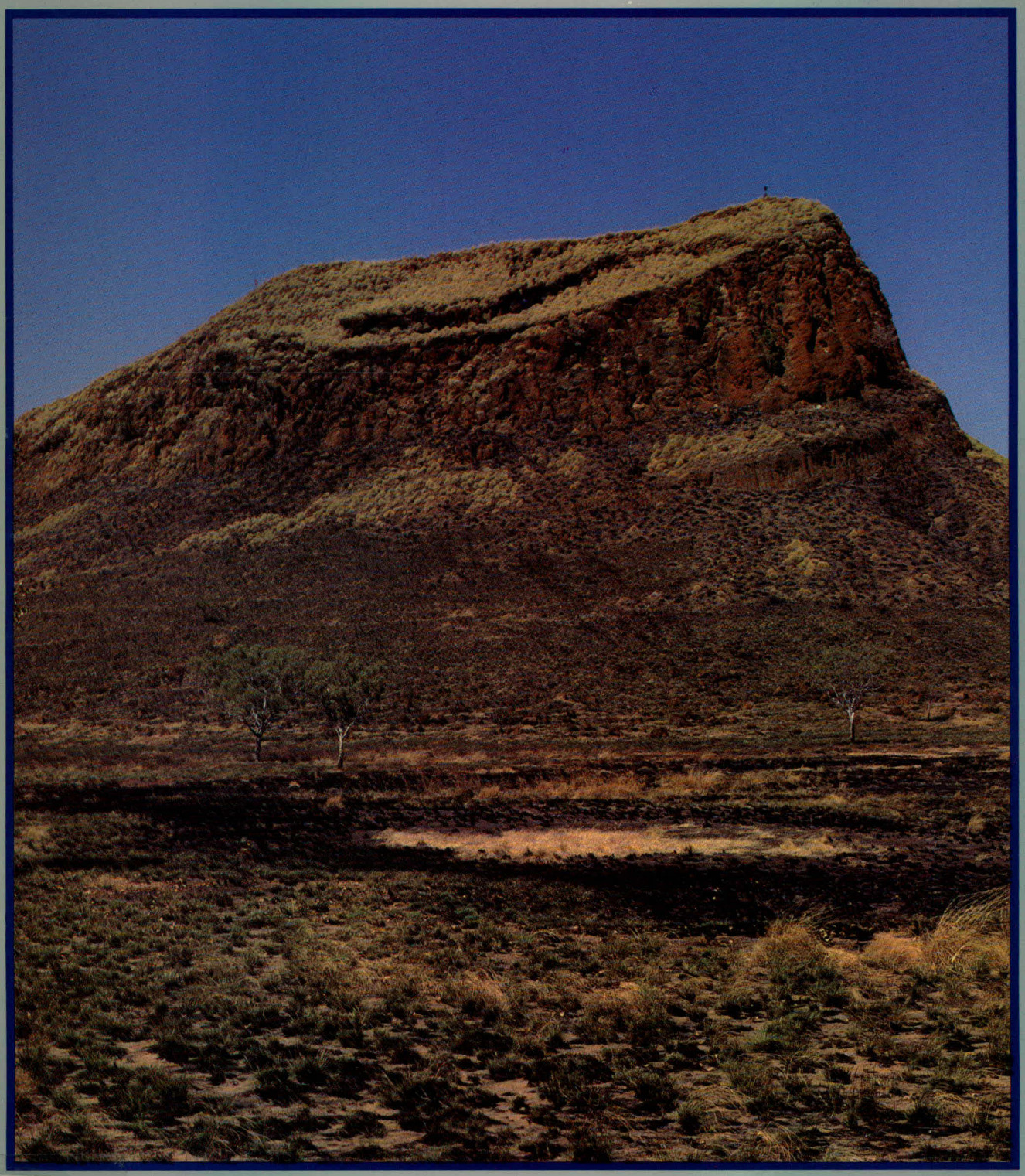

VOLUME 9 NUMBER 1 MARCH 1984

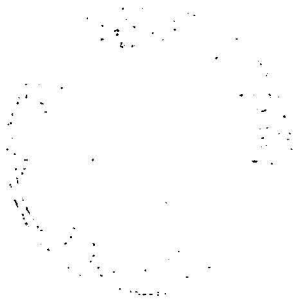

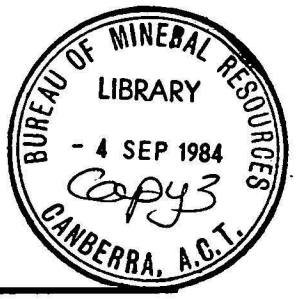

BMR JOURNAL
OF AUSTRALIAN GEOLOGY & GEOPHYSICS

VOLUME 9 NUMBER 1 MARCH 1984

CONTENTS

Front cover: Mount North, an intrusion of lamproite in the West Kimberley region of Western Australia. New age determinations on this and other similar intrusions, including diamond-bearing pipes, are presented in this issue in a paper by A. L. Jaques & others.

AUSTRALIAN GOVERNMENT PUBLISHING SERVICE CANBERRA 1984

Department of Resources and Energy

Minister: Senator the Hon. Peter Walsh

Secretary: A. J. Woods

Bureau of Mineral Resources, Geology and Geophysics

Director: R. W. R. Rutland

Editor, BMR Journal: I. M. Hodgson

The BMR Journal of Australian Geology & Geophysics is a quarterly journal of research and related activities. Contributions are from officers of the BMR, from BMR officers working in collaboration with others, or requested work sponsored by the BMR. In addition to articles, the Journal may include shorter notes and discussion of papers published in it. Discussion of papers is invited from anyone.

Annual subscription to the Journal is $27 (Australian), which includes surface postage (Airmail rates are available on application). Individual numbers, if available, cost $8.60. Subscriptions etc., made payable to the Australian Government Publishing Service, should be sent to Mail Order Sales, Australian Government Publishing Service, GPO Box 84, Canberra, A.C.T. 2601, Australia.

Other matters concerning the Journal should be sent to the Director, marked for the attention of the Editor, BMR Journal.

ISSN 0312-9608

Printed by Graphic Services Pty Ltd, 516-518 Grand Junction Road, Northfield, S.A. 5085

BMR Journal of Australian Geology & Geophysics, 9, 1-7

The age of the diamond-bearing pipes and associated leucite lamproites of the West Kimberley region, Western Australia

A.L. Jaques[1], A.W. Webb[2], C.M. Fanning[2], L.P. Black[1], R.T. Pidgeon[3], John Ferguson[1], C.B. Smith[4], & G.P. Gregory[5]

New K-Ar and Rb-Sr ages obtained for 14 separate lamproite intrusions in the Fitzroy area of the West Kimberley region of Western Australia confirm the early Miocene ages previously obtained for the Fitzroy lamproites. Similar (early Miocene) ages were obtained for the leucite lamproite intrusions and one of the newly discovered diamondiferous pipes of olivine lamproite resembling kimberlite. This is consistent with their close spatial association in the field and their petrologic and geochemical similarities. There is a small difference in age between the northernmost intrusions of the Ellendale area (20-22 Ma) and those further south in the Noonkanbah area (18-20 Ma). The early Miocene ages of the West Kimberley diamond pipes make these the youngest primary source of diamond yet found.

Introduction

The recent discovery of diamond (Atkinson & others, 1982, 1984) in kimberlitic rocks intimately associated with the leucite lamproites of the Fitzroy area of the West Kimberley region of Western Australia (Wade & Prider, 1940; Prider, 1960) has renewed interest in the province and, in particular, in these unusual rocks. Petrological and geochemical studies of these newly discovered kimberlitic intrusions indicate that, although resembling micaceous kimberlite, they are olivine-rich lamproites directly related to the leucite lamproites (Fitzroy lamproites), with which they form a consanguineous ultrapotassic (lamproite) suite (Jaques & others, 1982, 1984). Accurate dating of the age of intrusion of the Fitzroy lamproites therefore constrains the age of intrusion of the diamond-bearing pipes.

Controversy has surrounded the age of intrusion of the Fitzroy lamproites. Prider (1960) and Kaplan & others (1967) considered them to be Jurassic on the basis of limited Rb-Sr dating. Wellman (1973) disputed the Jurassic ages and presented concordant K-Ar ages on a number of different minerals, which gave consistent early Miocene ages (17-20 Ma). A number of subsequent publications and recent regional geological maps (e.g. GSWA, 1979), however, have preferred the older (Jurassic) ages for the Fitzroy lamproites, possibly because this age is in better accord with known tectonic activity in the region.

In this paper we present new K-Ar ages for mineral separates from 13 separate intrusions, mostly of leucite lamproite composition, together with new Rb-Sr dates on both the leucite lamproites and one of the newly discovered olivine-rich lamproites, which contains diamond at grades greater than 5 cts/100 tonnes. The new data confirm Wellman's (1973) early Miocene ages for intrusion of the suite and indicate small but systematic differences in age within the province. The Tertiary ages obtained for the diamond-bearing lamproites make these the youngest pipes yet found.

Geology

Recent company exploration has greatly increased the number of recorded intrusions in the Fitzroy area of the West Kimberley region, and over 100 separate intrusions are now known (Atkinson & others, 1984; Jaques & others,1984). The majority of the intrusions occur as vents, pipes, plugs, sills, and rare dykes in a broad belt that extends south from the King Leopold Mobile Belt, at the southern margin of the Kimberley Block, across the Lennard Shelf to the southern margin of the Fitzroy Trough, at the northern edge of the Canning Basin (Fig. 1). Within this belt are three main fields (Fig. 2), located in the north on the Lennard Shelf (Ellendale field), on the shelf margin (Calwynyardah field), and in the south in the Fitzroy Trough (Noonkanbah field). A smaller cluster of pipes intrudes the King Leopold Mobile Zone some 100 km further east, to the north of Fitzroy Crossing. Olivine-rich (kimberlitic) rocks are mostly confined to the Ellendale field, whereas intrusions in the Noonkanbah field are mostly leucite-rich lamproite. Diamondiferous pipes occur in all four areas, however.

Petrological and geochemical studies indicate a continuum from olivine-rich lamproite, resembling micaceous kimberlite, through lamproite containing both olivine and leucite, to the leucite-rich lamproites described by Wade & Prider (1940) and Prider (1960), which contain phlogopite, diopside, or potassic richterite as the main mafic phases. The olivine lamproites consist of coarse olivine macrocrysts in a fine-grained to glassy groundmass, containing olivine, phlogopite, diopside, apatite, perovskite, spinel, and glass, and, in coarser-grained types, potassic richterite and wadeite. The leucite lamproites are strongly porphyritic with the major phenocryst minerals including one or more of: olivine, phlogopite, diopside, potassic richterite, and leucite. Details are given in Wade & Prider (1940), Prider (1960), and Jaques & others (1984).

Analytical methods

The dating was carried out on whole rock samples and mineral separates obtained by standard heavy-liquid separation techniques, followed by hand picking. Sample locations and descriptions are given in an Appendix.

K-Ar dating was carried out at the Australian Mineral Development Laboratories (AMDEL) using techniques based on McDougall (1966) and Cooper (1963). A more complete description is given in Webb (1976). The bulk of the Rb-Sr dating was carried out at the ANU and BMR laboratories, using a mixed ^{85}Rb, ^{84}Sr spike, following Williams & others (1975) and Page & others (1976). Additional analyses were made at AMDEL following similar techniques based on Compston & others (1965). All $^{87}Sr/^{86}Sr$ values are normalised to the average value obtained on the MSZ mass spectrometer at ANU for NBS 987 of 0.71027 (McCulloch & others, 1983).

K-Ar results

The K-Ar ages obtained in this study together with the analytical data are presented in Table 1. The ages range from

1. Bureau of Mineral Resources, Canberra City ACT 2601
2. Australian Mineral Development Laboratories, Flemington St., Frewville, South Australia 5063
3. Western Australian Institute of Technology, Kent St., Bentley, Western Australia 6102
4. CRA Exploration Pty. Ltd., 21 Wynyard St., Belmont, Western Australia 6104.
5. Seltrust Mining Corp. Pty Ltd, 200 Adelaide Tce, Perth, Western Australia 6000.

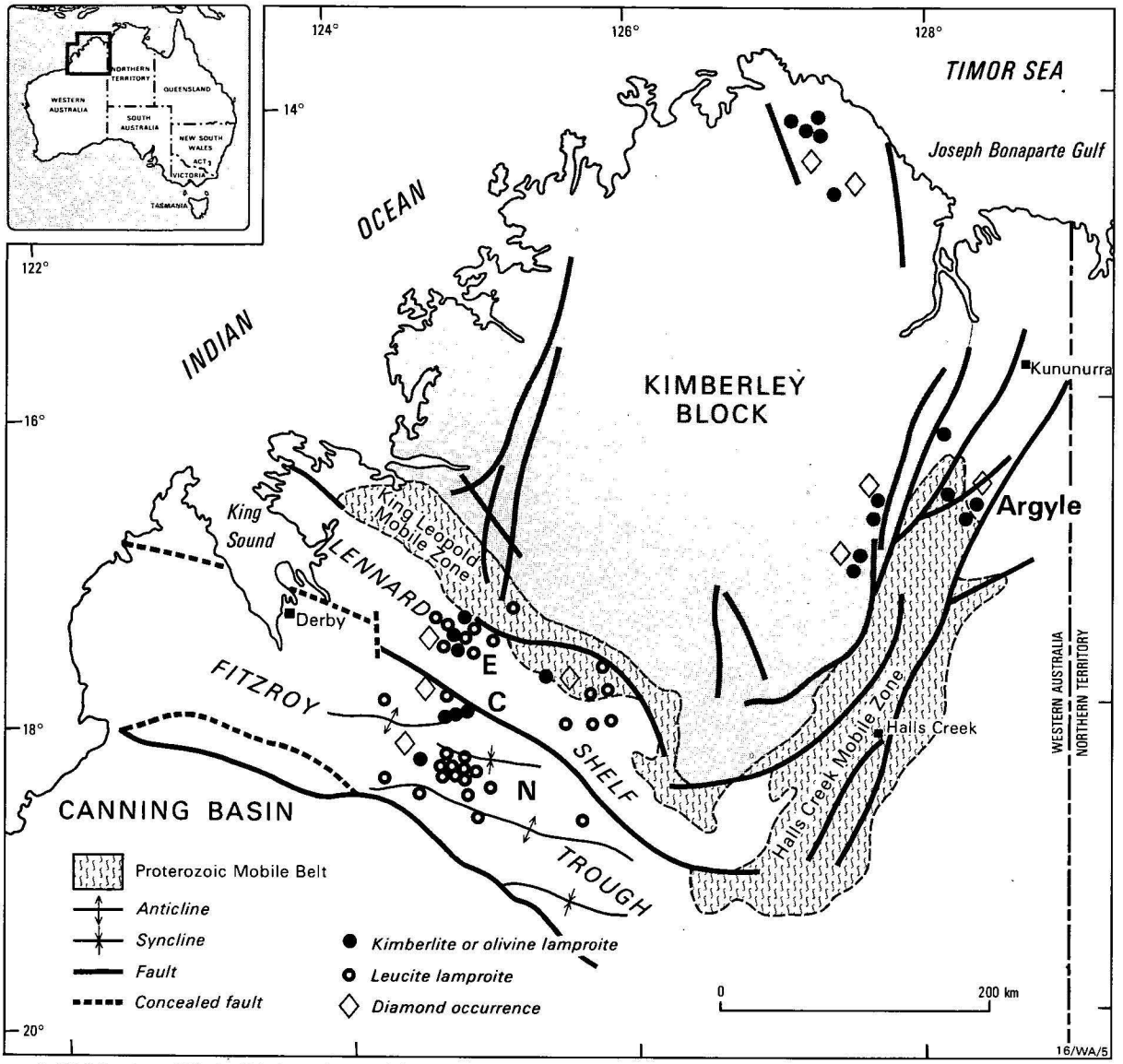

Figure 1. Distribution of kimberlitic intrusions, olivine and leucite lamproites, and diamond occurrences in relation to major tectonic features of the Kimberley region, Western Australia.

E = Ellendale field, C = Calwynyardah field, N = Noonkanbah field.

22 Ma in the northernmost diatremes at Winjana and Mount Percy to about 18–20 Ma for the southernmost lamproite plugs in the Noonkanbah field.

The ages determined on different phlogopite fractions from five different samples, ranging from olivine-phlogopite-leucite lamproite to tuffaceous phlogopite-rich crater sediments for the Camarotoechia Bore pipe, range from 21.3 to 22.6 Ma. This is only slightly greater than that expected from analytical uncertainty ($1\sigma = \pm 1\%$). The oldest and youngest ages were obtained from detrital phlogopites in crater sediments, whereas phlogopites from the magmatic and tuffaceous lamproite samples gave ages in good agreement (22.1, 22.5, and 22.0 Ma). Whether this spread in ages reflects complex igneous activity within the pipe or the fact that detrital phlogopites are more susceptible to Ar diffusion is not clear. However, primary and detrital phlogopites have similar K and ^{40}Ar contents, which with the concordant ages (within instrumental uncertainty) suggest that ^{40}Ar and K gain or loss in detrital phlogopites is negligible. The fact that the anomalously young age (sample 79211067) has a significantly lower $^{40}Ar^*/^{40}Ar$ total than the other samples suggests a greater uncertainty for this date. A reproducible age was obtained from two different samples from the Water Reserve Sill (Table 1).

In general, the ages obtained from diopside and phlogopite separates are in good agreement (Table 1). For example, diopside and phlogopite from Machell's Pyramid (sample 81210157) gave ages of 18.5 and 18.2 Ma, respectively. However, in two samples from 'P' Hill, while diopside from 81210147 and phlogopite from 81210145 are in fair agreement (20.5 ± 1.0 and 19.7 ± 0.2 Ma), diopside from 81210145 gave a significantly younger age (18.4 ± 0.9 Ma). This difference is marginally greater than would be expected solely from experimental error (i.e. 6.6% compared to $\pm$ 5% for the diopside). The small amount of sample available prohibited duplication of the K analysis of the diopside, and it is possible that there is a higher uncertainty in the K analysis for this sample. The age difference may, therefore, be due to analytical error.

The youngest age (17.0 ± 0.9 Ma) was obtained on diopside from a diopside-leucite lamproite from Mount Gytha (Table 1). The high uncertainty associated with this age overlaps, at the 95 per cent confidence level, the lower age limit given by phlogopite (and diopside) from the adjacent Machell's Pyramid (i.e. 17.9 cf. 18.2 ± 0.28 Ma). Since, on geological grounds, it seems likely that the two intrusions are closely related, the upper age limit (17.9 Ma) is preferred for Mount Gytha.

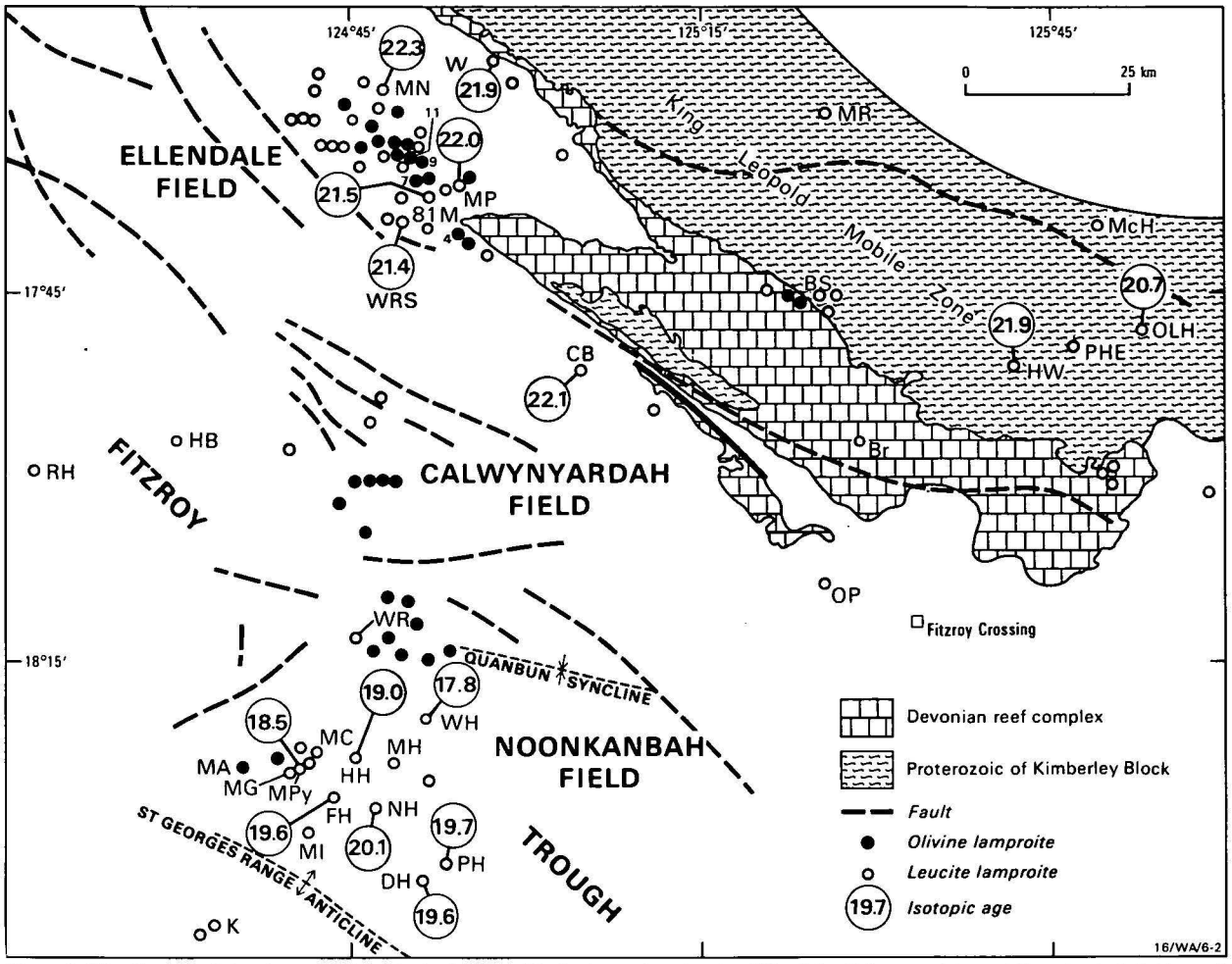

Figure 2. Distribution of the ultrapotassic rocks in the West Kimberley region,showing Ellendale, Calwynyardah, and Noonkanbah fields, and a summary of K-Ar isotopic ages.

Main lamproite bodies from north to south are: W= Winjana, MN = Mt North, MR = Mt Rose, 4 = Ellendale 4, 7 = Ellendale 7, 9 = Ellendale 9, 11 = Ellendale 11, MP = Mt Percy, 81-M = 81-Mile Vent, WRS = Water Reserve Sill, CB = Camarotoechia Bore, McH = McKinrick Hill, BS = Big Spring, OLH = Old Leopold Hill, PHE = Prairie Hill East, HW = Hooper West, BR = Brooking Creek, RH = Rice Hill, HB = Hason's Bore, OP = Oscar Plug, WR = White Rocks, WH = Walgidee Hills, MC = Mt Cedric, HH = Howes Hill, MH = Mamilu Hill, MA = Mt Abbott, MG = Mt Gytha, MPy = Machell's Pyramid, FH = Fishery Hill, NH = Noonkanbah Hill, MI = Mt Ibis, PH = 'P' Hill, DH = Djada (Dadja) Hill, K = Kalyeeda Hills.
Note: A number of smaller lamproite intrusions not shown. Locations taken from published 1:250 000 geological maps and unpublished data provided by CRA Exploration Pty Ltd. Data from Wellman (1973) (using revised decay constants), this study, and Nixon & others (1982) (for Howes Hill, west, lamproite).

The new ages compare with the Miocene K-Ar ages obtained by Wellman (1973) on a variety of minerals from three separate intrusions of the Fitzroy lamproites. Wellman's (1973) concordant mineral ages, regarded as 'best estimates', have been recalculated using the revised decay constants of Steiger & Jager (1977). Agreement between these recalculated ages (Table 2) and the new ones (Table 1) is excellent. For example, the revised age for the Mount North lamproite (22.3 Ma) compares with the 21-22 Ma obtained for other intrusions of the Ellendale field. Similarly, the mean of the revised ages for the Walgidee Hills intrusion (17.8 Ma) is in excellent agreement with the 17.5 ± 0.2 Ma obtained in this study. The K-Ar ages obtained in both Wellman's and this study are further supported by the 19 Ma reported by Nixon & others (1982) for the Howes Hill (west) lamproite. This agrees closely with the K-Ar ages obtained for the other Noonkanbah field lamproites and provides further support for the slight difference in age observed between the northernmost and southernmost lamproites.

Rb-Sr dating

Studies by Powell & Bell (1970) and, more recently, McCulloch & others (1983) have shown that the lamproites of the West Kimberley region have high contents of Rb and Sr (250–3000 ppm Rb, 1000–2000 ppm Sr), and high Rb/Sr and $^{87}Sr/^{86}Sr$ (0.3–0.4 and 0.711–0.720, respectively). These Rb/Sr and initial $^{87}Sr/^{86}Sr$ values are amongst the highest reported for mantle-derived ultrabasic and basic igneous rocks. McCulloch & others (1983) observed large variations in initial $^{87}Sr/^{86}Sr$ both throughout the West Kimberley province and within individual fields, precluding any assumptions regarding common initial ratios.

Leucite lamproites

Rb and Sr analyses were made on phlogopite separates and total-rock samples from Mount Percy, 81-Mile Vent, and Walgidee Hills (Table 3), and on potassic richterite, perovskite, and apatite separates from an additional sample from the Walgidee Hills intrusion (Table 3). Although the phlogopites are insufficiently enriched in ^{87}Rb relative to ^{86}Sr to allow age estimates independent of initial-ratio assumptions, reasonably reliable estimates were obtained from regression lines through the phlogopite-whole-rock data from Mount Percy and 81-Mile Vent. These gave ages of 20.8 and 21.6 Ma, respectively, which are in reasonable agreement with the K-Ar ages obtained for these intrusions (Table 1). Phlogopite from Walgidee Hills (sample 81210184) is much less enriched in ^{87}Rb and the age obtained from the phlogopite–whole-rock pair for this sample, 9.3 Ma, is much

Table 1. Summary of K-Ar results for Fitzroy lamproites

Locality and sample nos	Minerals analysed	K (%)	$^{40}Ar^*$ (x 10^{-10}moles/g)	$\frac{^{40}Ar^*}{^{40}Ar\ total}$	Age (Ma)
Mt Percy					
81210047	Phlog	8.64,8.66	3.325	0.740	22.0 ± 0.3
Camarotoechia Bore					
79211068	Phlog	8.67,8.67	3.419	0.693	22.6 ± 0.2
79211064	Phlog	8.69,8.72	3.417	0.597	22.5 ± 0.2
80210059	Phlog	8.58,8.60	3.317	0.628	22.1 ± 0.3
79211063	Phlog	8.69,8.69	3.335	0.633	22.0 ± 0.2
79211067	Phlog	8.65,8.69	3.224	0.192	21.3 ± 0.3
Hooper West					
81210083	Phlog	8.71,8.70	3.321	0.811	21.9 ± 0.2
Winjana					
80210109	Phlog	7.66,7.68	2.935	0.725	21.9 ± 0.2
81-Mile Vent					
79211054	Phlog	8.96,8.95	3.364	0.786	21.5 ± 0.2
Water Reserve Sill					
79211079	Phlog	8.47,8.49	3.165	0.580	21.4 ± 0.2
79211080	Phlog	8.39,8.41	3.132	0.569	21.4 ± 0.2
Noonkanbah Hill					
81210122	Phlog	8.59	3.005	0.663	20.1 ± 0.2
'P' Hill					
81210147	Diop	0.136,0.137	0.049	0.173	20.5 ± 1.0
81210145	Phlog	7.90	2.714	0.779	19.7 ± 0.2
	Diop	0.115	0.037	0.145	18.4 ± 0.9
Djada (Dadja) Hill					
79211057	Phlog	8.53	2.918	0.768	19.6 ± 0.2
Fishery Hill					
81210151	Phlog	8.66	2.954	0.737	19.6 ± 0.2
Machell's Pyramid					
81210157	Diop	0.123,0.122	0.039	0.127	18.5 ± 0.9
	Phlog	8.45,8.44	2.676	0.721	18.2 ± 0.2
Walgidee Hills					
81210184	Phlog	7.86,7.86	2.390	0.760	17.5 ± 0.2
Mt Gytha					
81210154	Diop	0.282,0.283	0.084.	0.262	17.0 ± 0.9

Phlog = phlogopite, Diop = diopside. * denotes radiogenic Ar.
$^{40}K/K$ = 0.01167 atom %, λ_β = 4.962 x $10^{-10}yr^{-1}$, λ_ϵ = 0.5811 x $10^{-10}yr^{-1}$.

Errors refer to standard deviation.

Table 2. Previous K-Ar ages* (Wellman, 1973) recalculated using the revised decay constants

Locality and sample nos.	Minerals analysed	Age (Ma)
Mount North		
69-1331	Phlog	22.3
70-1321	Phlog	22.2
		Mean 22.2 ± 0.1
Old Leopold Hill		
69-1330	Phlog	20.9
	Leuc. P	19.9
	WR	20.4
70-1320	Phlog	20.7
	Leuc. P	21.4
		Mean 20.7 ± 0.6
Walgidee Hills		
69-1329	Prid	17.6
	K-Richt	17.6
69-1332	K-Richt	17.9
	Phlog	18.0
		Mean 17.8 ± 0.2

* Only the concordant mineral ages suggested as 'best estimates' by Wellman are presented.
Phlog = phlogopite, Leuc. P = leucite pseudomorphs, WR = whole rock, Prid = priderite, K-Richt = potassium richterite.

younger than the K-Ar age obtained for this sample (Table 1) and others from the Walgidee Hills intrusion (Table 2). In view of the large uncertainties associated with this estimate and the possibility of resetting of the isotopic systems by either slow cooling of the intrusion or late deuteric alteration (extensive in most Walgidee Hills rocks), no significance can be attached to this apparent age. The mineral phases in sample 81210167 are extremely enriched in common Sr (up to 3% SrO in perovskite) and, consequently, their small $^{87}Rb/^{86}Sr$ values preclude any estimate of age. Rb-Sr data available for three whole-rock samples from the Walgidee Hills intrusion (sample 81210184, Table 3; WAK 25 and 30, McCulloch & others, 1983) are plotted together with the data for the mineral separates from samples 81210167 and 81210184 (Table 3) in Figure 3. The data are not colinear. An isochron (model 3) obtained on the three whole-rock samples and the

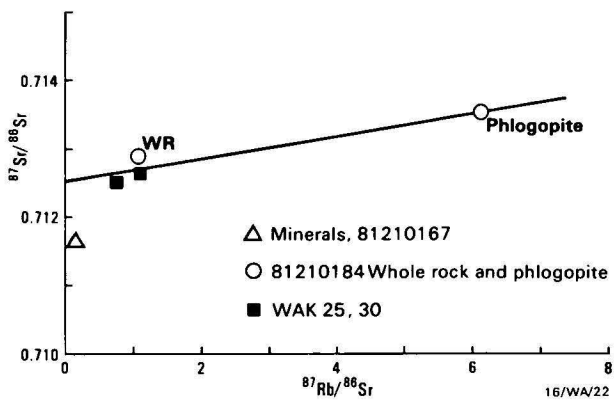

Figure 3. Rb-Sr isotopic systems of whole rocks and minerals for Walgidee Hills.

Whole-rock data for WAK 25 and 30 from McCulloch & others (1983).

Table 3. Rb-Sr data for the West Kimberley lamproites

Locality and Sample Nos.	Mineral Analysed	Rb (ppm)	Sr (ppm)	$^{87}Rb/^{86}Sr$	$^{87}Sr/^{86}Sr$	Rb/Sr age (Ma)
Mount Percy						
80210047	Phlog	628.3	16.82	108.3	0.74828	20.8
	WR	658.2	1840	1.034	0.71654	
81 Mile Vent						
79211054	Phlog	629	74.9	24.28	0.72297	21.6
	WR	652	2077	0.9077	0.71581	
Walgidee Hills						
81210167	Diop	1.823	2204	0.0024	0.7116 ± 1(2 σ)	
	K-Richt	37.07	2684	0.0399	0.7116 ± 1(2 σ)	
	Perov	3.171	24770	0.0004	0.7116 ± 1(2 σ)	
	Apatite	7.397	30586	0.0007	0.7117 ± 1(2)	
81210184	Phlog	496	237	6.056	0.7135	9.3
	WR	427	1153	1.0698	0.71287	
Ellendale No. 9						
	WR(A)	660	1150	1.654	0.7118	13.0
	Phlog(A)	752	442	4.903	0.7124	
	WR(B)	624	1222	1.474	0.7114	25.2
	Phlog(B)	737	327	6.495	0.7132	
	WR(C)	610	1460	1.206	0.7115	23.3
	Phlog(C)	826	376	6.343	0.7132	
	Phlog(D) (xenolith)	820	237	9.966	0.7144	

Phlog = Phlogopite; WR = Whole-rock; Diop = diopside; Perov = perovskite.
$^{85}Rb/^{87}Rb$ = 2.600, $^{88}Sr/^{86}Sr$ = 8.3752, $\lambda\ ^{87}Rb$ = 1.42 x 10^{-11} yr^{-1}. All $^{87}Sr/^{86}Sr$ values normalized to NBS 987 value of 0.71027.
Rb/Sr ages calculated from phlogopite - whole-rock pairs (see text).

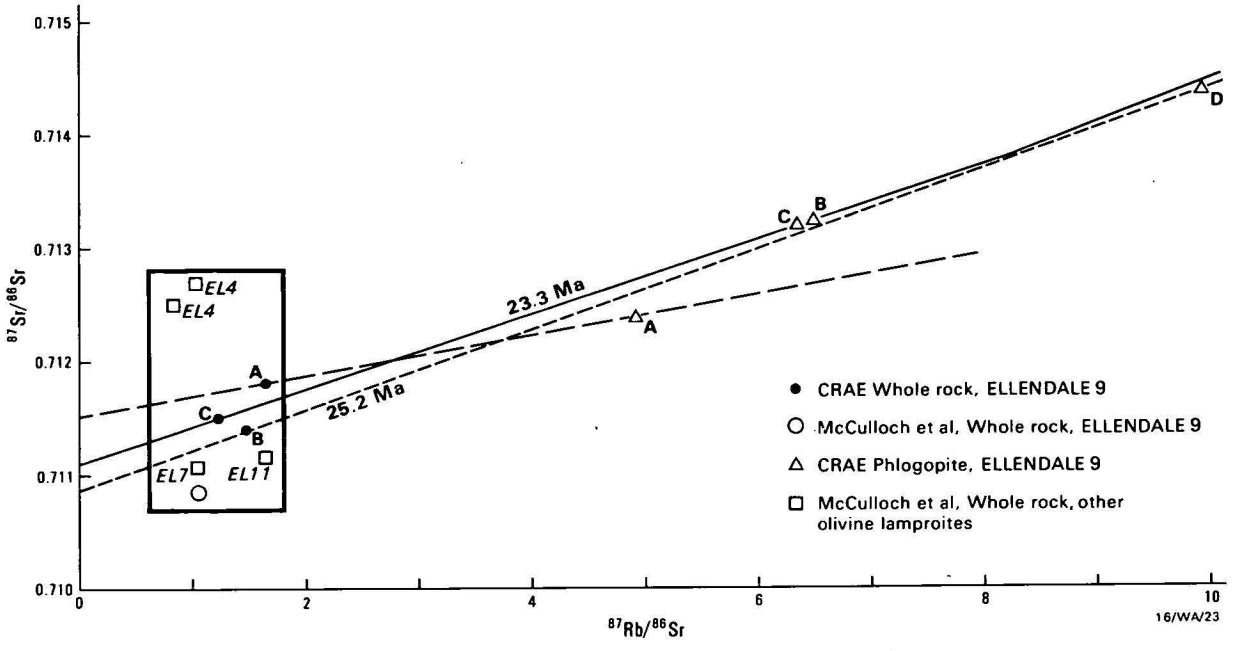

Figure 4. Rb-Sr isotopic systems of whole rocks and phlogopites in olivine lamproites from the Ellendale field.
Data from Table 3 and McCulloch & others (1983) for Ellendale pipes 4, 7, and 11.

phlogopite separate gave an age of 11.5 ± 10.4 Ma with an initial ratio of 0.71252 ± 0.00046. This initial ratio differs from that implied by the mineral separates in sample 81210167 (0.7116), suggesting isotopic heterogeneity within this intrusion.

Olivine lamproites

Rb-Sr analytical results on whole rocks and phlogopites from drill-core samples from Ellendale No. 9 olivine lamproite pipe are reported in Table 3 and plotted, together with Rb-Sr whole-rock data obtained by McCulloch & others (1983) on other olivine lamproites from the Ellendale field, in Figure 4. The Rb-Sr whole-rock points from the four separate olivine lamproite pipes do not define a single isochron, but form a cluster of points within an area defined as 0.7117 ± 0.0011 ($^{87}Sr/^{86}Sr$) and 1.2 ± 0.6 ($^{87}Rb/^{86}Sr$). In addition to isotopic variation shown by the four olivine lamproite pipes of the Ellendale field, isotopic heterogeneity within a single pipe is also evident. For example, the four Rb-Sr whole-rock data

points from Ellendale No. 9 olivine lamproite pipe (three reported in Table 3, and one from McCulloch & others, 1983) are not colinear, and, therefore, cannot be used to determine the age of the pipe. Consequently, Rb-Sr ages of the pipe have been derived from phlogopite-whole-rock pairs (Table 3). Ages calculated from the slopes of whole-rock-phlogopite tie lines (Fig. 4) are: Group A, 13.0 Ma (initial $^{87}Sr/^{86}Sr$ = 0.7115); Group B, 25.2 Ma (initial $^{87}Sr/^{86}Sr$ = 0.7109); and Group C, 23.3 Ma (initial $^{87}Sr/^{86}Sr$ = 0.7111). The near coincidence of tie lines through phlogopite-whole-rock pairs of samples B and C and the extension of these lines to include the data point phlogopite D, as shown in Figure 4, suggests an age for Ellendale pipe 9 of 24 ± 1 Ma. This is in reasonable agreement with, although slightly older than, the Rb-Sr ages obtained for leucite lamproite intrusions from the Ellendale field, and confirms the close spatial and temporal relationship between the olivine lamproites and leucite lamproites inferred from field relations.

The present results confirm the unusually high initial $^{87}Sr/^{86}Sr$ values of the olivine lamproites of the Ellendale field reported by McCulloch & others (1983), and support the observation that, in general, the leucite lamproites are much more radiogenic and exhibit a much wider range in initial $^{87}Sr/^{86}Sr$ than the olivine lamproites. Only the lamproites from Walgidee Hills (McCulloch & others, 1983; Table 3) fall within the olivine lamproite field in Figure 4. McCulloch & others (1983) interpret the isotopic systems of the West Kimberley lamproites in terms of interaction of enriched and depleted mantle components, and suggest that ancient enrichment events (>1000 Ma) are required to explain the observed Sr (and Nd) isotopic compositions.

The Rb-Sr data presented here support the K-Ar ages obtained by Wellman (1973) and in this study. The Tertiary ages contrast with the Jurassic ages obtained previously by Rb-Sr dating (Compston, in Prider, 1960; Kaplan & others, 1967). Possible reasons for the difference were discussed by Wellman (1973). They include the small enrichments in radiogenic strontium of the minerals analysed, the poor precision of many of the earlier measurements, and the fact that many of the earlier determinations either assumed initial $^{87}Sr/^{86}Sr$ values or pooled results from separate intrusions or different phases of the same intrusion. Powell & Bell (1970), McCulloch & others (1983), and this work (see previous discussion) have shown that large differences in $^{87}Sr/^{86}Sr$ exist between the lamproites, precluding any assumptions regarding common initial $^{87}Sr/^{86}Sr$. There is also a large range in initial $^{143}Nd/^{144}Nd$ (ϵ_{Nd} = — 15.2 to —7.4), which is generally consistent with the range in initial Sr ratios, but essentially independent of age correction.

Conclusions

The new K-Ar and Rb-Sr ages obtained for 14 separate intrusions confirm the early Miocene ages obtained previously for the Fitzroy lamproites by Wellman (1973). The new data, coupled with Wellman's (1973) recalculated using revised decay constants, show a range in age from slightly more than 20 Ma (21–22 Ma) for the northern lamproites in the Ellendale field to slightly less than 20 Ma (18–20 Ma) in the Noonkanbah area (Fig. 2). These young isotopic ages are consistent with the palynological evidence obtained from a pipe in the Calwynyardah field (Atkinson & others, 1984) and the preservation of crater facies rocks in the West Kimberley pipes. Erosion of not more than a few hundred metres of the pipes since their emplacement is also evidenced by the presence of crater sediments in some of the diatremes.

The similarity in ages between the newly discovered, diamond-bearing, olivine-rich (i.e. kimberlitic) lamproites and the better known leucite lamproites is consistent with the geological, petrological, and geochemical data, which indicate that the kimberlitic intrusives are olivine-rich members of the lamproite suite, constituting with the latter a consanguineous ultrapotassic (lamproite) suite (Jaques & others, 1982, 1984). The young Tertiary ages obtained on the West Kimberley rocks make these intrusives the youngest primary diamond-bearing rocks yet found.

The apparent southward younging of the intrusions of the West Kimberley region suggests a crude linear migration (north to south) of magmatic activity with time, analogous to volcanism associated with 'hot spots'. However, at least locally, the major factor controlling the distribution of intrusions appears to have been structural: west-northwesterly trending faults at the margin of the Fitzroy Trough, northerly trending fractures in the Kimberley Block, Lennard Shelf, and Fitzroy Trough, and east-west en-echelon faults and folds within the Fitzroy Trough (Atkinson & others, 1982, 1984; Jaques & others, 1982). Unlike other ultrapotassic provinces (e.g. East Africa), the lamproitic rocks of the West Kimberley do not appear to be related in time of intrusion to a major rifting episode. The Miocene magmatism clearly post-dates both formation of the Fitzroy Trough, where the major sedimentation took place in the Devonian to Carboniferous (Forman & Wales, 1981), and rifting associated with the break up of Gondwanaland in the late Jurassic. It also predates the collision between the Australian continent and Timor, which took place in the late Cainozoic (<15 Ma; Berry & Grady, 1981).

Acknowledgements

ALJ and JF gratefully acknowledge support from CRA Exploration Pty Ltd and Seltrust Mining Corp Pty Ltd. We thank Richard Rudowski for careful mineral separations, and John Lewis and Peter Wellman for helpful discussions and, together with the reviewers, for comments on the draft manuscript. AWW and CMF publish by permission of the Managing Director, AMDEL.

References

Atkinson, W.J., Hughes, F.E., & Smith, C.B., 1982 - A review of the kimberlitic rocks of Western Australia. *Terra Cognita*, 2, 204.

Atkinson, W.J., Hughes, F.E., & Smith, C.B., 1984 - A review of the kimberlitic rocks of Western Australia. *In* Kornprobst, J. (Editor), Kimberlites and related rocks *Developments in Petrology*, 9, 195-225; *Elsevier, Amsterdam.*

Berry, R.F., & Grady, A.E., 1981 - Deformation and metamorphism of the Aileu Formation, north coast, East Timor, and its tectonic significance. *Journal of Structural Geology*, 3, 143-167.

Compston, W., Lovering, J.F., & Vernon, M.J., 1965 - The rubidium-strontium age of the Bishopville aubrite and its component enstatite and feldspar. *Geochimica et Cosmochimica Acta*, 29, 1085-1099.

Cooper, J.A., 1963 - The flame photometric determination of potassium in geological materials used for potassium-argon dating. *Geochimica et Cosmochimica Acta*, 27, 525-546.

Derrick, G.M., & Gellatly, D.C., 1972 - New leucite lamproites from the West Kimberley, Western Australia. *Bureau of Mineral Resources, Australia, Bulletin* 125, 103-119.

Forman, D.J., & Wales, D.W., 1981 - Geological evolution of the Canning Basin, Western Australia. *Bureau of Mineral Resources, Australia, Bulletin* 210.

GSWA, 1979 - Geological map of Western Australia, 1:2 500 000. *Geological Survey of Western Australia, Perth.*

Jaques, A.L., Gregory, G.P., Lewis, J.D., & Ferguson, J., 1982 - The ultrapotassic rocks of the West Kimberley region, Western Australia, and a new class of diamondiferous kimberlite. *Terra Cognita*, 2, 251-252.

Jaques, A.L., Lewis, J.D., Smith, C.B., Gregory, G.P., Ferguson, J., Chappell, B.W., & McCulloch, M.T., 1984 - The diamond-bearing ultrapotassic (lamproitic) rocks of the West Kimberley region, Western Australia. *In* Kornprobst, J. (Editor), Kimberlites and related rocks. *Developments in Petrology*, 9, 225-255; *Elsevier, Amsterdam.*

Kaplan, G., Faure, D., Elloy, R., & Heilammer, R., 1967 - Contribution a l'etude de l'origine des lamproites. *Bulletin de Centre de Recherche PAUSNPA*, 1, 153-159.

McCulloch, M.T., Jaques, A.L., Nelson, D.R., & Lewis, J.D., 1983 - Nd and Sr isotopes in kimberlites and lamproites from Western Australia: an enriched mantle origin. *Nature*, 32, 400-403.

McDougall, I., 1966 - Precision methods of potassium-argon isotopic age determination on young rocks. *In* Runcorn, S.K. (Editor), Methods and techniques in geophysics, 2, 279-304; *London, Interscience.*

Nixon, P.H., Thirlwall, F.F., & Buckley, F., 1982 - Kimberlite-lamproite consanguinuity. *Terra Cognita*, 2, 252-254.

Page, R.W., Blake, D.H., & Mahon, M.W., 1976 - Geochronology and related aspects of acid volcanics, associated granites, and other Proterozoic rocks in The Granites-Tanami region, northwestern Australia. *BMR Journal of Australian Geology & Geophysics*, 1, 1-13.

Powell, J.L., & Bell, K., 1970 - Strontium isotope studies of alkalic rocks. Localities from Australia, Spain and the Western United States. *Contributions to Mineralogy and Petrology*, 27, 1-10.

Prider, R.T., 1960 - The leucite lamproites of the Fitzroy Basin, Western Australia. *Journal of the Geological Society of Australia*, 6, 71-118.

Steiger, R.H., & Jager, E., 1977 - Subcommission on geochronology: convention on the use of decay constants in geo- and cosmochronology. *Earth and Planetary Science Letters*, 36, 359-362.

Wade, A., & Prider, R.T., 1940 - The leucite-bearing rocks of the West Kimberley area, Western Australia. *Quarterly Journal of the Geological Society of London*, 98, 39-98.

Webb, A.W., 1976 - The use of the potassium-argon method to date a suite of granitic rocks from southeastern South Australia. *AMDEL Bulletin*, 21, 25-36.

Wellman, P., 1973 - Early Miocene potassium-argon age for the Fitzroy Lamproites of Western Australia. *Journal of the Geological Society of Australia*, 19, 471-474.

Williams, I.S., Compston, W., Chappell, B.W., & Shirahase, T., 1975 - Rubidium-strontium age determinations on micas from a geologically controlled, composite batholith. *Journal of the Geological Society of Australia*, 22, 497-506.

Appendix
Location of specimens

Mt Percy
Sample 81210047. Phlogopite-leucite lamproite with coarse (up to 1 cm) phlogopite phenocrysts. SE side of hill. Ellendale 044513*

Camarotoechia Bore
Sample 79211068. Tuffaceous quartz-rich sandstone with detrital phlogopite. NE side of pipe.
Sample 79211064. Lapilli tuff of olivine-phlogopite-leucite lamproite with phlogopite phenocrysts up to 3 mm. SE side of pipe.
Sample 80210059. Lapilli tuff of olivine-phlogopite-leucite lamproite. Costean on NE side of pipe.
Sample 79211063. Olivine-phlogopite-leucite lamproite with phlogopite (and olivine) phenocrysts up to 3 mm. Costean on SE side.
Sample 79211067. Tuffaceous quartz sandstone with detrital phlogopite. Costean on outer margin of NE side of pipe. Leopold Downs 201251.

Winjana
Sample 80210109. Carbonated tuff-breccia of phlogopite lamproite. Costean in Ellendale No. 17 pipe. Lennard 101701.

Hooper West
Sample 81210083. Olivine-phlogopite-leucite lamproite with phenocrysts of phlogopite up to 0.75 cm. Centre of outcrop. Hooper 865138.

81-Mile Vent
Sample 79211054. Phlogopite-leucite lamproite with coarse phenocrysts of phlogopite up to 1 cm. Fitzroyite zone on E side (cf Derrick & Gellatly, 1973, Fig. 2). Ellendale 994504.

Water Reserve Sill
Samples 79211079, 79211080. Phlogopite-olivine-leucite lamproite with phlogopite and olivine phenocrysts. Costean No. 3 in sill. Ellendale 930496.

Noonkanbah Hill
Sample 81210122. Lapilli tuff of phlogopite-leucite lamproite with phlogopite phenocrysts. Fitzroyite breccia zone on SE side (cf. Prider, 1960, Fig. 10). Hardman 893614.

'P' Hill
Sample 81210147. Olivine-diopside-leucite lamproite with phenocrysts of olivine, diopside and leucite. Fitzroyite zone on E side of hill. Hardman 022548.
Sample 81210145. Phlogopite-potassic richterite-diopside-leucite lamproite with phenocrysts of diopside, leucite, olivine and phlogopite. Wolgidite zone on SW side of hill (cf. Prider, 1960, Fig. 8). Hardman 021548.

Djada (Dadja) Hill
Sample 79211057. Phlogopite-diopside-leucite lamproite with phenocrysts of phlogopite, diopside and leucite. Wyomingite zone (cf. Prider, 1960, Fig. 9). Kalyeeda 961499.

Fishery Hill
Sample 81210151. Lapilli tuff of phlogopite-leucite lamproite with phlogopite and leucite phenocrysts. Fitzroyite breccia zone on W side of hill (cf Prider, 1960, Fig. 6). Hardman 833632.

Machell's Pyramid
Sample 81210157. Phlogopite-diopside-leucite lamproite with phenocrysts of phlogopite, diopside and leucite. Fitzroyite zone on SE flank of Machell's Pyramid (cf. Prider, 1960, Fig. 5). Hardman 779678.

Walgidee Hills
Sample 81210184. Phlogopite-diopside-olivine-potassic richterite-leucite lamproite with phenocrysts of phlogopite. NE margin of intrusion. Hardman 982752.
Sample 81210167. Olivine-diopside-potassic richterite lamproite. Central outcrop of intrusion. Hardman 974745.

Mt Gytha
Sample 81210154. Diopside-leucite lamproite with phenocrysts of diopside and leucite. Outcrop in central saddle of intrusion. Hardman 773677.

Ellendale 9
Sample B. Phlogopite-olivine lamproite with phenocrysts of phlogopite and olivine. From centre of western lobe of crater, borehole 9AC 86 at 53 - 60 m depth. Ellendale 9667257077.

* 1:100 000 map sheet name and grid reference of locality.

BMR Journal of Australian Geology & Geophysics, 9, 9-12

Late Proterozoic peralkaline intrusives of the Alligator Rivers region, Northern Territory

P.G. Stuart-Smith & R.S. Needham

The Mudginberri and Maningkorrirr Phonolites in the Alligator Rivers region consist of swarms of discordant peralkaline dykes that intrude Archaean to late Early Proterozoic rocks. Samples have given a Rb-Sr isotopic age of 1316 Ma. The dykes are phonolitic in composition and typically porphyritic, containing alkali feldspar, nepheline, sodic pyroxene, and minor biotite and apatite. In some, small globules of mostly alkali feldspar may be products of liquid immiscibility. The dykes intrude part of the stable North Australian Craton and may represent late differentiates of concealed alkaline magma, as there are no other alkaline intrusive rocks known in the region. Alternatively, they may have formed by incipient melting in the upper mantle and deep crust.

Introduction

The peralkaline Mudginberri and Maningkorrirr Phonolites were first defined by Needham & Smart (1972) and Needham & others (1975), and have been briefly described by Smart & others (1976) and Needham & others (1979). They are among the oldest peralkaline rocks in Australia. Most other occurrences are Mesozoic or Cainozoic in age and are in southeastern Australia, although Early Proterozoic peralkaline rocks occur in the Yilgarn Block, Western Australia (Libby & others, 1978). The nearest known rocks of similar composition are the potassic ultramafic to feldspar-rich plutonic rocks of the Mordor Complex in central Australia, which have given a Rb-Sr age of 1210±90 Ma (Langworthy & Black, 1978).

The phonolites consist of swarms of dykes that intrude Archaean (2500 Ma) to late Early Proterozoic rocks (about 1800 Ma) of the Pine Creek Geosyncline in the Alligator Rivers region of the Northern Territory (Needham & others, 1980; Fig. 1). The Mudginberri Phonolite has given an age of 1316±40 Ma*, and is the youngest dated Precambrian unit in the region. Although Middle Proterozoic (1645 Ma, age determined from interbedded basalt) sandstone of the Kombolgie Formation crops out extensively in the area, contact relationships are not clear. Dyke-like bodies of massive chlorite rock within this sandstone above the Jabiluka orebody may be highly altered Mudginberri Phonolite (Gustafson & Curtis, 1983).

Field relations

The Mudginberri Phonolite intrudes granitoid rocks of the Archaean Nanambu Complex (Needham, 1982). It comprises typically dark greenish grey, fine-grained, generally porphyritic rocks, forming dykes less than 10 m wide and rarely exceeding 400 m in outcrop length. The dykes are straight, parallel-sided, and apparently steeply dipping, but bifurcate in places. Most are oriented northwest; a few trend northeast. Their most concentrated development is 6–17 km southwest of Mudginberri Homestead, where at least five northwest-trending dykes intrude a garnetiferous leucogneiss. In this area, owing to poor exposure of the country rock, contacts are not exposed, but have been intersected by two drill holes (Needham, 1976). Elsewhere, exposed contacts are limited to Granite Hill, an outcrop 4 km south of Jabiluka, near the eastern margin of the Nanambu Complex, where several dykes up to 1 m wide intrude foliated granitoid rocks. At this locality they are clearly discordant and have narrow unaltered chilled margins. Neither contact aureoles, flow structures, nor xenoliths are apparent.

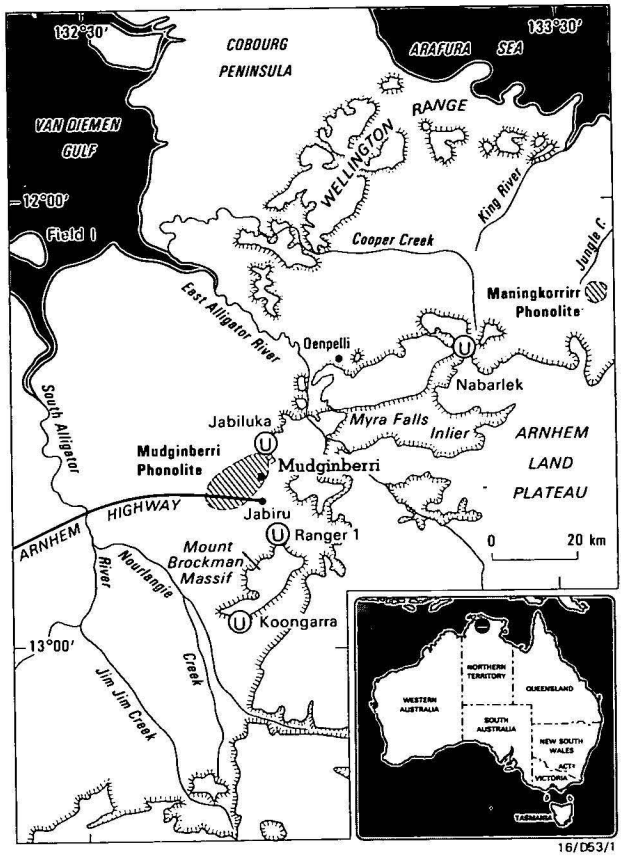

Figure 1. Locality map. Hatched area indicates location of dyke swarms

The Maningkorrirr Phonolite is exposed in an area of about 6 km², 3 km east of the headwaters of Jungle Creek and 34 km northeast of Nabarlek, where numerous straight, parallel-sided, steeply dipping dykes intrude granitoid migmatite of the Nimbuwah Complex. They are mostly 30–50 cm wide, although some are as wide as 1 m, and up to 1 km long, and are oriented northeast or northwest. The dykes are typically dark grey-green, fine to medium-grained, and commonly porphyritic. Many fine-grained and less porphyritic varieties are deeply weathered to pink ferruginised rocks in places. In the centre of the widest and longest dyke a wedge-shaped 'raft' composed of up to 50 per cent sanidine phenocrysts, possibly indicates a near-horizontal direction of flow. A similar direction is indicated elsewhere in the same dyke by arc-like accumulations of phenocrysts across the dyke (Fig. 2).

In places the dykes contain partly assimilated xenoliths of granitoid migmatite, which indicate hybridisation of incorporated material at depth during or before intrusion (Needham & others, 1975). The margins of the dykes are

*All age determinations for the Alligator Rivers Region mentioned in this paper are from Page & others (1980).

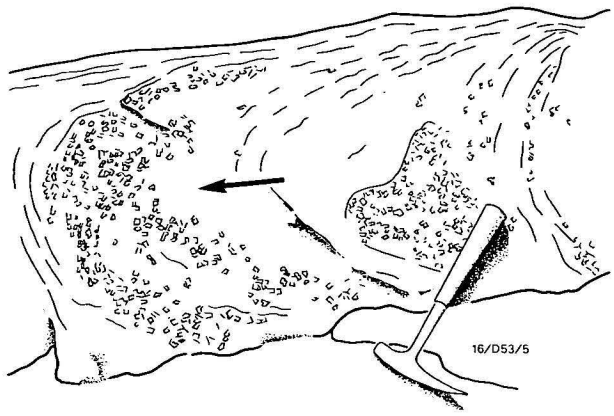

Figure 2. Accumulations of sanidine phenocrysts indicating flow direction (shown by arrow), Maningkorrirr Phonolite

sharp, and show no evidence of assimilation or contact effects on a macroscopic scale.

Petrography

The dykes show a wide range in composition. Mafic varieties predominate in the Mudginberri Phonolite, whereas more felsic varieties are dominant in the Maningkorrirr Phonolite.

The more felsic dykes range from fine, even-grained, dark green rocks to coarse porphyritic varieties. Phenocrysts constitute up to 50 per cent of the rock and are mainly euhedral alkali feldspar (albite or anorthoclase) with minor sodic pyroxene, nepheline, kaersutite and apatite. The groundmass is subtrachytic, and consists of sanidine laths, dark green titanium-rich aegirine-augite microlites and minor nepheline. Secondary carbonate and chlorite are present in places.

The more mafic dykes are typically dark green to grey, fine to medium-grained, and porphyritic. Phenocrysts of nepheline, sodic pyroxene, biotite,and apatite are abundant, but feldspar does not form phenocrysts.

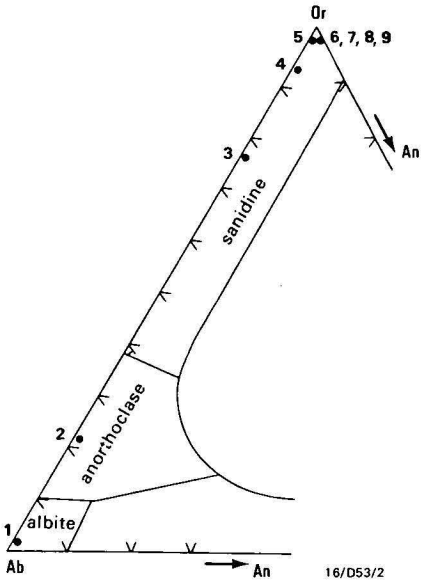

Figure 3. Feldspar compositions determined by electron microprobe
1. Phenocryst, Maningkorrirr Phonolite, BMR Sample No. 75080343
2. Phenocryst, Maningkorrirr Phonolite, BMR Sample No. 75080315
3. Groundmass, Maningkorrirr Phonolite, BMR Sample No. 75080343
4. Groundmass, Maningkorrirr Phonolite, BMR Sample No. 75980315
5,6. Groundmass, Maningkorrirr Phonolite, BMR Sample No. 72121302
7,8,9. Globule, Mudginberri Phonolite, BMR Sample No. 75080284

The groundmass is similar in composition to the felsic varieties, but the feldspar is orthoclase and subordinate to nepheline (Fig. 3). It is finer-grained than the felsic varieties, and probably crystallised after rather than during emplacement, as it lacks the flow textures characteristic of the more felsic dykes. Pyroxene phenocrysts are typically euhedral zoned crystals with pale coloured cores of augite or sodian augite (Fe_2O_3=O, Na_2O = 0.64%) and outer rims of dark green aegirine augite (Fe_2O_3=9.37%, Na_2O=4.60%) (Table 1). Their composition is relatively constant and appears to be independent of the host rock composition. The outermost rims probably have a similar composition to the dark green titaniferous aegirine-augite microlites, which grew outward from the margins of phenocrysts, radially into the groundmass. The proportion and composition of pyroxene in the groundmass remains fairly constant in all varieties (Table 1).

Table 1. Pyroxene compositions determined by electron microprobe

	1	2	3	4	5	6
SiO_2	51.23	50.28	51.29	51.61	51.60	52.87
TiO_2	5.42	3.36	0.76	0.88	0.74	0.92
Al_2O_3	1.23	1.92	2.38	2.43	1.78	0.78
*Fe_2O_3	16.88	9.37	9.62	9.12	5.13	0.00
FeO	6.89	6.50	6.91	7.82	7.85	6.15
MnO	0.33	0.27	0.34	0.23	0.35	0.12
MgO	2.38	8.08	7.69	7.28	10.15	14.70
CaO	5.31	16.11	16.80	16.15	20.20	23.81
K_2O	0.00	0.00	0.00	0.00	0.00	0.00
Na_2O	10.33	4.60	4.21	4.48	2.20	0.64
Total	100.00	100.49	100.00	100.00	100.00	100.00

*Fe_2O_3calculated by stoichiometry on the basis of 4 cations per 6 oxygen cations
1. Titanian aegirine-augite microlite, BMR Sample No. 72121302
2. Aegirine-augite phenocryst rim, BMR Sample No. 72121302
3. Aegirine-augite phenocryst, BMR Sample No. 75080284
4. Aegirine-augite phenocryst, BMR Sample No. 75080284
5. Sodian augite phenocryst core, BMR Sample No. 75080284
6. Augite phenocryst, BMR Sample No. 72121302

Nepheline commonly forms tabular zoned phenocrysts or glomeroporphyritic aggregates, which in places are altered to natrolite, and may be up to 50 per cent of the rock. Subhedral groundmass nepheline is extensively altered to natrolite and rarely preserved.

Apatite is a common accessory mineral in all varieties, particularly in the mafic varieties, where it forms slightly rounded euhedral phenocrysts, which mostly contain small rounded inclusions of carbonate.

An unusual feature is the presence of small rounded or dumbbell-shaped globules up to 2 mm across, in a dyke of the Mudginberri Phonolite, at Granite Hill (Needham & others, 1979). The globules constitute about 10 per cent of the rock and consist of subhedral orthoclase, and minor natrolite, carbonate and aegirine-augite. The natrolite is probably altered nepheline, as natrolite forms pseudomorphs after nepheline phenocrysts in the same rock. The phases in the globules are identical in composition to those in the groundmass; however, orthoclase constitutes about 70 per cent of the globules compared to less than 35 per cent of the groundmass.

Similar globules occur in a dyke of the Maningkorrirr Phonolite. They are rounded to irregular and consist of carbonate, subhedral sanidine, and aegirine-augite microlites. Euhedral aegirine-augite crystals protrude into the globules in places. Secondary amphibole alteration of the pyroxene in the globules and the adjacent groundmass is common. The term 'ocelli' was used by Needham & others (1979) to describe the globules and has been used by Philpotts & Hodgson (1968), Ferguson & Currie (1971), and Philpotts (1971, 1976) to describe similar textures in alkaline rocks.

Table 2. Chemical analyses of some rocks from the Mudginberri and Maningkorrirr Phonolites

	1	2	3	4	5
SiO_2	50.77	49.80	49.18	58.37	54.15
TiO_2	1.67	1.28	1.36	0.44	0.86
Al_2O_3	15.77	17.66	13.70	18.17	18.95
Fe_2O_3	9.63*	7.51*	6.46	6.01	6.19
FeO*			3.57	0.46	1.24
MnO	0.20	0.21	0.24	0.17	0.18
MgO	2.19	1.22	2.33	0.25	0.27
CaO	4.31	3.45	7.34	0.80	0.86
Na_2O	4.91	9.63	5.83	9.22	10.96
K_2O	4.53	3.23	3.60	3.88	3.85
P_2O_5	0.55	0.19	1.52	0.11	0.11
H_2O+	4.56	5.00	4.11	1.23	2.18
H_2O-					
CO_2			0.00	0.20	0.80
	99.09	99.18	99.24	99.31	100.60
CIPW Norms					
Ns	-	0.86	-	0.43	2.73
Or	26.77	19.09	21.27	22.93	22.75
Ab	30.10	22.33	25.07	48.55	35.40
An	7.61	-	0.58	-	-
Ne	6.20	27.37	13.14	12.62	22.01
Ac	-	4.34	-	3.79	4.37
Di	8.54	13.55	21.81	1.75	-
Ol	7.09	2.96	3.45	5.82	7.10
Mt	2.80	-	3.02	-	-
Il	3.17	2.43	2.58	0.84	1.63
Ap	1.30	0.45	3.60	0.26	0.26
Cc	-	-	-	0.45	1.82
	93.58	93.38	94.52	97.44	98.07

*Total iron as Fe_2O_3.
CIPW Norm calculations: Fe calculated on the basis that Fe^{3+} = 20% total Fe (Hughes & Hussey, 1976)

1. Mudginberri Phonolite, BMR Sample No. 74121329, Needham, 1976
2. Mudginberri Phonolite, BMR Sample No. 74121335, Needham, 1976
3. Mudginberri Phonolite, BMR Sample No. 75080284, Ferguson & Winer, 1980
4. Maningkorrirr Phonolite, BMR Sample No. 75080313, Ferguson & Winer, 1980
5. Maningkorrirr Phonolite, BMR Sample No. 75080315, Ferguson & Winer, 1980

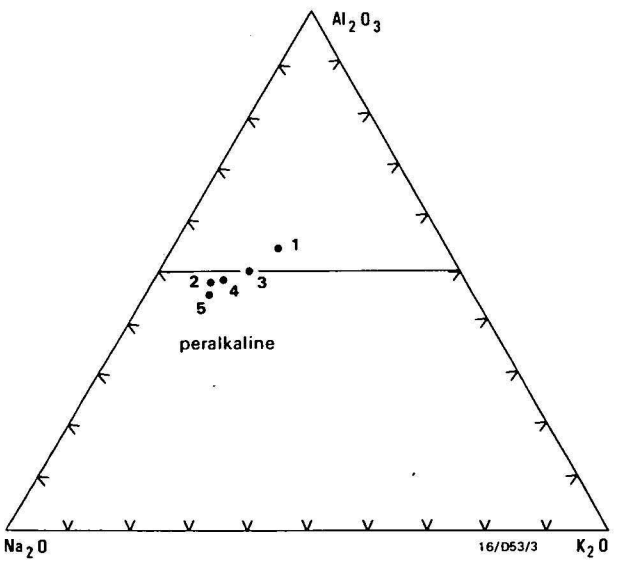

Figure 4. Molecular proportion of Na_2O, K_2O, and Al_2O_3 of analysed samples (Table 2)
1-3, Mudginberri Phonolite; 4,5, Maningkorrirr Phonolite

Chemistry

All samples of the Mudginberri and Maningkorrirr Phonolites show some degree of weathering, as evidenced by high Fe_2O_3/FeO values and high H_2O content (Table 2). All but one sample of Mudginberri Phonolite are peralkaline (Fig. 4) and show a wide range in composition in the fields of phonolitic tephrite, tephritic phonolite, nepheline trachybasalt and phonolite (Fig. 5). Most variation occurs in the Mudginberri Phonolite samples, which are more mafic than the Maningkorrirr Phonolite, containing higher MgO and CaO, and lower SiO_2. Normative nepheline ranges between 6 per cent and 27 per cent; normative plagioclase is only present in the Mudginberri Phonolite.

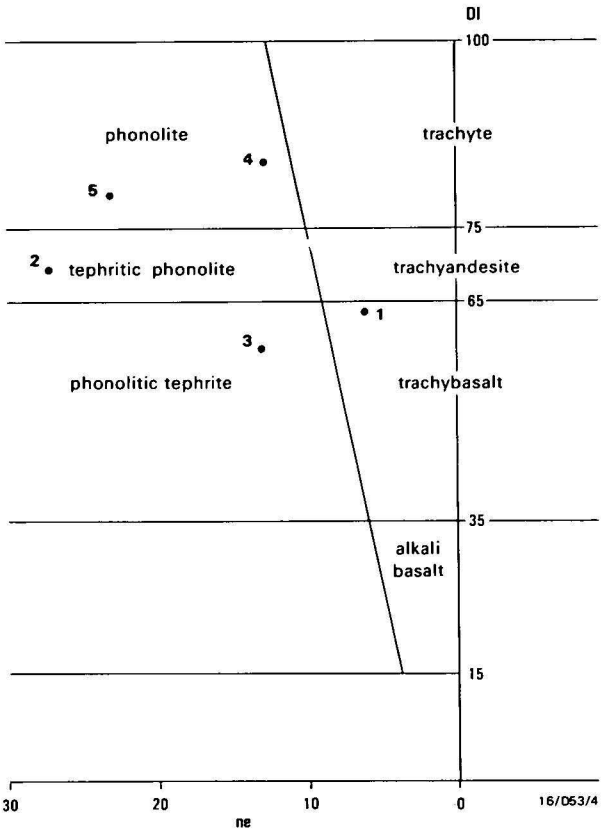

Figure 5. Classification of volcanic rocks based on Differentiation Index (DI) and degree of silica saturation (Normative ne) after Johnson & others (1978)
1-3, Mudginberri Phonolite; 4,5, Maningkorrirr Phonolite.

Discussion

Alkaline magmas have a strong tendency to immiscibility (Freestone, 1978), a process thought to be responsible for the development of globular textures (Philpotts & Hodgson, 1968; Ferguson & Currie, 1971; Philpotts, 1971, 1976). Immiscibility has also been invoked to account for globular structures and compositional variation in basic igneous bodies in southeastern Australia (Mackenzie & White, 1970; Barron, 1981).

The globules in the Mudginberri and Maningkorrirr Phonolites were possibly formed by a sudden drop in pressure, related to tapping of the magma chamber, which would have triggered volatile release, initiated an immiscible magma relationship (Barron, 1981), and terminated crystallisation of phenocrysts of sodic pyroxene, nepheline, biotite, apatite and alkali feldspar. This suggests that the

magma consisted of a mush containing these phenocrysts and small immiscible droplets of volatile-enriched liquid.

The surface tension of the globules appears generally to have prevented phenocrysts from penetrating them, except for rare aegirine-augite crystals, which show dark green titanium-rich rims where they protrude into the droplets. After emplacement of the dykes both liquid phases crystallised rapidly.

The peralkaline rocks probably evolved as low temperature melts, possibly as the end products of fractional crystallisation from a more mafic alkaline magma. However, there is no other alkaline magmatism of about the same age known in the Alligator Rivers region. Alternatively, their genesis may be related to incipient melting in the upper mantle and deep crust. The lack of xenoliths, however, and small amount of volatiles suggest that ascent of the peralkaline magma was not rapid, and that fractionation took place. Some degree of crustal contamination is indicated by a high initial $^{87}Sr/^{86}Sr$ ratio of 0.7063 ± 0.0004 (Page & others, 1980). The dykes intruded the stable North Australian Craton probably along deep fracture zones. There was possibly some reactivation of faults, mostly initiated between 1800 and 1600 Ma ago (Needham & Stuart-Smith, 1980) at the time of dyke intrusion. Emplacement was also aided by the low density, and volatile content of the magma.

Acknowledgements

P.G. Smart assisted with field observations and sample collection. John Ferguson provided samples and petrological data, and is also thanked for his encouragement. Nick Ware (Research School of Earth Sciences, Australian National University) gave assistance with the microprobe analyses, and A.L. Jaques and John Ferguson critically read the manuscript.

References

Barron, L.M., 1981 — An example of liquid immiscibility. *Geological Survey of New South Wales, Quarterly Notes.* April 1981, 4-15.

Ferguson, J., & Currie, K.L., 1971 - Evidence of liquid immiscibility in alkaline ultrabasic dykes at Callander Bay, Ontario. *Journal of Petrology,* 12(3), 561-585.

Ferguson, J., & Winer, P., 1980 - Pine Creek Geosyncline: Statistical treatment of whole rock geochemical data. Ferguson, J. & Goleby, A.B. (Editors), Uranium in the Pine Creek Geosyncline, *International Atomic Energy Agency, Vienna,* 191-208.

Freestone, I.C., 1978 - Liquid immiscibility in alkali-rich magmas. *Chemical Geology,* 23, 115-123.

Gustafson, L.B., & Curtis, L.W., 1983 - Post Kombolgie metasomatism at Jabiluka, Northern Territory, Australia, and its significance in the formation of high-grade uranium mineralisation in Lower Proterozoic Rocks. *Economic Geology,* 78, 1, 26-56.

Hughes, C.J., & Hussey, E.M., 1976 - M and Mg values in igneous rocks: proposed usage and a comment on currently employed Fe_2O_3 corrections. *Geochemica et Cosmochimica Acta,* 40, 485-486.

Johnson, R.W., Mackenzie, D.E., & Smith, I.E.M., 1978 - Volcanic rock associations at convergent plate boundaries: reappraisal of the concept using case histories from Papua New Guinea. *Geological Society of America Bulletin,* 89, 96-106.

Langworthy, A.P., & Black, L.P., 1976 - The Mordor Complex: A highly differentiated potassic intrusion with kimberlitic affinities in central Australia. *Contributions to Mineralogy & Petrology,* 67, 51-62.

Libby, W.G., Lewis, J.D., & Gower, C.F., 1978 - Contributions to the geology of the Eastern Goldfields Province. *Geological Survey of Western Australia, Report,* 9.

Mackenzie, D.E., & White, A.J.R., 1970 - Phonolite globules in basanite from Kiandra, Australia. *Lithos,* 3, 309-317.

Needham, R.S., 1976 - BMR rotary-percussion and auger drilling in the Cahill and East Alligator 1:100 000 Sheet Areas, Alligator River region, 1972-3. *Bureau of Mineral Resources Australia, Record* 1976/43.

Needham, R.S., 1982 - Cahill, Northern Territory. *Bureau of Mineral Resources, Australia, 1:100 000 Geological Map Commentary.*

Needham, R.S., & Smart, P.G., 1972 - Progress report, Alligator River Party, NT, 1971, *Bureau of Mineral Resources, Australia, Record* 1972/1.

Needham, R.S., & Stuart-Smith, P.G., 1980 - Geology of the Alligator Rivers Uranium Field. *In* Ferguson, J., & Goleby, A.B. (Editors), Uranium in the Pine Creek Geosyncline. *International Atomic Energy Agency, Vienna,* 233-257.

Needham, R.S., Smart, P.G., & Watchman, A.L., 1975 - Progress report, Alligator River Party, NT, 1972 (Oenpelli region). *Bureau of Mineral Resources, Australia, Record* 1975/39.

Needham, R.S., Ferguson, J., & Prichard, C.E., 1979 - Excursion Guide - *International Symposium on the Pine Creek Geosyncline, Australia, Sydney, June 4-8, 1979* (Special publication).

Needham, R.S., Crick, I.H., & Stuart-Smith, P.G., 1980 - Regional geology of the Pine Creek Geosyncline. *In* Ferguson, J., & Goleby, A.B. (Editors), Uranium in the Pine Creek Geosyncline. *International Atomic Energy Agency, Vienna,* 1-22.

Page, R.W., Compston, W., & Needham, R.S., 1980 - Geochronology and evolution of the late Archaean basement and Proterozoic rocks in the Alligator Rivers Uranium Field, Northern Territory, Australia. *In* Ferguson, J., & Goleby A.B. (Editors), Uranium in the Pine Creek Geosyncline. *International Atomic Energy Agency, Vienna,* 39-68.

Philpotts, A.R., 1971 - Immiscibility between feldspathic and gabbroic magmas, *Nature,* 229, 107-109.

Philpotts, A.R., 1976 - Silicate liquid immiscibility: its probable extent and petrogenetic significance. *American Journal of Science,* 276, 1147-1177.

Philpotts, A.R., & Hodgson, G.J., 1968 - Role of liquid immiscibility in alkaline rock genesis. *23rd International Geological Congress,* 2, 175-188.

Smart, P.G., Wilkes, P.G., Needham, R.S., & Watchman, A.L., 1975 - Geology and geophysics of the Alligator Rivers region. *In* Knight, C.L. (Editor), Economic Geology of Australia and Papua New Guinea, Volume 1 — Metals. *Australasian Institute of Mining and Metallurgy, Monograph* 5, 285-301.

BMR Journal of Australian Geology & Geophysics, 9, 13-18

The Mud Tank Carbonatite, Strangways Range, central Australia

P.W. Crohn[1] & D.H. Moore[2]

The Mud Tank Carbonatite at the eastern end of the Strangways Range, about 100 km northeast of Alice Springs, was the first to be recognised in Australia. Crystalline carbonate rocks containing apatite, magnetite and zircon occur in a northeast-trending zone about 2 km long and up to 700 m wide, and in a second, much smaller, lens about 2 km to the southwest. The rocks show banding, owing to differences in texture and composition, and can be broadly divided into crystalline carbonate rocks with subordinate apatite, magnetite, phlogopite, chlorite, and soda-amphibole; foliated micaceous carbonate rocks rich in pale brown phlogopite; and feldspathic carbonate rocks with various amounts of sodic plagioclase, clinopyroxene, green-brown amphibole, and brown biotite. This last group is considered to be largely of hybrid origin. Calcite and dolomite occur in various proportions in all the rock types. Country rocks are schists and gneisses of the Early Proterozoic Arunta Block. Trace element concentrations, particularly of niobium and rare earths, are within established ranges for carbonatites, but well below economic values. On the other hand, zircon crystals of gem quality are present in the soil and colluvium overlying the carbonatite, and vermiculitic mica has developed in the weathered zone within about 40 m of the surface.

Introduction

The Mud Tank Carbonatite is located at latitude 23°01'S longitude 134°16'E, about 100 km north-northeast of Alice Springs, (Fig. 1). Attention was first drawn to this locality through the presence of detrital magnetite, apatite, and zircon, which are widely scattered over the area underlain by the carbonatite. The occurrence was first described by H.B. Owen (1944), who examined it as a possible source of phosphate in 1944 and considered the carbonate rocks to be metamorphosed limestones. In 1966, the area was investigated by B.T. Williams of Geopeko Ltd, who mapped four areas of outcropping carbonate rocks and carried out a programme of four diamond-drill holes, totalling 350 m. In his account of the area, Williams (1967) briefly considered that some of the rocks could be carbonatites, but rejected the idea, mainly because of the prominent banding, which he regarded as relict bedding. P.W. Crohn first became interested in the area in 1967 after seeing a number of Canadian carbonatite complexes.

Following a preliminary account by Crohn & Gellatly (1969), a petrological study was undertaken by Gellatly (1969), and four more diamond-drill holes, totalling about 550 m, were drilled by the Mines and Water Resources Branch, Northern Territory Administration, in the same year (Crohn, 1971). Other recent investigations have included a regional gravity survey (Flavelle, 1965), and a low-level aeromagnetic survey (Tipper, 1966), both undertaken by the Bureau of Mineral Resources, age determinations by Black & Gulson (1978), and isotopic studies of the carbonate rocks by Moore & Grey (1973) and Wilson (1979). More recently, the area has again been under investigation by the Northern Territory Department of Mines and Energy to assess its economic potential as a source of vermiculite (D.H. Moore, in prep.).

Field occurrence

The main occurrence consists of an irregular northeast-trending lens of crystalline carbonate rocks, some 2 km long and from 200 to 700 m wide, which crops out intermittently in three low, gently sloping hills. A second, considerably smaller lens lies about 2 km to the west-southwest, (Fig. 2).

The carbonate rocks are highly altered and in part ferruginised at the surface. In places they show banding, owing to differences in texture and the content of non-carbonate minerals, mainly mica, magnetite, and apatite. The trend of the banding is generally northeasterly, parallel to the long axis of the occurrence and to the trend of the surrounding schists and gneisses. Individual bands range from a few centimetres to more than a metre in width.

Apatite generally occurs as massive aggregates, some of which are up to 60 cm across, and individual grains of more than 2 cm are not uncommon. Magnetite forms twinned octahedra up to 10 cm across and occasional larger aggregates. Mica generally occurs as plates up to about 2 cm across, and zircon as relatively squat prismatic crystals up to 5 cm long and 2 cm across.

Small lenses and irregular masses of amphibolite (soda-amphibole, biotite, minor plagioclase, diopside, calcite and dolomite) and sodic pegmatite (sodic plagioclase, biotite, soda-amphibole and/or aegirine-augite, minor calcite and/or dolomite), generally less than 3 m across, also occur within the carbonatite, but their contacts are not exposed.

The host rocks are schists and gneisses, calc-silicate rocks and basic igneous rocks of the Early Proterozoic Arunta Block. In places, these can be traced to within about 20 m of the carbonatite, but the actual contacts are not exposed, although they have been located approximately by auger drilling and intersected in two places by diamond drilling (Mines and Water Resources Branch diamond-drill holes A and B). In these drill holes, relationships at the major contacts are obscured by extensive shearing and associated weathering, but in DDH A there is a suggestion of minor occurrences (? veins) of carbonate rocks within the host rocks up to 25 m from the main contact. Very minor alteration of the gneiss has been recorded by Moore (1973), who noted the replacement of (?) aegirine by soda-amphibole for distances of up to 50 cm from the carbonate contact.

Magnetite-rich zones within the complex give rise to a number of distinctive magnetic anomalies of up to 1800 gammas, which indicate a steep north-westerly dip for the bodies responsible for them, in good agreement with observed dips on the layering of the outcropping carbonate rocks (Tipper, 1969).

Structural setting

The carbonatite lies on the axis of a major regional gravity high, which extends in a general east-west direction for at least 600 km, and includes the Papunya Gravity Ridge to the west and the Illogwa Gravity High to the east (Flavelle, 1965).

A major structural feature, the northwest-trending Woolonga Lineament, passes about 8 km southwest of the carbonatite.

[1] 1 Durham Road, Surrey Hills, Vic. 3127.
Formerly Department of Mines and Energy, Darwin, NT.

[2] The Broken Hill Pty Co. Ltd, P.O. Box 559, Camberwell, Vic. 3124.
Formerly Department of Mines and Energy, Alice Springs, NT.

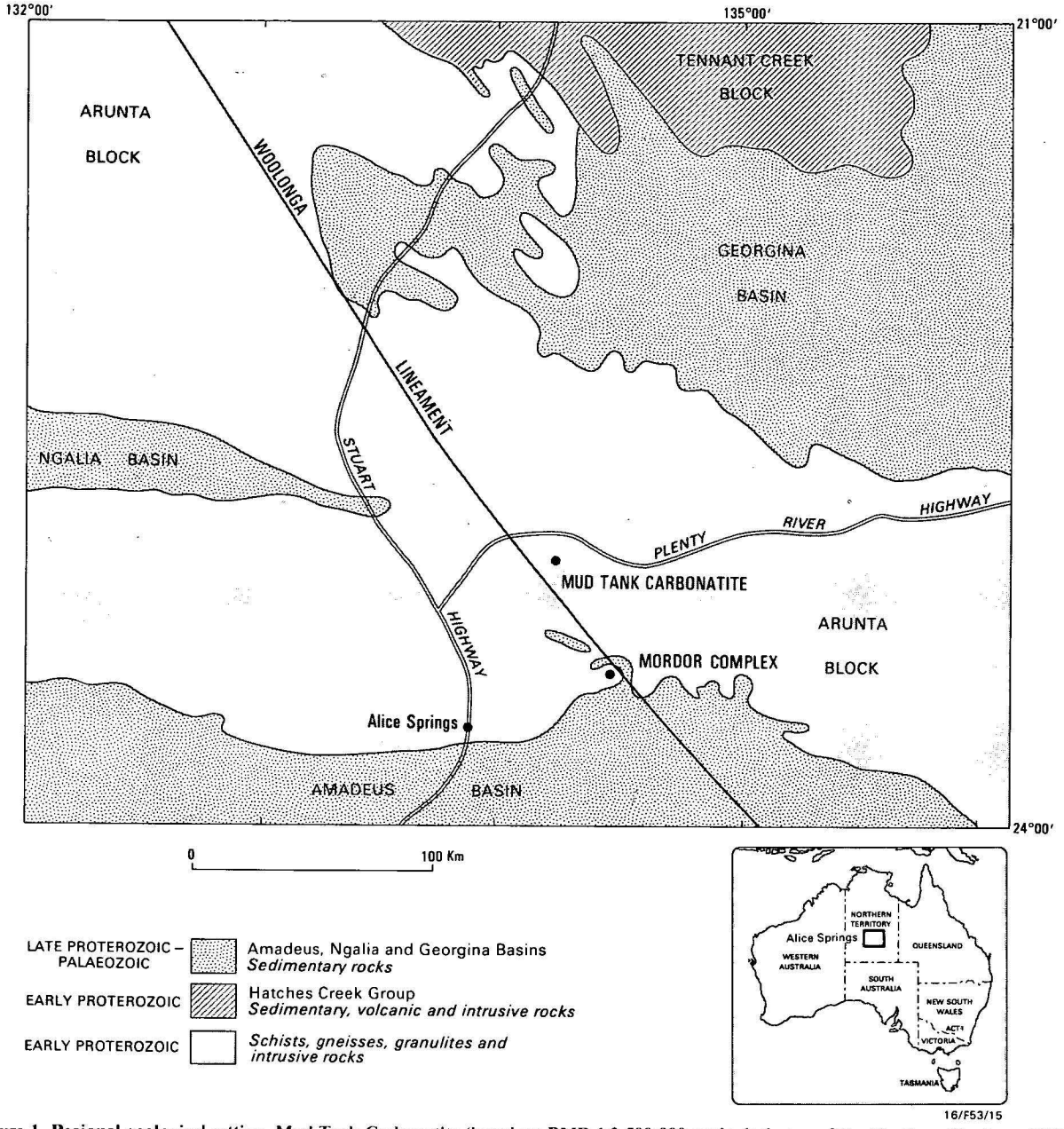

Figure 1. Regional geological setting, Mud Tank Carbonatite (based on BMR 1:2 500 000 geological map of the Northern Territory, 1976).

This also has been traced for several hundred kilometres, in part by its effect on the gravitational pattern, and may represent a deep-seated structural feature (Fig. 1) (Anfiloff & Shaw, 1973).

In the immediate vicinity of the carbonatite, the host rocks, mainly quartz-muscovite schists with minor garnet granulites and amphibolites, show some evidence of shearing and recrystallisation, suggestive of another shear zone with a northeasterly trend, parallel to the long axis of the carbonatite and complementary to the Woolonga Lineament. This may be a pre-carbonatite structure, which has partly controlled the emplacement of the carbonatite, with subsequent movement giving rise to shearing and faulting within the carbonatite and along its contacts with the host rocks. The largest fault cutting the carbonatite has an apparent displacement of about 300 m, east block north.

The Woolonga Lineament also passes close to another alkaline intrusion. The Mordor Complex (Langworthy & Black, 1978) is an alkaline ultramafic intrusion some 50 km southeast of the Mud Tank Carbonatite. This complex is cut by veins and small irregular masses of carbonates, suggesting possible carbonatitic affinities, but it has been dated at 1210 ± 90 Ma (Langworthy & Black, 1978) compared to 730 Ma for the Mud Tank Carbonatite (Black & Gulson, 1978).

Petrology

The rocks of the Mud Tank Carbonatite complex can be divided into a number of groups. Those most closely resembling typical carbonatites as recorded from other occurrences are crystalline carbonate rocks with subordinate apatite, magnetite, phlogopite, chlorite, and soda-amphibole, which are relatively abundant throughout the complex. Either calcite or dolomite may predominate, with the latter tending to form the larger grains (Gellatly, 1969). Ilmenite is commonly associated with the magnetite, and biotite takes the place of phlogopite in some specimens. Zircon is a minor constituent, and pyrite is occasionally present. According to Gellatly, the proportion of major constituents in the thin sec-

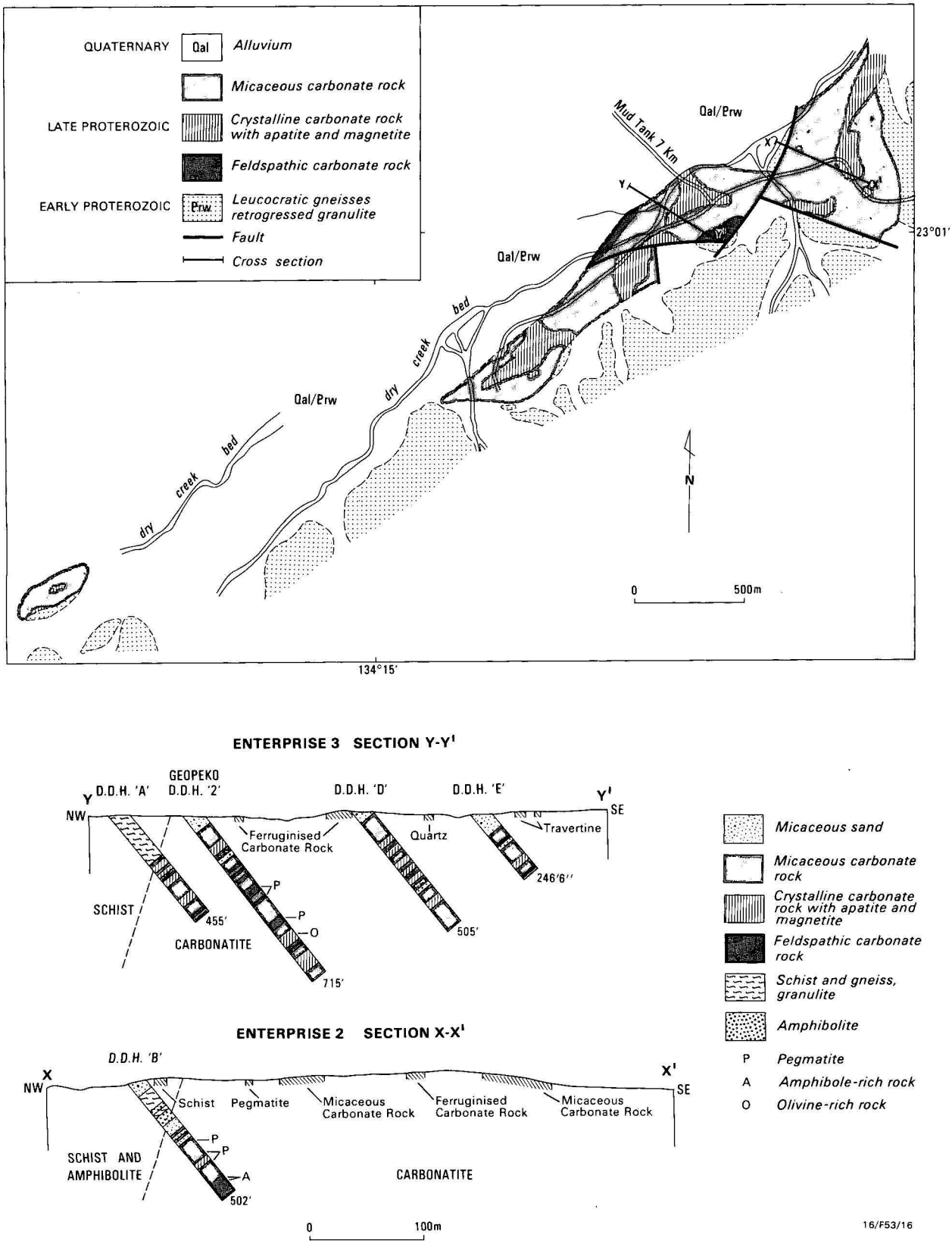

Figure 2. Geology of the Mud Tank Carbonatite (after Moore, in prep.).
Drill-hole cross-sections, after Crohn, 1971.

tions examined by him included calcite 5-90%, dolomite 5-65%, biotite 0-50%, apatite 1-65%, magnetite and ilmenite trace -2%, and the rock types included dolomitic sövite, dolomitic magnetite sövite, biotite sövite, calcitic beforsite and calcite-apatite beforsite. Gellatly and Black & Gulson (1978) recorded reverse pleochroism in the phlogopite, but this was not seen by Moore & Grey (1973) or by us.

The most abundant group of rocks, however, consists of foliated micaceous carbonate rocks, in which pale brown phlogopite, in places somewhat chloritised, is a major constituent, and is responsible for the strongly foliated appearance of these rocks. Subordinate soda-amphibole and minor apatite and magnetite are again typically present. These rocks are under-represented in outcrop, because they are not particularly resistant to erosion, but they make up just on two-thirds of all core recovered from diamond-drill holes in the carbonatite, and, by extrapolation from recent auger drilling results, they are believed to underlie most of the non-outcropping portions of the complex.

A third group of rocks contains feldspar (typically sodic plagioclase) as well as carbonates, and possibly represents a series intermediate between carbonatites and 'normal' igneous rocks. The feldspar in one specimen from Geopeko DDH Enterprise 2 was identified by Gellatly (1969) as andesine (Ab_{34}); other specimens show sericitised cores indicative of zoning (Crohn, 1971). The rocks also contain various amounts of green-brown amphibole, brown biotite, and subordinate clinopyroxene. Apatite, iron oxides and pyrite may again be present in minor amounts. Although widely distributed, this is a relatively minor phase and individual occurrences appear to be generally small. They bear some resemblance to fenites as recorded from other carbonatite complexes, but differ in occurring within the carbonatite complex rather than in the contact zone of the country rock (Fig. 2), and also in their contents of calcite and/or dolomite, which are not found in typical fenites (Le Bas, 1981).

There are also minor occurrences of rocks composed almost entirely of amphibole and biotite in various proportions, and often in close association with the feldspathic carbonate rocks, and one Geopeko drill hole intersected a 30-cm band composed almost entirely of large serpentinised olivine crystals.

Pegmatites are another minor but fairly widely distributed phase, and typically consist of sodic plagioclase, subordinate carbonates, biotite, minor soda-amphibole and/or aegirine-augite, and accessory apatite.

Where some of these different rock types are seen in juxtaposition in diamond-drill cores, contacts are generally gradational over distances of a few centimetres or tens of centimetres. An exception is provided by the feldspathic carbonate rocks, which in places show sharp contacts against the crystalline carbonate rocks, but their age relationships have not been established. The pegmatites also generally show sharp contacts against all other rock types and probably represent a late phase. Gellatly (1969) suggested that these may represent rheomorphic fenites. However, in that case, it is difficult to see why they should apparently occur only within the carbonatite complex rather than in the country rock, and they would be expected to form one of the earliest, rather than one of the last, phases of the complex. The olivine-rich band, on the other hand, is associated with a zone of strongly sheared carbonate rocks and may represent a narrow infaulted wedge or an inclusion carried up during the emplacement of the complex from an originally remote, possibly much deeper location.

From their wide distribution, crystalline texture, and relatively simple mineralogy, it is considered that both the crystalline carbonate rocks and the foliated micaceous carbonate rocks are the products of crystallisation from a carbonatite magma. The foliated micaceous carbonate rocks show considerable variation, particularly in mica content, and their crystallisation may have occurred concurrently with some movement and segregation of constituents during the last stages of consolidation.

The feldspathic carbonate rocks and the amphibole-rich rocks, on the other hand, appear to represent the products of crystallisation from a magma that was undergoing considerable modification, either by differentiation or by assimilation of pre-existing rocks, either country rocks or earlier phases of the carbonatite. In particular, a characteristic even-grained granular or slightly porphyroblastic texture of some of the feldspathic carbonate rocks is suggestive of a hybrid origin. They may represent xenoliths of gneisses or granulites in an advanced stage of assimilation, and some of the amphibole-rich rocks may similarly represent remnants of amphibolite xenoliths. Their origin, as previously indicated, has some of the characteristics of fenitisation, although their spatial distribution and mineralogy differ from those of typical fenites. The results of age determination studies also support the view that these rocks are not part of the main sequence of crystalline carbonate rocks and foliated micaceous carbonate rocks.

Geochemistry

Trace element determinations have been carried out on 13 samples of diamond-drill core from the deepest Geopeko drill hole (Crohn & Gellatly, 1968; Gellatly, 1969), and on 88 scrape samples at 6-m intervals from all Mines and Water Resources Branch cores (Crohn, 1971) (Table 1).

The highest value for niobium was obtained from a specimen containing suspected pseudomorphs after pyrochlore. Copper, zinc, cobalt, nickel, vanadium, chromium, and titanium are higher than average in magnetite-bearing and pyrite-bearing specimens, while at least some of the high values for rare earths (La, Pr, Nd and Y) tend to be associated with apatite-rich samples. Most elements did not show any regular distribution patterns, but barium and strontium tended to show generally higher values in the lower portion of DDH E, i.e. towards the base of the complex.

In general, the trace element concentrations fall within the range exhibited by carbonatites. Gellatly (1969) made a number of specific comparisons, in which he found, among others: Niobium comparable to values recorded from Spitzkop (South Africa), Darkainle (Somali Republic), and Sangu (Tanzania); barium and strontium comparable to Tundulu (Malawi), Dorowa (Zimbabwe), and Shawa (Zimbabwe); lanthanum and yttrium comparable to Mbeya (Tanzania) and Darkainle; and neodymium and praseodymium comparable to Sangu.

Table 1. Trace element values, Mud Tank Carbonatite

Nb	< 20-450 ppm	Cu	10-300ppm
Ba	175-3000	Zn	< 100-100
Sr	40-1500	Pb	2-6
La	< 100-1000	Co	8-125
	(one sample > 1000)	Ni	10-530
Pr	< 100-100	V	10-900
Nd	< 300-300		(one sample > 1000)
Y	16-200	Cr	10-60
Rb	< 3-500		

Ba, La, Cu, Co, Ni — direct reading optical spectrography.
Other elements — optical emission spectrography.

Isotopic and age determination studies

A study of strontium isotopes by Moore & Grey (1973) generally supported a carbonatite origin for the Mud Tank Carbonatite, as did studies of oxygen and carbon isotopes by Wilson (1979).

Age determinations by Black & Gulson (1978) indicated ages of 732 ± 5 Ma from U-Pb in zircon, and 735 ± 75 Ma from whole rock Rb-Sr analyses of the carbonate rocks. These do not coincide with any other known igneous or metamorphic event in this general area, and are substantially younger than the surrounding Early Proterozoic rocks.

Results from two feldspathic carbonate rocks and one amphibole-rich rock did not fall on the isochron for the remaining samples, supporting the suggestion that they are contaminated or temporally distinct phases. Determinations based on Rb-Sr in three biotite samples gave ages of 319, 349, and 329 Ma, indicating that these have been affected by younger earth movements or metamorphism, possibly related to the Alice Springs Orogeny.

Economic potential

Interest was originally directed to this occurrence as a possible source of phosphate (Owen, 1944; Williams, 1967), but, on the available evidence, the apatite content of the unaltered rocks is too low for development, and the near-surface enriched material, probably resulting from selective leaching of the carbonate fraction of the rocks, is insufficient to support a mining operation. Rare-earth, niobium, and base-metal concentrations also appear to be below economic levels.

With regard to zircon, most of the larger crystals are flawed and discoloured, but smaller specimens of gem-quality material are not uncommon, and the area now regularly attracts fossickers searching for this type of material in the soil and colluvium overlying the carbonatite.

The mica of the carbonatite within the weathered zone (generally within about 40 m of the surface) and in the overlying soil and colluvium, shows bloating properties, i.e. it expands on heating to several times its original volume, and may therefore have commercial value for thermal insulation or as a soil conditioner or light-weight aggregate. The bloating material was originally called vermiculite (Crohn, 1971), but has recently been identified by X-ray crystallography as a member of the hydrobiotite/hydrophlogopite series (Moore, in prep.). Current investigations by the Northern Territory Department of Mines and Energy are largely designed to test the possibility of economically developing this material.

Comparison with other carbonatites

Most recorded carbonatites, including such well-documented occurrences as Palabora (South Africa), Oka (Canada) and Alnö (Sweden) occur in ring structures, are closely associated with alkaline intrusive rocks, and have given rise to extensive fenitisation (alkali metasomatism) of their host rocks. They generally also occur close to major structural lineaments and show distinctive trace element values and stable isotope ratios (Le Bas, 1981). The Mud Tank Carbonatite conforms in occurring close to a major lineament (the Woolonga Lineament) and in its geochemical and isotopic characteristics, but lacks the ring structure, the associated alkalic rocks (except for very minor pegmatites), and the fenitisation (except for the development of soda-amphibole in the host gneisses within about 50 cm of the carbonatite contact).

A limited number of carbonatites comparable to the Mud Tank Carbonatite in shape and in the absence of associated alkalic rocks have, however, been recorded. They include Sangu and Songwe Scarp in Tanzania (Tuttle & Gittins, 1966), Newania in India (Viladkar, 1980) and an occurrence in the Ukrainian Shield (Kapustin & others, 1978). These may represent deeper levels of erosion than the typical ring complexes. In addition, the Indian and Ukrainian examples are associated with sodic rather than potassic fenitisation, which Le Bas (1981) also considered to be characteristic of deeper levels of erosion. Comparable sodic fenitisation is not typical of ring complexes. However, one recorded example from Sokli in Finland is of interest in that this complex is thought to consist of a core of magmatic carbonatite surrounded by a zone of meta-carbonatite — carbonate and carbonate-silicate rocks resulting from the replacement of pre-existing, possibly mafic rocks by CO_2-rich fluids from the carbonatite magma (Vartianen & Paarma, 1979).

The Mud Tank Carbonatite, has only given rise to very minor fenitisation of the surrounding gneisses, but the mineralogy of the feldspathic carbonate rocks, the amphibolite-rich rocks, and the pegmatites is, in each case, indicative of enrichment in sodium rather than potassium. Moreover, the suggested hybrid origin of the feldspathic carbonate rocks and the amphibole-rich rocks appears to bear some resemblance to that of the Sokli metacarbonatites, and the pegmatites may be the products of crystallisation from an alkali-rich residual fluid containing those components that in other carbonatite complexes have penetrated the host rocks to give rise to typical fenitic aureoles.

Acknowledgement

References to unpublished reports of the Northern Territory Department of Mines and Energy are included by permission of the Secretary of that Department, which is gratefully acknowledged.

References

Anfiloff, W. & Shaw, R.D., 1973 - The gravity effects of three large uplifted granulite blocks in separate Australian shield areas. *In* Mather, R.S., & Angus-Leppan, P.V. (editors), *Proceedings: Symposium on Earth's gravitational field and secular variations in position. Sydney, 1973.* 273-278.

Black, L.P., & Gulson, B.L., 1978 - The age of the Mud Tank Carbonatite, Strangways Range, Northern Territory. *BMR Journal of Australian Geology & Geophysics,* 3, 227--232.

Crohn, P.W., & Gellatly, D., 1969 - Probable carbonatites in the Strangways Range area, Central Australia. *Australian Journal of Science, 31, 335-336.*

Crohn, P.W., 1971 - Investigations at the Strangways Range carbonatite locality, Northern Territory, 1969-1970. *Mines Branch, Northern Territory Administration; Records Northern Territory Geological Survey* 1971/1 (unpublished).

Flavelle, A.J., 1965 - Helicopter gravity survey by contract - Northern Territory and Queensland, 1965. *Bureau of Mineral Resources, Australia, Record* 1965/212.

Gellatly, D.C., 1969 - Probable carbonatites in the Strangways Range area, Alice Springs 1:250 000 Sheet area SF 53/14: petrography and geochemistry. *Bureau of Mineral Resources, Australia, Record* 1969/77.

Jensen, H.I., 1943 - Notes on the phlogopite mine, Strangways Range area. *Bureau of Mineral Resources, Australia, Unpublished Report, Resident Geologist's Office, Alice Springs.*

Kapustin, Y.L., Lapitski, E.M., Pogrebnoy, V.T., Storchak, P.N., & Kochanov, Y.N., 1978 - The carbonatite zone of the Ukrainian Shield. *International Geology Review, 20, 1131-1140.*

Langworthy, A.P., & Black, L.P., 1978 - The potassic Mordor Complex, central Australia. *Contributions to Mineralogy and Petrology,* 67, 51-62.

Le Bas, M.J., 1981 - Carbonatite magmas. *Mineralogical Magazine,* 44, 133-140.

Moore, A.C., 1973 - Carbonatites and kimberlites in Australia: a review of the evidence. *Minerals Science and Engineering,* 5(2), 81-91.

Moore, A.C., & Grey, C.M., 1973 - Carbonatites of the Strangways Range, central Australia: evidence from isotopes. *Journal of the Geological Society of Australia,* 20(1), 71-73.

Moore, D.H., in prep. - The Mud Tank vermiculite prospect, Alice Springs 1:250 000 Sheet area SF 53/14. *Northern Territory Government, Department of Mines and Energy, Northern Territory Geological Survey Records* (unpubl.).

Owen, H.B., 1944 - Report on an occurrence of apatite on Alcoota Station, Alice Springs District, Northern Territory. *Bureau of Mineral Resources, Australia, Record* 1944/44.

Stillwell, F.A. 1943 - Rock specimens from Strangways Range, Northern Territory. *Mineragraphic Investigations of the Council for Scientific and Industrial Research, Report No.* 288.

Tipper, D.B., 1966 - Strangways Range aeromagnetic survey, Northern Territory, 1965. *Bureau of Mineral Resources, Australia, Report* 136.

Tuttle, D.F. & Gittins, J. (editors) 1966 - Carbonatites. *J. Wiley, London.*

Vartianen, H., & Paarma, H., 1979 - Geological characteristics of the Sokli Carbonatite Complex, Finland. *Economic Geology,* 74, 1296-1306.

Viladkar, S.G., 1980 - The fenitised aureole of the Newania carbonatite, Rajasthan. *Geological Magazine,* 117, 285-292.

Williams, B.T., 1967 - Report on the investigation of the Enterprise 2 group of prospects, Strangways Range, Northern Territory. *Geopeko Ltd, unpublished report.*

Wilson, A.F., 1979 - Contrast in isotopic composition of oxygen and carbon between the Mud Tank Carbonatite and the marble in the granulite terrane of the Strangways Range, Central Australia. *Journal of the Geological Society of Australia,* 26(1-2), 39-44.

BMR Journal of Australian Geology & Geophysics, 9, 19-32

Petrology and geochemistry of Proterozoic dolerites from the Mount Isa Inlier

D.J. Ellis* & L.A.I. Wyborn

The Precambrian Mount Isa Inlier in northwest Queensland is extensively cut by numerous dolerite intrusions. At least two distinct episodes of dolerite intrusion have been recognised in each of the three major tectonic units: the western succession, basement sequence, and eastern succession. Olivine and quartz tholeiites predominate. The rocks in the western succession and basement sequence display little chemical variation with time. Those of the eastern succession display greater chemical variations. The most likely present-day tectonic analogue is that of an intracontinental rift. There is no evidence in the composition of the mafic igneous rocks to suggest that they were formed in a subduction-related environment such as an island arc or continental margin.

Introduction

The Proterozoic Mount Isa Inlier (Geological Survey of Queensland, 1975) of northwestern Queensland was subdivided into three major tectonic units by Carter & others (1961): two depositional basins — the western and eastern successions — separated by an older basement sequence of felsic and mafic volcanics and granitic rocks. Mafic igneous rocks occur throughout these three major tectonic units (Fig. 1), with the mafic volcanic rocks being concentrated in the lower half of the stratigraphic column (Fig. 2).

In the western succession, metabasalts occur near the base and top of the *Bottletree Formation* (Blake & others, 1981), but the main mafic volcanic unit is the *Eastern Creek Volcanics* (Carter & others, 1961), which are part of the Haslingden Group and overlie the Bottletree Formation. The Eastern Creek Volcanics crop out over 4000 km² in a north-trending belt some 300 km long. Other western succession mafic volcanics include the *Jayah Creek Metabasalt* and the *Oroopo Metabasalt,* which crop out well south of Mount Isa, near Ardmore; Blake & others, (1981) considered them to be the probable metamorphosed equivalents of the Eastern Creek Volcanics.

The *Magna Lynn Metabasalt* of the Tewinga Group (Derrick & others, 1976a), is the major mafic volcanic unit of the basement sequence.

In the eastern succession, the main mafic volcanic units are the *Soldiers Cap Group* (Carter & others, 1961), a succession of schist and amphibolite that crops out southeast of Cloncurry in a north-northwest-trending belt about 100 km long by 35 km wide and up to 1600 m thick, and the *Marraba Volcanics* (Carter & others, 1961), which cover about 600 km² and are exposed in a complexly folded and faulted arcuate belt (the Duck Creek and Bulonga Anticlines). Some basalt flows occur locally in other parts of the eastern succession and include the *Wakeful Metabasalt Member* of the Mitakoodi Quartzite (Derrick & others, 1976b) and the *Lime Creek Metabasalt Member* of the Corella Formation (Derrick & others, 1977). Minor metabasalts also occur in the *Double Crossing Metamorphics, Kuridala Formation, Doherty Formation,* and *Staveley Formation* (Blake & others, 1981).

The first comprehensive study of the Precambrian geology of the Mount Isa Inlier was that of Carter & others (1961). More recently, the Bureau of Mineral Resources and the Geological Survey of Queensland carried out geological mapping at 1:100 000 scale in the inlier, and much of this work is summarised by Plumb & others (1980) and Blake (1980). Papers dealing specifically with mafic igneous rocks include Walker (1958), Walker & others (1960), Robinson (1968), Smith & Walker (1971), Wilson (1978), and Scott & Taylor (1982). Of special interest to this paper is the work of Glikson & others (1976) and Glikson & Derrick (1978), who studied the geochemistry of the mafic volcanic rocks in the northern part

* Department of Geology, University of Tasmania, PO Box 252C, Hobart, Tasmania 7001.

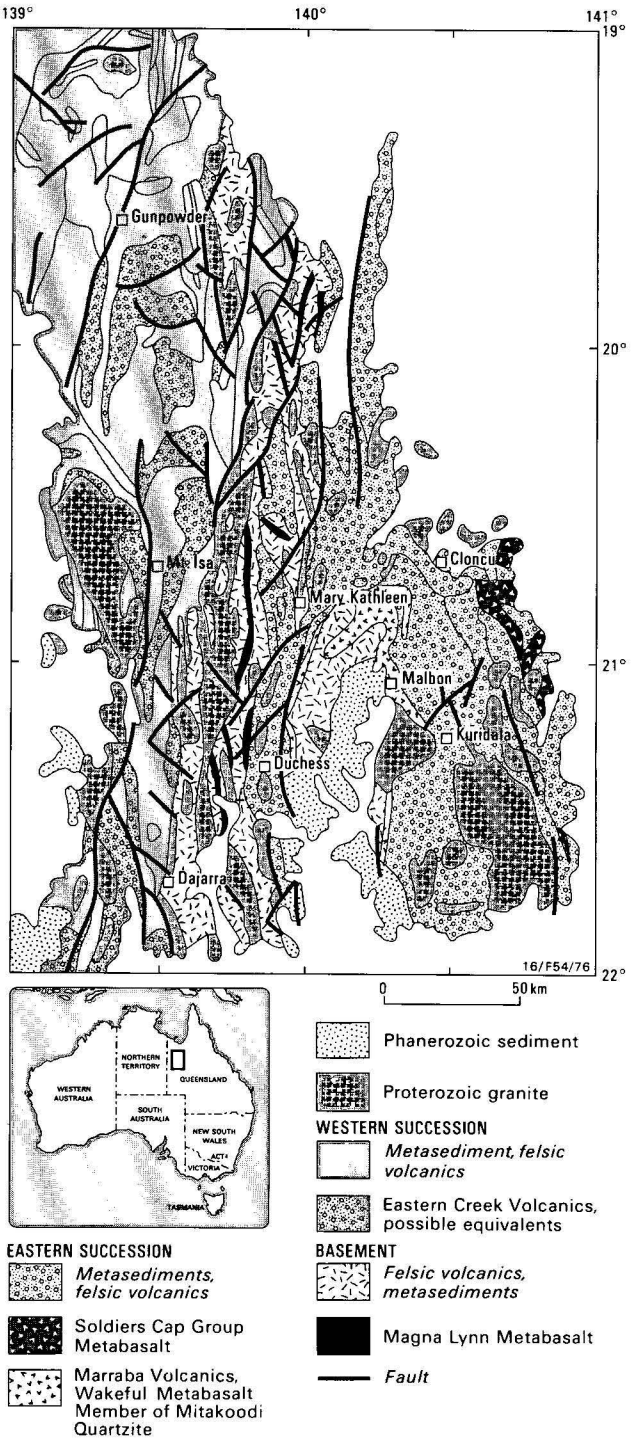

Figure 1. Geological sketch map of the Mount Isa Region, northwestern Queensland.

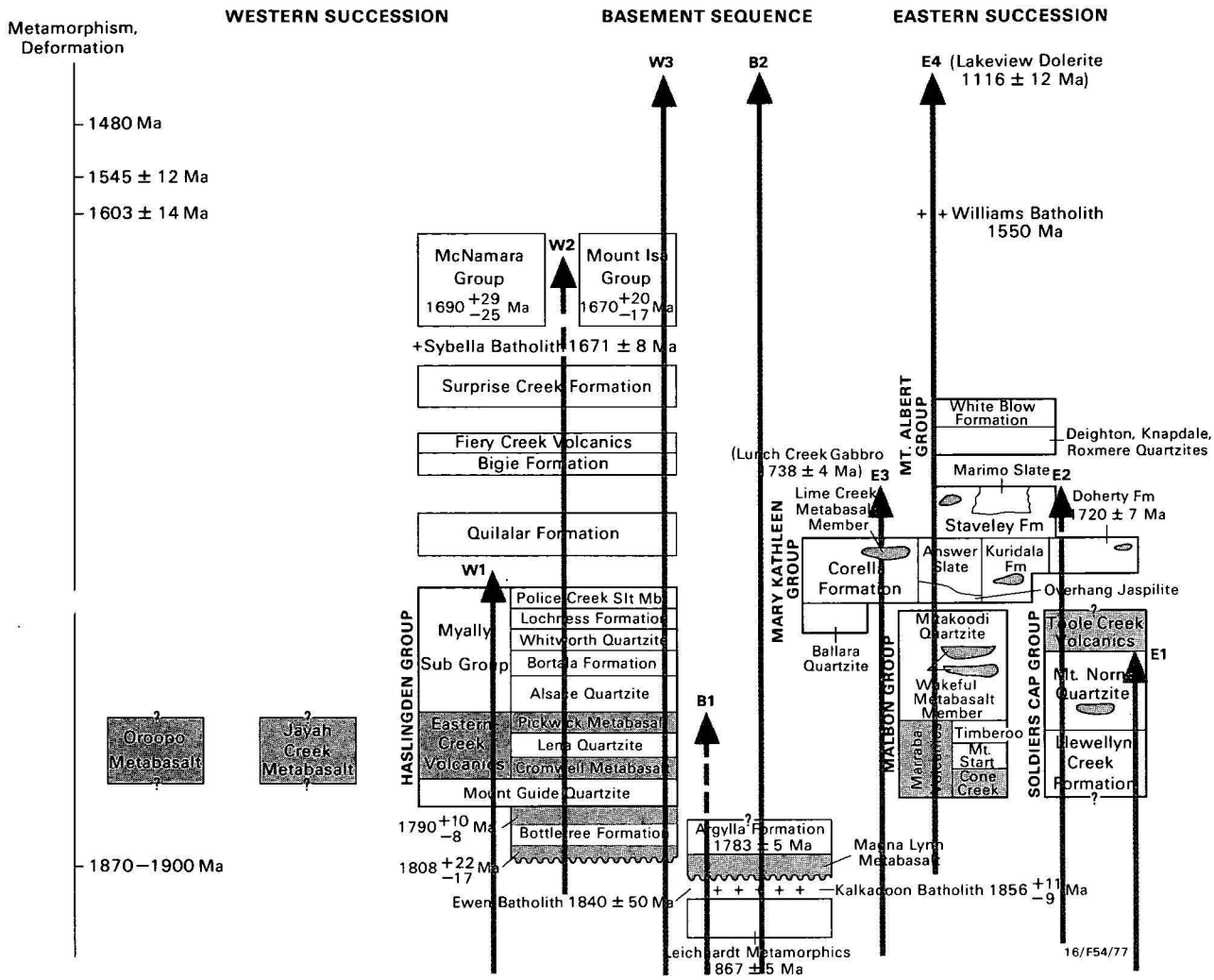

Figure 2. Stratigraphy. Based on data from Plumb & others, 1980, Blake 1980, Wyborn & Page (1983), Page (1983a, 1983b) and Blake & others (1984).

of the Mount Isa Inlier and found a marked east-west change in their composition. They concluded that the geochemistry of the Eastern Creek Volcanics correlated with that of continental flood basalts, whereas that of the Soldiers Cap Group in the eastern succession showed certain affinities with ocean floor tholeiites. In contrast, Bultitude & Wyborn (1982) did not find an east-west change in the composition of the mafic volcanic rocks in the southern third of the Mount Isa Inlier (i.e. south of latitude 21°).

In this study, detailed sampling of the dolerite dykes was carried out to complement that done on the extrusive rocks. Most of the samples were collected in a west-east belt through the centre of the Mount Isa Inlier, essentially between the towns of Mount Isa, Mary Kathleen, and Cloncurry. The dolerite intrusions have been divided spatially into three broad groups — those of the western succession, basement sequence, and eastern succession, and each of these has been further subdivided into groups corresponding to periods of magmatic activity. Time differences between the various groups of dolerites have been defined from their field relations to sedimentary units, folding, metamorphism, and episodes of granite intrusion. The field relationships, petrography, and chemistry of 88 dolerite samples are presented and characteristics of these dolerites and volcanics are discussed in the context of present-day analogues.

Classification

Of the dolerites analysed, eight are metasomatised and eighty are believed to have essentially retained their original geochemical characteristics. All chemical analyses in Tables 2-4 are adjusted to a volatile free basis. Weight percentages of the various oxides (volatile-free) are plotted in Figures 6, 8, and 10 as a function of differentiation index (D.I. of Thornton & Tuttle, 1960) with $Fe_2O_3 = 2.0$ per cent. The full analyses are listed in Wyborn (in prep.). The development of metamorphic mineral assemblages in many of these rocks renders classification based on petrographic criteria impossible, and a chemical classification is used here, following the terminology proposed by MacDonald & Katsura (1964), Green & Ringwood (1967), and Irvine & Baragar (1971).

Plots of the conventional total alkalis-silica diagram (Fig. 3) show that most of the rocks can be classified as subalkaline. Only two of the samples that plot in the alkaline field are nepheline-normative (74205557*, 74205684; 0.1 and 0.69 Ne, respectively); the remainder are hypersthene-normative and considered to be tholeiitic in chemistry. Of the latter, rocks that contain normative olivine are classified as olivine tholeiite, and those with normative quartz are classified as quartz tholeiite. On an FMA Diagram (Fig. 4), all analysed groups of dolerites show trends of iron enrichment and belong to the tholeiite suite.

Alteration

In places, the basic igneous rocks have been metasomatised, and samples of massive dolerites and the very altered parts of the same intrusions have been analysed (Table 1) to study the

*Total iron as FeO

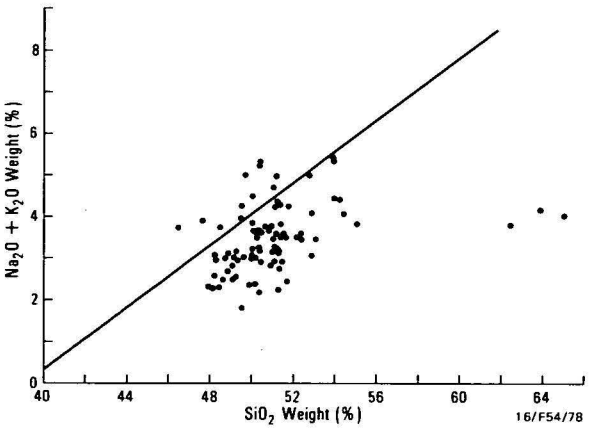

Figure 3. Plot of SiO_2 *vs* Na_2O + K_2O contents in Mount Isa mafic igneous rocks.

Table 1. Chemical analyses of metasomatised mafic rocks.

Sample No.	1 74205594	2 74205595	3 74205598	4 74205596	5 73205374	6 73205375	7 74205608	8 74205609	9 74205539	10 74205651
Type*	mBI	cBI	mBI	cBI	mBI	bBI	mBI	bBI	sE2	sE2
Major elements										
SiO_2	60.94	33.47	50.57	47.88	51.56	49.08	48.62	49.89	48.11	44.71
TiO_2	1.54	3.26	1.18	3.33	2.45	2.51	1.14	0.83	1.36	2.26
Al_2O_3	12.24	12.67	14.31	13.35	13.20	12.70	15.11	16.16	13.03	12.05
Fe_2O_3	3.10	2.27	3.23	2.06	3.04	6.62	1.66	1.59	4.56	5.48
FeO	6.35	12.30	8.55	7.45	10.00	9.80	9.65	8.00	7.90	12.50
MnO	0.20	0.35	0.25	0.07	0.10	0.12	0.18	0.18	0.08	0.21
MgO	1.76	12.80	6.07	14.20	5.57	4.60	7.36	6.83	6.40	5.54
CaO	7.19	3.04	9.32	0.93	8.29	7.57	10.16	10.01	9.00	9.19
Na_2O	3.31	0.28	2.71	0.12	2.22	2.03	2.02	1.70	4.11	3.05
K_2O	0.38	0.64	0.70	0.02	0.84	1.59	0.95	2.10	1.15	0.72
P_2O_5	0.50	0.53	0.12	0.76	0.25	0.27	0.13	0.14	0.18	0.12
H_2O^+	0.75	6.95	1.54	7.84	1.10	1.47	1.89	1.62	0.99	1.37
H_2O^-	0.07	0.17	0.08	0.32	0.04	0.11	0.05	0.04	0.03	0.09
CO_2	0.05	0.05	0.05	0.05	0.05	0.22	0.05	0.05	0.10	0.05
$S(SO_3)$	0.02	0.02	0.04	0.04	0.02	0.035	0.06	0.03	0.22	0.36
Total	98.40	98.38	98.67	98.38	98.72	98.68	98.98	98.49	96.98	97.34
Trace elements ppm										
Ba	312	463	956	10	210	775	309	434	58	256
Rb	9	35	43	2	45	91	44	118	72	30
Sr	242	31	215	13	116	127	182	208	144	141
Y	102	51	23	54	51	43	18	27	26	25
Pb	11	2	11	3	3	4	6	7	2	6
Zr	623	266	75	235	160	166	79	103	70	75
Zn	116	272	395	176	64	44	135	90	35	86
Cu	128	15	170	10	38	130	162	52	410	330
Ni	10	50	63	48	18	33	235	140	85	95
Cr	10	40	130	75	60	35	125	280	140	30
V	60	370	350	300	480	460	275	205	385	770
Sc	10	15	20	10	25	10	15	20	20	25
Cl%	0.05	0.05	0.05	0.05	0.05	0.05	0.05	0.05	1.03	1.30
Ratios										
Ti	9.01	31.76	33.02	33.28	31.96	33.71	26.98	21.03	35.65	47.4
Zr	61.02	43.32	34.88	39.50	34.78	37.30	40.87	44.21	30.43	26
Y	29.97	24.92	32.09	27.23	33.26	28.99	32.10	34.76	33.91	26
K/Rb	350	152	135	83	155	145	179	147	133	199

*m = Massive
c = chlorite bearing
b = biotite bearing
s = scapolite bearing

effect of this. and chemical analyses of these samples are given in Table 1. Three main mineralogical changes have been observed: the production of chlorite, biotite, and scapolite.

Chlorite is common in sheared samples and, from a comparison of the chlorite-rich samples and massive rocks (Table 1, Nos. 1 vs 2 and 3 vs 4), it appears that Si, Ca, Na, and Cu are removed from the system, whereas Ti, Mg, and H_2O increase, K/Rb decreases, and the Ti-Zr-Y ratio is altered. Copper, in particular, is affected, and many shear zones are sites of copper sulphide mineralisation in a calcite-quartz gangue. These results may be compared with the work of Smith & Walker (1971), who found that deformation of greenstone adjacent to the Mount Isa orebody and its conversion to pale green chlorite schist resulted in depletion in Ba, Ca, Cu, K, Na, and Si, and, to a lesser extent, Co, Fe, Mn, Ni, and Ti.

Biotite is commonly formed by metasomatism during shearing. This alteration is virtually absent from the western succession, but common in the basement and eastern succession. Examples of massive rock–schistose biotite rock pairs are shown in Table 1, Nos. 5 vs 6 and 7 vs 8, and the most obvious effect is the large increase in K_2O, with smaller increases in Ba and Rb. The other elements are more erratic in their behaviour. In contrast to the development of chlorite schists (Table 1, Nos 1–4), Ca is not removed from the system, K/Rb and the Ti-Zr-Y ratios are not altered, and Na/K decreases. This indicates that those basic rocks that show even slight petrographic evidence of alteration have had their K, Ba, and Rb contents altered, whereas certain elemental ratios are not affected.

Scapolite has developed in some of the metamorphosed dolerites, particularly in the eastern succession. From a comparison with some average analyses, it can be seen that the development of scapolite during metasomatism involves an increase in S, Cl, Na, Cu, and Na/K (Table 1, Nos. 9, 10). The introduced fluid phase must have been rich in Na and Cl, and was probably derived from the Corella Formation. The high Cu content in these samples indicates that Cu has also been concentrated, but other element ratios are generally unaffected by the formation of scapolite.

Western succession dolerites

Three groups of dolerite intrusions are recognised in the western succession: (W1) and (W2), which were intruded before the regional metamorphic event(s), and a younger group (W3), which appears to be unmetamorphosed.

The *W1 dykes and sills* intrude the Mount Guide Quartzite, Eastern Creek Volcanics, and the Myally Subgroup. Intrusions within the Myally Subgroup are mostly sills, whereas those in the Eastern Creek Volcanics occur as dykes. The dykes are from several metres to 30 metres wide, and locally sheared. Because of extensive faulting, they can rarely be traced for more than a few kilometres. They predate the earliest metamorphic event, which has been dated in this area at 1610±3 Ma (Page *in* Blake & others, 1984).

East of the Mount Isa Fault, the W1 dolerites contain mineral assemblages typical of lower greenschist grade, and igneous textures are well preserved. Tremolite/actinolite is the dominant ferromagnesian mineral occurring with chlorite, epidote, sphene, and magnetite. The opaque oxides are typically mantled by sphene. In the more siliceous dolerites, granophyric intergrowths of quartz and feldspar are preserved in the groundmass. Remnant pyroxene has been seen in one thin section (73205349*).

*Registered BMR sample number

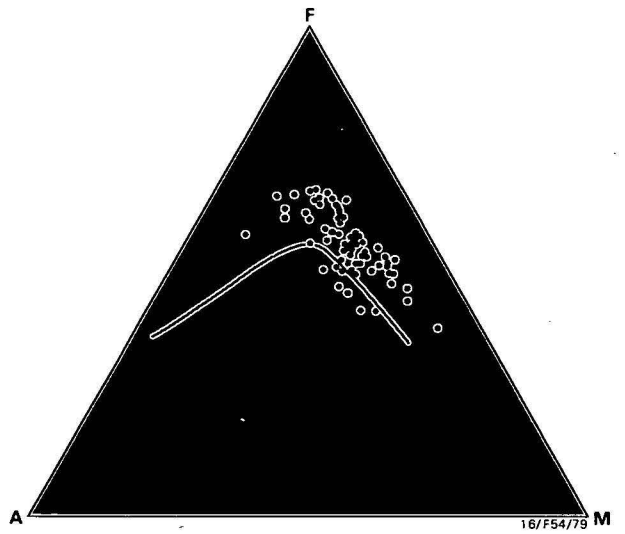

Figure 4. FMA plot of all mafic igneous rocks.

Table 2. Chemical analyses of western succession dolerite dykes and related rocks.

Sample No.	1 71201436	2 71201446	3 73205326	4 73205346	5 73205347	6 73205349	7 73205352	8 74205643	9 74205644	10 74205685	11 74205634	12 74205635A	13 74205635B	14 74205635C	15 74205636C	16 74205637	17 74205641	18 73205350	19 73205353	20 73205354	21 73205358	22 73205359	23 73205360	24 73205361	25 73205364	26 74205649
Type	W1	W1	W1	W1	W1	W1	W1	W1	W1	W1	W2	W2	W2	W2	W2	W2	W2	W3	W3	W3	W3	W3	W3	W3	W3	W3
Major elements																										
SiO_2	50.25	50.38	50.01	50.37	48.33	48.05	51.34	48.29	51.14	49.14	48.75	49.17	62.39	63.91	65.10	50.02	52.91	47.91	48.98	51.40	48.48	50.04	53.96	55.52	51.20	52.32
TiO_2	1.21	0.86	0.94	2.56	0.88	0.92	1.63	1.69	1.58	1.21	1.86	1.83	1.62	0.96	0.85	1.61	1.98	0.98	0.94	1.29	3.29	1.29	2.30	1.68	2.24	2.41
Al_2O_3	16.99	16.95	17.20	15.60	16.75	16.01	14.43	14.14	14.44	16.14	14.97	14.88	15.19	13.02	12.34	14.05	14.49	16.21	15.35	15.15	14.02	15.67	13.02	15.90	13.24	13.21
Fe_2O_3	2.31	1.83	1.69	2.99	1.84	2.43	3.88	5.17	4.79	1.66	1.98	1.71	2.19	1.11	1.21	2.86	1.48	2.41	1.89	3.52	4.17	2.37	4.51	5.14	3.94	4.02
FeO	9.08	8.50	7.81	10.63	10.56	9.02	8.83	9.72	8.76	10.39	10.29	10.32	5.36	5.38	5.21	9.02	9.97	10.66	9.23	6.30	11.80	9.79	10.44	6.68	11.37	11.42
MnO	0.18	0.18	0.18	0.21	0.19	0.20	0.20	0.22	0.20	0.19	0.19	0.19	0.09	0.09	0.09	0.19	0.16	0.19	0.19	0.21	0.22	0.20	0.23	0.16	0.23	0.21
MgO	6.23	6.67	8.85	3.57	8.84	9.41	5.50	6.00	5.71	7.79	7.02	7.65	2.70	5.35	5.49	7.35	5.40	8.31	8.09	7.43	4.18	6.83	3.57	2.10	5.06	4.13
CaO	10.70	11.14	8.73	8.20	10.17	11.54	10.21	11.41	10.28	10.47	10.99	10.90	5.46	5.81	5.56	11.23	8.82	10.84	12.76	10.27	9.70	10.41	6.21	5.95	7.46	8.40
Na_2O	2.15	2.45	2.21	3.90*	1.75	1.30	2.16	2.55	2.10	2.04	2.40	2.30	2.82	2.04	2.02	2.11	2.25	1.53	1.88	3.18	2.40	2.28	3.47	4.60	2.32	2.35
K_2O	0.78	0.95	2.29	1.36	0.61	1.05	1.65	0.56	0.81	0.87	0.63	0.74	1.86	2.151	2.00	0.80	1.89	0.86	0.65	1.13	1.39	0.98	1.90	1.87	2.67	1.23
P_2O_5	0.13	0.09	0.10	0.61	0.09	0.08	0.17	0.24	0.20	0.11	0.32	0.32	0.32	0.18	0.13	0.26	0.65	0.10	0.07	0.12	0.37	0.13	0.41	0.40	0.27	0.31
Trace elements ppm																										
Ba	183	133	602	716	142	170	844	490	340	175	309	289	377	1047	936	373	1280	186	99	482	325	316	342	488	320	286
Rb	32	33	101	15	24	34	39	11	36	29	18	24	94	98	87	32	58	25	26	29	64	40	64	79	77	57
Sr	185	197	226	261	176	190	179	184	166	182	304	290	245	164	157	272	368	176	187	242	145	155	121	180	276	157
Y	22	15	16	40	14	13	29	40	39	18	20	24	27	26	28	20	50	14	13	22	41	22	45	52	35	40
Pb	9	13	12	7	6	7	10	7	7	3	10	2	18	17	12	6	19	5	6	6	10	6	11	9	11	6
Zr	94	51	48	242	57	43	104	166	174	59	75	82	566	299	366	75	320	58	44	78	170	87	197	192	128	156
Zn	100	97	132	138	102	126	122	146	135	126	116	112	78	93	66	106	138	106	82	101	159	120	160	142	142	157
Cu	186	40	58	20	92	128	220	80	160	127	85	80	45	52	45	78	70	98	164	180	368	178	86	62	155	112
Ni	92	102	234	12	220	235	68	95	133	158	110	125	40	110	103	230	148	202	134	126	48	136	24	10	53	63
Cr	110	185	430	20	95	205	120	5	10	85	275	270	45	285	330	285	175	60	450	390	10	165	25	5	50	200
V	275	310	275	250	240	30	420	345	370	305	315	330	220	150	125	245	265	280	300	340	700	360	280	130	400	370
Sc	15	15	10	10	10	15	10		20	15	20	15	10	15	10	25	15	10	10	10	20	15	20	15	20	25
CIPW norm																										
Q	0.79						3.33		6.12				21.90	22.11	24.36	1.42	4.42				2.04		6.51	6.42	1.94	8.08
Or	4.61	5.61	13.54	8.04	3.61	6.21	9.75	3.31	4.79	5.141	3.72	4.37	10.99	12.71	11.82	4.73	11.17	5.08	3.84	6.68	8.22	5.79	11.23	11.05	15.78	7.27
Ab	18.19	20.73	18.70	33.00	14.81	11.00	18.28	21.58	17.77	17.26	20.31	19.46	23.86	17.26	17.09	17.25	19.04	12.95	15.91	26.91	20.31	19.29	29.36	38.92	19.63	19.88
An	34.41	32.45	30.25	21.05	36.05	34.75	24.81	25.49	27.59	32.32	28.22	28.10	23.30	20.02	18.70	26.51	23.86	34.82	31.53	23.73	23.38	29.63	14.34	17.22	17.83	21.95
Ne																				21.24	18.62	17.41	11.53	8.03		
Di	14.67	18.24	10.06	13.12	11.33	17.86	20.30	24.22	18.08	15.55	19.86	19.61	1.40	6.20	6.52	22.45	12.97	13.56	25.62	9.47	14.31	18.87	15.19	6.79	19.75	16.93
Hy	21.39	12.47	7.42	10.68	19.97	15.63	14.41	13.81	15.27	16.47	12.50	14.91	11.56	17.86	17.84	19.24	21.12	20.23	9.44	4.14		2.81				
Ol		6.00	15.58	3.60	9.70	9.10		0.33		8.32	8.24	6.86						7.42	8.99	5.10	6.05	3.44	6.54	7.45	5.71	5.83
Mt	3.35	2.65	2.45	4.30	2.67	3.52	5.63	7.50	6.94	2.41	2.87	2.48	3.18	1.61	1.75	4.15	2.15	3.49	2.74	2.45	6.25	2.45	4.37	3.19	4.25	4.58
Il	2.30	1.63	1.79	4.86	1.67	1.75	3.10	3.21	3.00	2.30	3.53	3.48	3.08	1.82	1.61	3.06	3.76	1.86	1.79	0.28	0.87	0.31	0.97	0.94	0.64	0.73
Ap	0.31	0.21	0.24	1.44	0.21	0.19	0.40	0.57	0.47	0.26	0.75	0.75	0.75	0.42	0.31	0.61	1.53	0.24	0.17							
Ratios																										
D.I.	23.5	26.3	32.2	41.0	18.4	17.21	31.36	24.9	28.7	22.4	24.0	23.8	56.7	52.08	53.3	24.0	34.6	18.0	19.7	33.6	30.6	25.1	47.10	56.4	37.4	35.2
A	14.3	16.7	19.7	23.5	10.0	10.1	17.5	13.1	13.3	22.4	24.0	23.8	56.7	52.08	53.3	24.0	19.7	9.97	11.6	20.1	16.0	14.7	22.7	32.3	19.8	15.6
F	55.3	50.6	41.6	60.5	52.5	49.2	57.4	61.6	60.6	53.0	53.5	53.0	50.2	40.4	40.2	53.5	54.6	55.34	51.2	45.2	66.4	54.6	62.2	57.2	60.1	66.4
M	30.4	32.7	38.7	16.0	37.5	40.6	25.2	25.3	26.1	34.2	33.3	33.6	18.2	33.4	34.5	33.3	25.7	34.68	37.2	34.7	17.6	30.7	15.1	10.5	20.1	18.0
Rb/Sr	.173	.167	.447	.057	.136	.179	.218	.060	.217	.159	.059	.083	.383	.597	.554	.117	.157	.142	.139	.120	.441	.258	.529	.439	.279	.363
Na_2O/K_2O	2.76	2.58	0.96	2.87	2.87	1.24	1.31	4.55	2.59	2.34	3.81	3.11	1.51	.95	1.00	2.64	1.19	1.78	2.89	2.81	1.73	2.32	1.83	2.46	0.87	1.91
K/Rb	202	239	188	753	211	256	351	423	187	249	290	256	164	182	191	207	270	285	207	323	180	203	246	196	288	179

Table 3. Chemical analyses of basement dolerite dykes.

Sample No.	1 73205374	2 73205376	3 74205555	4 74205557	5 74205590	6 74205598	7 74205599	8 74205600	9 74205601	10 74205603	11 74205606	12 74205608	13 74205614	14 74205645	15 74205646	16 71201414	17 71201416	18 73205372	19 73205373
Type	B1	B1	B1	B1	B1	B1	B1	B1	B1	B1	B1	B1	B1	B1	B1	B2	B2	B2	B2
Major elements																			
SiO_2	52.87	50.23	50.80	51.11	53.12	52.13	50.33	48.59	51.50	50.05	48.23	50.13	51.59	54.55	50.41	51.02	50.53	51.24	51.16
TiO_2	2.51	1.08	1.26	1.25	1.77	1.22	0.61	0.81	1.25	1.01	0.62	1.18	1.38	2.32	0.77	1.76	1.57	1.57	1.47
Al_2O_3	13.54	15.39	13.93	13.76	14.15	14.75	17.10	15.13	14.41	16.22	17.38	15.58	14.85	16.31	15.72	13.53	13.92	13.76	13.79
Fe_2O_3	3.12	0.82	3.53	2.96	3.92	3.33	1.56	1.96	2.67	1.62	1.22	1.71	2.61	2.861	1.44	2.42	2.17	2.76	2.40
FeO	10.25	10.10	9.20	9.15	10.57	8.81	7.08	8.32	9.621	9.67	9.24	9.95	9.59	9.36	8.89	11.79	11.37	10.33	10.68
MnO	0.10	0.18	0.19	0.13	0.26	0.26	0.39	0.26	0.37	0.27	0.25	0.19	0.30	0.16	0.17	0.23	0.22	0.20	0.22
MgO	5.71	8.25	7.08	6.99	4.76	6.26	8.74	10.71	6.59	6.89	9.26	7.59	6.64	2.31	8.35	6.00	6.47	6.85	6.70
CaO	8.50	11.48	10.17	9.79	7.67	9.61	10.58	11.65	9.81	10.26	11.12	10.48	9.42	7.51	12.01	9.85	9.99	10.12	10.31
Na_2O	2.28	2.15	2.69	3.85	2.73	2.79	2.14	1.20	3.03	2.24	1.52	2.08	2.81	3.52	1.88	2.34	3.20	2.12	2.28
K_2O	0.86	0.21	1.02	0.88	0.81	0.72	1.39	1.30	0.64	1.63	1.06	0.98	0.68	0.64	0.31	0.92	0.41	0.89	0.87
P_2O_5	0.26	0.10	0.14	0.13	0.24	0.12	0.08	0.07	0.11	0.14	0.11	0.13	0.13	0.56	0.05	0.15	0.15	0.15	0.13
Trace elements ppm																			
Ba	210	78	129	206	64	956	198	506	72	374	136	309	258	1224	70	138	126	177	121
Rb	45	6	44	38	52	43	85	89	30	120	68	44	29	23	11	56	15	47	59
Sr	116	127	129	139	87	215	175	183	162	209	175	182	146	211	214	177	212	173	156
Y	51	23	22	25	42	23	18	18	23	20	16	18	27	62	10	27	25	25	23
Pb	3	3	2	4	8	11	8	42	12	12	14	6	7	12	5	6	5	2	4
Zr	160	68	60	65	174	75	70	40	73	81	36	79	95	296	28	101	89	91	85
Zn	64	66	88	55	49	395	148	240	290	133	165	135	184	116	90	130	125	118	118
Cu	38	142	200	150	180	170	78	300	70	100	80	162	110	92	132	224	194	210	248
Ni	18	188	90	100	53	63	293	345	68	155	200	235	125	30	130	84	96	80	73
Cr	60	205	200	150	110	130	880	970	125	125	210	125	180	5	225	95	130	130	100
V	480	290	355	380	330	350	140	240	275	275	160	275	340	100	260	390	420	375	340
Sc	25	15	15	20	15	20	15	15	30	20	15	15	20	20	25	20	10	20	25
CIPW norm																			
Q	8.25				7.73	2.74							0.99	9.88		1.66		2.58	1.25
Or	5.08	1.24	6.03	5.20	4.79	4.26	8.22	7.86	3.78	9.63	6.27	5.79	4.02	3.78	1.83	5.44	2.42	5.26	5.14
Ab	19.29	18.19	22.76	32.4	23.10	23.61	18.11	10.15	25.64	18.95	12.86	17.60	23.78	29.78	15.91	19.80	27.07	17.94	19.29
An	24.18	31.73	22.93	17.7	23.97	25.60	32.95	32.06	23.83	29.39	37.47	30.29	25.90	26.82	33.54	23.70	22.41	25.40	24.83
Ne				0.10															
Di	13.42	20.18	21.76	24.60	10.41	17.46	15.42	20.45	19.85	16.97	13.86	17.14	16.43	5.74	21.01	20.11	21.69	19.60	21.03
Hy	19.89	20.06	17.25		20.40	18.91	11.11	13.39	19.53	10.56	11.95	19.86	22.18	14.14	22.26	22.11	13.39	21.87	21.90
Ol		5.11	1.45	13.07			10.60	11.73	0.87	9.90	14.39	4.31			1.78		6.54		
Mt	4.52	1.19	5.12	4.29	5.68	4.83	2.26	2.84	3.87	2.35	1.77	2.48	3.78	4.15	2.09	3.51	3.15	4.00	3.48
Il	4.77	2.05	2.39	2.37	3.36	2.32	1.16	1.54	2.37	1.92	1.18	2.24	2.62	4.41	1.46	3.34	2.98	2.98	2.79
Ap	0.61	0.24	0.33	0.31	0.57	0.28	0.19	0.17	0.26	0.33	0.26	0.31	0.31	1.32	0.12	0.35	0.35	0.35	0.31
Ratios																			
D.I.	32.6	19.4	28.8	37.7	35.6	30.6	26.3	17.8	29.4	28.6	19.1	23.4	28.8	43.45	17.74	26.9	29.5	25.8	25.7
A	14.3	10.9	15.9	20.0	15.6	16.0	16.7	10.6	16.2	17.5	11.5	13.7	15.6	22.4	10.5	13.9	15.3	13.2	13.7
F	59.8	50.9	53.8	50.5	63.4	55.3	42.0	43.9	54.7	51.4	47.2	52.3	54.7	65.2	49.6	60.5	57.3	56.9	57.0
M	25.9	38.2	30.3	29.5	21.0	28.7	41.3	45.5	29.1	31.1	41.3	34.0	29.7	12.4	39.9	25.6	27.4	29.9	29.3
Rb/Sr	.388	.047	.341	.273	.598	.200	.486	.486	.185	.574	.388	.241	.199	.109	.051	.316	.071	.271	.378
Na_2O K_2O	2.65	10.23	2.64	4.37	3.37	3.87	1.54	0.92	4.73	1.37	1.44	2.12	4.13	5.50	6.06	2.54	7.80	2.38	2.62
K/Rb	158	290	192	192	129	139	136	121	177	113	129	185	195	231	234	136	227	157	122

Table 4. Chemical analyses of eastern succession dolerite dykes.

Sample No.	1 74205475	2 74205476	3 74205514	4 74205520	5 74205531	6 74205532	7 74205536	8 74205522	9 74205523	10 74205524	11 74205527	12 74205567	13 74205658	14 74205666	15 74205666	16 74205670	17 74205671	18 74205672	19 74205675	20 74205683	21 74205657	22 74205684	23 74205652	24 74205650
Type	E2	E2	E2	E2	E2	E2	E2	E2	E2	E2	E2	E2	E2	E2	E2	E2	E2	E2	E2	E2	E2	E1	E3	E3
Major elements																								
SiO_2	51.15	50.25	51.21	51.32	49.56	50.41	50.18	52.80	50.90	51.09	53.96	50.25	49.20	49.33	49.06	49.88	50.08	49.59	50.43	54.25	50.39	49.49	46.43	50.71
TiO_2	1.32	1.35	1.10	1.49	2.70	2.42	1.36	2.05	1.75	1.55	0.83	2.79	1.04	1.43	0.87	0.90	0.91	1.27	1.77	1.89	1.66	1.65	2.09	1.33
Al_2O_3	14.85	14.83	14.24	13.71	12.89	13.33	16.23	13.61	13.37	13.98	14.43	13.76	15.05	15.89	15.43	14.72	16.23	14.31	14.42	11.58	13.27	13.88	12.33	14.70
Fe_2O_3	1.65	1.24	2.17	4.15	5.72	5.70	2.60	3.22	3.08	2.33	1.67	2.73	1.46	3.97	1.92	1.48	1.21	1.53	3.26	3.52	3.46	1.42	9.08	3.39
FeO	10.35	11.31	10.18	9.62	10.89	8.30	8.44	8.49	12.17	8.64	8.03	10.12	11.31	9.06	9.17	10.34	9.79	11.58	11.49	11.62	12.03	12.65	10.03	9.83
MnO	0.23	0.25	0.22	0.19	0.15	0.10	0.14	0.14	0.22	0.19	0.15	0.14	0.20	0.18	0.19	0.20	0.19	0.23	0.19	0.28	0.20	0.21	0.17	0.12
MgO	6.32	7.09	6.75	5.97	4.79	5.46	6.14	6.14	5.68	6.27	6.65	5.15	9.42	6.35	8.13	7.64	6.83	7.44	4.76	3.31	5.80	6.42	6.24	6.14
CaO	11.22	10.47	10.85	9.04	8.69	8.68	10.99	8.26	9.44	11.53	9.42	10.81	9.81	10.51	13.33	12.34	10.98	10.85	9.76	8.67	9.83	10.47	9.77	10.00
Na_2O	2.62	2.40	2.51	3.07	3.24	4.49	2.99	4.11	2.39	3.43	2.37	3.16	2.13	2.85	1.63	1.61	2.78	2.61	3.06	4.08	2.87	3.54	2.18	2.85
K_2O	0.94	0.66	0.66	1.29	1.06	0.79	0.80	0.98	0.81	0.85	2.14	0.75	0.50	0.33	0.22	0.81	0.95	0.48	0.68	0.39	0.36	0.44	1.57	0.79
P_2O_5	0.13	0.13	0.11	0.16	0.31	0.30	0.13	0.20	0.19	0.14	0.14	0.34	0.08	0.11	0.06	0.08	0.07	0.01	0.17	0.49	0.14	0.15	0.09	0.12
Trace elements ppm																								
Ba	190	129	462	325	170	72	97	90	272	288	333	109	139	211	49	96	130	79	158	82	237	82	116	198
Rb	50	42	49	85	39	36	24	47	47	17	139	17	19	8	10	47	74	31	21	6	9	6	74	34
Sr	205	292	166	139	167	137	181	125	144	177	91	175	132	219	139	115	219	176	152	76	123	76	169	170
Y	26	25	21	27	38	38	23	33	32	37	28	81	19	31	16	16	15	19	32	25	30	25	19	26
Pb	7	3	3	18	4	2	2	6	8	7	9	7	8	2	2	4	3	2	5	2	2	2	5	2
Zr	96	68	60	87	141	126	96	116	100	88	99	152	54	86	38	39	34	53	88	90	83	90	58	78
Zn	126	190	112	100	64	46	40	44	118	82	94	59	110	60	96	135	112	124	78	96	90	96	38	48
Cu	160	145	138	145	105	22	118	32	128	40	80	20	65	22	135	220	112	162	35	140	220	140	445	172
Ni	75	120	53	58	45	48	100	53	70	65	115	70	170	68	133	93	98	100	40	65	103	65	105	110
Cr	185	110	105	125	75	110	230	90	90	110	300	60	105	250	220	200	120	225	70	125	85	125	5	175
V	340	330	320	405	505	505	265	475	370	360	255	550	270	380	315	305	225	340	470	350	390	350	770	355
Sc	15	15	35	25	10	20	20	20	15	25	25	20	10	30	15	15	20	20	20	20	20	20	20	15
CIPW norm																								
Q	2.08			0.36	1.81				2.65		1.82	0.19							0.40	5.58	0.85		0.40	
Or	5.56	4.02	3.90	7.62	6.27	4.67	4.73	5.79	4.79	5.02	12.65	4.43	2.96	1.95	1.30	4.79	5.61	2.84	4.02	2.31	2.13	2.60	9.28	4.67
Ab	15.40	20.31	21.24	25.97	27.41	37.99	25.30	34.77	20.22	29.02	20.05	26.74	18.02	24.11	13.79	13.62	23.52	22.08	25.89	34.52	24.28	28.68	18.44	24.11
An	29.58	27.69	25.64	19.82	17.50	13.89	28.51	15.80	23.37	20.24	22.42	21.15	30.03	29.60	34.14	30.55	29.01	25.92	23.61	12.14	22.27	20.69	19.22	24.99
Ne																						0.69		
Di	20.89	19.38	22.66	19.71	19.47	22.03	20.62	19.47	18.52	29.54	19.16	24.98	14.85	17.87	25.84	24.84	20.65	22.55	19.81	23.74	21.28	25.27	23.21	19.63
Hy	21.28	18.11	20.94	17.30	13.40	3.05	7.79	13.92	22.23	0.44	19.28	12.46	18.52	16.04	16.55	18.67	3.57	10.72	17.78	12.05	20.71		12.08	18.76
Ol		5.84	0.12			4.82	6.40	1.22		9.08			11.34	1.72	3.81	3.49	14.01	11.03				16.55		0.09
Mt	2.39	1.80	3.15	6.02	8.29	8.26	3.77	4.67	4.47	3.38	2.71	3.96	2.12	5.76	2.78	2.35	1.75	2.22	4.73	5.10	5.02	2.06	13.16	4.91
Il	2.51	2.56	2.09	2.83	5.13	4.60	2.58	3.89	3.32	2.94	1.58	5.30	1.98	2.72	1.65	1.71	1.73	2.41	3.36	3.59	3.15	3.13	3.97	2.53
Ap	0.31	0.31	0.26	0.38	0.73	0.71	0.31	0.47	0.45	0.33	0.33	0.80	0.19	0.26	0.14	0.19	0.17	0.24	0.40	1.01	0.33	0.35	0.21	0.28
Ratios																								
D.I.	23.0	24.3	25.1	33.9	35.5	42.7	30.0	40.6	27.7	34.0	34.5	31.4	30.0	26.1	15.1	18.4	29.1	24.9	30.31	42.4	27.3	32.0	28.2	28.78
A	13.0	7.7	14.2	18.3	17.0	21.7	18.2	22.4	13.3	19.9	21.5	18.0	10.6	14.2	8.8	11.0	17.3	13.0	16.2	19.6	13.2	16.4	13.2	16.0
F	57.3	39.0	55.5	56.7	64.0	55.8	52.4	50.6	63.1	50.9	46.9	58.4	51.2	57.4	52.6	54.2	51.2	55.6	63.2	66.0	63.0	58.3	64.8	57.1
M	29.9	53.3	30.3	25.0	19.0	22.5	29.4	27.0	23.6	29.2	31.6	23.6	38.2	28.4	38.6	34.8	31.5	31.4	20.6	14.4	23.8	25.3	22.0	25.9
Rb Sr	.224	.144	.295	.611	.233	.263	.132	.376	.326	.096	1.52	.097	.144	.036	.072	.408	.338	.176	.138	.079	.073	.079	.437	.200
Na_2O K_2O	1.94	3.53	3.80	2.38	3.06	5.68	3.74	4.19	2.95	4.03	1.11	4.21	4.26	8.64	7.41	2.00	2.92	5.44	4.50	10.46	7.97	8.04	1.39	3.61
K Rb	156	134	112	126	103	182	277	173	143	415	128	366	218	342	183	143	106	128	269	539	233	609	176	193

Table 4 (cont'd)

Sample No.	25 74205615	26 74200097	27 74205525	28 73205369	29 74205622	30 74205673	31 74205674	32 74205676	33 74205678	34 74205693	35 74205699	36 74205701
Type	E3	E4	E4	E4	E4	E4	E4	E4	E4	E4	E4	E4
Major elements												
SiO_2	53.67	49.30	51.23	48.80	48.92	50.67	51.05	51.05	50.88	51.78	51.27	51.34
TiO_2	1.09	2.66	0.48	2.69	2.60	1.24	1.19	1.26	1.21	1.82	1.80	3.50
Al_2O_3	16.05	14.20	15.20	12.84	13.33	14.36	14.21	14.51	14.37	13.87	13.74	13.60
Fe_2O_3	2.65	4.16	0.49	4.41	3.61	2.27	2.48	3.14	2.80	3.64	3.26	5.27
FeO	7.29	11.26	8.75	11.93	11.97	8.82	8.75	8.53	8.79	8.21	8.59	9.90
MnO	1.14	0.24	0.16	0.25	0.24	0.18	0.18	0.19	0.19	0.20	0.19	0.20
MgO	5.31	4.74	11.74	5.99	5.83	7.34	7.84	7.18	7.42	6.89	7.20	4.39
CaO	8.60	10.02	9.60	10.01	9.99	10.70	11.29	10.53	10.43	9.11	10.24	6.74
Na_2O	2.70	2.15	1.19	2.00	2.37	2.20	1.98	2.00	1.82	2.34	2.10	2.76
K_2O	2.31	0.86	1.08	0.72	0.75	1.61	0.93	1.50	1.98	1.99	1.45	1.95
P_2O_5	0.15	0.40	0.06	0.36	0.39	0.10	0.10	0.11	0.11	0.17	0.16	0.35
Trace elements ppm												
Ba	481	265	173	228	189	111	188	156	427	497	215	387
Rb	130	46	87	41	38	75	31	65	108	109	74	68
Sr	202	141	101	133	133	216	157	180	190	225	254	207
Y	26	50	12	47	48	21	22	21	23	26	24	44
Pb	8	2	3	4	7	4	5	8	4	7	2	22
Zr	165	194	39	158	157	69	66	70	68	116	111	240
Zn	90	160	94	165	165	105	105	112	118	98	124	250
Cu	110	70	128	90	80	177	180	175	190	177	197	360
Ni	108	50	293	73	68	103	100	88	95	110	133	70
Cr	120	70	1100	160	135	260	335	245	235	175	265	65
V	300	450	200	420	420	325	350	295	320	360	375	395
Sc	15	5	15	20	15	30	15	15	20	15		
CIPW norm												
Q	2.23	4.48		3.59	1.44		0.83	1.02		1.83	2.12	6.62
Or	13.65	5.08	6.03	4.26	4.43	9.52	5.50	8.87	11.70	11.76	8.57	11.53
Ab	23.18	18.19	22.76	16.92	20.05	18.61	16.75	16.92	15.40	19.80	17.77	23.35
An	24.68	26.55	22.93	23.94	23.52	24.56	27.14	26.19	25.20	21.47	23.79	18.96
Ne												
Di	13.93	5.08	21.76	19.31	19.47	22.76	23.01	20.66	21.09	18.36	21.12	10.00
Hy	16.05	16.60	17.25	19.65	20.01	14.13	20.69	19.14	19.04	17.67	18.11	14.44
Ol			1.45			3.81	0.96					
Mt	3.84	6.06	5.12	6.39	5.23	4.02	3.60	4.55	4.06	5.28	4.73	7.64
Il	2.07	5.05	2.39	5.11	4.94	2.35	2.26	2.39	2.30	3.46	3.42	6.65
Ap	0.35	0.94	0.33	0.85	0.92	0.24	0.24	0.26	0.26	0.40	0.38	0.83
Ratios												
D.I.	39.1	27.8	28.8	24.8	25.9	28.1	23.1	26.8	27.1	33.4	28.5	41.5
A	25.0	13.1	15.9	10.9	12.8	16.8	13.3	15.7	16.7	18.9	15.8	19.7
F	48.7	66.3	53.8	65.0	63.3	50.8	50.9	52.0	50.6	51.0	52.1	62.0
M	26.3	20.6	30.3	24.1	23.9	32.4	35.8	32.3	32.7	30.1	32.1	18.3
Rb Sr	.643	.326	.861	.308	.286	.347	.197	.36	.568	.484	.291	.328
Na_2O K_2O	1.17	2.50	1.10	2.78	3.16	1.36	2.13	1.33	0.92	1.17	1.45	1.41
K Rb	147	155	103	146	164	178	249	192	152	152	163	238

Table 5. Representative analyses of mafic igneous rocks from various geological settings.

	1	2	3	4	5	6	7
Major elements							
SiO_2	49.9	49.3	53.8	50.0	51.98	51.9	51.5
TiO_2	1.51	1.6	2.0	3.2	1.21	1.1	1.2
Al_2O_3	17.2	15.6	13.9	13.5	14.48	15.5	16.3
Fe_2O_3	2.0	3.5	2.6	1.9	1.37	1.0	2.8
FeO	6.9	7.8	9.3	12.5	8.92	9.7	7.9
MnO	0.17	0.2	0.2	0.25	0.16	0.3	0.17
MgO	7.2	6.5	4.1	4.4	7.59	8.2	5.9
CaO	11.8	10.3	7.9	8.3	10.33	9.7	9.8
Na_2O	2.7	2.7	3.0	2.9	2.04	1.8	2.5
K_2O	0.16	0.5	1.5	1.4	0.84	0.7	0.86
P_2O_5	0.3	0.4	0.7	0.14	0.1	0.21	
Trace elements ppm							
Ba	14				195		
Rb	10						
Sr	130				175		
Y	43						
Pb					11		
Zr	95				20		
Zn							
Cu	77						
Ni	97				95		
Cr	297				315		
V	292				235		
Sc	61						
Ratios							
K Rb	133						
Na_2O K_2O	17	5.4	2.0	2.07	2.4	2.6	2.9

1. Oceanic tholeiite (av. of 10 analyses) (Engel & others, 1965, Table 2).

2. Average Picture Gorge Basalt, Columbia Plateau (Waters, 1961, p. 592).

3. Average Yakima Basalt, Columbia Plateau (Waters, 1961, p. 592).

4. Average Late Yakima Ellensburg Basalt, Columbia Plateau (Waters, 1961, p. 594).

5. Chilled Diabase, Palisades Sill (Walker, 1969, Table 8).

6. Average Karoo Chilled Basalt (Walker & Poldervaart, 1949, Table 17, water-free basis).

7. Average Continental Tholeiite (Manson, 1967).

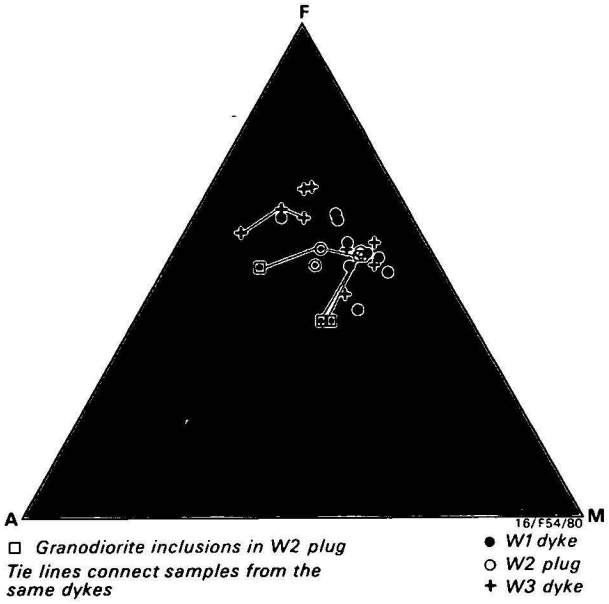

Figure 5. FMA plot for western succession dolerites.

W1 dolerites from west of the Mount Isa Fault have been regionally metamorphosed to amphibolite facies (Wilson, 1972), and commonly contain hornblende (green-yellow to green-brown pleochroism). Recrystallisation has destroyed igneous textures and produced medium-grained equigranular rocks with typical granoblastic textures.

Chemical analyses of ten samples of W1 dolerite dykes are shown in Table 2, Nos. 1–10. They are mostly olivine tholeiites and quartz tholeiites with SiO_2 ranging from 48.05 to 51.34 per cent. They show a trend of iron enrichment when plotted on the FMA diagram (Fig. 5). There is a slight increase in SiO_2 (48–51%) with differentiation, which is accompanied by an increase in Na_2O, K_2O, TiO_2, Ba, Sr, and Zr, and a decrease in CaO, MgO, Cr, and Ni (Fig. 6). Such features are consistent with crystal fractionation involving removal of Mg-silicates (olivine, pyroxene) and plagioclase from a common parental magma, and indicate, with the possible exception of sample 73205326, which has probably been altered, that these rocks may be considered as representing variants of a single magmatic group (Fig. 6). Sample 73205349 could be considered close to the parental magma composition.

The *W2 dolerites* occur as numerous plugs intruding the Sybella Granite west of Mount Isa. They crop out as low hills on alluvial plains, e.g. Kitty Plain east of May Downs Homestead. Net-vein complexes are commonly found at the edges of these plugs, (Joplin, 1955; Blake, 1981) and it is highly probable that these dolerites and granites were emplaced at the same time (Walker & Skelhorn, 1966). A U-Pb zircon date of 1671±8 Ma has been obtained by Page (*in* Blake & others, 1984) on the Sybella Granite.

The dolerite in these plugs is medium to coarse-grained, and has ophitic to subophitic textures. Plagioclase (An_{54}–An_{14}), orthopyroxene, clinopyroxene, biotite, and minor actinolite, magnetite, pyrite, ilmenite, and chalcopyrite constitute a typical assemblage. The biotite and amphibole are both of magmatic origin, with the biotite often forming rims around the opaque oxides. The amphibole rims pyroxenes, and in places the biotite, and in some cases it is interstitial to all these minerals. Quartz, when present, is restricted to the groundmass. Accessory apatite is also found.

Contacts between granitic veins and the enclosing dolerite mass are transitional in texture and composition; there is usually a gradation from biotite and amphibole-poor dolerite, through biotite-rich and amphibole-rich zones, to granodiorite and then granite. The granodiorites consist of coarse-grained (up to 1 cm) laths of plagioclase feldspar (labradorite with rims of albite), biotite, amphibole, and in some cases orthoclase, together with interstitial quartz and alkali feldspar. The amphibole is yellow-green hornblende. Accessory zircon, magnetite, ilmenite, pyrite, and chalcopyrite are also present.

Analyses of the dolerites from these plugs are shown in Table 2, Nos. 11–17. Samples 74205634, 74205635A, 74205637, and 74205641 (Table 2, Nos. 11, 12, 16, & 17) are either olivine or quartz tholeiites and of similar composition, with the exception of 74205641, which is slightly more differentiated. Sample 74205636B (Table 2, No. 13) extends the trend defined by the dolerites and was probably formed by differentiation. It has modal magnetite, and is depleted in MgO and Cr; these differences can be explained by removal of pyroxene from the host dolerite. In contrast, samples 74205635C and 74205636C (Table 2, Nos. 14 & 15) do not lie on this differentiation trend and are distinct in compositions. They are enriched in SiO_2, K_2O, Rb, and Zr, depleted in TiO_2, total iron, MgO, CaO, Sr, Zn, Cu, and V, and have high K/Na compared to the adjacent dolerite. They are probably samples of Sybella Granite contaminated by dolerite as a result of net-veining.

The *W3 dykes* are discordant to the regional structures and cut the earlier W1 dykes. They are 10–1000 m wide, and individual dykes are up to 50 km long, though discontinuous because of faulting. These dykes must be younger than 1480 Ma, the approximate age of the youngest metamorphic event in the region (Page, 1981). They have a massive bouldery outcrop and a coarse-grained ophitic texture with fresh clinopyroxene clearly visible in hand specimen. Other minerals present include plagioclase, minor orthopyroxene, and magnetite, with traces of biotite, hornblende, and interstitial quartz and albite.

Chemical analyses of these dykes are given in Table 2, Nos. 18–26. There is a wide systematic variation in the composition of individual dykes, which can be explained in terms of crystal differentiation from a common parent magma. The variations shown in Figure 6 are consistent with the removal of olivine, pyroxene, and calcic plagioclase from the basic members of this group to produce the more differentiated samples. Plots on the FMA diagram (Fig. 5) show a trend of iron enrichment: 73205361 is the most differentiated sample (Table 2, No. 24) and trends towards alkali enrichment and depletion in iron. Concomitant with the iron enrichment shown on this diagram, TiO_2, SiO_2, Na_2O, K_2O, P_2O_5, Ba, Rb, and Zr also increase, whereas CaO, Al_2O_3, MgO, Sr, and Ni decrease.

The least differentiated samples of the W3 dolerite dykes (73205350, 73205353, Table 2, Nos. 18 & 19) are very similar in composition to the W2 dolerite plugs, except for slight depletions in TiO_2, P_2O_5, and Sr. They are almost identical in composition to the least differentiated examples of the metamorphosed W1 dolerite dykes that they intrude (73205347, 73205349; Table 2, Nos. 5 & 6).

Basement dolerites

The older basement sequence occurs in four major blocks: the Kalkadoon–Leichhardt, Blockade, Ewen, and Malbon blocks (Plumb & others, 1980), and they are intruded extensively by dolerite. Two distinct groups can be distinguished in the Kalkadoon–Leichhardt and Blockade blocks: older, metamorphosed (B1) dykes and younger, unmetamorphosed (B2) dykes.

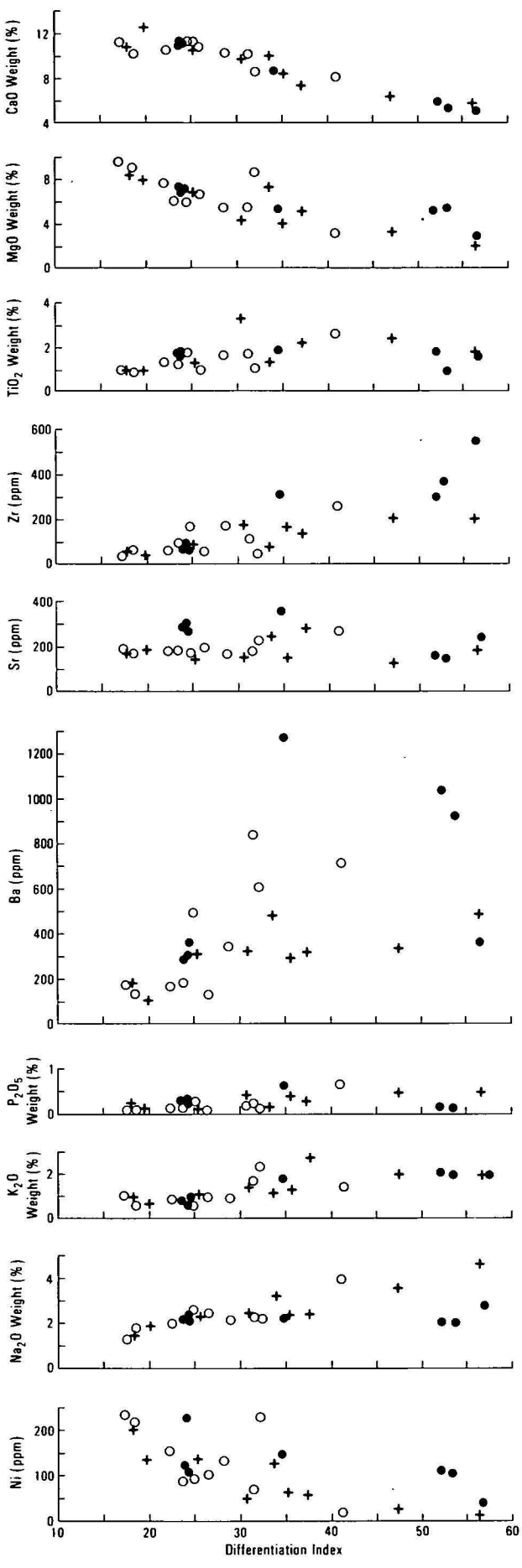

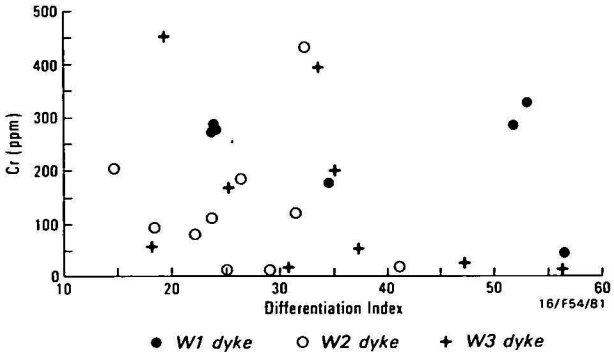

Figure 6. W1 and W2 dolerite compositions *vs* D.I.

The *B1 dykes* form a conjugate set oriented mainly north-northwest and north-northeast, and, in several areas, roughly east-trending dykes cut these. The rocks are only weakly magnetic, compared with most other mafic igneous rocks of the Mount Isa Inlier, which are strongly magnetic (Blake & others, in press).

The B1 dolerite dykes have been metamorphosed to amphibolite facies, with local retrogression along shear zones to biotite and chlorite schists. The amphibolite facies dolerites have either partly or wholly retained their igneous texture. Euhedral laths of calcic plagioclase are zoned from cores of An_{50} to rims of albite; they are very pale brown, owing to the presence of traces of iron, and are generally devoid of inclusions. In several specimens, the plagioclase has rims of albite, in part optically continuous with that of the quartz-albite micropegmatite of the groundmass, which is also of igneous origin. The hornblende varies from large ragged crystals to subidiomorphic prismatic blades, with blue-green-yellow pleochroism, and is usually optically homogeneous. Magnetite is commonly rimmed with sphene, and in some cases is entirely replaced by it. Garnet has only rarely been found in thin section (e.g. 74205591). Some metamorphic quartz is also present, especially in shear zones, where it occurs with albite and chlorite. Some B1 dykes are mineralised along the shear zones, and copper sulphide-quartz-calcite assemblages are common. Copper mines such as 'Referee', 'Queen Elizabeth', and 'Azurite' are located in sheared B1 dykes.

The fifteen analysed B1 dolerites (Table 3, Nos. 1-15) can be classified as subalkaline on the total alkalies silica diagram (Fig.3) with one exception (74205557, Table 3, No. 4), which contains 0.10 per cent normative Ne. All other samples are olivine tholeiites or quartz tholeiites, with 48.23 to 54.55 per cent SiO_2. The B1 dolerites, like the western succession dolerites, show a wide but systematic variation in composition. They display a marked trend of iron enrichment (Fig. 7) and Cr depletion, with the least differentiated sample, 74205600 (Table 3, No. 8), containing 970 ppm Cr, whereas the most differentiated sample, 74205645 (Table 3, No. 14), has only 5 ppm Cr. There is an increase in SiO_2, TiO_2, Na_2O, P_2O_5, and Zr and a decrease in MgO, CaO, Sr, Ni, and Cr with differentiation (Fig. 8), suggesting that B1 basement dykes represent a consanguineous group of rocks related to one another through low-pressure crystal fractionation.

Although the abovementioned elements show systematic variations in concentration with differentiation, K_2O, Ba, and Rb are irregular (Fig. 8), possibly indicating that several samples have been altered. It has already been shown that the development of biotite schist from the basic rocks involved an increase in K_2O, Rb, and Ba without significantly affecting the other elements present.

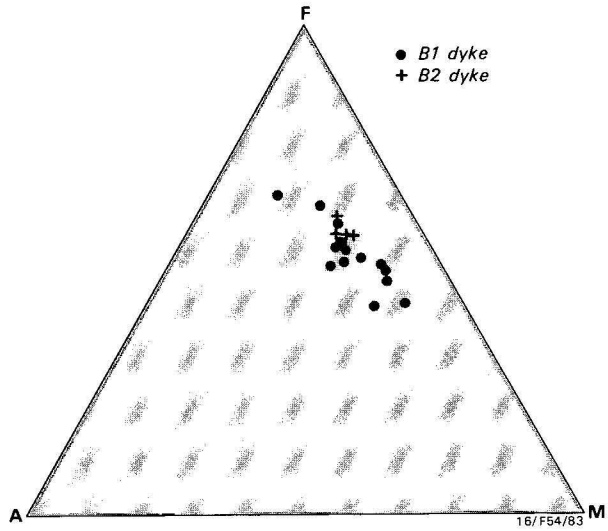

Figure 7. FMA plot of basement dolerites.

Field relations indicate that the metamorphosed east-trending B1 dykes were cut by north-trending B1 dykes. However, there is no obvious difference in composition between samples 74205606 and 74205608 (Table 3, Nos. 11 & 12) from an east-trending dyke and samples 74205600 and 74205601 (Table 3, Nos. 8 & 9) from a north-trending dyke.

The *B2 dykes* are fresh and unmetamorphosed and may be consanguineous with the E4 and W3 dykes from the eastern and western successions, respectively. B2 dykes consist of zoned plagioclase (An_{60}-An_{20}), clinopyroxene, minor orthopyroxene, magnetite, rare biotite, and brown-green hornblende, and some interstitial micrographic quartz and albite. Locally, plagioclase shows some alteration to sericite and the pyroxene to chlorite.

Only four B2 dolerite dykes have been analysed (Table 3, Nos. 16–19). Sample 71201414 is from a dyke that cuts that represented by sample 71201416. Samples 73205372 and 73205373 are from one dyke that cuts across the basement/eastern succession contact northwest of Mary Kathleen. The dyke rocks are olivine tholeiite or quartz tholeiite, and show little variation in composition, with SiO_2 ranging from 50.02 to 51.24 per cent. They are very similar in both major and trace-element abundances to the B1 dolerite dyke samples of comparable differentiation index (Fig. 8).

Eastern succession dolerites

Four groups of dolerite intrusions have been recognised in the eastern succession; three older groups E1, E2, and E3, which predate the regional metamorphism of 1550±15 Ma (Page, 1983a), and a younger, post-metamorphic E4 group. The E2 group is the most widespread; E1, E3, and E4 groups are less abundant.

The earliest *E1 intrusions* occur as concordant, folded sills within the Soldiers Cap Group on CLONCURRY*. One example occurs between Weatherly Creek, near the top of the Llewellyn Creek Formation, and is conformable with the Snake Creek Crossfold (Glikson & Derrick, 1970). A second metadolerite sill, 250 m thick, intrudes schists of the Mount Norna Quartzite, southeast of Mount Avarice near Cloncurry. It has been strongly folded and dislocated by faulting.

* 1:100 000 Sheet areas are shown in capital letters.

E1 dolerites are metamorphosed to amphibolite grade and typically consist of hornblende, plagioclase, opaques, and quartz, with minor sphene, epidote, talc, sericite, biotite, and scapolite. The one chemical analysis of an E1 dolerite sill (Table 4, No. 22) has been affected by metasomatism.

The *E2 dolerite* dyke swarms on CLONCURRY cut the Snake Creek Crossfold and the E1 dolerite sills. The largest of these dykes is 12 km long and up to 15 m wide, and forms narrow elevated ridges where it transgresses pelitic and arenaceous sediments. On MARY KATHLEEN and MARRABA, the E2 dolerites occur as metamorphosed sills and dykes intruding all units older than the Deighton Quartzite (Fig. 2) and form discontinuous bodies within fault blocks.

The E2 dolerites are petrographically variable because of the spatial variations in metamorphic grade, and the possibility of there being more than one generation of intrusion within the E2 group cannot be dismissed. Amphibolite grade rocks are abundant in a north-south belt that runs through the Mary Kathleen area, and here the dolerites contain plagioclase, hornblende, clinopyroxene, sphene, quartz, biotite, epidote, and scapolite.

Less metamorphosed dolerites occur to the east, in the area between Mary Kathleen and Cloncurry. These show some relict ophitic textures, with zoned laths of plagioclase, ophitic hornblende, and interstitial quartz-albite micropegmatite. The feldspar is a pale brown colour, zoned from cores of An_{50} to rims of albite. The amphiboles commonly have distinct rims of hornblende surrounding cores of actinolite, and in some cases, include quartz in a poikiloblastic texture. The opaque oxides often display a regular change in form with prograde metamorphism. Where original titanomagnetite has exsolved ilmenite along rational (111) planes (or vice versa), then, at the lowest grades of metamorphism, the ilmenite is preferentially replaced by sphene. At higher grades, the sphene often disappears and is replaced by green or blue-green hornblende. The effect is the development of a reticulate network of aligned magnetite blades with interspersed amphibole.

Although the E2 dolerites all show trends towards iron enrichment on a FMA diagram (Fig. 9), in detail they have a wide range in composition, which can be explained in terms of low-pressure crystal fractionation from a range of parent magmas (Fig. 10). The distribution of the different chemical types of dykes is not random, as there is an easterly zonation in composition, and several groupings will be discussed.

Chemical analyses of the first group of E2 dolerites, which intrude the Argylla and Corella Formations, northwest of Mary Kathleen, are given in Table 4, Nos. 1–7. Except for sample 74205531 (Table 4, No. 5), the range of composition of these dykes can be explained by crystal fractionation from a common parent magma. With differentiation, MgO ranges from 7.09 to 4.79 per cent, and there is a systematic increase in TiO_2, Na_2O, total iron, and SiO_2, and a decrease in MgO, CaO, Ba, Sr, and Ni (Fig.10). Sample 74205531 appears to be unrelated to the other samples, and has higher TiO_2 and lower SiO_2.

Five samples of another group of E2 dolerites, which intrude the Wonga Granite were analysed (Table 4, Nos. 8–12). SiO_2 ranges from 50.25 to 53.96 per cent. Samples 74205522, 74205523, 74205524, and 74205567 (Table 4, Nos. 8, 9, 10, 12, respectively) have similar K_2O, Al_2O_3, MgO, Rb, Sr, and Cr. However, the variations in abundance of other elements cannot be explained adequately in terms of crystal fractionation from a common parental magma (Fig. 10), and their original compositions have probably been altered, e.g. sample

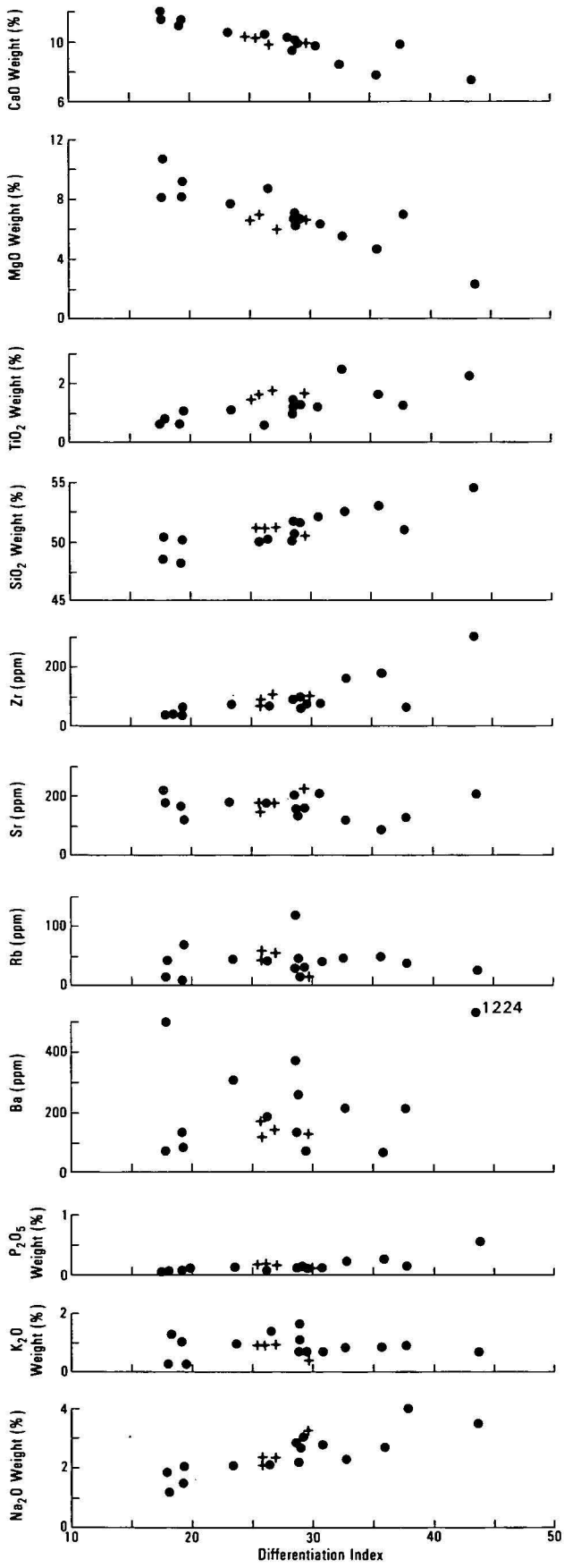

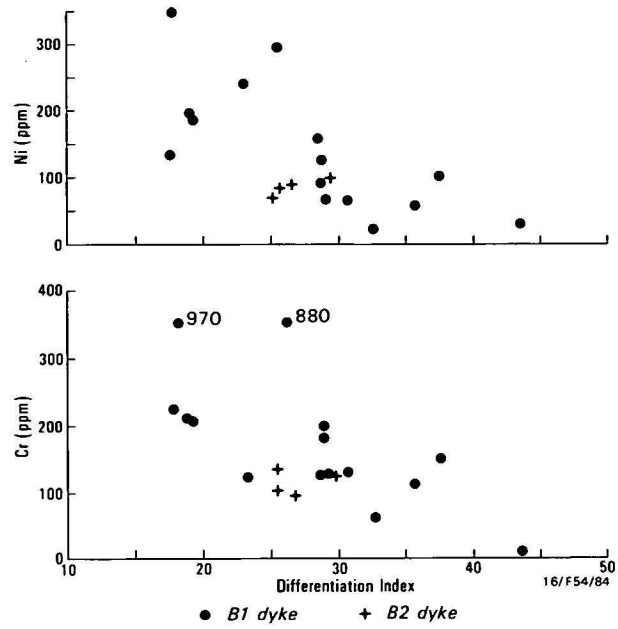

Figure 8. B1 & B2 dolerite compositions *vs* D.I.

74205527 (Table 4, No. 11) contains 2.14 per cent K_2O, and is also richer in SiO_2, MgO, Rb, and Cr, and poorer in TiO_2.

Most of the E2 dolerites intruding the Marraba Volcanics have been metasomatised and contain scapolite and biotite. Two chemical analyses of the least altered dykes are presented in Table 4 (Nos. 13 & 14): they are olivine tholeiites, characterised by low K_2O (0.50 and 0.33%), and differ in composition from the preceding E2 dykes in having Al_2O_3 and lower K_2O.

The group of E2 dolerites from near Kuridala crops out as metamorphosed, folded sills, cut by east-trending E4 dolerite dykes. The six analysed E2 dolerite samples (Table 4, Nos. 15–20), can be classified as olivine or quartz tholeiites, with 49.06 to 54.25 per cent SiO_2. Except for sample 74205671 (Table 4, No. 17) they appear to be a comagmatic group of sills with related chemical features. They show a linear trend of iron enrichment on the FMA diagram (Fig. 9) and there is an increase in SiO_2, TiO_2, total iron. Na_2O, and P_2O_5, and a decrease in Al_2O_3, MgO, CaO, Ni, and Cr with differentiation. Sample 74205671 does not fall along the trend defined by the other samples. It is richer in Al_2O_3, K_2O, Rb, and Sr, and apparently unrelated by low-pressure fractionation processes to the other rocks.

An E2 dolerite southeast of Cloncurry, 74205684, (Table 4, No. 21) is poor in Al_2O_3 and K_2O, has moderate to high K/Rb and high Na_2O/K_2O, and is similar to the E1 dolerite (Table 4, No. 21).

E3 dolerite intrusions are only slightly metamorphosed and occur as irregular dykes, sills, and plugs in the Corella Formation and Marimo Slate. The largest E3 intrusion is the Lunch Creek Gabbro (Derrick & others, 1978), a layered lopolithic or sill-like mass northeast of Mary Kathleen. The age of the Lunch Creek Gabbro was determined at 1738±4 Ma (Page, 1983a) and it is essentially coeval with the Burstall Granite. Possible E3 correlatives of the Lunch Creek Gabbro have been noted to the south on DUCHESS, where dykes containing hypersthene, olivine, and rare scapolite occur ('do_4' dolerites of Carter & others, 1961); examples are the Mount Earle and Myubee Igneous Complexes (Blake & others, 1981).

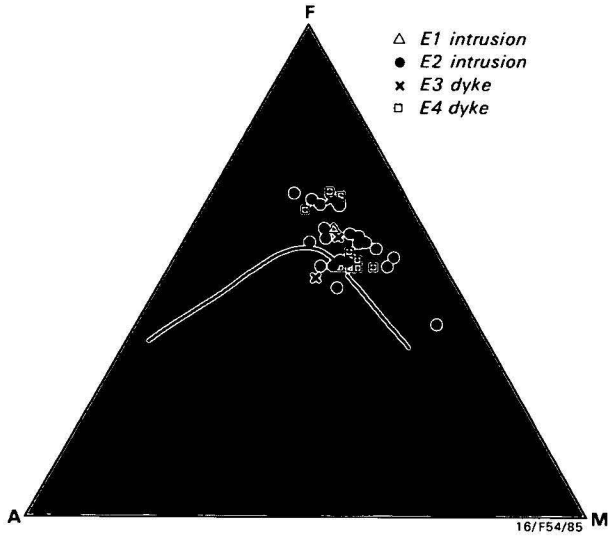

Figure 9. FMA plot for eastern succession dolerites.

Other E3 intrusions include dolerite plugs marked as 'do_4' on southwestern CLONCURRY (Glikson & Derrick, 1970), intruding the Corella Formation and Marimo Slate. These intrusions are generally circular and show sharp contacts with the country rock.

Petrographically, the E3 intrusions differ from the E2 intrusions in that they typically have relict igneous clinopyroxene and plagioclase. Although the E3 dolerites have only been weakly affected by the regional metamorphism, they may, in fact, be the same age as some E2 dolerites.

The Lunch Creek Gabbro consists of zoned phenocrysts of plagioclase, hypersthene, clinopyroxene, ilmenite, magnetite, biotite, actinolite-hornblende, and quartz. Opaque oxides are typically rimmed by biotite, which in turn is rimmed by amphibole, both of which are of igneous origin. Amphibole may form a thin sheaf around the pyroxenes and also occurs interstitially to these other minerals. Derrick (1980) recorded rare olivine.

The plugs on CLONCURRY are ophitic dolerites, consisting of zoned phenocrysts of plagioclase (An_{48} to An_{60}), relict clinopyroxene, quartz, opaque oxides, sphene, actinolite, cummingtonite, and hornblende. Plagioclase laths are up to 3 mm long, have a pale brown-pink colour, and are commonly clouded with sericite. Relict colourless augite is partly replaced by actinolite and commonly rimmed with blue-green hornblende. Quartz occurs both interstitially and as a graphic intergrowth with plagioclase. Opaque oxides are commonly rimmed with sphene.

Chemical analyses of the E3 dolerites are given in Table 4, Nos. 23–25. Sample 74205615 (Table 4 No. 25) of the Lunch Creek Gabbro is notably potassic, with Na_2O/K_2O = 1.17. Of the two samples of E3 dolerites near Cloncurry, sample 74205652 (No. 23) is very iron rich and plots in the alkaline field of the total alkalis-silica diagram of MacDonald & Katsura (1964). It is low in silica (46.43% SiO_2), quite potassic (Na_2O/K_2O = 1.39), and may be altered. Sample 74205650 (Table 4, No. 24), from another E3 dolerite, is an olivine tholeiite, and appears to be unrelated chemically to 74205652. It has a similar MgO content, but higher SiO_2 and lower K_2O and total iron. It is somewhat akin to a metamorphosed E2 dyke farther east (74205657; Table 4, No. 21).

The *E4 dolerites* cut all regional structures and rock types, and are up to 30 km long. They are not metamorphosed and are possibly lateral equivalents of the W3 and B2 dykes of the western succession and basement sequence. E4 dolerites from the Mary Kathleen, Kuridala, and McKinlay River areas have been sampled in this study, including the Lakeview Dolerite (Derrick & others, 1978), whose age has been determined by Rb-Sr at 1116±12 Ma (Page 1983a).

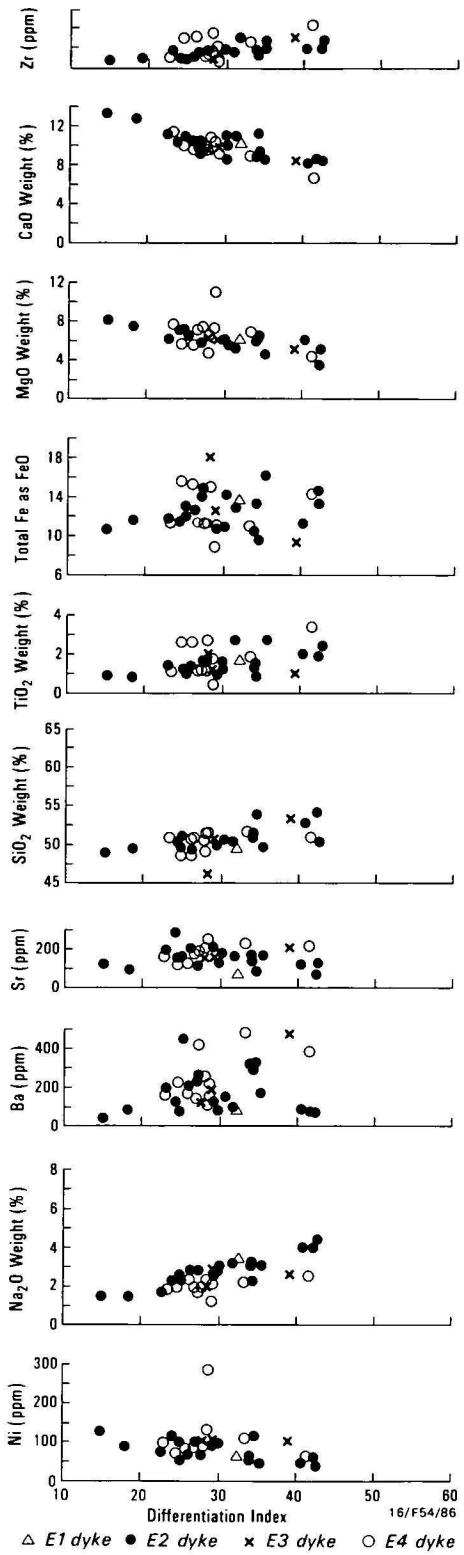

Figure 10. Eastern succession dolerite compositions vs D.I.

The Lakeview Dolerite, which cuts the Burstall Granite, the Corella Formation, and earlier E3 and E2 dykes, has a fine-grained, dense, chilled margin and a coarse-grained core. The chilled margin consists of sparse phenocrysts of euhedral plagioclase, clinopyroxene, and orthopyroxene in a very fine-

grained groundmass of plagioclase, pyroxene, and magnetite; possibly representing devitrified glass. Two generations of plagioclase phenocrysts are present (about 3 x 2 and 1 x 0.5 mm, respectively, in size). Twinned, euhedral to rounded augite phenocrysts (av. 1 mm) are more abundant than pale pink hypersthene phenocrysts of similar habit. The coarser-grained dolerite has a subophitic texture, with an average grain size of 1-2 mm. Zoned euhedral phenocrysts of plagioclase (An_{50} cores), clinopyroxene, orthopyroxene, and magnetite are the main minerals present. Interstitial green-brown hornblende, minor biotite, accessory pyrite, apatite, and secondary chlorite, serpentine, and sericite complete the assemblage. The hornblende and biotite are of igneous origin.

The east-trending E4 dolerites near Kuridala are up to 25 m wide and 16 km long, and cut the Williams Batholith, the Kuridala and Staveley Formations, and folded and metamorphosed E2 dolerites. They have a subophitic texture and consist of euhedral to subhedral phenocrysts of plagioclase (An_{60}-An_{45}), augite, hypersthene, anhedral magnetite, accessory pyrite, and rare chalcopyrite. Interstitial quartz, biotite, and green-brown hornblende may also be present. Patches of secondary chlorite and serpentine are often found, and the plagioclase is extensively sericitized. Carter & others (1961) reported rare pigeonite from these rocks.

To the southeast, east-west-trending E4 dolerite dykes near the McKinlay River cut the Williams Batholith, Soldiers Cap Group, and Doherty Formation. They have a subophitic texture and contain clinopyroxene, orthopyroxene, zoned calcic plagioclase, magnetite, minor interstitial brown-green hornblende, biotite, and quartz-albite micrographic intergrowths in the groundmass. With an increase in the amount of quartz present, there is a concomitant increase in biotite and hornblende. Where these dykes have intruded calc-silicate rocks of the Doherty Formation, marginal assimilation has resulted in assemblages containing diopside, wollastonite, siderite, hydrogarnet, and up to 80 percent plagioclase (An_{34}-An_{25}).

Rocks from three E4 dykes from the Mary Kathleen area were analysed (Table 4, Nos. 26-29). Samples from the Lakeview Dolerite, 73205369 and 74205622 (Table 5, Nos. 28 & 29), and another dyke north of Mary Kathleen (74200097; Table 3, No. 26) are quartz tholeiites with similar compositions. A sample from a third dyke (74205525; Table 4, No. 27) is an olivine tholeiite.

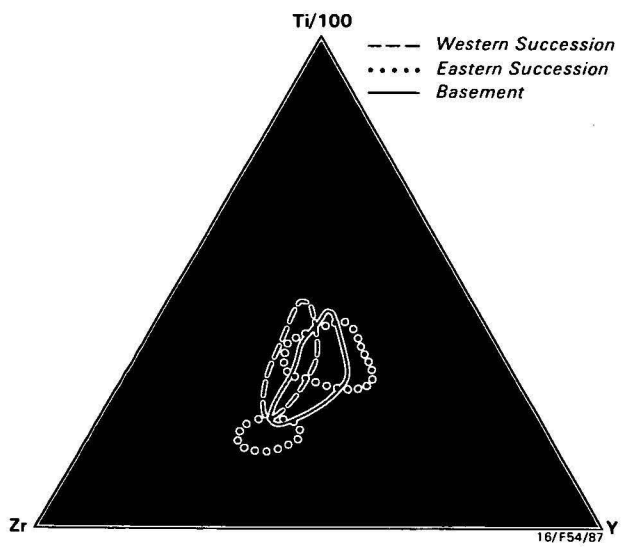

Figure 11. Ti-Zr-Y plots of the range in compositions of all mafic igneous rocks.

Chemical analyses of the E4 dolerite dykes from Kuridala (Table 4, Nos. 30-33) are either olivine-normative or quartz-normative and distinct from the E4 dykes of the Mary Kathleen area in their high K_2O and Sr. They can be termed 'potassic tholeiites', with Na_2O/K_2O as low as 0.92.

Chemical analyses of three E4 dykes from the KcKinlay River area are presented in Table 4 (Nos. 34, 35, 36). Two of the analysed dykes, 74205693 and 74205699 (Table 4, Nos. 34 & 35), are very similar in composition to the potassic tholeiites from Kuridala. However, the McKinlay samples are slightly richer in TiO_2. The other analysed dyke from this area, (sample 74205701; Table 4, No. 36), is slightly more differentiated, and can be related to the other dykes by low-pressure crystal fractionation, involving the removal of calcic plagioclase and pyroxene. It is richer in TiO_2, total iron, Na_2O, and P_2O_5, and poorer in MgO, CaO, Ni, and Cr than the other dykes in the McKinlay area.

Discussion

General chemical variations

The dolerites of the western succession and the basement sequence are fairly uniform in composition (Figs. 6, 8), whereas the dolerites of the eastern succession tend to be more heterogeneous and show some spatial and temporal variations in composition (Fig. 10). The variations in composition within any one group of dolerites can largely be explained in terms of crystal differentiation from a common parent. In contrast, variations in composition between the groups of dolerite must be explained by other processes, such as different conditions of melting within the likely source regions. There are some chemical differences between the dolerites from the three tectonic units, e.g. there is a consistent decrease in Y relative to Ti and Zr in an easterly direction (Fig. 11).

Relationships to mafic volcanic units

As the variation in composition between the various dolerite groups and the mafic volcanics is subtle, it is not possible, with the limited trace element data available, to chemically relate specific dolerite groups to any mafic volcanic unit. On field evidence alone, the W2, W3, B2, E3, and E4 groups post-date any volcanic formation. Compositionally, the W1 group could be feeders only to the Pickwick Metabasalt, and those W1 dolerites intruding the Myally Group obviously post-date these mafic volcanics. The B1 group dolerites have always been regarded as feeders to the Magna Lynn Metabasalt (Derrick & others, 1977a). However, these dolerite dykes are weakly magnetic compared to the Magna Lynn Metabasalt, which is strongly magnetic (Blake & others, in press), and the two units may in fact be of different ages. Some of the E2 group may be feeders to any of the numerous metabasalt units within the eastern succession.

Chemical variation in the dolerites, both between and within the three tectonic units, is not marked as the west-east variation in composition of metabasalts noted by Glikson & others (1976) and Glikson & Derrick (1978). These authors found that their samples of the Eastern Creek Volcanics from the western succession contained higher levels of incompatible elements, such as TiO_2, K_2O, P_2O_5, and Rb, and could be mainly classified as continental tholeiites, whereas the metabasalts from the eastern succession, such as the Soldiers Cap Group and the Marraba Volcanics, contained low levels of these elements and would be mainly classified as ocean-floor tholeiites. They further suggested this showed evidence of an eastwards transition into a continental margin environment. However, as pointed out by Bultitude & Wyborn (1982), the change in composition actually occurs within the Eastern

Creek Volcanics, with the lowermost Cromwell Metabasalt Member being more enriched in incompatible elements than the uppermost Pickwick Metabasalt Member, which in fact is not significantly different, compositionally, from metabasalt units within the basement sequence and the eastern succession.

It is relevant that few of the dolerite dykes are significantly enriched in incompatible elements. All the W1 or B1 dykes, which predate the metamorphism and some of which could be regarded as possible feeders to the Eastern Creek Volcanics, are compositionally similar to the Pickwick Metabasalt Member, and in turn, to most metabasalts of the Mount Isa Inlier. On the other hand, some dolerites in the eastern succession, notably in the E2 and E4 groups are enriched in incompatible elements. Therefore, there is no systematic spatial variation in composition of the mafic igneous rocks that could be attributed to crustal thickness, and it is more likely that factors such as source composition or degree of partial melting or both have controlled the degree of enrichment in incompatible elements.

Comparison with mafic igneous rocks from different tectonic environments

In the western succession, most W1 dykes have low TiO_2, somewhat similar to the average Karroo chilled basalt (Table 5, No. 6). Specimen 74205685 (Table 2, No. 10) is very similar in major-element composition to the chilled margin of the Palisades sill (Table 5, No. 5). The most differentiated dyke, 73205326 (Table 2, No. 4), has 2.56 per cent TiO_2 and is similar to basalts from other continental basaltic provinces.

The W3 dykes are similar in major and trace-element abundances and K/Rb to continental tholeiites, although they contain less Ba and Sr. The least differentiated rocks are very similar in major-element contents to the average Karroo chilled basalt (Table 5, No. 6); the more fractionated W3 dykes contain more TiO_2, Na_2O, and less MgO. Correlatives of these dykes are found in other continental flood basalts, especially examples of the Columbia River basalt (e.g. Table 5, Nos. 2-4).

In the basement sequence, the least differentiated examples of the B1 dykes, generally contain less K_2O, TiO_2, Ba, Rb, and Sr than most continental tholeiitic rocks (Table 5, No. 7), but not as little as most oceanic tholeiites (Table 5, No. 1). The dolerites are also similar in major-element composition to the chilled zones of the Stillwater and Skaergaard intrusions, having slightly higher CaO and lower Al_2O_3 (Carmichael & others, 1974, table 9-15).

In the eastern succession, most of the E2 dolerites (Table 4) are similar in most elements to examples of continental tholeiites, but, although they have distinctly lower Ba, Rb, Sr, and K_2O, the value for these elements is not as low as ocean floor tholeiites (Table 5, No. 1). Furthermore, the low values for these elements are still comparable to values listed by Carmichael & others (1974, table 9-5) for continental basaltic magmas of the Karoo Province of South Africa.

The analysed sample of the E3 Lunch Creek Gabbro has high potassium and low titanium, and is probably from a fractionated part of the intrusion. According to Derrick (1980), the gabbro represents a 'subalkaline, hydrous tholeiitic or calc-alkaline magma type fractionated from picrite to coarse pegmatoidal leucogabbros'.

Most E4 dykes from the Mary Kathleen area (Table 4, Nos. 26, 28, 29) are comparable in major and trace-element content to continental tholeiitic lavas, and differ from ocean-floor tholeiites in having higher TiO_2, K_2O, Ba, and Rb, and lower Sr. One TiO_2-poor dyke (Table 4, No. 27) is quite potassic (Na_2O/K_2O ⁵ 1.1) and has much lower TiO_2, Ba, and Na_2O/K_2O than continental tholeiite.

The tholeiites of the E4 dykes from the Kuridala area, (Table 4, Nos. 30-33) have high Rb contents and low K/Rb, like continental tholeiites, but have lower Ba, which is characteristic of many of the Mount Isa mafic rocks. The E3 and E4 dolerites are much more potassic than other continental tholeiites, (0.72-2.31% K_2O), though the average nonporphyritic Central Basalt from Mull (Bailey & others, 1924) and the average Victorian 'labradorite basalt' (Edwards, 1938) contain 1.3 and 1.23 per cent K_2O, respectively.

Present day tectonic analogue

The Mount Isa region is dominated by a bimodal range in igneous rock compositions — basalt and dolerite vs rhyolite, dacite, and granite (Bultitude & Wyborn, 1982). These compositions indicate a rifting rather than a subduction- related environment such as an island arc or continental margin (e.g. Christiansen & Lipman, 1972; Martin & Piwinski, 1972). Continental margins usually have an abundance of andesitic volcanism, which is absent at Mount Isa. There, a predominance of shallow-water sediments and felsic igneous rocks of crustal origin argues against an oceanic environment such as an island arc or ocean floor, which usually includes ophiolites and can also include blueschist metamorphic rocks, both of which are absent from Mount Isa, where the facies of metamorphism is greenschist-amphibolite.

Another reason for rejecting a subduction related environment for the Mount Isa Inlier lies in the time scale we are considering. The basic volcanism and dolerite dyke emplacement in the Mount Isa region extended over a period of at least 700 Ma, the difference between 1800 Ma, the date of the Magna Lynn Metabasalt (Page, 1983b) to 1116±12 Ma, the date of the Lakeview Dolerite (Page, 1983a). At present, it takes the oceanic crust of the order of 100 Ma from the time of generation at a spreading ridge until it descends a subduction zone. Since the Mesozoic era, nearly 10 000 km of oceanic plate seems to have descended beneath Japan (Uyeda, 1978). If subduction did operate at Mount Isa, with the same sea-floor spreading rate as now, then, over a 700 Ma period, at least 70 000 km of oceanic crust would have been subducted. This would have resulted in an enormous volume of andesitic lava at Mount Isa, evidence for which is lacking.

Conclusions

Mafic rocks of the western succession and basement sequence are very uniform in composition and similar to other continental tholeiite suites, although elements such as K_2O, TiO_2, Ba, Rb, and Sr tend to be low, and K/Rb exceptionally so. The eastern succession mafic rocks are the most heterogeneous, but are still dominated by rocks of continental tholeiitic composition. Olivine-tholeiites and quartz-tholeiites are the dominant rock types, and the variations in composition of rocks in any one group can largely be explained by crystal differentiation from a common parent.

The most likely present-day analogue is that of an intracontinental rift. There is no evidence for a subduction-related tectonic environment such as an island arc or continental margin.

Acknowledgements

We have benefited from helpful discussions with D.H. Blake, G.M. Derrick, A.L. Jaques, R.M. Hill, R.J. Bultitude, R.N. England, C.M. Mock, T.A. Noon, K. R. Walker, I. H. Wilson and A.Y. Glikson. D.H. Blake, J.W. Sheraton, J.Ferguson, and W.E. Cameron provided helpful reviews.

References

Bailey, E.B., Clough, C.T., Wright, W.B., Richey, J.E., & Wilson, G.V., 1924 - Tertiary and post-Tertiary geology of Mull, Loch Aline and Oban. *Memoirs of the Geological Survey of Scotland* 1924.

Blake, D.H., 1980 - The early geological history of the Proterozoic Mount Isa Inlier, northwestern Queensland: an alternative interpretation. *BMR Journal of Australian Geology & Geophysics*, 5, 243-256.

Blake, D.H., 1981 - Intrusive net-veined complexes in north Queensland. *BMR Journal of Australian Geology & Geophysics*, 6, 1981, 95-99.

Blake, D.H., Bultitude, R.J., & Donchak, P.J.T., 1981 - Definitions of newly named and revised Precambrian stratigraphic and intrusive rock units in the Duchess and Urandangi 1:250 000 sheet areas, Mount Isa Inlier, northwestern Queensland. *Bureau of Mineral Resources, Australia, Report* 233; *BMR Microform* MF164.

Blake, D.H., Page, R.W., Wyborn, L.A.I., & Etheridge, M.A., 1984 - The Mount Isa base-metal province. *BMR Yearbook* 1983, 50.

Blake, D.H., Bultitude, R.J., Donchak, P.J.T., Wyborn, L.A.I., & Hone, I.G., in press - Geology of the Duchess-Urandangi region, Mount Isa Inlier, Queensland. *Bureau of Mineral Resources, Australia, Bulletin* 219.

Bultitude, R.J., & Wyborn, L.A.I., 1982 - Distribution and geochemistry of volcanic rocks in the Duchess - Urandangi Region. *BMR Journal of Australian Geology & Geophysics*, 7, 99-112.

Carter, E.K., Brooks, J.H., & Walker, K.R., 1961 - The Precambrian mineral belt of northwestern Queensland. *Bureau of Mineral Resources, Australia, Bulletin* 51.

Carmichael, I.S.E., Turner, F.J., & Verhoogen, J., 1974 - Igneous petrology. *McGraw Hill Inc., New York.*

Christiansen, R.L., & Lipman, P.W., 1972 - Cenozoic volcanism and plate-tectonic evolution of the Western United States. *Philosophical Transactions of the Royal Society of London, Series A*, 271, 249-284.

Derrick, G.M., 1980 - Marraba, Queensland. *Bureau of Mineral Resources, Australia, 1:100 000 Geological Map Commentary.*

Derrick, G.M., Wilson, I.H., & Hill, R.M. 1976a - Revision of stratigraphic nomenclature in the Precambrian of northwestern Queensland. I: Tewinga Group. *Queensland Government Mining Journal* 77, 97-102.

Derrick, G.M., Wilson, I.H., & Hill, R.M., 1976b - Revision of stratigraphic nomenclature in the Precambrian of northwestern Queensland. IV: Malbon Group. *Queensland Government Mining Journal* 77, 515-517.

Derrick, G.M., Wilson, I.H., & Hill, R.M., 1977b - Revision of stratigraphic nomenclature in the Precambrian of northwestern Queensland. VI: The Mary Kathleen Group. *Queensland Government Mining Journal* 78, 15-23.

Derrick, G.M., Wilson, I.H., & Hill, R.M., 1978 - Revision of stratigraphic nomenclature in the Precambrian of northwestern Queensland. VIII: Igneous rocks. *Queensland Government Mining Journal*, 79, 151-156.

Edwards, A.B., 1938 - The Tertiary volcanic rocks of central Victoria. *Quarterly Journal of the Geological Society of London* 94, 243-320.

Engel, A.E.J., Engel, C.G., & Havens, R.G., 1965 - Chemical characteristics of oceanic basalts and the upper mantle. *Geological Society of America Bulletin* 76, 719-734.

Geological Survey of Queensland, 1976 - Queensland geology scale 1:250 000. *Department of Mines, Brisbane.*

Glikson, A.Y., & Derrick, G.M., 1970 - The Proterozoic metamorphic rocks of the Cloncurry 1:100 000 Sheet area, (Soldiers Cap Belt) northwestern Queensland. *Bureau of Mineral Resources, Australia, Record* 1970/24.

Glikson, A.Y., & Derrick, G.M., 1978 - Geology and geochemistry of Middle Proterozoic basic volcanic belts, Mount Isa/Cloncurry, northwestern Queensland. *Bureau of Mineral Resources, Australia, Record* 1978/48.

Glikson, A.Y., Derrick, G.M., Wilson, I.H., & Hill, R.M., 1976 - Tectonic evolution and crustal setting of the middle Proterozoic Leichhardt River fault trough, Mount Isa region, northwestern Queensland. *BMR Journal of Australian Geology & Geophysics* 1, 115-129.

Green, D.H., & Ringwood, A.E., 1967 - The genesis of basaltic magmas. *Contributions to Mineralogy and Petrology* 15, 103-190.

Irvine, T.N., & Baragar, W.R.A., 1971 - A guide to the chemical classification of the common volcanic rocks. *Canadian Journal of Earth Sciences* 8, 523-548.

Joplin, G.A., 1955 - A preliminary account of the petrology of the Cloncurry Mineral Field. *Proceedings of the Royal Society of Queensland*, 62, 33-67.

MacDonald, G.A. & Katsura, T., 1964 - Chemical composition of Hawaiian lavas. *Journal of Petrology*, 5, 82-133.

Manson, V., 1967 - Geochemistry of basaltic rocks: major elements. *In* Hess, H.H., & Poldervaart A. (editors), Basalts; the Poldervaart treatise on rocks of basaltic composition. *Wiley New York.*

Martin, R.F., & Piwinski, A.J., 1972 - Magmatism and tectonic settings. *Journal of Geophysical Research*, 77, 4966-4976.

Page, R.W., 1981 - Depositional ages of the stratiform base metal deposits at Mount Isa and McArthur River, Australia, based on U-Pb zircon dating of concordant tuff horizons. *Economic Geology*, 76, 648-658.

Page, R.W., 1983a - Chronology of magmatism, skarn formation and uranium mineralisation, Mary Kathleen, Queensland, Australia. *Economic Geology*, 78, 838-853.

Page, R.W., 1983b - Timing of superposed volcanism in the Proterozoic Mount Isa Inlier, Australia. *Precambrian Research*, 21, 223-245.

Plumb, K.A., Derrick, G.M., & Wilson, I.H., 1980 - Precambrian geology of the McArthur River-Mount Isa region, northern Australia. *In* Henderson, R.A., & Stephenson, P.J. (editors), The geology and geophysics of northeastern Australia. *Geological Society of Australia, Queensland Division, Brisbane.*

Robinson, W.B., 1968 - Geology of the Eastern Creek Volcanics. *Proceedings of the Australasian Institute of Mining and Metallurgy*, 226, 89-96.

Scott, K.M., & Taylor, G.F., 1982 - Eastern Creek Volcanics as the source of copper at the Mammoth Mine, northwest Queensland. *BMR Journal of Australian Geology & Geophysics*, 7, 93-98.

Smith, S.E., & Walker, K.R., 1971 - Primary element dispersions associated with mineralisations at Mount Isa, Queensland. *Bureau of Mineral Resources, Australia, Bulletin* 131.

Thornton, C.P., & Tuttle, O.F., 1960 - Chemistry of igneous rocks: I. Differentiation Index. *American Journal of Science*, 258, 664-684.

Uyeda, S., 1977 - Some basic problems in the trench-arc- back arc system. *In* M. Talwani & Pitman W.C. (editors), Island arcs, deep sea trenches and back arc basins. *American Geophysical Union, Maurice Ewing Series* 1, 1-14.

Walker, F., & Poldervaart, A., 1949 - Karroo dolerites of the Union of South Africa. *Geological Society of America Bulletin* 60, 591-706.

Walker, G.P.L., & Skelhorn, R.R., 1966 - Some associations of acid and basic rocks. *Earth Science Reviews*, 2, 93-109.

Walker, K.R., 1958 - A study of the basic igneous rocks of the Lower Proterozoic of northwestern Queensland with special reference to their metamorphism and metasomatism in relation to the geological sequence of events. *Ph.D Thesis, Australian National University.*

Walker, K.R., 1969 - The Palisades Sill, New Jersey: A reinvestigation. *Geological Society of America, Special Paper* 111.

Walker, K.R., Joplin, G.A. Lovering, J.F., & Green, R., 1960 - Metamorphic and metasomatic convergence of basic igneous rocks and lime-magnesia sediments of the Precambrian of northwestern Queensland. *Journal of the Geological Society of Australia* 6, 149-178.

Waters, A.C., 1961 - Stratigraphic and lithological variations in the Columbia River basalt. *American Journal of Science*, 259, 583-611.

Wilson, C.J.L., 1972 - Structural features west of Mount Isa. *Journal of the Geological Society of Australia*, 22, 457-76.

Wilson, I.H., 1978 - Volcanism on a Proterozoic continental margin in northwestern Queensland. *Precambrian Research* 7, 205-235.

Wyborn, L.A.I., in preparation - Geochemical analyses from the Mt Isa Region. *Bureau of Mineral Resources, Australia, Report.*

Wyborn, L.A.I., & Page, R.W., 1983 - The Proterozoic Kalkadoon and Ewen Batholiths, Mount Isa Inlier, Queensland: source, chemistry, age, and metamorphism. *BMR Journal of Australian Geology & Geophysics* 8, 53-69.

Appendix. Sample localities

Table 1. Metasomatised basic rocks

Analysis No.	Sample No.	Type	Rock type	Grid ref.	1:100 000 Sheet area
1	74205594	B1	metadolerite	781530	Prospector
2	74205595	B1	chlorite schist	781530	"
3	74205598	B1	dolerite	778530	"
4	74205596	B1	chlorite schist	778530	"
5	73205374	B1	dolerite	849218	Mary Kathleen
6	73205375	B1	biotite schist	849218	" "
7	74205608	B1	dolerite	753501	Prospector
8	74205609	B1	biotite schist	753501	"
9	74205539	E2	scapolite dolerite	910420	Prospector
10	74205651	E2	scapolite dolerite	545060?	Cloncurry

Table 2. Western succession dolerites

Analysis No.	Sample No.	Type	Formation dolerite intrudes	Grid ref.	1:100 000 Sheet area
1	71201436	W1	Cromwell Metabasalt Member	478981	Mary Kathleen
2	71201446	W1	" "	487987	" "
3	73205326	W1	Whitworth Quartzite	586726	Prospector
4	73205346	W1	" "	494604	"
5	73205347	W1	Cromwell Metabasalt Member	477683	"
6	73205349	W1	Alsace Quartzite	484563	"
7	73205352	W1	Lena Quartzite Member	476527	"
8	74205643	W1	Mt Guide Quartzite	321958	Mount Isa
9	74205644	W1	" " "	321958	Mount Isa
10	74205685	W1	Cromwell Metabasalt Member	481078	Mary Kathleen
11	74205634	W2	Sybella Granite	300225	Mount Isa
12	74205635A	W2	" "	300225	" "
13	74205635B	W2	" "	300225	" "
14	74205635C	W2	" "	300225	" "
15	74205636C	W2	" "	300225	" "
16	74205637	W2	" "	311227	" "
17	74205641	W2	" "	311977	" "
18	73205350	W3	Cromwell Metabasalt Member	468497	Prospector
19	73205353	W3	Bortala Formation	514587	"
20	73205354	W3	Cromwell Metabasalt Member	561548	"
21	73205358	W3	Pickwick Metabasalt Member	561548	"
22	73205359	W3	Bortala Formation	586580	"
23	73205360	W3	Lochness Formation	649513	"
24	73205361	W3	Quilalar Formation	655527	"
25	73205364	W3	" "	685650	"
26	74205649	W3	Tewinga Group undivided	557090	Dajarra

Table 3. Basement sequence dolerites

Analysis No.	Sample No.	Type	Formation dolerite intrudes	Grid ref.	1:100 000 Sheet area
1	73205374	B1	Leichhardt Metamorphics	849218	Mary Kathleen
2	73205376	B1	Corella Formation	900282	" "
3	74205	B1	Argylla Formation	909459	Prospector
4	74205557	B1	" "	943329	"
5	74205590	B1	Kalkadoon Granodiorite	793532	"
6	74205598	B1	" "	778530	"
7	74205599	B1	" "	772528	"
8	74205600	B1	Leichhardt Metamorphics	762523	"
9	74205601	B1	" "	762523	"
10	74205603	B1	" "	755526	"
11	74205606	B1	" "	754502	"
12	74205608	B1	" "	751502	"
13	74205614	B1	" "	731469	"
14	74205645	B1	Kalkadoon Granodiorite	505956	Dajarra
15	74205646	B1	Tewinga Group undivided	517932?	"
16	71201414	B2	Leichhardt Metamorphics	846237	Mary Kathleen
17	71201416	B2	" "	846237	" "
18	73205372	B2	Corella Formation	792119	" "
19	73205373	B2	" "	795131	" "

Table 4. Eastern succession dolerites

Analysis No.	Sample No.	Type	Formation dolerite intrudes	Grid ref.	1:100 000 Sheet area
1	74205475	E2	Corella Formation	877658	Prospector
2	74205476	E2	" "	874637	"
3	74205514	E2	" "	997561	Quamby
4	74205520	E2	Argylla Formation	890640	Prospector
5	74205531	E2	" "	917456	Prospector
6	74205532	E2	" "	915457	"
7	74205536	E2	" "	906426	"
8	74205522	E2	Wonga Granite	933448	"
9	74205523	E2	" "	937449	"
10	74205524	E2	" "	925453	"
11	74205527	E2	" "	939448	"
12	74205567	E2	" "	913507	"
13	74205658	E2	Cone Creek Metabasalt Member	246721	Malbon
14	74205666	E2	" "	257729	"
15	74205667	E2	Kuridala Formation	464467	"
16	74205670	E2	" "	470462	"
17	74205671	E2	" "	478472	"
18	74205672	E2	" "	471480	
19	74205675	E2	" "	509455	Mt Angelay
20	74205683	E2	" "	510430	" "
21	74205657	E2	Llewellyn Creek Formation	640870	Cloncurry
22	74205684	E1	Toole Creek Volcanics	663007	"
23	74205652	E3	Corella Formation	548922	"
24	74205650	E3	" "	482078	"
25	74205615	E3	" "	027047	Marraba
26	74200097	E4			Prospector
27	74205525	E4	Wonga Granite	938448	"
28	73205369	E4	Corella Formation	997967	Marraba
29	74205622	E4	" "	035047	"
30	74205673	E4	Kuridala Formation	502453	Mt Angelay
31	74205674	E4	" "	508458	" "
32	74205676	E4	Williams Batholith	532402	" "
33	74205678	E4	Doherty Formation	540462	" "
34	74205693	E4	" "	894117	Selwyn
35	74205699	E4	" "	894117	"
36	74205701	E4	" "	858089	"

BMR Journal of Australian Geology & Geophysics, 9, 33–40

A mica, pyroxene, ilmenite megacryst-bearing lamprophyre from Mt Woolooma, northeastern New South Wales

A.L. Jaques & D.J. Perkin

A narrow lamprophyre dyke, dated at 85 Ma, intrudes Early Carboniferous sediments at Mount Woolooma in northeast New South Wales. The lamprophyre contains megacrysts of titanbiotite (Mg_{18-21}, 7–8% TiO_2) and rare Ti-Al salite (Mg_{67-72}, 6–9% Al_2O_3), ilmenite (5% MgO), titanphlogopite (Mg_{61}, 9% TiO_2) and apatite. The host rock consists of lamprophyric-textured titanphlogopite (Mg_{62-70}, 7–8% TiO_2), diopside-salite, olivine, kaersutite, and Ti-magnetite in a K-feldspar-rich base. The rock resembles a minette (mica-lamprophyre), but its bulk composition is richer in SiO_2 and Al_2O_3 (53–54% SiO_2 anhydrous, ~16% Al_2O_3), and poorer in MgO (3%), Ni and Cr (30 ppm) than many minettes elsewhere. The Mount Woolooma minette forms part of a diverse assemblage of alkaline igneous rocks from the Scone–Gloucester area. These include alkali olivine basalt, teschenite, biotite alnoite, kimberlite, and leucite monchiquite, many of which carry mantle xenoliths/xenocrysts and/or megacrysts.

Introduction

Mica lamprophyres (minettes) are now recognised as an important rock association: many carry xenoliths of garnet lherzolite and share chemical similarities with micaceous kimberlites (e.g. Bachinski & Scott, 1979; Roden & Smith, 1979; Roden, 1981; Rogers & others, 1982). The significance of the lamprophyre suite is reinforced by the occurrence of diamond in recently discovered olivine-rich lamproites (potash- and magnesia-rich lamprophyres) of the West Kimberley region of Western Australia (Atkinson & others, 1984; Jaques & others, 1984). This paper describes a small lamprophyre dyke from Mount Woolooma in the Rouchel District of the Scone–Gloucester area of northeastern New South Wales. The dyke was found by one of us (DJP) in 1980 during an attempt to relocate a leucite(?) monchiquite plug found by students of Sydney University during mapping of the Glenbawn Dam region in 1966. The lamprophyre is of interest because it carries megacrysts of titanbiotite, clinopyroxene, and ilmenite, and is compositionally unlike other megacryst-bearing rocks described from this region.

Geology

The lamprophyre occurs as a poorly exposed dyke in dissected country on the northern slopes of Mount Woolooma (Fig. 1). The dyke is 1–3 m wide, subvertical, and extends for a little over 100 m in an east-west direction (Fig. 2). It intrudes thinly bedded, fossiliferous marl, mudstone, and shale of the Early Carboniferous Waverley Formation (Roberts & Oversby, 1974). Basaltic lavas of the Eocene Barrington Tops volcanic field cap ridges immediately east and south (Wilkinson, 1969; Wellman & McDougall, 1974; Mason, 1982), and a small plug-like body of alkali olivine basalt, containing peridotite nodules and megacrysts, lies immediately to the north (Fig. 2). The Mount Woolooma lamprophyre has been dated by the K-Ar method (mica separates) as late Cretaceous, 85.3 ± 0.4 Ma (Table 1).

The lamprophyre contains sparse (<5%) subhedral to euhedral megacrysts of biotite up to 1 cm long in a very fine-grained, phlogopite-rich groundmass. Rare megacrysts of black lustrous clinopyroxene up to 2.5 cm across, associated with crystals of ilmenite up to 1 cm long, were found in one sample.

Table 1. Summary of K-Ar data

Sample	%K	$^{40}Ar^*$ ($\times 10^{-10}$ moles g^{-1})	$^{40}Ar^*/^{40}Ar$ Total	Age (Ma)
Mica (812105003)	6.817 6.814	10.325	0.886	85.3 ± 0.4

$^{40}K/K$ = 1.167×10^{-4} mol./mol.; λ_β = $4.962 \times 10^{-10} yr^{-1}$; λ_ϵ = $0.581 \times 10^{-10} yr^{-1}$.
Analyst: A.W. Webb (AMDEL Report GS 2679/83.

Contacts with the country rock marls are sharp and little affected. The margins of the lamprophyre are commonly veined by carbonate, and mica megacrysts show a weak flow alignment near the contact.

Petrography

Thin sections show similar petrography. Sparse mica megacrysts up to 6 mm long lie in a lamprophyric-textured groundmass, in which euhedral microphenocrysts of phlogopite and diopside up to 0.3 mm are seriate to smaller euhedra of phlogopite, diopside, olivine, rare hornblende, and titanomagnetite. A glassy base is crowded with microlites of phlogopite, diopside, apatite, titanomagnetite, and rare ilmenite. Coarser-grained vein-like segregations contain laths of alkali feldspar in a crystalline K-feldspar-rich base. Sparse subhedral to euhedral phenocrysts of diopside up to 0.6 mm across, commonly with highly sieved cores, were observed in several thin sections. On megascopic and microscopic evidence, the Mount Woolooma lamprophyre is a minette (mica lamprophyre), using the nomenclature of Streckeisen (1978).

The mica megacrysts have strongly pleochroic (α = yellowish brown, β = γ = dark brown) biotite cores with sharp narrow rims (mostly 50μm) of red-brown pleochroic phlogopite (= pale yellow, β = γ = brownish red). The megacrysts are strongly resorbed and embayed, and some have kink-bands, indicating solid-state deformation. The inner rim is commonly marked by the presence of granules of magnetite and/or amoeboid-shaped inclusions of glassy groundmass material. Several of the megacrysts contain rounded inclusions of highly altered silicate (formerly K-feldspar?) now mainly zeolite, secondary K-feldspar, and magnetite. Tiny granules of magnetite occur along cleavage traces of some mica megacrysts.

The clinopyroxene megacrysts occur as large (up to 2 cm), strongly embayed anhedra free of exsolution. A clear core is surrounded by a reaction zone, commonly 0.2–0.6 mm wide, composed of less aluminous clinopyroxene (commonly in quench form), phlogopite, amphibole, magnetite, and glass. The outer part of the reaction zone generally consists of a narrow rim of quench diopside, which is commonly strongly zoned.

Ilmenite megacrysts accompany the clinopyroxene megacrysts as rare strongly rounded and embayed anhedra rimmed by phlogopite. One titanphlogopite megacryst 1.2 mm across was found with these megacrysts. This mica is strongly pleochroic (α = pale straw yellow, β = γ = foxy

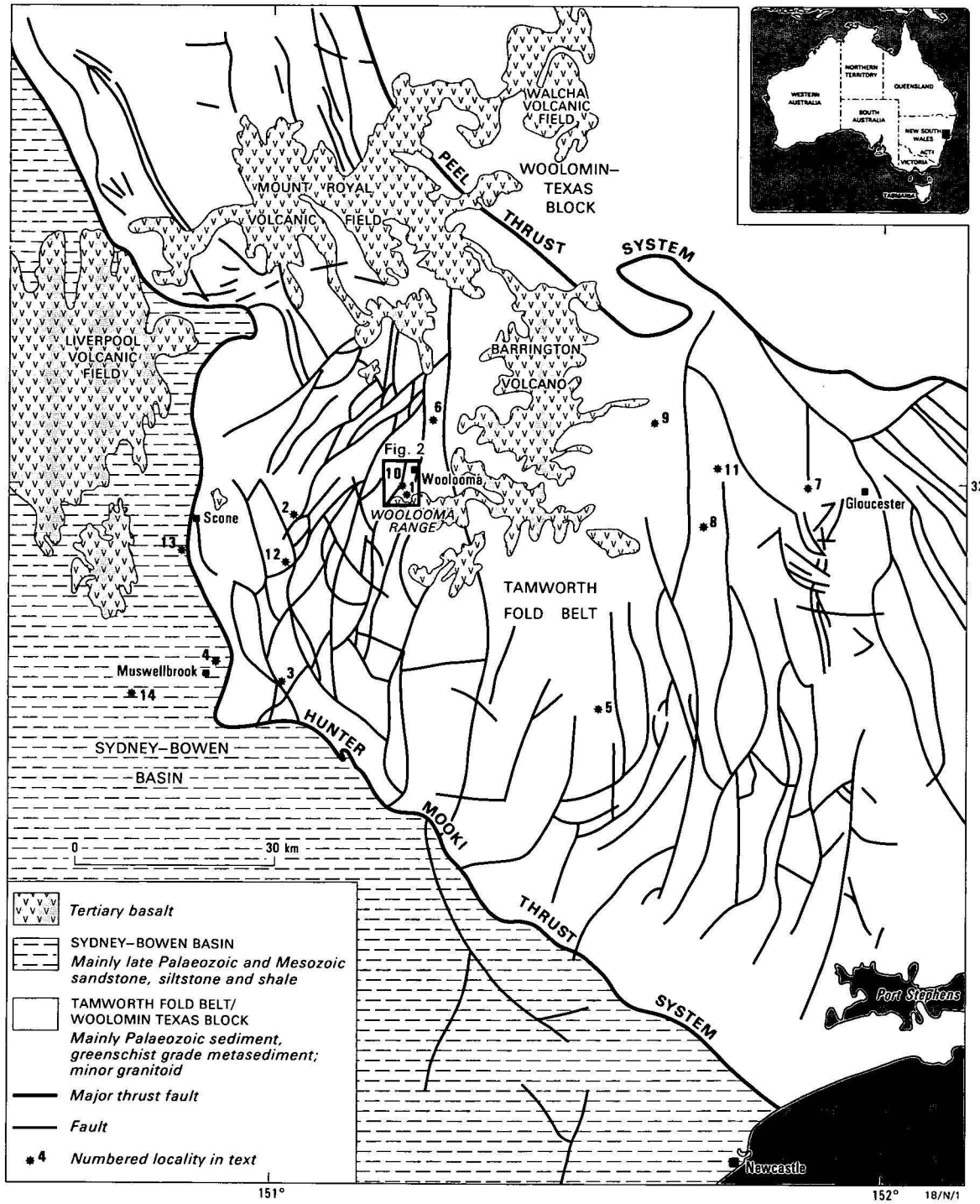

Figure 1. Simplified geology of the Scone - Gloucester area.

brownish red) and partly encased in the reaction zone surrounding the clinopyroxene megacryst.

Apatite was seen in one thin section as an elongate grain (approximately 1 mm x 0.25 mm) with strongly rounded margins; also present is a rounded xenocryst of strained quartz approximately 1 mm in diameter, which encloses a small oval-shaped crystal of K-feldspar.

The diopside phenocrysts (particularly those in sample 5) and many of the microphenocrysts have strongly sieved cores replaced by very fine-grained aggregates of phlogopite, magnetite and, in some cases, amphibole.

Megacrysts

Mica. The mica megacrysts are predominantly titanbiotites of uniform composition with high Ti and Fe contents, very low MgO contents, and low 100 Mg/(Mg + Fe) ratios (17.8–20.9; Table 2). They have low to moderate Na_2O contents (0.3–0.5%) and very low Cr_2O_3, MnO, and NiO. Structural formulae show low Si contents (Si = 5.3 atoms per 22 O atoms) with the Al in tetrahedral coordination. There is a deficiency of octahedral cations (0.5 cations) relative to ideal mica stoichiometry, suggesting that Ti is accommodated largely by the substitution $2\,Mg^{2+}_{VI} \rightleftharpoons Ti^{4+}_{VI} + \square_{VI}$ (Forbes & Flower, 1974).

A single phlogopite megacryst, $Mg_{60.6}$, has a higher TiO_2 content than the titanbiotite megacrysts and the groundmass titanphlogopites (Table 2); it is less magnesian and poorer in SiO_2 than the groundmass titanphlogopites.

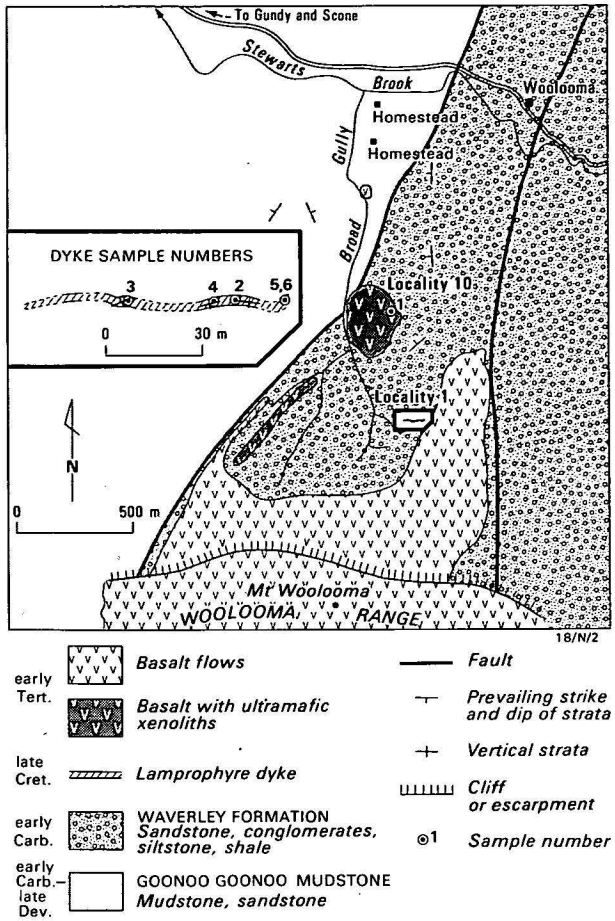

Figure 2. Geological map of the Mount Woolooma region.
(Based on mapping by students of Sydney University, University of New South Wales, and Roberts & Oversby (1974)). Sample numbers in inset have the BMR prefix 8121500.

Mica megacrysts with high TiO_2 contents are relatively common in alkali basalts (e.g. Irving, 1974; Wilkinson, 1975; Ellis, 1976), but most are titanphlogopite. Wilkinson (1962) reported titanobiotites (Mg_{55}, 6–8% TiO_2) from analcite-basalt from Spring Mountain. Irving (1974) described titan-biotite megacrysts as Fe-rich as $Mg_{35.6}$ (7.8% TiO_2) from the Anakies, Victoria. Ellis (1976) also reported similar or slightly more Mg-rich micas in a nepheline mugearite and in pyroxenite xenoliths. Similar micas (Mg_{50-66}) also occur in amphibolite-rich and apatite-rich xenoliths in dykes near Kiama (Wass, 1979a). To our knowledge, mica megacrysts as Fe-rich as those of the Mount Woolooma lamprophyre have not previously been reported.

Clinopyroxene. The clinopyroxene megacrysts are sodian, titanian, aluminous salites poor in Cr_2O_3 (Table 2), and show a limited range in Ca-Mg-Fe (Fig. 4). The cores are less calcic, and more aluminous, and have the lowest Mg-values (Figs. 4, 5). Al is partitioned between the tetrahedral and octahedral sites in the ratio 1:1 (Al^{IV}/Al^{VI} = 0.8–0.9). The cores are replaced by less aluminous, more calcic, and less sodic pyroxene together with phlogopite, magnetite, and amphibole in the reaction zone. Narrow rims of less Al- and Na- rich pyroxene, richer in Ca, and with a higher Mg-value (Table 2) overlap compositions of the more Al-rich phenocryst pyroxenes (Fig. 5). In general, there is a negative correlation of TiO_2, Al_2O_3, and Na_2O contents, and a positive correlation of Al^{IV}/Al^{VI} ratio with Mg-value (Fig. 5). The pyroxenes show a marked increase in Al^{IV}/Al^{VI} ratio from the megacryst cores through the reaction zone to the narrow rim (Fig. 5).

Table 2. Representative microprobe analyses of megacrysts

	1	2	3	4	5	6
SiO_2	34.08	36.02	48.98	49.26	0.68	35.90
TiO_2	6.96	7.29	1.54	1.63	44.47	9.31
Al_2O_3	14.68	15.26	9.22	4.68	1.53	15.23
V_2O_3	0.15	-	-	-	0.27	-
Fe_2O_3					16.37*	
FeO	27.72	12.56	9.86	8.49	30.88	13.99
MnO	0.20	-	-	-	0.15	-
MgO	4.11	13.84	11.14	13.17	5.32	12.09
CaO	0.27	-	17.44	22.02	0.23	0.17
Na_2O	0.50	0.55	2.16	0.58	-	0.33
K_2O	9.09	9.58	-	-	-	9.86
Total	97.76	95.10	100.35	99.82	99.90	96.87
100 Mg / $(Mg + Fe^{2+})$	20.9	66.3	66.8	73.4	23.5	60.6
Ca			42.9	46.9		
Mg			38.1	39.0		
Fe			18.9	14.1		

* Fe_2O_3 calculated from ABO_3 stoichiometry
Mineral analyses were made using the TPD energy-dispersive electron microprobe at the Australian National University (Reed & Ware, 1975; Ware, 1981).
1. Biotite megacryst core, sample 81215004.
2. Phlogopite rim on biotite megacryst, sample 81215004.
3. Clinopyroxene megacryst core, sample 81215006.
4. Clinopyroxene megacryst rim, sample 81215006.
5. Ilmenite megacryst, sample 81215006.
6. Titanphlogopite megacryst, sample 81215006.

The clinopyroxene megacrysts are broadly comparable with the Al-augites and salites found as megacrysts in alkali basalts and associated lavas elsewhere (e.g. Binns & others, 1970; Irving, 1974; Ellis, 1976; Wass, 1979a). However, the Mount Woolooma megacrysts are more Fe-rich than usual and resemble Fe-rich pyroxene megacrysts in basanitic dykes in the Kiama area (Wass, 1979b), in a nephelinite sill in the Nandewar Mountains (Wilkinson, 1975), and in basanites in the Massif Central (Wass, 1979a).

Ilmenite. The ilmenite megacrysts are relatively uniform in composition, with 100 Mg/(Mg + Fe^{2+}) ratios ~ 23–24, geikelite contents of 15.7–19.8%, and hematite contents of 19.1–26.7%. They are comparable with, although somewhat richer in hematite than, those reported from eastern Australia (e.g. Binns, 1969; Ellis, 1976).

Microphenocrysts/groundmass

Phlogopite. Pale coloured titanphlogopite rims the biotite megacrysts and forms microphenocryst and groundmass phases. It is much poorer in FeO and richer in MgO than the biotite megacrysts, but has similar high TiO_2 and Al_2O_3 contents (Table 2; Fig. 3). Small differences exist in Na, Ca, and Mn contents between the two mica generations. The titanphlogopite rims on the biotite megacrysts, the microphenocrysts, and the groundmass phlogopites overlap in TiO_2 and Al_2O_3 contents and Mg/(Mg+Fe) ratios (Fig. 3). These phlogopites show minor amounts of Al^{VI} in their structural formulae, indicating very limited solid solution towards eastonite, but the dominant solid solution is annite – phlogopite.

Clinopyroxene. Clinopyroxene is present as microphenocrysts, groundmass prisms, and very rare phenocrysts. They are of diopside – salite composition and show limited Ca-Mg-Fe variation (Fig. 4). The microphenocrysts, the groundmass grains, and the phenocrysts show similar Ca-Mg-Fe contents except for lower Ca in the phenocrysts. Ti and Al vary (1–2% TiO_2, 2.4–6.2% Al_2O_3) with the most Ti-rich and Al-rich grains occurring as fine-grained granules in the

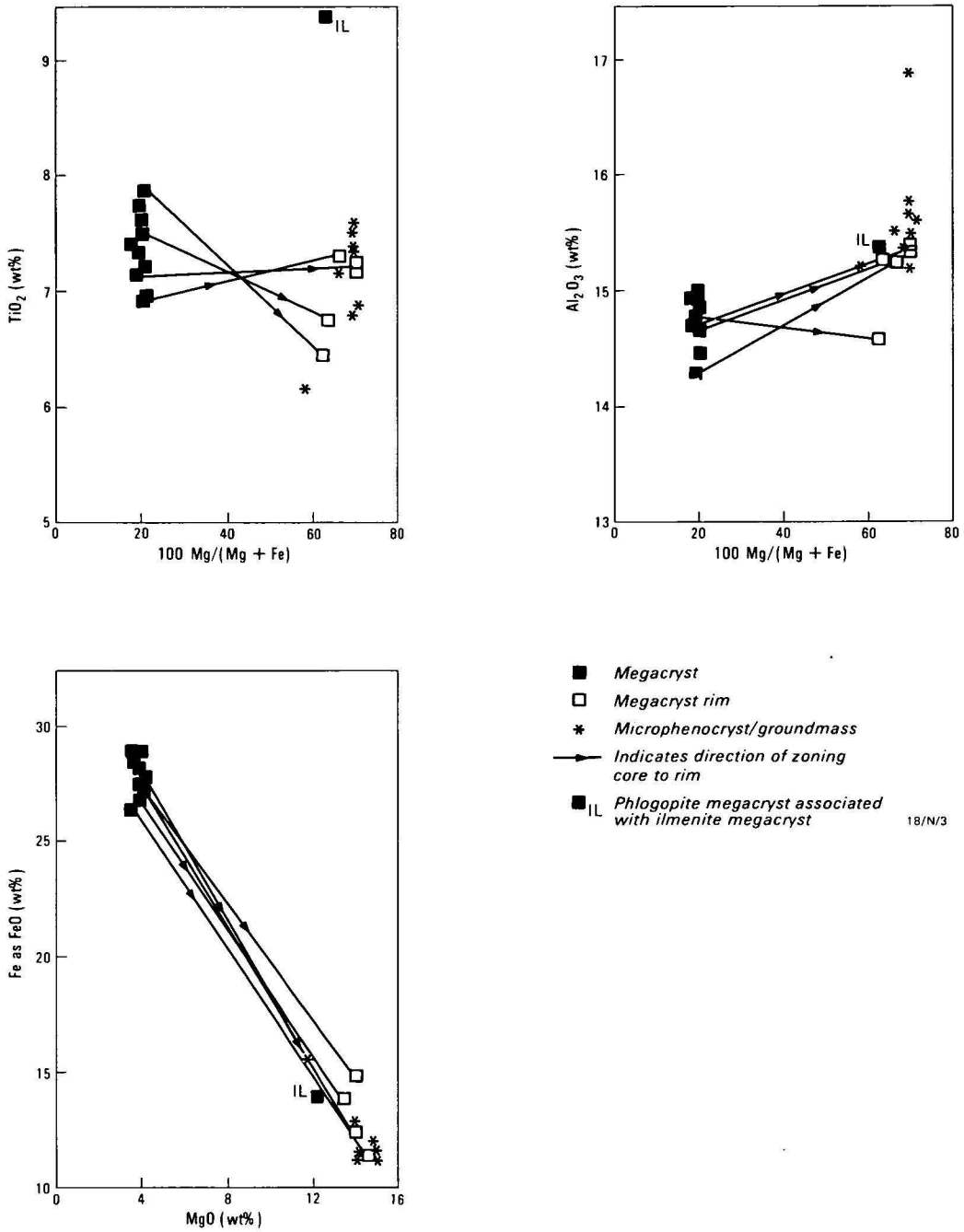

Figure 3. Compositional variation of micas in the Mount Woolooma minette. Note clear distinction of titanbiotite megacrysts (solid squares) from groundmass and microphenocryst phlogopite.

groundmass. Na contents are low, but range up to 0.9% Na_2O. The microphenocryst and groundmass pyroxenes have higher Al^{IV}/Al^{VI} ratios than the megacrysts and phenocrysts, and there is a correlation of grainsize with lower Al^{IV}/Al^{VI} ratio (Fig. 5).

Olivine. Olivine is comparatively Fe-rich (Fo_{71-73}) and contains appreciable amounts of Mn and Ca (0.3–0.45% MnO, 0.2–0.35% CaO). They are too Fe-rich to have crystallised from basaltic melts with an $Mg/(Mg+Fe^{2+})$ ratio of their host rock (assuming $K_{D\ ol\text{-}liquid}$ in the range 0.3–0.4, e.g. Roeder & Emslie, 1970; Nicholls, 1974). This suggests a lower original Fe^{3+}/Fe^{2+} than that of the rock analysis (Table 3). Olivine (or its alteration products) is common in minettes (e.g. Rock, 1977), but is usually more Mg-rich than those reported here (e.g. Roden & Smith, 1979).

Amphibole. Rare red-brown pleochroic kaersutite occurs as subhedral to euhedral grains in the groundmass of some samples. It is rich in Ti and Al (Table 3) with high Na and K contents. Ti contents and $Mg/(Mg+Fe)$ ratios are comparable with those of co-existing phlogopite.

FeTi oxides. Titaniferous magnetite forms as abundant euhedra in the groundmass. It has high Ti contents (up to 20% TiO_2) and moderate amounts of Al_2O_3 and low MgO contents (Table 3). An average composition is $Ti_{0.5}\ Fe^{3+}_{0.7}\ Fe^{2+}_{1.4}\ Al_{0.2}\ Mg_{0.2}\ O_4$. Rare ilmenite grains found in one sample proved too small for analysis.

K-feldspar and groundmass. The groundmass is partially recrystallised to K-feldspar ($Ab_{48-58}\ Or_{46-37}$). One sample contains narrow vein-like segregations of coarser-grained groundmass containing abundant fine laths of alkali feldspar.

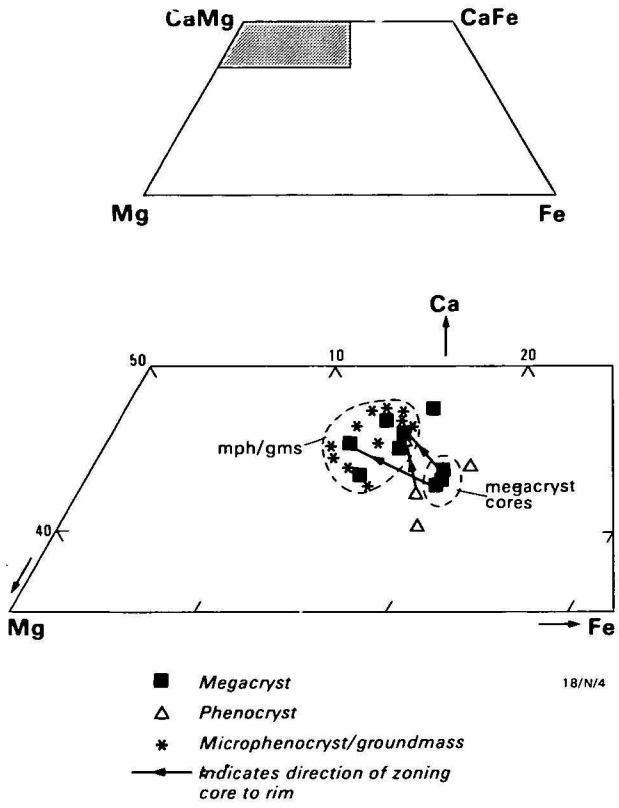

Figure 4. Portion of pyroxene quadrilateral showing compositional variation of pyroxenes in Mount Woolooma minette.

Table 3. Representative microprobe analyses of microphenocryst and groundmass phases.

	1	2	3	4	5	6
SiO_2	36.23	51.70	51.67	37.64	39.60	0.67
TiO_2	7.59	0.15	1.00	-	6.07	19.98
Al_2O_3	15.18	2.26	2.57	0.25	11.63	3.94
V_2O_3	-	-	-	-	-	-
Fe_2O_3	-	-	-	-	-	25.78*
FeO	11.48	11.67	8.40	25.44	11.44	45.81
MnO	-	0.42	-	0.45	-	0.50
MgO	14.92	14.17	14.77	35.83	12.37	3.21
CaO	0.09	19.41	21.01	0.34	11.60	0.10
Na_2O	0.50	0.24	0.29	-	2.45	-
K_2O	9.43	-	-	-	1.51	-
Cl	-	-	-	-	0.06	-
Total	95.41	100.02	99.71	99.96	96.72	100.50
100 Mg	69.8	68.4	75.8	71.5	65.8	11.1
$(Mg+Fe^{2+})$						
Ca		40.2	43.7		30.7	
Mg		40.9	42.7		45.5	
Fe		18.9	13.6		23.7	

*Fe_2O_3 calculated from AB_2O_4 stoichiometry.
1. Phlogopite, microphenocryst/groundmass, sample 81215004.
2. Diopside phenocryst, sample 81215005.
3. Diopside, groundmass, sample 81215003.
4. Olivine, groundmass, sample 81215003.
5. Kaersutite, groundmass, sample 81215002.
6. Titanomagnetite, groundmass, sample 81215003.

Geochemistry

The three samples of the Mount Woolooma minette are very similar in composition, with intermediate silica contents, high Al_2O_3 and alkali contents ($Na_2O + K_2O = 8$–9%), and low MgO, FeO, CaO, and Mg/(Mg+Fe) ratios (Table 4). Their CIPW norms contain minor nepheline (4–5%) and anorthite, and abundant albite and orthoclase; differentiation indices are high (58–60). K_2O/Na_2O ratios lie in the range 0.6 to 1, and the rocks compare with a 'shoshonitic lamprophyre' group of Rock (1977).

The Mount Woolooma minette differs markedly in chemical composition from the mica lamprophyres of the Navajo volcanic field (Roden & Smith, 1979; Roden, 1981; Rogers & others, 1982) and Spanish Peaks, Colorado (Jahn & others, 1979), in having much higher Na_2O and Al_2O_3, lower MgO, and a low Mg/(Mg+Fe) ratio; a feature of these and many other minettes are their high Mg/(Mg+Fe) ratios (>0.6) and dominance of K over Na. The Mount Woolooma minette more closely resembles the 'average' minette composition given by Velde (1971), apart from being richer in Al_2O_3 and Na_2O, and poorer in MgO (Table 4). There are also differences in trace-element contents: the Mount Woolooma rocks lack the high abundances of Ni, Cr, and Sc, and extreme enrichment in light rare-earth elements and other 'incompatible' elements, such as Pb, Th, U, Zr, Nb, P etc., which appear to be diagnostic of minettes (e.g. Bachinski & Scott, 1979; Jahn & others, 1979; Roden, 1981; Rogers & others, 1982).

The Mount Woolooma lamprophyre differs from most of the mildly alkaline rocks of intermediate composition previously described from northern and central New South Wales, which include hawaiite, mugearite, and benmoreite of distinctly sodic suites (e.g. Abbott, 1969; Wilkinson, 1969; Ewart & others, 1976, 1980; Middlemost, 1981). The Na_2O/K_2O ratio is similar to the shoshonites and latites of the Gerringong

Table 4. Chemical analyses of Mt Woolooma lamprophyre

	1	2	3	4	5
SiO_2	49.94	49.90	49.95	51.17	46.49
TiO_2	2.00	1.98	2.00	1.36	2.26
Al_2O_3	16.27	16.23	16.30	13.87	15.43
Fe_2O_3	2.72	2.96	2.87	3.27	3.27
FeO	5.18	4.98	5.01	4.16	8.00
MnO	0.13	0.13	0.13		0.11
MgO	3.46	3.43	3.27	6.91	9.30
CaO	5.05	5.24	4.78	6.58	9.49
Na_2O	5.10	4.30	4.80	2.12	3.19
K_2O	3.25	4.18	3.85	5.49	1.30
P_2O_5	0.38	0.38	0.58		0.71
Loss	6.01	5.80	5.64	3.72	0.46
Total	99.48	99.52	98.99	98.65	100.08
Trace elements (ppm)					
Sc	9	9	7		24
V	121	119	119		175
Cr	33	28	33		278
Ni	33	31	30		176
Cu	15	15	15		43
Zn	116	111	116		85
Ga	24	23	23		16
As	1	1	1		1
Rb	88	84	90		13
Sr	1432	1446	1146		825
Y	17	17	18		21
Zr	287	285	291		219
Nb	49	47	49		55
Sn	<2	2	2		<2
Ba	1084	1201	912		296
La	26	26	29		35
Ce	54	56	59		59
Nd	39	34	37		30
Pb	<2	<2	<2		2
Bi	<2	<2	<2		<2
Th	3	3	4		4
U	<1	<1	<1		<1
Mg/(Mg + Fe^t)	0.447	0.444	0.434	0.634	0.602
K_2O/Na_2O	0.64	0.97	0.80	2.59	0.41

1. Mt Woolooma lamprophyre, 81215002.
2. Mt Woolooma lamprophyre, 81215003.
3. Mt Woolooma lamprophyre, 81215004.
4. Average of 64 minettes (Velde, 1971)
5. Alkali olivine basalt, 81215001, northern slope of Mt Woolooma.

Analyses by BMR, using XRF, AAS, and wet chemical methods (Sheraton & Labonne, 1978).

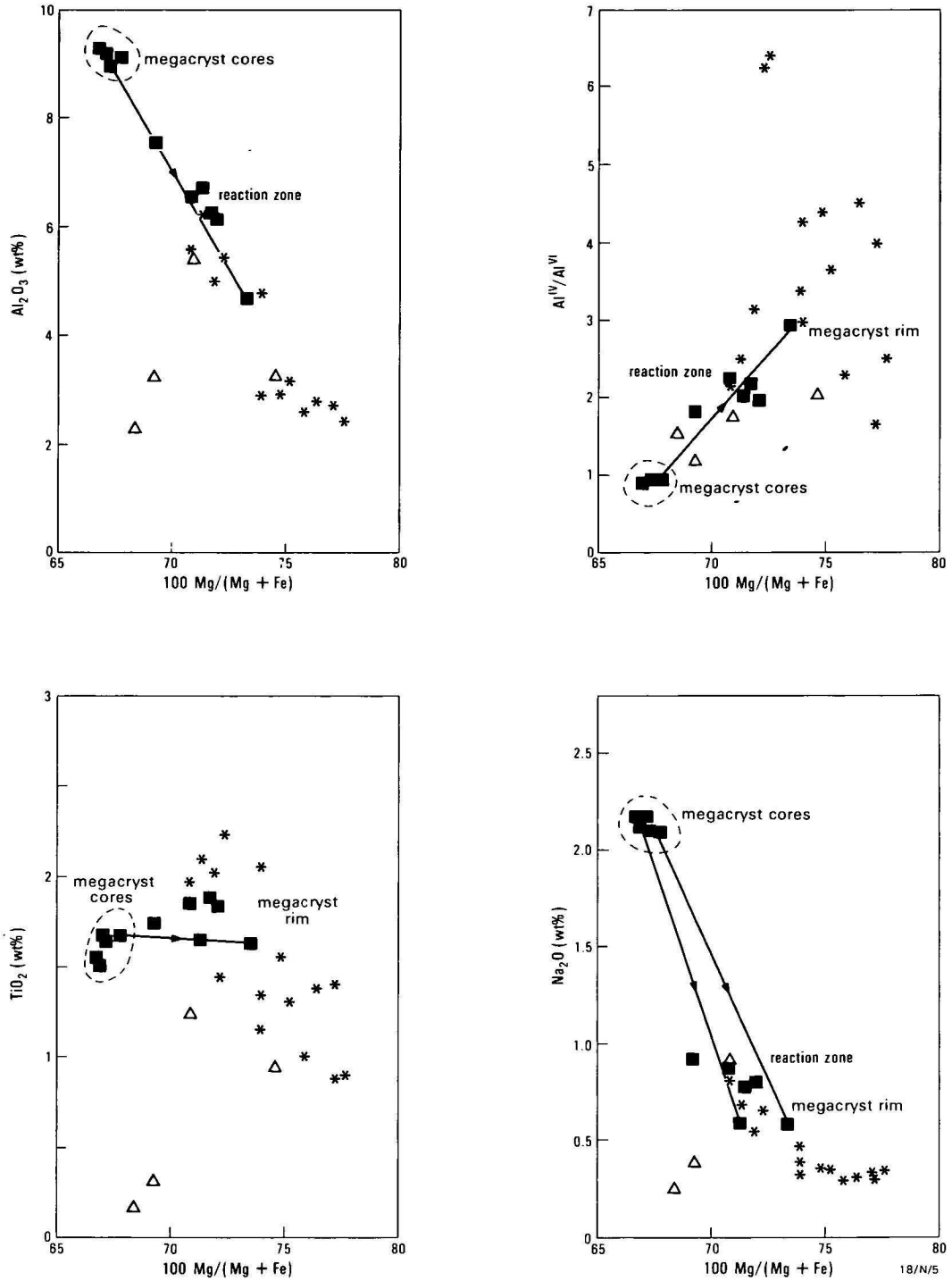

Figure 5. Compositional variation of Al_2O_3, Al^{IV}, TiO_2 and Na_2O with 100 Mg/(Mg+Fe) in pyroxenes from Mount Woolooma minette. Note the clear distinction of the megacryst cores and the trend of the reaction zone and outer rim towards the microphenocryst/groundmass compositions. Symbols as in Figure 4.

Volcanics of the south coast of New South Wales (cf. Joplin, 1971), but alkalis are higher and CaO lower. Wilshire & Binns (1961) reported megacryst-bearing and xenolith-bearing lamprophyres, mostly monchiquite, but few analyses are available; Joplin (1971) cited analyses of several nepheline-monchiquites that are distinctly more undersaturated than the Mount Woolooma lamprophyre.

Discussion

Origin and significance of the megacrysts

Similar megacrysts are widely recorded from alkali basalt suites in eastern Australia and are generally held to have crystallised at high pressure (e.g. Wilshire & Binns, 1961; Binns & others, 1970; Irving, 1974; Wilkinson, 1975; Ellis, 1976; Wass & Irving, 1976; Wass, 1979a). In some evolved rocks of intermediate composition, e.g. hawaiite, mugearite, benmoreite etc., the megacrysts are thought to result from crystal fractionation at high pressure (lower crust or upper mantle) from more mafic parent magmas (basanite, alkali olivine basalt etc.) derived from the mantle (e.g. Green & others, 1974).

The megacrysts in the Mount Woolooma lamprophyre suggest high-pressure crystallisation from the host rock or a more mafic magma. The high Al_2O_3 contents and low Al^{IV}/Al^{VI} ratios of the megacryst pyroxene, particularly, are good

evidence for high-pressure crystallisation (cf. Wass, 1979a). The biotite megacrysts are inferred to have crystallised at high temperature under oxidising conditions, since high Ti in micas is favoured by high temperature and fO_2 (Arima & Edgar, 1981). The solid state deformation shown by some biotites suggests a xenocrystal origin, at least for some of the megacrysts. However, the marked similarity in Al and Ti contents of the megacrysts and the groundmass phlogopite suggests that the megacrysts may have crystallised from a magma with similar TiO_2 and Al_2O_3 content: Barton (1979) found that mica compositions in potassic alkaline rocks were related to bulk magma compositions. Because the Mount Woolooma biotite megacrysts are much more Fe-rich than the equilibrium (groundmass and rim) phlogopite in the rock, a cognate origin requires marked changes in either the Fe-Mg partitioning between mica and melt with temperature, pressure, water pressure, and/or oxygen fugacity, or a change in the $Mg/(Mg+Fe^{2+})$ ratio of the melt at lower pressure (near surface). The latter could arise either by oxidation of Fe^{2+} to Fe^{3+} or a decrease in total Fe in the melt. Oxidation by the reaction biotite + O_2 = phlogopite + Fe-oxide could explain the abundance of magnetite in the groundmass and the presence of magnetite granules at the phlogopite rims. However, the estimated Fe^{3+} contents of the groundmass phlogopites (Fe^{3+} assumed – ΔT = 8-Al-Si) are generally lower than the biotite cores. Thus, if a significant change in oxidation state occurred, it was buffered by the magnetite. The rimming of the titanbiotite megacrysts with coexisting groundmass phlogopite matches Fe-rich brown biotite (Type I mica) in kimberlite containing more Mg-rich groundmass (Type II) mica (cf. Smith & others, 1978). Type I micas are thought to be xenocrystal, perhaps derived from carbonatites (e.g. Smith & others, 1978); the origin of the biotite megacrysts in the Mount Woolooma minette remains obscure.

Relationship of the Mount Woolooma lamprophyre to other igneous rocks in the Scone - Gloucester region.

A wide range of igneous rocks occurs in the Scone - Gloucester area. The lavas of the Eocene Barrington Tops volcanic field (Wellman & McDougall, 1974) cover some 2400 km² and consist mainly of alkali olivine basalt, some tholeiitic olivine basalts, olivine-pyroxene basalts, ankaramites containing megacrysts of clinopyroxene, and rare theralites (Wilkinson, 1969; Mason, 1982). An analysis of an alkali olivine basalt (Table 4) from a small outcrop on the northern flank of Mount Woolooma (Fig. 2) is similar to previously published compositions from the Barrington Tops volcanic field.

Other alkaline basic volcanic and intrusive rocks, many carrying megacrysts or xenoliths, have been reported in the region (Fig. 1). They include: a small leucite(?) monchiquite body (Locality 2; D. Perkin, unpubl. data); 2 monchiquite plugs near Muswellbrook, which contain megacrysts of olivine, orthopyroxene, and possibly clinopyroxene (Localities 3 and 4; Wilshire & Binns, 1961); 2 eclogite localities, one 5 km north of Allyn Brook, 51 km east of Muswellbrook, and the other at Moonan Flat immediately north of Mt Woolooma (Localities 5 and 6; MacNevin, 1977); diamond-bearing 'parakimberlite' volcanic breccia and tuff in Prince Charlie Creek (Locality 7; MacNevin, 1977); 2 kimberlite pipes at Oaky Creek including AuK1 (Locality 8; Wilkinson, 1974; MacNevin, 1977; Stracke & others, 1979); biotite alnoite in the Cobakh River (Locality 9; F.L. Sutherland & J.D. Hollis, pers. comm., 1982); alkali basalt containing peridotite nodules (Locality 10) or peridotite nodules and megacrysts of deformed olivine, clinopyroxene orthopyroxene(?) and spinel (Locality 11; Wilshire & Binns, 1961; Wass & Irving, 1976), and olivine analcimite at Glenbawn Dam containing megacrysts of titanphlogopite and clinopyroxene (Locality 12; Irving, 1974); a carbonate-rich intrusion encountered in drill hole in the Scone area (Locality 13); teschenitic dykes and sills of late Permian-early Triassic age intruding the Permian Singleton Coal Measures in the area between Denman and Muswellbrook (Locality 14; Gamble, in press).

Of this diverse suite those most closely resembling the Mount Woolooma minette are the late Permian - early Triassic syenoteschenites (Gamble, in press). Although poorer in mica and containing abundant analcime, these differentiated slightly ne-normative rocks compare in differentiation indices and normative $An/(An+Ab)$ contents. Differences exist in MgO and TiO_2 contents and in the trace-element abundances. Although no chemical data are available, the megacryst-bearing monchiquite plugs reported by Wilshire & Binns (1961) also show some similarities with the Mount Woolooma minette.

The diverse suite of alkaline igneous rocks in the Scone - Gloucester area dates from at least the late Permian, and was most voluminous in the Barrington Tops volcano in the Eocene. The Mount Woolooma minette is only a minor phase of this activity and its precise relationship to other magmatic episodes and the magmatic evolution of the province are unclear.

Acknowledgements

We thank Dr D. Branagan (Sydney University) for information obtained by student mapping in the Glenbawn region in the period 1966 - 1971, J. Pyke and T. Slezak (BMR) for the chemical analyses, and N.G. Ware (ANU) for access to the TPD probe. Comments on the draft manuscript by M. Duggan, J. Knutson, and the journal referees are gratefully acknowledged. DJP thanks F.L. Sutherland and J.D. Hollis for helpful discussions.

References

Abbott, M.J., 1969 - Petrology of the Nandewar Volcano, N.S.W., Australia. *Contributions to Mineralogy and Petrology*, 20, 115-134.

Arima, M., & Edgar, A.D., 1981 - Substitution mechanisms and solubility of titanium in phlogopites from rocks of probable mantle origin. *Contributions to Mineralogy and Petrology*, 77, 288-295.

Atkinson, W.J., Hughes, F.E., & Smith, C.B., 1984 - A review of the kimberlitic rocks of Western Australia, *In* Kornprobst, J. (editor). Kimberlites and related rocks. *Developments in Petrology*, 11A, 195-225; *Elsevier, Amsterdam.*

Bachinski, W.S., & Scott, R.B., 1979 - Rare earth and other trace element contents of minettes (mica lamprophyres). *Geochimica et Cosmochimica Acta*, 43, 93-100.

Barton, M., 1979 - A comparative study of some minerals occurring in the potassium-rich alkaline rocks of the Leucite Hills, Wyoming, the Vico Volcano, western Italy, and the Toro-Ankole Region, Uganda. *Neues Jahrbuch fur Mineralogie, Abhandlungen*, 137, 113-134.

Binns, R.A., 1969 - High-pressure megacrysts in basanitic lavas near Armidale, New South Wales. *American Journal of Science*, 267-A, 33-49.

Binns, R.A., Duggan, M.B., & Wilkinson, J.F.G., 1970 - High pressure megacrysts in alkaline lavas from north eastern New South Wales. *American Journal of Science*, 269, 132-168.

Ellis, D.J., 1976 - High pressure cognate inclusions in the Newer Volcanics of Victoria. *Contributions to Mineralogy and Petrology*, 58, 149-180.

Ewart, A., Mateen, A., & Ross, J.A., 1976 - Review of mineralogy and chemistry of Tertiary central volcanic complexes in southeast Queensland and northeast New South Wales. *In* R.W. Johnson (editor), Volcanism in Australasia, 21-39; *Elsevier, Amsterdam.*

Ewart, A., Baxter, K., & Ross, J.A., 1980 - The petrology and petrogenesis of the Tertiary anorogenic mafic lavas of southern and central Queensland, Australia — possible implications for crustal thickening. *Contributions to Mineralogy and Petrology*, 75, 129-152.

Forbes, W.C., & Flower, M.J.F., 1974 - Phase relations of titanphlogopite, $K_2Mg_4TiAl_2Si_6O_{20}(OH)_4$: a refractory phase in the upper mantle? *Earth and Planetary Science Letters*, 22, 60-66.

Gamble, J.A., in press - Petrology and geochemistry of differentiated teschenite intrusions for the Hunter Valley, New South Wales, Australia.

Green, D.H., Edgar, A.D., Beasley, P., & Ware, N.G., 1974 - Upper mantle source for some hawaiites, mugearites and benmoreites. *Contributions to Mineralogy and Petrology*, 48, 33-44.

Irving, A.J., 1974 - Megacrysts from the Newer Basalts and other basaltic rocks of southeastern Australia. *Geological Society of America Bulletin*, 85, 1503-1514.

Jahn, B., Sun, S.S., & Nesbitt, R.W., 1979 - REE distribution and petrogenesis of the Spanish Peaks igneous complex, Colorado. *Contributions to Mineralogy and Petrology*, 70, 281-298.

Jaques, A.L., Lewis, J.D., Smith, C.B., Gregory, G.P., Ferguson, J., Chappell, B.W., & McCulloch, M.T., 1984 - The diamond-bearing ultrapotassic (lamproitic) rocks of the West Kimberley region, Western Australia. *In* Kornprobst, J. (editor), Kimberlites and related rocks. *Developments in Petrology*, 11A, 225-255; *Elsevier, Amsterdam.*

Joplin, G.A., 1971 - A petrography of Australian igneous rocks. Second Edition, *Angus and Robertson, Sydney.*

MacNevin, A.A., 1977 - Diamonds in New South Wales. *New South Wales Department of Mineral Resources and Development, Report* 42.

Mason, D.R., 1982 - Stratigraphy of western parts of the Barrington Tops Tertiary volcanic field. *In* Flood, P.G. & Runnegar, B., (editors), New England geology. *Department of Geology, University of New England, Armidale.* 133-139.

Middlemost, E.A.K., 1981 - The Canobolas complex, N.S.W., an alkaline shield volcano. *Journal of the Geological Society of Australia*, 28, 33-49.

Nicholls, I.A., 1974 - Liquids in equilibrium with peridotitic mineral assemblages at high water pressures. *Contributions to Mineralogy and Petrology*, 45, 289-316.

Reed, S.J.B., & Ware, N.G., 1975 - Quantitative electron microprobe analysis of silicates using energy-dispersive X-ray spectrometry. *Journal of Petrology*, 16, 499-519.

Roberts, J., & Oversby, B.S., 1974 - The Lower Carboniferous geology of the Rouchel District, New South Wales. *Bureau of Mineral Resources Australia Bulletin* 147.

Rock, N.M.S., 1977 - The nature and origin of lamprophyres: some definitions, distinctions and derivations. *Earth-Science Reviews*, 13, 123-169.

Roden, M.F., 1981 - Origin of coexisting minette and ultramafic breccia, Navajo Volcanic Field. *Contributions to Mineralogy and Petrology*, 77, 195-206.

Roden, M.F., & Smith, D., 1979 - Field geology and petrology of the Buell Park minette diatreme, Apache Country, Arizona. *In* Boyd, F.R., & Meyer, H.O.A. (editors), Kimberlites, diatremes and diamonds; their geology, petrology and geochemistry. *American Geophysical Union, Washington D.C.*

Roeder, P.L., & Emslie, R.F., 1970 - Olivine-liquid equilibrium. *Contributions to Mineralogy and Petrology*, 29, 275-289.

Rogers, N.W., Bachinski, S.W., Henderson, P., & Parry, S.J., 1982 - Origin of potash-rich basic lamprophyres: trace element data from Arizona minettes. *Earth and Planetary Science Letters*, 57, 305-312.

Sheraton, J.W., & Labonne, B., 1978 - Petrology and geochemistry of acid igneous rocks of northeast Australia. *Bureau of Mineral Resources, Australia, Bulletin* 169.

Smith, J.V., Brennesholtz, R., & Dawson, J.B., 1978 - Chemistry of micas from kimberlites and xenoliths — I. Micaceous kimberlites. *Geochimica et Cosmochimica Acta*, 42, 959-971.

Stracke, K.J., Ferguson, J., & Black, L.P., 1979 - Structural setting of kimberlites in southeastern Australia. *In* Boyd, F.R., & Meyer, H.O.A. (editors), Kimberlites, diatremes, and diamonds: their geology, petrology, and geochemistry. *American Geophysical Union, Washington D.C.* 71-91.

Streckeisen, A., 1978 - Classification and nomenclature of volcanic rocks, lamprophyres, carbonatites, and melilitic rocks: recommendations and suggestions of the IUGS subcommission of the Systematics of Igenous Rocks. *Neues Jahrbuch fur Mineralogie, Abhandlungen*, 134, 1-14.

Velde, D., 1971 - Les lamprophyres à feldspath alcalin et biotite: minettes et roches voisines. *Contributions to Mineralogy and Petrology*, 30, 216-239.

Ware, N.G., 1981 - Computer programs and calibration with the PIBS technique for quantitative electron probe analysis using a lithium-drifted silicon detector. *Computers & Geoscience*, 7, 167-184.

Wass, S.Y., 1979a - Multiple origins of clinopyroxenes in alkali basaltic rocks. *Lithos*, 12, 115-132.

Wass, S.Y., 1979b - Fractional crystallization in the mantle of late-stage kimberlitic liquids — evidence in xenoliths from the Kiama area, N.S.W., Australia. *In* Boyd, F.R., & Meyer, H.O.A. (editors), The mantle sample: inclusions in kimberlites and other volcanics. *American Geophysical Union, Washington D.C.* 366-373.

Wass, S.Y., & Irving, A.J., 1976 - XENMEG : a catalogue of occurrences of xenoliths and megacrysts in volcanic rocks of eastern Australia. *Australian Museum, Sydney.*

Wellman, P., & McDougall, I., 1974 - Potassium-argon ages on the Cainozoic volcanic rocks of New South Wales. *Journal of the Geological Society of Australia*, 21, 247-272.

Wilkinson, J.F.G., 1962 - Mineralogical, geochemical, and petrogenetic aspects of an analcime-basalt from the New England District of New South Wales. *Journal of Petrology*, 3, 192-214.

Wilkinson, J.F.G., 1969 - The Cainozoic igneous rocks of northeastern New South Wales. *Journal of the Geological Society of Australia* 16, 530-541.

Wilkinson, J.F.G., 1974 - Garnet clinopyroxenite inclusions from diatremes in the Gloucester area, New South Wales, Australia. *Contributions to Mineralogy and Petrology*, 46, 275-299.

Wilkinson, J.F.G., 1975 - Ultramafic inclusions and high pressure megacrysts from a nephelinite sill, Nandewar Mountains, northeastern New South Wales, and their bearing on the origin of certain ultramafic inclusions in alkaline volcanic rocks. *Contributions to Mineralogy and Petrology*, 51, 235-262.

Wilshire, H.G., & Binns, R.A., 1961 - Basic and ultrabasic xenoliths from volcanic rocks of New South Wales. *Journal of Petrology*, 2, 185-208.

BMR Journal of Australian Geology & Geophysics, 9, 41–47

Stratigraphic correlations in the Tennant Creek region, central Australia: Warramunga Group, Tomkinson Creek beds, Hatches Creek Group, and Rising Sun Conglomerate

D.H. Blake

The Proterozoic Warramunga Group, as previously mapped around Tennant Creek, is shown to consist of two sequences separated by a major angular unconformity. The older sequence, which is tightly folded and cleaved, hosts the gold-copper-ironstone lodes near Tennant Creek. The younger sequence, exposed north of Tennant Creek, is correlated with the lower Hatches Creek Group south of Tennant Creek. It is overlain conformably by the Tomkinson Creek beds, which are correlated with the middle and upper Hatches Creek Group. The Rising Sun Conglomerate, southeast of Tennant Creek, is a composite unit, consisting of Hatches Creek Group equivalents and unconformably overlying Cambrian rocks.

Introduction

Three long-standing problems concerning the geology of the Tennant Creek region in central Australia (Fig. 1) have been the nature of the contact between the Proterozoic Tomkinson Creek beds in the north and the underlying Warramunga Group, the possible correlation of the Tomkinson Creek beds with the Hatches Creek Group to the south, and the relative age of the Rising Sun Conglomerate. These problems have now been largely resolved, as reported in this paper, by examination and comparison of the sequences exposed near Tennant Creek with those in the Davenport and Murchison Ranges.

The Warramunga Group (Ivanac, 1954; Dodson & Gardener, 1978) hosts the economic gold-copper mineralisation around Tennant Creek. It is probably at least 3000 m thick, consists of mainly turbiditic greywacke, siltstone, and shale, with interlayered felsic volcanics, and is tightly folded, generally cleaved, and regionally metamorphosed to greenschist facies.

The Tomkinson Creek beds (Randal & Brown, 1969; Dodson & Gardener, 1978) are about 9000 m thick in the Tennant Creek region (Mendum & Tonkin, 1978). They consist largely of clean sandstones (quartz arenites and feldspathic quartz arenites, according to the classification of Pettijohn, & others, 1972), but also include siltstones, mudstones, carbonates, and a formation of basaltic lava, the Whittington Range Volcanics.

The Hatches Creek Group (Smith & others, 1961; Blake & others, 1983) overlies the Warramunga Group unconformably in the Davenport and Murchison Ranges, and has a maximum thickness of at least 10,000 m. It is generally similar in lithology to the Tomkinson Creek beds, but includes thick sequences of felsic volcanics and extensive basalt flows.

Both the Tomkinson Creek beds and Hatches Creek Group have been folded into a series of major anticlines and synclines and show the effects of low-grade regional metamorphism. The Warramunga and Hatches Creek Groups, but not the Tomkinson Creek beds, are intruded by granite, and all three units are intruded by dolerite.

The Rising Sun Conglomerate (Ivanac, 1954) overlies the Warramunga Group near the Nobles Nob mine southeast of Tennant Creek, and contains boulders of Hatches Creek Group-type rocks.

Review of previous work

The first systematic geological survey of the Tennant Creek region was by BMR in 1948–1950, and results were reported by Ivanac (1954). Subsequent surveys were carried out in 1958–59 (Crohn & Oldershaw, 1965), 1964 (Dunnet & Harding, 1967), and 1970–71 (Mendum & Tonkin, 1976; summarised in Dodson & Gardener, 1978). A broad reconnaissance survey of the Davenport and Murchison Ranges in 1956 was reported by Smith & others (1961). Reviews of the regional geology have been given by Crohn (1965, 1976) and Le Messurier (1976). Results of isotopic dating of igneous and metamorphic rocks from the Tennant Creek region have been given by Black (1977, 1981, in press).

Warramunga Group relationships

According to Ivanac (1954), the Warramunga Group grades northwards up into sandstone and conglomerate of the Tomkinson Creek beds, an arbitrary conformable contact between the two being taken at the first prominent sandstone ridge. Crohn & Oldershaw (1965), on the other hand, considered that the shape of the contact as shown on Ivanac's map suggested an unconformity. This suggestion was supported by Dunnet & Harding (1967), who stated that north of Tennant Creek the contact is either faulted or obscured by soil, but to the northwest it was a pronounced angular unconformity. Dunnet & Harding thought that there was some evidence to suggest that the Warramunga Group was gently folded, but not cleaved, before the Tomkinson Creek beds were laid down, and that the deposition of the Tomkinson Creek beds predated the main folding, metamorphism, and slaty cleavage development in the region. The contact between the Warramunga Group and Tomkinson Creek beds was also considered to be an unconformity by Crohn (1976), Le Messurier (1976), and Mendum & Tonkin (1976). In their account of the geology of the Tennant Creek region, Mendum & Tonkin did not remark on the pronounced angular unconformity reported by Dunnet & Harding, but claimed that the contact is a slight angular unconformity, best exposed in the ranges 65 km northwest of Tennant Creek, and that the Warramunga Group and Tomkinson Creek beds have had the same structural history.

Smith & others (1961) reported that in the Murchison Range the Warramunga Group is overlain unconformably by the Hatches Creek Group. This relationship has since been confirmed by several workers, including Mendum & Tonkin (1976), and Blake & others (1983). Mendum & Tonkin regarded this unconformity as being at least partly a décollement surface between two sequences of markedly different rock types that developed contrasting styles of folding during the same deformation event.

Tomkinson Creek beds and Hatches Creek Group correlations

Ivanac (1954) and, subsequently, Crohn & Oldershaw (1965) and Mendum & Tonkin (1976) suggested that the Tomkin-

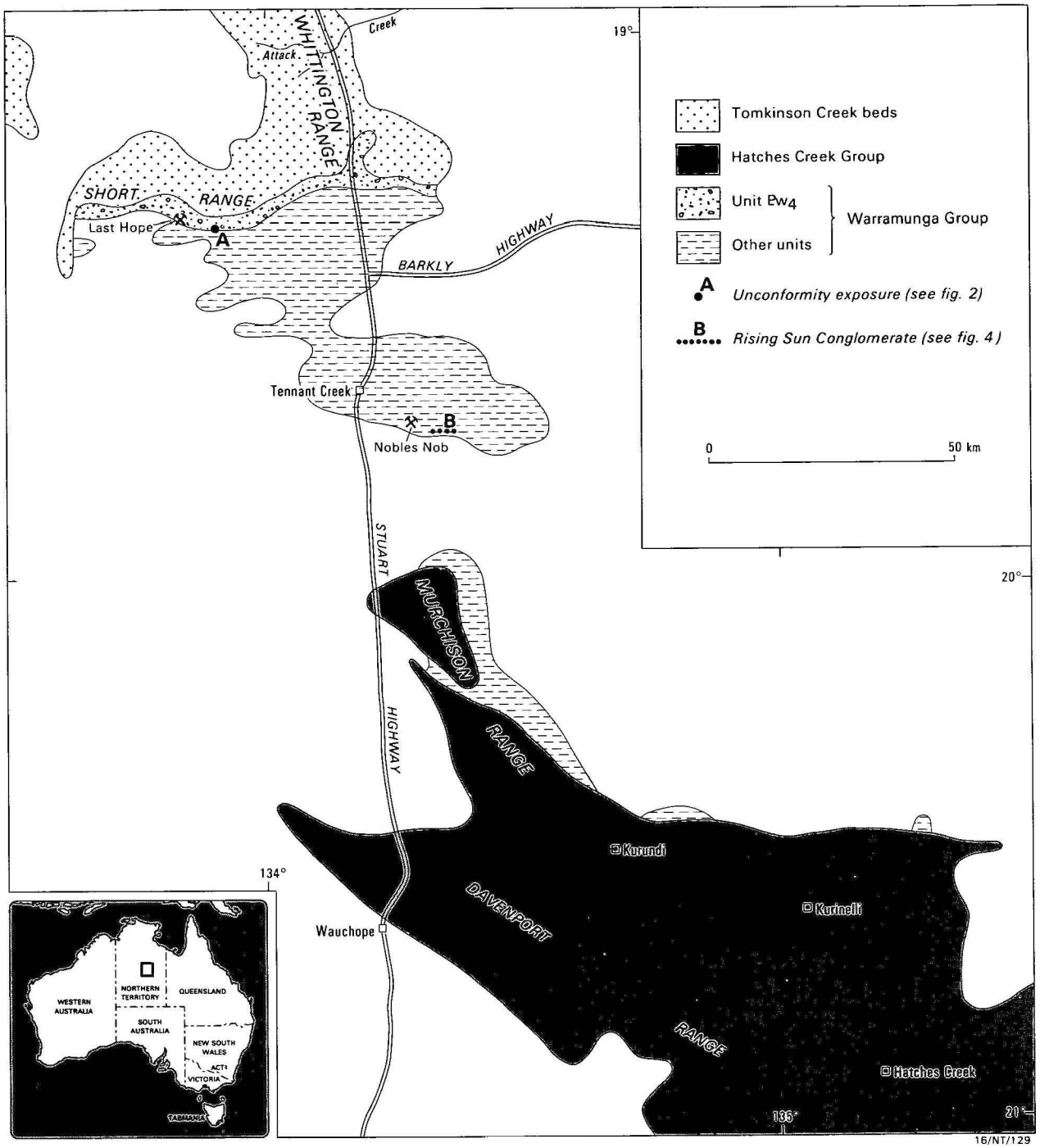

Figure 1. Geological locality map

son Creek beds are correlatives of the Hatches Creek Group. Mendum & Tonkin further suggested that a formation of basaltic lavas within the Tomkinson Creek beds, the Whittington Range Volcanics, correlated with basalt lavas in the Hatches Creek Group near Kurundi.

Rising Sun Conglomerate

As described by Ivanac (1954), the Rising Sun Conglomerate consists of about 15 m of conglomerate and a greater thickness of overlying cross-bedded quartz-rich arenites. It is unconformable on the Warramunga Group, is cut by hematite and quartz veins, and is intruded at its base by tongues of quartz-feldspar porphyry. In a more detailed description, Crohn & Oldershaw (1968) reported the Rising Sun Conglomerate to be about 60 m thick and to be unconformable on, rather than being intruded by, quartz-feldspar porphyry, as well as being unconformable on the Warramunga Group.

Present investigations

Davenport and Murchison Ranges

Recent research in the Davenport and Murchison Ranges has shown that the most extensively exposed sequence, that forming the Hatches Creek Group, can be subdivided into a number of readily mappable and laterally extensive sedimentary and volcanic formations (Fig. 3, Table 1). These are defined by Blake & others (in prep). Especially extensive are three ridge-forming units of white to pale pink or grey cross-bedded quartz arenites containing little or no matrix, the

Table 1. Summary of stratigraphy, Hatches Creek Group

Name	Max thickness (m)	Dominant lithology	Relationships
Yaddanilla Sandstone	1000	Ridge-forming quartz arenite	Conformable on Vaddingilla Formation
Vaddingilla Formation	800	Recessive siltstone, arenite	Conformable on Canulgerra Sandstone
Canulgerra Sandstone	500	Ridge-forming quartz arenite; interbedded recessive arenite, siltstone	Conformable on Lennee Creek Formation
Lennee Creek Formation	1500	Recessive arenite, siltstone, shale	Conformable on Alinjabon Sandstone
Alinjabon Sandstone	750	Ridge-forming quartz arenite, interbedded recessive arenite, siltstone, shale	Conformable on Errolola Sandstone
Errolola Sandstone	1200+	Ridge-forming quartz arenite	Conformable on Kudinga Basalt
Kudinga Basalt	600	Recessive altered basalt	Conformable on Frew River Formation
Frew River Formation	500	Recessive arenite, siltstone, mudstone, calcareous beds	Conformable on Coulters Sandstone
Coulters Sandstone	1000+	Ridge-forming quartz arenite	Conformable on Yeeradgi Sandstone, Arabulja Volcanics, Newlands Volcanics
Newlands Volcanics	2000+	Generally recessive feldspar and quartz-feldspar porphyry	Conformable on Unimbra Sandstone and Yeeradgi Sandstone
Arabulja Volcanics	300	Generally recessive feldspar porphyry	Conformable on Yeeradgi Sandstone
Yeeradgi Sandstone	800	Low-ridge-forming arenite	Conformable on Unimbra Sandstone
Unimbra Sandstone	1000?	Ridge-forming quartz arenite	Conformable on formations of lower Hatches Creek Group; unconformable on Warramunga Group
Epenarra Volcanics	1000+	Recessive felsic lava, pyroclastics rocks; interlayered low-ridge-forming arenite	Unconformable on Warramunga Group; interfingers with Kurinelli Sandstone, Rooneys Formation
Treasure Volcanics	3500?	Recessive felsic lava, interlayered ridge-forming quartz arenite	Conformable on and interfingers with Taragan Sandstone.
Mia Mia Volcanics	2000+	Recessive altered felsic tuff	Overlain by Unimbra Sandstone; base not exposed
Edmirringee Volcanics	1000+	Recessive basaltic and felsic lava	Conformable on and interfingers with Kurinelli Sandstone
Taragan Sandstone	1000?	Ridge-forming pebbly quartz arenite	Conformable on and interfingers with Kurinelli Sandstone; interfingers with Treasure Volcanics
Kurinelli Sandstone	2000?	Ridge-forming quartz arenite; recessive arenite, siltstone	Conformable on and interfingers with Epenarra Volcanics, Edmirringee Volcanics, Rooneys Formation; interfingers with Taragan Sandstone
Rooneys Formation	1200?	Low-ridge-forming to recessive arenite, siltstone	Conformable on and interfingers with Epenarra Volcanics; interfingers with Kurinelli Sandstone

Unimbra, Coulters, and Errolola Sandstones, and a unit of basalt lavas, the Kudinga Basalt, in the middle Hatches Creek Group. The basalt lavas noted by Mendum & Tonkin (1976) near Kurundi belong to the Edmirringee Volcanics of the lower Hatches Creek Group. The Unimbra Sandstone and younger formations form a largely layer-cake type of stratigraphy. The formations of the lower Hatches Creek Group, however, interfinger with one another (Blake & others, 1983), and are intruded by granophyre, dolerite, and gabbro sills, and granite plutons. Arenites in the lower Hatches Creek Group are commonly cross-bedded, but are generally less quartz-rich and contain more matrix material than the younger ridge-forming arenites. Cross-cutting quartz veins are common throughout. The sedimentary rocks of the group represent shallow marine to fluvial deposits (Sweet, *in* Blake & others, 1983), and the associated volcanics may result from both subaerial and subaqueous eruptions.

The Hatches Creek Group has been folded into a series of large, mainly tight, upright anticlines and synclines with an overall southeasterly trend. They are tens of kilometres long and have wavelengths of several kilometres. An axial plane cleavage is developed locally, mainly in the finer grained sedimentary and tuffaceous rocks. The deformation was accompanied by low-grade regional metamorphism and followed by granite intrusion at about 1640 Ma (L.P. Black, personal communication, 1983).

The base of the Hatches Creek Group has been seen only in the north, mainly in the Murchison Range. Here, a marked angular unconformity separates it from the underlying Warramunga Group — moderately to tightly folded greywacke, micaceous siltstone, shale, cherty mudstone, and jaspilite. The folds evident in the Warramunga Group typically have wavelengths of between 100 m and 1 km, limbs intersecting at 45°–90°, variable trends, and, commonly, an axial plane slaty cleavage. They are markedly different in both size and style to those affecting the Hatches Creek Group.

The unconformity between the Warramunga and Hatches Creek Groups, where exposed, has a local relief of several hundred metres. Depressions in the unconformity surface contain felsic lavas, tuffs, and volcaniclastic sediments of the Epenarra Volcanics of the lower Hatches Creek Group, and highs on the unconformity surface are overlain directly by the Unimbra Sandstone of the middle Hatches Creek Group, which elsewhere is conformable on the Epenarra Volcanics. The field evidence is that the Warramunga Group was tightly folded, cleaved, uplifted, and eroded before the Hatches Creek Group was laid down, and was refolded during the deformation of the Hatches Creek Group.

Both the Hatches Creek and Warramunga Groups are overlain unconformably by flat-lying Middle Cambrian conglomerate, sandstone, siltstone, and chert, locally fossiliferous (trilobites, brachiopods, hyolithids), which have been assigned to the Gum Ridge Formation and Sandover Beds of the Georgina Basin succession (e.g., Smith & others, 1961). Conglomerate is present mainly at the base of the Cambrian succession and consists mostly of boulders and cobbles of quartz arenite and conglomeratic arenite, derived from the Hatches Creek Group, in a sparse, poorly sorted, sandy matrix. Interbeds and lenses of indurated fine to coarse-grained sandstone show cross-bedding and ripple

marks. Unlike the Hatches Creek and Warramunga Groups, the Cambrian rocks are not cut by quartz veins or igneous intrusions.

Whittington and Short Ranges

On the Tennant Creek 1:250 000 geological map (Dodson & Gardener, 1978), the Whittington and Short Ranges north of Tennant Creek (Fig. 1) are shown as being formed of Tomkinson Creek beds overlying unit Pw$_4$ of the Warramunga Group. The Tomkinson Creek beds here have been subdivided into five formations (Mendum & Tonkin, 1976), details of which are given in Table 2. The basal part consists of pale cross-bedded quartz arenites containing sparse to abundant pebbles of mainly vein quartz and quartzite. These and younger arenites of the Tomkinson Creek beds are identical in lithology to arenites in the middle and upper Hatches Creek Group. The basal beds overlie Warramunga Group unit Pw$_4$, a sequence of reddish-brown, lithic or feldspathic arenites with interbedded, locally cleaved siltstone and, in places, quartz arenite like that in the overlying basal Tomkinson Creek beds; many of the arenites are cross-bedded. Bedding in this sequence is parallel to that of the overlying Tomkinson Creek beds, and nowhere has an angular unconformity been found to separate the two sequences. Both sequences are intruded by what appear to be sills of recessive, intensely weathered dolerite.

On the south side of the Short Range, the Tomkinson Creek beds and underlying unit Pw$_4$ have very steep to vertical dips and face consistently north, forming a series of long, parallel, easterly trending, strike ridges up to 30 m high. South of these are lower hills formed of tightly folded and commonly cleaved greywacke, siltstone, and shale, mapped as unit Pw$_3$ of the Warramunga Group by Mendum & Tonkin (1976). Although contacts between Pw$_3$ and Pw$_4$ are generally concealed, a major angular unconformity clearly separates the two units, as the east-trending bedding in Pw$_4$ cuts obliquely across bedding in adjacent Pw$_3$ rocks. An exposure of this unconformity was found at grid reference 38518609 (Fig. 2; locality A in Fig. 1), where subvertical northerly striking beds of greywacke (Pw$_3$) are overlain by arenites of Pw$_4$ dipping 85° north. A few hundred metres north of this exposure, folded greywacke is again exposed: here, it is faulted against north-dipping arenites of Pw$_4$ to the south and is inferred to be overlain unconformably by north-dipping Pw$_4$ to the north.

Lithological comparison of the sequences exposed in the Whittington and Short Ranges with those in the Murchison and Davenport Ranges indicates that unit Pw$_4$ of the Warramunga Group probably correlates with the lower Hatches Creek Group, and the basal part of the Tomkinson Creek beds probably correlates with the Unimbra Sandstone of the middle Hatches Creek Group. Unit Pw$_3$ and other units of the Warramunga Group, except Pw$_4$, are equivalent to the Warramunga Group exposed in the Murchison Range. Proposed correlations are shown in Figure 3.

Rising Sun Conglomerate outcrop area

Rocks that have been mapped as Rising Sun Conglomerate form a low east-trending strike ridge 15–20 km east-southeast of Tennant Creek (Fig. 1). This ridge (Fig. 4) is separated from irregular steep-sided hills and ridges to the north, formed of folded and cleaved greywacke and siltstone of the Warramunga Group (unit Pw$_6$ of Mendum & Tonkin, 1976, and Dodson & Gardener, 1978), by a depression, in which there are scattered exposures of pinkish quartz-feldspar porphyry.

The porphyry has fragmental and eutaxitic textures, and represents an ignimbritic extrusion. Its northern edge cuts across bedding in the Warramunga rocks, and is highly irregular in detail, indicating that it overlies the Warramunga Group with an erosional unconformity. To the south, it grades up into highly altered purplish tuff, containing quartz

Table 2. Summary of stratigraphy, Tomkinson Creek beds (mainly after Mendum & Tonkin, 1976)

Name	Max thickness (m)	Dominant lithology	Relationships
Attack Creek Formation	800+	Recessive calcareous and dolomitic siltstone, mudstone and arenite in lower part; low-ridge-forming quartz arenite and recessive beds in upper part	Conformable on Short Range Sandstone
Short Range Sandstone	800	Ridge-forming quartz arenite	Conformable on Morphett Creek Formation
Morphett Creek	3000?	Ridge-forming quartz arenite in lower part; recessive mudstone, siltstone, and arenite in upper part	Conformable on Whittington Range Volcanics
Whittington Range	450	Recessive weathered basalt lava	Conformable on Hayward Creek Formation
Hayward Creek Formation	3000?	Ridge-forming quartz arenite, pebbly near base	Conformable on rocks mapped as unit Pw$_4$ of Warramunga Group

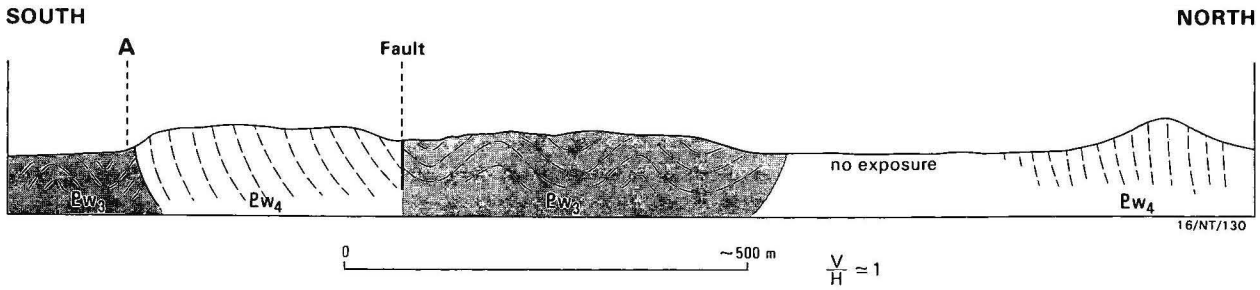

Figure 2. Section from south to north across locality A on the south side of the Short Range (see Fig. 1), showing relationships between units Pw$_3$ and Pw$_4$.
A marked angular unconformity is exposed at A. (Folding in Pw$_3$ is schematic)

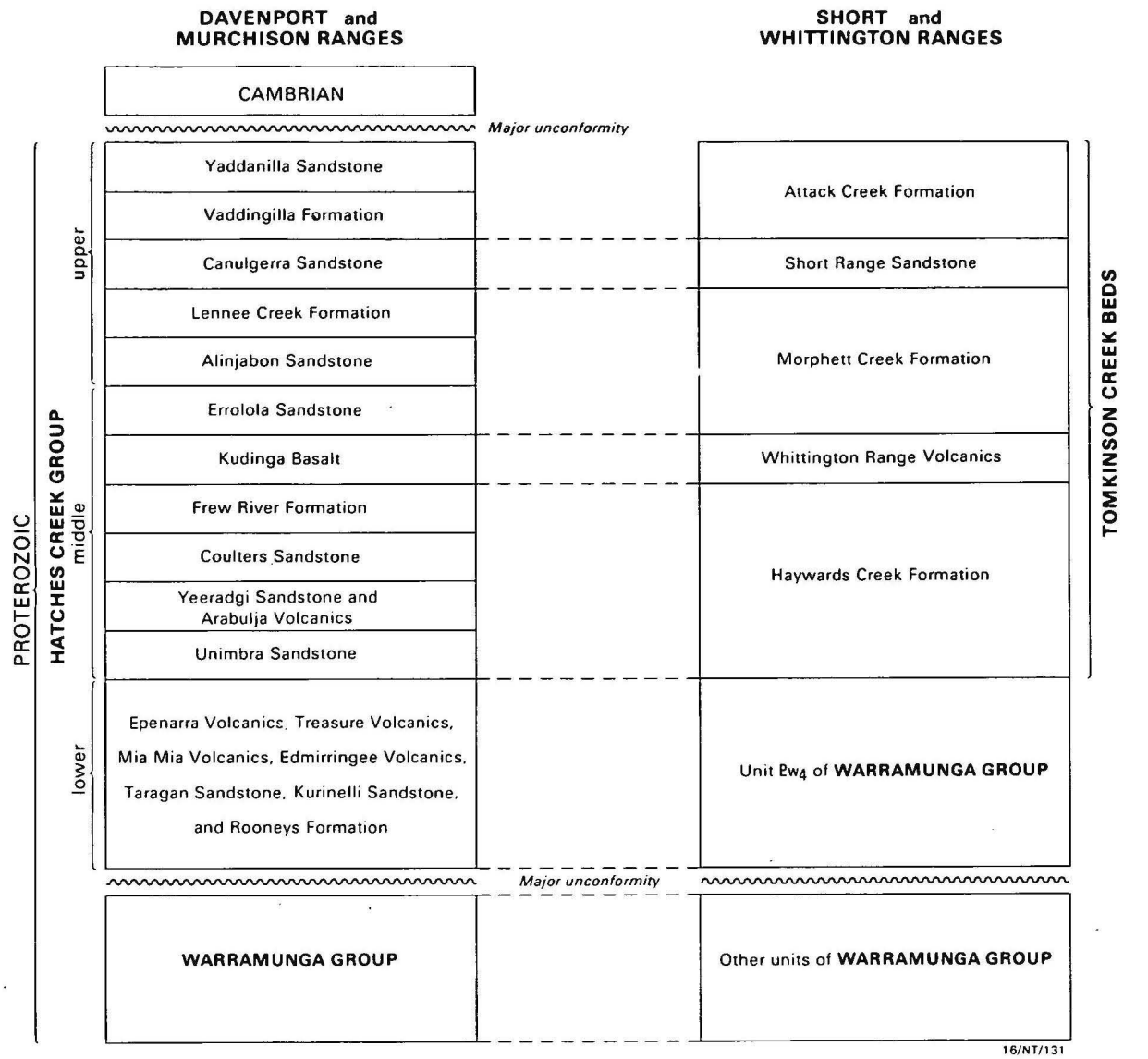

Figure 3. Correlations of the sequences exposed in the Davenport and Murchison Ranges south of Tennant Creek with those in the Short and Whittington Ranges north of Tennant Creek

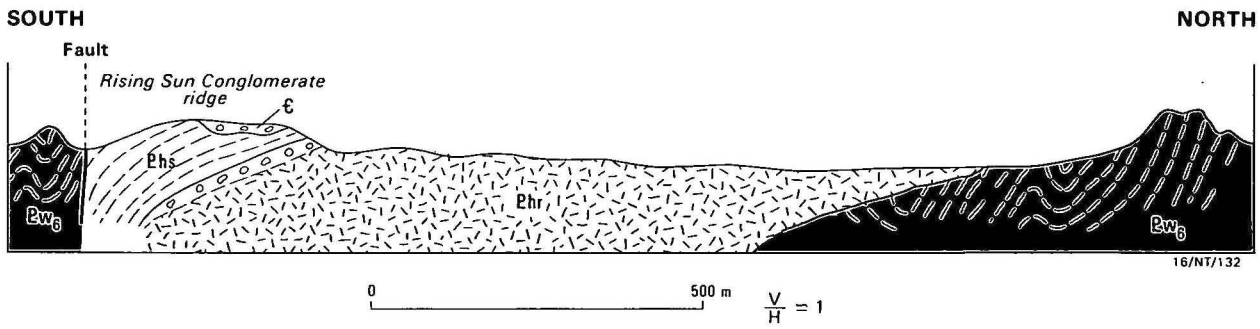

Figure 4. Section from south to north across the Rising Sun Conglomerate ridge (see Fig. 1 for location).
Pw_6, Warramunga Group; Phr, correlative of the Epenarra Volcanics, Hatches Creek Group; Phs, correlative of the Unimbra Sandstone, Hatches Creek Group; €, Cambrian conglomerate. (Folding in Pw_6 is schematic)

and altered feldspar phenocrysts. The tuff is overlain by bedded conglomerate 0–6 m thick, dipping 20° south, and consisting of well-rounded to subangular pebbles and cobbles, mostly of fine-grained quartzite, in a purplish volcaniclastic matrix similar in appearance to the underlying tuff.

The conglomerate and tuff are succeeded conformably by cross-bedded quartz arenite, which forms the bulk of the Rising Sun Conglomerate ridge. The quartz arenite is mainly whitish to pale pink and medium-grained, and some is slightly feldspathic. Many bedding planes are strewn with mudstone/siltstone pellets. There are also beds of maroon fine-grained arenite and siltstone in the predominantly quartz arenite sequence, which is probably about 60 m thick (Crohn & Oldershaw, 1965), and some cross-cutting quartz veins. Bedding steepens to the south, where the sequence is faulted against Warramunga Group rocks.

On the crest of the ridge, the southerly dipping arenites are overlain unconformably by coarse conglomerate containing some flat-lying lenses of ripple-marked, medium to fine-grained lithic arenite. The conglomerate is formed of well-rounded to subrounded boulders and cobbles, mainly of quartz arenite and pebbly to conglomeratic arenite of Hatches Creek Group type, in a generally sparse sandy matrix. Boulders derived from this conglomerate partly mantle the sides of the ridge. The unconformity beneath the conglomerate is an irregular erosional surface, cutting across bedding in the underlying sequence, and has a local relief of several metres. Similar boulder conglomerate is exposed on a low mound north of the ridge about 1.8 km southeast of the Nobles Nob mine, where it may lie directly on Warramunga Group rocks.

By analogy with the sequences exposed in the Davenport and Murchison Ranges, the following correlations can be made: the ridge-forming arenites correlate with the Unimbra Sandstone of the middle Hatches Creek Group, the conformably underlying conglomerate, tuff, and porphyry are correlatives of the Epenarra Volcanics of the lower Hatches Creek Group, and the unconformably overlying boulder conglomerate is equivalent to that commonly present at the base of the middle Cambrian Gum Ridge Formation and Sandover beds.

Implications for mineral exploration

With one possible exception, the lodes in the Tennant Creek region are confined to those Warramunga Group rocks that predate the Hatches Creek Group. The exception is at the Last Hope gold mine (Ivanac, 1954), situated 50 km northwest of Tennant Creek (Fig. 1), where the host rocks for the mineralisation may belong to unit Pw_4, equivalent to the lower Hatches Creek Group. At this mine, the gold occurs in quartz veins cutting sandstone, siltstone, shale, and probably dolerite, an occurrence similar to that found near Hatches Creek and Kurinelli (Ryan, 1961; Blake & Wyche, 1983) in the Davenport Range, but not elsewhere in the Tennant Creek goldfield. At the other Tennant Creek mines, the gold and copper lodes are associated with ironstones (quartz-hematite- magnetite bodies). The Hatches Creek Group and correlatives are not considered to be prospective for gold and copper-bearing ironstone lodes of the Tennant Creek type, although they are prospective for auriferous quartz vein lodes, especially in the vicinity of altered dolerite.

Conclusions

The Warramunga Group north of Tennant Creek, as described by Ivanac (1954), Mendum & Tonkin (1976), and Dodson & Gardener (1978), includes correlatives of the lower Hatches Creek Group. These correlatives, which have been mapped mainly as unit Pw_4 of the Warramunga Group, are overlain conformably by the Tomkinson Creek beds, and overlie, with a marked angular unconformity, rocks mapped as unit Pw_3 of the Warramunga Group. They need to be defined as a separate stratigraphic unit, because they belong to neither the Warramunga Group *sensu stricto* nor the Tomkinson Creek beds of Randal & Brown (1969) and Dodson & Gardener (1978).

Unit Pw_3 and other units of the Warramunga Group exposed near Tennant Creek (except Pw_4) belong to the Warramunga Group *sensu stricto*. They correspond in general to the Warramunga Group rocks in the Murchison Range to the south, and were tightly folded, cleaved, metamorphosed, and eroded before the Tomkinson Creek beds and the Hatches Creek Group and their correlatives were deposited.

The Tomkinson Creek beds in the Short and Whittington Ranges, north of Tennant Creek, can be correlated with the middle and upper parts of the Hatches Creek Group in the Murchison and Davenport Ranges. The Whittington Range Volcanics, a basaltic formation within the Tomkinson Creek beds, probably correlate with the Kudinga Basalt in the middle Hatches Creek Group.

The Rising Sun Conglomerate of previous workers consists partly of southerly dipping Hatches Creek Group equivalents (correlatives of the Epenarra Volcanics of the lower Hatches Creek Group and the conformably overlying Unimbra Sandstone of the middle Hatches Group), which overlie folded Warramunga Group rocks unconformably, and partly of flat-lying Cambrian conglomerate, which is unconformable on the Hatches Creek Group equivalents.

Gold-copper-ironstone lodes of the Tennant Creek type are probably confined to those Warramunga Group rocks that predate the Hatches Creek Group.

Acknowledgements

Critical reviews of the manuscript by A.J. Stewart and R.S. Needham are gratefully acknowledged.

References

Black, L.P., 1977 – A Rb–Sr geochronological study in the Proterozoic Tennant Creek Block, central Australia. *BMR Journal of Australian Geology & Geophysics*, 2, 111–122.

Black, L.P., 1981 – Age of the Warramunga Group, Tennant Creek Block, Northern Territory. *BMR Journal of Australian Geology & Geophysics*, 6, 253–257.

Black, L.P., in press – U-Pb zircon ages and a revised chronology for the Tennant Creek Inlier, N.T. *Australian Journal of Earth Sciences.*

Blake, D.H., & Wyche, S., 1983 – Geology of the Hatches Creek region 1:100 000 map sheet, Northern Territory. *Bureau of Mineral Resources, Australia Record* 1983/18.

Blake, D.H., Stewart, A.J., Sweet, I.P., & Hoatson, D.M., 1983 – Project 2B.04: Davenport gold-tungsten province. *Bureau of Mineral Resources, Australia, Yearbook* 1983.

Blake, D.H., Stewart, A.J., Sweet, I.P., Wyche, S., & Horsfall, C.L., in preparation. Definitions of newly named and revised Precambrian rock units in the Davenport and Murchison Ranges, central Australia (Northern Territory). *Bureau of Mineral Resources, Australia, Report 257.*

Crohn, P.W., 1965 – Tennant Creek gold and copper field. *In* McAndrew, J. (editor), Geology of Australian ore deposits. Second Edition, *Eighth Commonwealth Mining and Metallurgical Congress, Australia and New Zealand 1965 Publications*, 1, 176–182.

Crohn, P.W., 1978 - Tennant Creek-Davenport Proterozoic Basins - regional geology and mineralization. *In* Knight, C.L. (Editor), Economic geology of Australia and New Guinea. Volume 1 - Metals. *Australasian Institute of Mining and Metallurgy, Monograph* 5, 421-424.

Crohn, P.W., & Oldershaw, W., 1965 - The geology of the Tennant Creek one mile sheet area, N.T. *Bureau of Mineral Resources, Australia, Report* 83.

Dodson, R.G., & Gardener, J.E.F., 1978 - Tennant Creek, Northern Territory - 1:250 000 Geological Series. *Bureau of Mineral Resources, Australia Explanatory Notes* 58/5314.

Dunnet, D., & Harding, R.R., 1967 - Geology of the Mount Woodcock 1-mile sheet area, Tennant Creek, N.T. *Bureau of Mineral Resources, Australia, Report* 114.

Ivanac, J.F., 1954 - The geology and mineral deposits of the Tennant Creek Gold-field, Northern Territory. *Bureau of Mineral Resources, Australia, Bulletin* 22.

Le Messurier, P., 1976 - Notes on the Tennant Creek gold-copper-bismuth field. *In* Stewart, A.J., & others, Precambrian structures and metamorphic rocks of central Australia and Tennant Creek, N.T. *25th International Geological Congress, Excursion Guide* 47C.

Mendum, J.R., & Tonkin, P.C., 1976 - Geology of Tennant Creek 1:250 000 Sheet area, Northern Territory. *Bureau of Mineral Resources, Australia, Record* 1976/68 *BMR Microform* MF96.

Pettitjohn, F.J., Potter, P.E., & Siever, R., 1972 - Sand and sandstone. *Springer-Verlag, Berlin.*

Randal, M.A., & Brown, M.C., 1969 - Helen Springs, Northern Territory — 1:250 000 Geological Series. *Bureau of Mineral Resources, Australia, Exploratory Notes* SE/53-6.

Ryan, G.R., 1961 - The geology and mineral resources of the Hatches Creek wolfram field, Northern Territory. *Bureau of Mineral Resources, Australia, Bulletin* 6.

Smith, K.G., Stewart, J.R., & Smith, J.W., 1961 — The regional geology of the Davenport and Murchison Ranges, Northern Territory. *Bureau of Mineral Resources, Australia, Report* 58

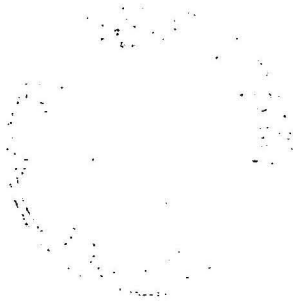

BMR Journal of Australian Geology & Geophysics, 9, 49-68

Structure and evolution of the southern Solomon Sea region

H.L Davies[1] P.A. Symonds[1] & I.D. Ripper[2]

The evolution of the southern Solomon Sea region is deduced from a review of geological, geophysical, and bathymetric data, and previously unpublished seismic reflection profiles. Although the Solomon Sea is bounded to the north by a classical active arc-trench subduction system, the situation to the south is less certain. There, the Solomon Sea is bounded to the north by a classical active arc-trench Woodlark Rise. On seismic profiles, the Trobriand Trough has the appearance of an active trench, and it is associated with active andesite volcanoes. But it is virtually aseismic, indicating that it is inactive or that subduction is proceeding only slowly. If the Trough is active, then it forms the southwestern boundary of the Solomon Plate. If it is inactive, the plate boundary may be transitional, coinciding with a diffuse zone of shallow earthquakes on the Papuan peninsula. The southeastern boundary may be a postulated transform fault on the line of the Woodlark Rise. The lithosphere of the Solomon Sea Basin probably formed by back-arc spreading in the Early Tertiary. As a result of subduction to the northeast, northwest, and southwest, the lithosphere has been anticlinally folded about east-west and north-south axes, causing elevation of the Huon Peninsula and southern New Ireland, and the development of small flanking extensional basins. Miocene to Holocene volcanics of southeastern Papua mostly have the character of an arc-trench suite, and are probably related to Miocene-Quaternary subduction at the Trobriand Trough. The Trobriand Basin, an east-west trending basin south of the Trobriand Trough, contains up to 5000 m of Miocene and younger sediments, and probably developed as a fore-arc basin related to subduction at the Trobriand Trough. Seismic reflection profiles indicate that the Trobriand Basin extends further east than was previously recognised and is bounded southeastwards by rifting associated with the formation of the Woodlark Basin. The same rifting caused Plio-Quaternary elevation of the D'Entrecasteaux Islands and Papuan peninsula, and the development of small rift basins, such as the Goodenough Basin, and is linked with rhyolite volcanism on Fergusson Island.

Introduction

The Solomon Sea is one of several marginal seas and small ocean basins that characterise the Melanesian borderland north and northeast of the Australian continent. Lying between the Solomon Islands and New Guinea, it is bounded on the north by the islands of New Britain and New Ireland and on the south by those of southeast Papua (Figs. 1, 2).

The main morphologic features of the Solomon Sea (Fig. 2) are a rhomb-shaped central basin (the Solomon Sea Basin), 700 km long and 350 km wide; the New Britain Trench, to the northwest and northeast; and the Trobriand Trough and Woodlark Rise, to the south and southeast, respectively. The floor of the central basin lies at water depths of 3-5 km; it is broadly arched in the east and more tightly so in the west, about an east-west axis; and is also broadly arched about a north-south axis.

The New Britain Trench is 6-8.5 km deep, and remarkable for a 70° change in strike between 152°30' and 153°10'E. In the west, it appears to bifurcate: a narrow trough extends westward to a closed basin, which we have termed the Finsch Deep (from the nearby Finsch coast of the Huon Peninsula), and a broader trough extends southwestward to form what we have termed the 149° Embayment (centred on 149°E).

The Trobriand Trough, 5-5.3 km deep and 300 km long, is broader in profile and shallower than the New Britain Trench. It is bounded southward by the Trobriand Platform, a broad reef-strewn shallow shelf that extends from the Papuan peninsula eastward to the Woodlark Rise. The Woodlark Rise is a broad elevated area less than 1 km deep, extending northeast from Woodlark Island, and bounded southwards by the Woodlark Basin.

A broad closed basin northwest of Bougainville Island is here termed the Feni Deep (from nearby Feni Island), and there are several small basins between the D'Entrecasteaux Islands and the Papuan peninsula, and narrow troughs located centrally in the Huon Gulf and St George's Channel (Fig. 3).

Purpose of study and main conclusions

In this paper we address the question of the structure and evolution of the southern Solomon Sea region. The structure of the northern and northeastern Solomon Sea is relatively simple, and we discuss this only briefly. We focus attention, rather, on the Solomon Sea Basin itself, and on its complex southern margin and adjacent platforms, basins, and land areas. For this area, we present a review of regional geological and geophysical data and, in particular, some previously unpublished seismic reflection profiles.

We conclude that the floor of the Solomon Sea Basin is a doubly arched segment of oceanic lithosphere that is, or was until recently, being subducted on three sides, leaving only its

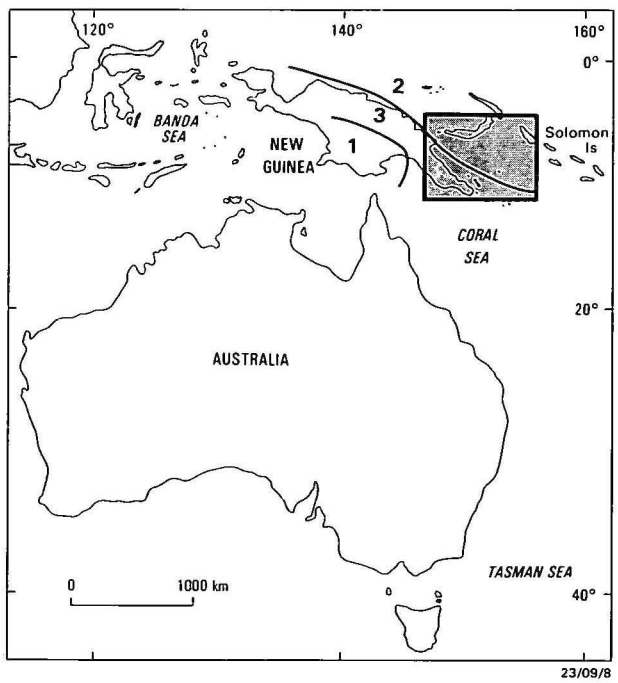

Figure 1. Locality map, showing the three major structural divisions of Papual New Guinea.
(1) craton and epi-cratonic sediments (2) marginal seas and islands constructed by Cainozoic volcanic activity, and (3) complex zone of interaction, including elements of (1) and (2) and deep-seated metamorphic and ultramafic rocks.

[1]Division of Marine Geosciences & Petroleum Geology, BMR
[2]Geophysical Observatory, Geological Survey of Papua New Guinea, PO Box 323, Port Moresby, PNG.

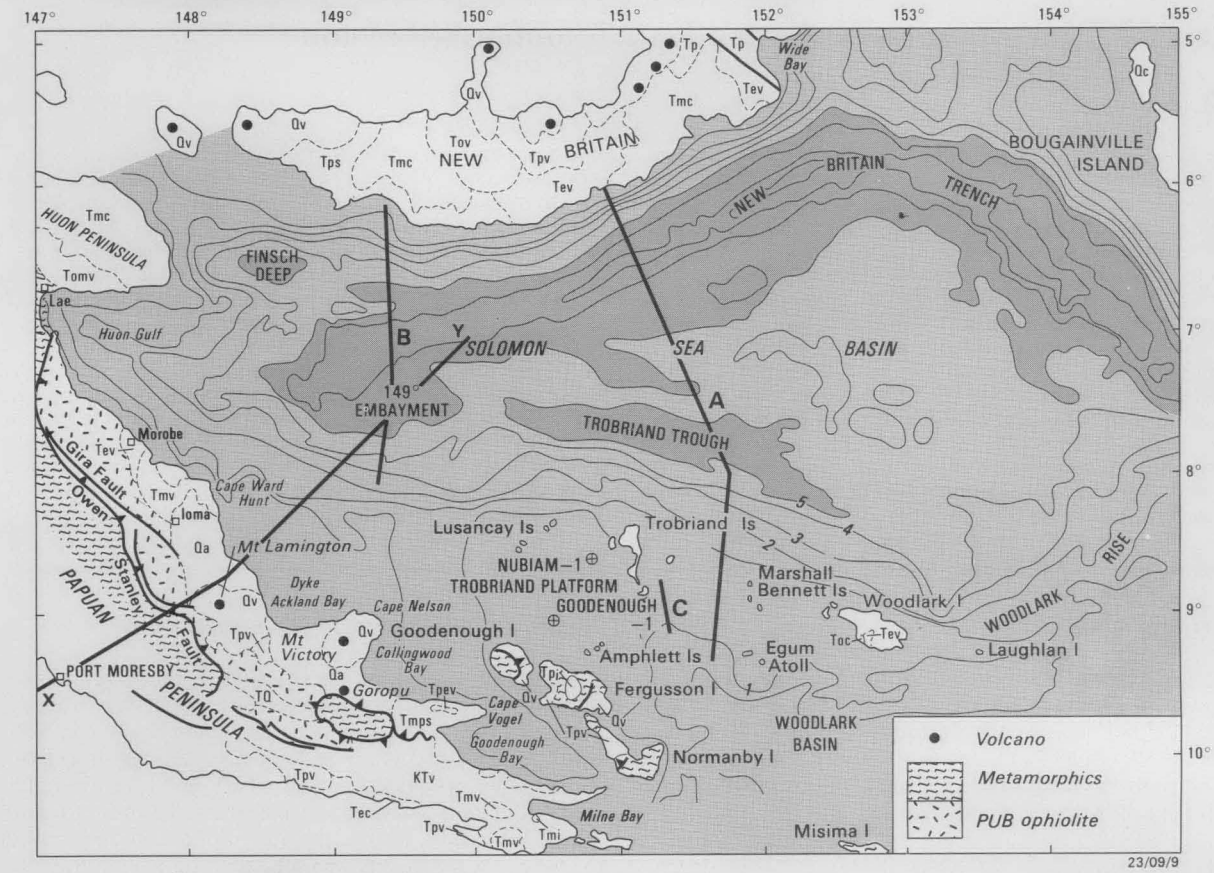

Figure 2. Solomon Sea region geology and bathymetry.

K–Cretaceous, T–Tertiary, Q–Quaternary, pe–Palaeocene, e–Eocene, o–Oligocene, m–Miocene, p–Pliocene, a–alluvium, v–volcanics, s–sediments, c–carbonate, i–intrusive rocks. Shows locations of crustal structure section X-Y and seismic profiles: A – Gulf profile (Fig. 8); B – BMR profile (Fig. 9); C – BMR profile (Fig. 10). Oil exploration well Nubiam-1 and Goodenough-1 are shown. Bathymetric contours at 1 km intervals.

southeastern flank as a transform-type passive margin. Southward subduction in the Neogene–Quaternary was related to the development of the Trobriand Basin on the Trobriand Platform and to Neogene–Quarternary andesitic volcanism in southeastern Papua. Since the Pliocene, this tectonic and volcanic regime has been disturbed by rifting associated with the opening of the Woodlark Basin. The physical character of the Solomon Sea Basin lithosphere is compatible with an Early Tertiary age.

Regional setting

Papua New Guinea geology may be described in terms of three provinces (Fig. 1): (1) a stable craton in the southwest, (2) a region of marginal seas and islands constructed by Cainozoic volcanic activity in the northeast, and, between the two, (3) a structurally complex zone that includes elements of both the other provinces and deep-seated metamorphic and ultramafic rocks. The central complex zone forms most of the higher ground along the axis of the island of New Guinea; it has been termed the New Guinea mobile belt (Dow & others, 1972; Bain, 1973; Dow, 1977) or the (central) orogenic belt (Jaques & Robinson, 1977; Davies, 1978; R.W. Johnson, 1979). The Solomon Sea lies between provinces (2) and (3).

In plate tectonic terms, the Solomon Sea Basin coincides with, or at least forms part of, the Solomon Plate, one of several minor plates that occupy a zone between the Indo-Australian and Pacific Plates in the Papua New Guinea region (Fig. 3; Davies & Smith, 1971; Johnson & Molnar, 1972; Curtis, 1973; Krause, 1973; Denham, 1973). The northern boundary of the Solomon Plate is marked by the New Britain Trench (Denham, 1969; Johnson & Molnar, 1972; R.W. Johnson, 1979). The southern boundary is more complex, and is discussed more fully in a separate section of the paper. It may coincide with the Woodlark Rise (this paper) and the Trobriand Trough (Hamilton, 1979; Ripper, 1982b; this paper), or with the Woodlark Basin spreading ridge–transform system and a diffuse zone or variety of alignments on or near the Papuan peninsula (Johnson & Molnar, 1972; Curtis, 1973; Luyendyk & others, 1973; Krause, 1973; Taylor, 1975; and this paper).

Convergence of the Indo-Australian and Pacific plates is estimated to be at a rate of 10–11 cm/yr on azimuth about 070° (Le Pichon, 1970), and convergence of the Solomon and South Bismarck minor plates, 9.2–12.5 cm/yr (review of other authors by R.W. Johnson, 1979).

Geology

In this section we briefly review the geology of the land areas surrounding the Solomon Sea and the offshore Trobriand Basin as revealed in two exploratory wells. The land areas have been mapped by the Bureau of Mineral Resources and the Geological Survey of Papua New Guinea, and the results reported in 1:250 000-scale maps and explanatory notes, and in some wider-ranging papers (e.g., Blake & Miezitis, 1967; Davies & Smith, 1971; Jaques & Robinson, 1977; Page & Ryburn, 1977).

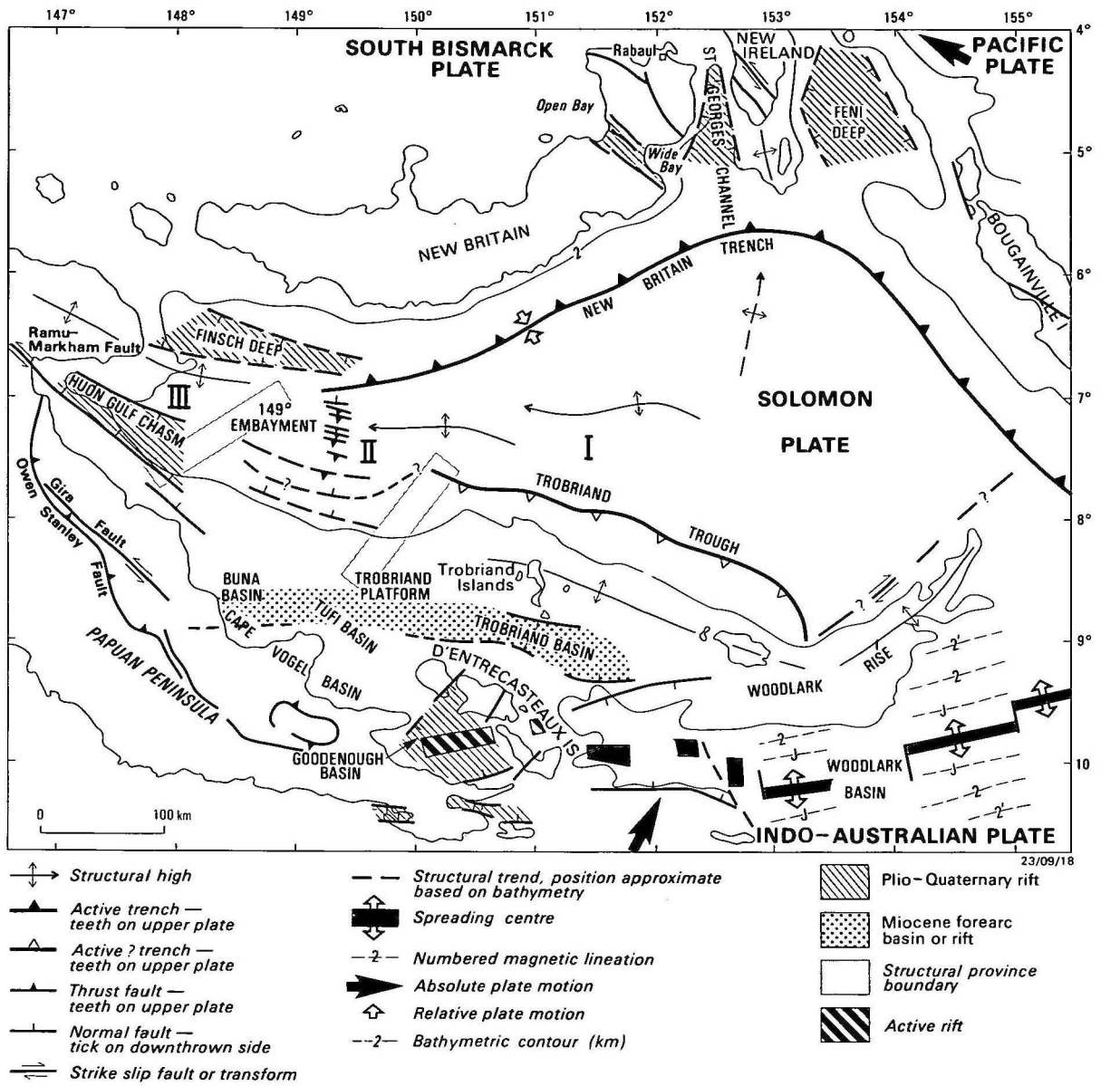

Figure 3. Structural interpretation map of the Solomon Sea region.
Shows the major structural elements and faults, and structural provinces (I, II and III) along the southern margin of the Solomon Sea Basin. The Trobriand Trough is a trench which is either inactive or associated with a slow rate of subduction (see text). Magnetic lineation numbering in the Woodlark Basin is after Weissel & others (1982). The Trobriand, Tufi, Buna and Goodenough Basins are all considered to be sub-basins of the Cape Vogel Basin following Bickel (1976).

The islands northwest and northeast of the Solomon Sea, and the Huon Peninsula were constructed by Cainozoic island-arc volcanism and associated sedimentation. On New Britain, late Eocene volcanics are partly overlain by less widely developed late Oligocene volcanics (Page & Ryburn, 1977). On the Huon Peninsula, the Eocene rocks are predominantly argillaceous and grade upwards into late Oligocene and early Miocene volcanics (Jaques & Robinson, 1977). On New Ireland, the oldest dated volcanics and intrusives are Oligocene (Hohnen, 1978), and on Bougainville Island, probably Oligocene (Blake & Miezietis, 1967). On all the islands and the Huon Peninsula, the older volcanics are overlain by early to middle Miocene carbonate, which, on New Britain and Bougainville, is in turn overlain by Plio-Quaternary volcanics.

Basement geology of the southern Solomon Sea region

The geology of the southern Solomon Sea region is summarised in Fig. 4. The basement rocks of the Papuan peninsula and adjacent islands formed by continent-island arc collision in the Eocene (Davies & Smith, 1971; Davies, 1980a). Metamorphosed partly Cretaceous sediments and Late Cretaceous metabasalt of the subducted plate now form the main range of the Papuan penisula and the high ground of the adjacent islands. These are overlain, with faulted contact, by peridotite and ?Cretaceous gabbro and basalt of the Papuan ultramafic belt ophiolite (PUB ophiolite, Davies, 1968, 1971, 1980a, 1980b), which are, in turn, overlain by Palaeocene and Eocene island arc-type volcanics (Tev and Tpev in Fig. 2; Davies, 1980a; Walker & McDougall, 1982). Late Cretaceous and middle Eocene submarine tholeiites of the southeastern peninsula (KTv in Fig. 2; Kutu volcanics of Smith & Davies, 1976) may be part of the same collision system.

Lava, pillow lava, pyroclastics, and sediments that form the basement of Woodlark Island are probably part of the Palaeocene–Eocene island arc. They have not been dated, but are overlain unconformably by late Oligocene limestone that contains a re-worked probable-Eocene large benthonic

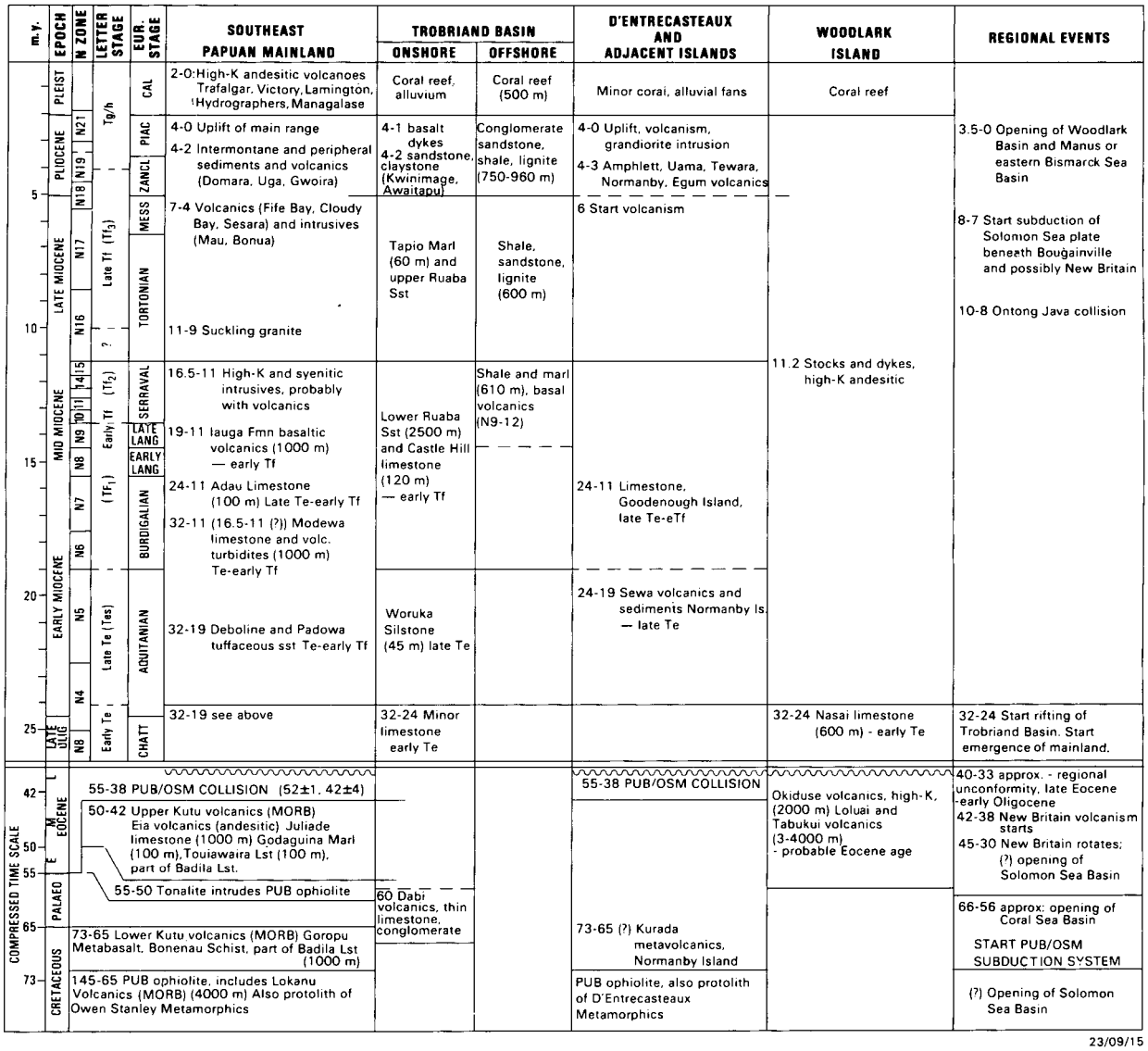

Figure 4. Summary of geology, southern Solomon Sea region.
PUB - Papuan ultramafic belt; OSM - Owen Stanley Metamorphics.

foraminifer (Terpstra, 1964; Trail, 1967; McGee, 1978a, 1978b; forams re-examined by D.J. Belford, personal communication 1983). On the other hand, Ashley & Flood (1981) suggested that the volcanics are early and late Miocene, and thus part of the younger cover volcanics, described below.

Cover sequence

The Eocene and older basement rocks of the Papuan peninsula and islands are unconformably overlain by late Oligocene and younger sediments and volcanics (Fig. 4), collectively referred to here as the cover sequence.

The greatest development of the cover sequence is in the Cape Vogel Basin and its sub-basins (Fig. 3; Bickel, 1976), the best known of which is the Trobriand Basin, an east–west basin between the Trobriand and D'Entrecasteaux Islands, which has been explored for petroleum. Seismic reflection surveys in this sub-basin indicate a maximum sediment thickness of 5000 m, and two wells drilled on structural highs penetrated 2300–2500 m of middle Miocene and younger sediment above volcanic 'basement' (Tjhin, 1976).

The well sections (Fig. 5) include up to 610 m of middle Miocene marine shale and marl, overlain by up to 660 m of late Miocene shale, sandstone, and lignite, partly marine and partly fluvio-deltaic. This is overlain, in turn, by up to 955 m of Pliocene fluvial sandstone and conglomerate in Goodenough-1 well, and 750 m of Pliocene mixed fluvio-deltaic and marine sediments in Nubiam-1, with up to 500 m of Quaternary shallow marine carbonate making up the remainder of the section (Tjhin, 1976; Garside & Stoen, 1973; Stoen & Garside, 1973; some revision of micropalaeontological ages by D.W. Haig and G. Francis, personal communication, 1983).

Volcanic rocks of cover sequence

Volcanic rocks of the cover sequence are of special interest to us because they may be related to subduction at the Trobriand Trough. These rocks have been studied by Smith (1976a) and the results presented in a number of papers (Jakes & Smith, 1970; Smith, 1972, 1973, 1976b; Smith & others, 1977; Johnson & others, 1978a, 1978b; Smith & others, 1979; Smith, 1982). Information from these papers and other sources is summarised in Table 1, and potash and silica variation are illustrated in Figure 6.

Most of the volcanic rocks have the chemical and physical characteristics of an arc–trench suite (Smith, 1982). Exceptions are the rhyolites of Fergusson Island, which are rift-

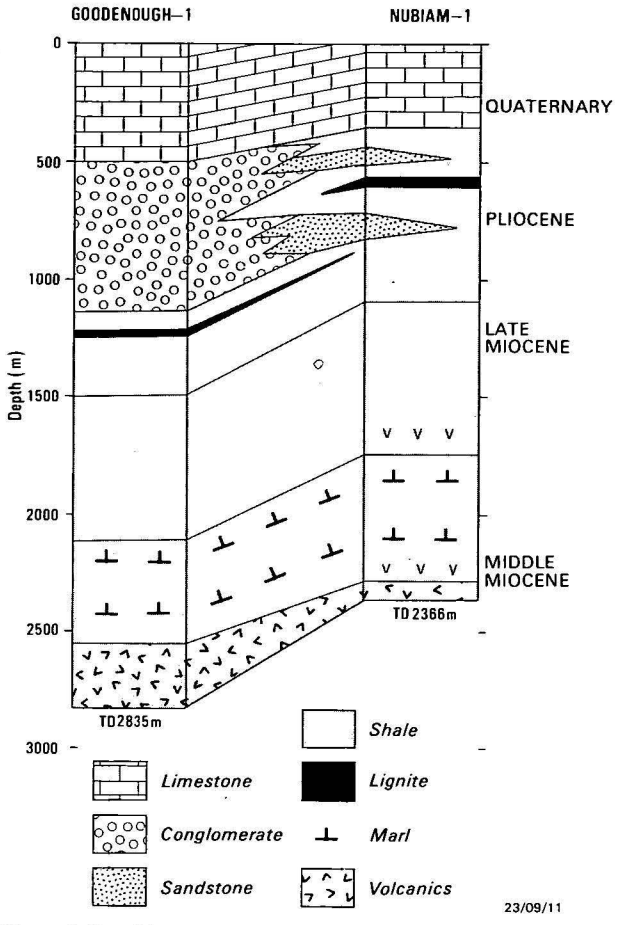

Figure 5. Simplified lithologic log of Goodenough–1 and Nubiam–1 exploration wells drilled in Trobriand Basin.

related (Smith, 1976b). We envisage that the volcanics of arc–trench affinity were erupted in successive volcanic arcs, broadly coincident in location, starting in the Miocene, continuing through the Pliocene and into the Quaternary, and including the currently active large central volcanoes Lamington and Victory.

The Miocene volcanics are poorly studied, but are thought to be generally basaltic; the only analyses are of pyroclastics from Cape Ward Hunt, which are basaltic (our unpublished data), and from the Calvados Chain, which are high-K andesites (Smith, 1976a; nomenclature of Johnson & others, 1978a, and Gill, 1981).

The Plio-Quaternary volcanics are mostly medium to high-K andesites, with minor development of trachybasalt and dacite, and less common tholeiite and alkali basalt (Table 1). They have chemical affinities with the Plio-Quaternary volcanics of the Papua New Guinea highlands, Bougainville Island, and the Rabaul area on northeastern New Britain (Johnson & others, 1978a; Johnson, 1982), and are characterised by a relatively high content of alkali and incompatible elements, variable to high Ni and Cr, strongly fractionated LREE-enriched rare earth patterns, and variable but generally low strontium isotope initial ratios. Initial ratios for volcanic rocks from the islands are tightly grouped with the range 0.7041 ± 2, indicating derivation from a homogeneous mantle source, with no evidence of crustal contamination (Smith & Compston, 1982). Initial ratios for volcanic rocks from the Papuan peninsula, on the other hand, are widely variable, in the range 0.7036–0.7054 (Page & Johnson, 1974; Smith & Compston, 1982). The wide variation in isotope ratios compares with that found in the Papua New Guinea highlands, where it has been attributed to contamination of mantle-source magma by continental crust, through which the magma rose (Hamilton & others, 1983).

Smith (1982) grouped the arc–trench volcanics into a southern belt, characterised by K-rich more basaltic rocks, and a northern belt of more andesitic rocks. We note the presence of andesitic volcanics in the southern belt, the convergence of the two belts in the Managalase area southeast of Mount Lamington, and the reconnaissance nature of the mapping

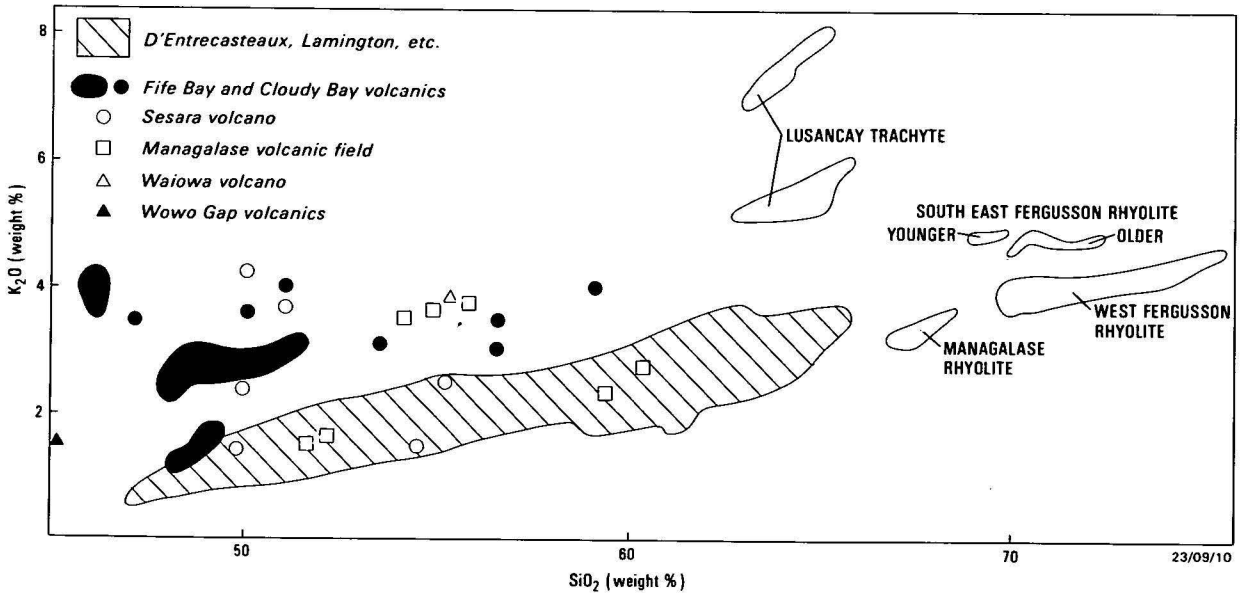

Figure 6. K_2O v. SiO_2 plot of Plio-Quaternary volcanics of southern Solomon Sea region.

Most volcanics plot within the hachured area; this includes volcanics from the Lamington. Hydrographers, Victory, Trafalgar, Goodenough, Normanby, Amphletts, Egum, and Calvados Chain eruptive centres, and some of the Managalase and Sesara volcanics. The dark area is the field of Fife Bay and Cloudy Bay volcanics. Illustration based on data of Smith (1976a, fig. 5-2), Ruxton (1976), Jakes & Smith, (1970), and Arculus & others (1983).

Table 1. Neogene–Quaternary volcanics of southern Solomon Sea region

Miocene

Cape Ward Hunt
Iauga Formation: Agglomerate of porphyritic basalt, deposited in littoral environment; early Tf (early to middle Miocene) age from benthonic foraminifera: Paterson & Kicinski (1956) and authors' unpublished data. More than 1000 m thick.

Milne Bay area
Modewa limestone and volcanogenic turbidites, composition not known but probably high-K andesitic by correlation with nearby intrusives. Te to early Tf age (late Oligocene to middle Miocene) from benthonic foraminifera (Smith & Davies 1973a, 1973b). Debolina and Padowa tuffaceous sandstone, details as for Modewa volcanogenic turbidites. More than 1000 m thick.

Trobriand Basin
Marine tuff, agglomerate, lava?, associated with shale and marl at and near base of section in Goodenough-1 and Nubiam-1 wells Fig 5; Tjhin, 1976) some tuff is late Miocene, but most volcanics are middle Miocene, N9-12 (Tjhin, 1976; palaeontological ages reviewed by D.W. Haig; G. Francis, pers. comm., 1983).

Western Calvados Chain
Pyroclastic deposits and lavas of high-K andesite composition (Smith, 1973, 1976a) on Pana Tinani Island.

Pliocene

North of Musa valley
Sesara volcanics: Agglomerate, tuff and lava of high-K basalt and high-K andesite composition (Ruxton, 1966); K-Ar age 5.2–5.9 Ma (Ruxton & McDougall, 1967). Musa volcanic member of Domara River Conglomerate is high-K basaltic agglomerate (Smith & Davies, 1976) of late Pliocene K-Ar age.

South coast of Papuan peninsula
Fife Bay and Cloudy Bay volcanics are high-K alkali basalt, trachybasalt, minor olivine tholeiite and medium-K andesite, previously described as shoshonites (Kesson & Smith, 1972; Smith & Davies, 1976). Age from lack of volcanic landform, and because mapped as unconformable on middle Miocene volcanics and sediments (Smith & Davies, 1973a, b). Smith (1976a, 1982) proposed middle Miocene age because chemically similar to middle Miocene intrusives.

Amphlett Group, Uama & Tewara Islands
Medium to high-K andesitic pyroclastics, structurally tilted, are remnants of probably major Pliocene volcanic complex north and northeast of Fergusson Island; Pliocene K-Ar ages Amphlett Group (Smith, 1976a).

Egum Atoll
High-K andestic volcanics exposed on one island have Pliocene K-Ar age (Smith, 1976a).

Normanby Island
Central western Normanby Island has extensive cover of high-K andesite with some trachybasalt and dacite (compositions from Smith, 1976a; Rb-Sr age 3.2 Ma from Smith & Compston, 1982).

SE Goodenough Island
Pliocene? andesitic lava and agglomerate form low plateau (Davies & Ives, 1965).

Misima Island
Agglomerate and tuff (Kobel Volcanics, de Keyser, 1961; age revised by D.W. Haig, pers. comm. 1983).

SW Fergusson & SE Fergusson Island, Sanaroa Island
The late Miocene and Pliocene rhyolite suite of Fergusson Island is discussed with Quaternary rhyolites below.

Quaternary

Mount Lamington and Hydrographers Range; Mounts Victory and Trafalgar
There are two large active volcanic complexes on the north-east coast of the Papuan peninsula: the **Lamington–Hydrographers** complex in the northwest, and the **Victory–Trafalgar** complex on Cape Nelson. Both have horizontal dimensions in the range 80–100 x 45 km, and maximum elevations of 1600–1850 m above sea level, and both have been constructed by eruptions from a central vent that has migrated progressively 27 km westward and 22 km southwestward, respectively, with time. Both active cones are decorated with tholoids and minor flows of viscous lava, and in both cases the oldest part of the complex has subsided, relative to sea level, to form a sharply indented coastline.

Lamington lavas are high–K acid andesites and trachybasalts (Arculus & others, 1983); Hydrographers Range volcanics are similar, but may be generally less silicic, judging from the four analyses presented by Ruxton (1966). Victory and Trafalgar lavas include rock types almost identical with those from Lamington volcano, but the analysed samples have a wider range of silica content (50–64 per cent); as with Lamington-Hydrographers, there is a suggestion that the older lavas are less silicic (Jakes & Smith, 1972).

Lavas from the Hydrographers Range have K–Ar ages between 1.45 and 0.67 Ma (Ruxton & McDougall, 1967); these ages probably do not encompass the onset of volcanism.

Mangalase Plateau
A volcanic field southeast of Mount Lamington made up of many minor eruptive centres; compositions include high–K basalt, medium–K and high–K andesite and some rhyolite (chemical data from Ruxton, 1966).

South of Mount Victory
Several minor eruptive centres including the small vent, Waiowa or Goropu, which erupted in 1943 and is located on the trace of the main ophiolite thrust fault (Davies & Smith, 1974); high–K andesite (Ruxton, 1966, and see Fig 6).

Goodenough Island and northwestern Fergusson Island
Minor eruptive centres are dotted around massifs of metamorphic rocks, some are located on bounding (thrust) fault (Davies, 1973); high–K basic andesite and some olivine tholeiite and nepheline and hypersthene-normative trachybasalt (authors' synthesis of data presented by Smith, 1976a).

Lusancay Islands
High–K trachyte and dacite form small massive outcrops on two islands; silica content 63–66 per cent and potash 5.3–8 per cent; LREE enriched with extremely low HREE contents; K–Ar ages close to 1 Ma (Smith, 1976a; Smith & others, 1979; Smith & Compston, 1982).

Late Miocene to Quaternary

Rhyolite suite of Fergusson Island
Rhyolitic and associated minor mafic volcanics are exposed in western and southeastern Fergusson Island. The southeastern rhyolites extend to the nearby small islands, Sanaroa and Dobu.

The rhyolites of western Fergusson Island consist of an older suite on the Kukuia Peninsula and a younger suite, associated with active thermal areas, in the Iamalele–Fagalulu area. The older suite is faulted and jointed. It includes minor alkali basalt, trachybasalt and high–K basic andesite and is late Miocene and Pliocene in age (Rb–Sr ages 6.27 and 3.6 Ma; Smith & Compston, 1982). The younger suite forms lava domes and flows of Pleistocene and Holocene aspect.

Some of the rhyolitic volcanics of southeastern Fergusson Island and those of Sanaroa Island are jointed lava and ignimbrite of probably Pliocene age. Quaternary rhyolitic pumice, agglomerate, and lava form potentially active eruptive centres near the southeastern tip of Fergusson Island and on Dobu Island; these are associated with active thermal areas. The Quaternary rhyolitic volcanics are associated with rare flows and agglomerate of alkali basalt, transitional basalt, trachybasalt, and trachyte, and contain inclusions of the same (Smith, 1976a, 1976b; Smith & others, 1977; Smith & others, 1977; Smith & Johnson, 1981; some field observations and interpretation of aerial photographs by Davies & Ives, 1965, and authors' unpublished data).

Younger lavas from all three vents on southeastern Fergusson Island have uniform composition and are more alkalic and generally less silic than older lavas from the same area (Fig. 6; Smith, 1976b). Rhyolites of western Fergusson Island have more variable composition than those of the southeast, but are uniformly less alkalic (Fig. 6; data from Smith, 1976a).

program, and conclude that this grouping may not be well founded. We also hesitate to accept that there is a systematic increase in potash content southward (Smith, 1982, fig. 5), for, to us, his diagrams suggest an irregular distribution of K_2O values. The high-K trachyte and dacite that are found in two small exposures in the Lusancay Islands are chemically anomalous (Fig. 6), but similar rocks have been described from fore-arc regions of other convergent systems, for example, near the Japan Trench (Gill, 1981).

The rhyolites of southwestern and southeastern Fergusson Island and nearby small islands (Sanaroa and Dobu islands, off southeastern Fergusson Island) are associated with minor alkali basalt, transitional basalt, trachybasalt, and trachyte (Smith, 1976b). Initial strontium isotope ratios are low, with the exception of some rhyolites that have anomalously high values; the high values may be due to groundwater contamination of late-stage low-Sr fractionated melts (Smith & Compston, 1982; Smith & Johnson, 1981). Volcanics of the rhyolite suite range in age from 6.3 Ma to modern lavas and pumice from potentially active vents (Table 1; Smith & Compston, 1982).

Origin of the volcanics

Smith (1976b) concluded that the rhyolites of Fergusson Island are a rift- related suite of mantle origin, and presented evidence to show that those of southeastern Fergusson Island formed by differentiation of more basic magma. He linked the rifting with the opening of the Woodlark Basin, to the east.

For the arc-trench suite of volcanics he considered the possibility that they were related to southward subduction of the Solomon Plate, but concluded that this was unlikely. Rather, he linked the genesis of these volcanics to the development of thickened crust beneath the Papuan peninsula and consequent interaction between lower crust and upper mantle (Smith, 1982); others have related it to delayed partial melting of mantle that had been modified during an earlier convergent tectonic event (Johnson & others, 1978b).

We conclude in favour of the simpler explanation that the arc-trench suite of volcanics is related to subduction of the Solomon Plate at the Trobriand Trough, because we have evidence that the Trobriand Trough is, or was, an active trench (see under **Offshore structure**).

Lithosphere structure

The deep crustal structure of central and eastern New Britain and southern New Ireland was investigated by gravity and explosion seismic refraction surveys in 1967 and 1969, the Papuan peninsula by a similar survey in 1973, and the Solomon Sea and Ontong Java Plateau by gravity, magnetic, and ship-to-ship refraction surveys in 1966 and 1970 (Rose & others, 1968; Furumoto & others, 1970, 1973, 1976; Finlayson & others, 1972, 1976a, 1976b, 1977; Finlayson & Cull, 1973). The regional gravity field of the Papuan peninsula and islands was investigated prior to the refraction survey by St John (1967, 1970) and Milsom (1973a, 1973b).

The surveys indicated crust of normal oceanic thickness in the central Solomon Sea Basin, thickening to 35 km beneath New Britain and New Ireland, and up to 42 km beneath the Ontong Java Plateau. In the southern Solomon Sea region they showed that: (1) the crust beneath the central axis and southern slopes of the Papuan peninsula is about 32 km thick, and may extend, as a northeasterly dipping slab, into the mantle beneath the northeastern slopes of the peninsula (Fig. 7); (2) the Papuan ultramafic belt ophiolite complex dips northeast at 13–25° and may be continuous with the crust and upper mantle of the Solomon Sea; (3) the crust beneath the Trobriand Platform is 24 km thick, and thins to normal oceanic thickness beneath the Solomon Sea Basin; and (4) the crust further west, in the region of the 149° Embayment, is up to 20 km thick.

From a review of earthquake data, Ripper (1982b) concluded that the lithosphere of the Solomon Sea Basin is subducted not only northwards beneath New Britain and Bougainville Island, but also southwestwards beneath the Papuan peninsula, as is illustrated by the broken line in Figure 7. This is discussed more fully under **Seismicity**. The flexural response of the Solomon Sea lithosphere also is discussed under **Age of Solomon Sea Basin lithosphere**.

Onshore structure

The dominant surface structure of the land areas of the southern Solomon Sea region is the Owen Stanley fault system, which separates the Papuan ultramafic belt ophiolite, above, from metamorphics below (Figs. 2,3; Davies, 1968, 1971, 1980a). It is marked by a prominent sinuous valley northeast of the central axis of the Papuan peninsula, and by the change in slope from mountain to foothills in the D'Entrecasteaux Islands (Davies & Ives, 1965; Davies, 1973). The fault system typically has a shallow dip and has accommodated both initial thrusting and later dip-slip extensional faulting (Davies, 1980b; Davies & Jaques, in press; Davies & Warren, 1983). The inclined fault plane has been disrupted by later steep normal faults in places (Davies, 1971).

Minor eruptive centres are located on the surface trace of the Owen Stanley Fault system at several localities on the Papuan peninsula, including the recently active vent, Waiowa or Goropu (Fig. 2) , and on the trace of the equivalent fault on Goodenough Island (Davies, 1973).

The Gira Fault (Fig. 3) is a northwesterly trending left-lateral strike-slip fault, upon which part of the Papuan ultramafic belt ophiolite has been displaced by up to 90 km (Davies, 1968, 1971). It is currently active, as is indicated by local displacement of Holocene ultramafic talus deposits in the Ioma area (Davies, in prep.). The fault trends towards Lamington volcano, but may veer eastward beneath the alluvial plains north of Mount Lamington (interpretation of magnetic anomalies by CGG, 1969, and see below).

There is an east-west alignment of eruptive centres within the Lamington-Hydrographers volcanic complex, which reflects a deep-seated fault or zone of weakness. This aligns with an east-west segment of the Owen Stanley Fault system to the west, and is parallel with other lineaments in the volcanic complex (visible on Landsat imagery and aerial photographs). A similar, but more pronounced northeasterly alignment of eruptive centres in the Victory-Trafalgar volcanic complex is also interpreted as reflecting a deep-seated fault or zone of weakness.

Horst and graben structures in the southeast Papuan peninsula, both in the Musa Valley area, southwest of Mount Victory, and in the extreme southeast, are defined by east-west-trending normal faults (Davies, 1968, Fig 2; Jongsma, 1972); other sets of east-west normal faults define the off-shore Trobriand Basin (Tjhin, 1976).

Recently active north-northeasterly trending faults of small vertical displacement cut across the southeastern Papuan peninsula and are concentrated in the northwest around Lake

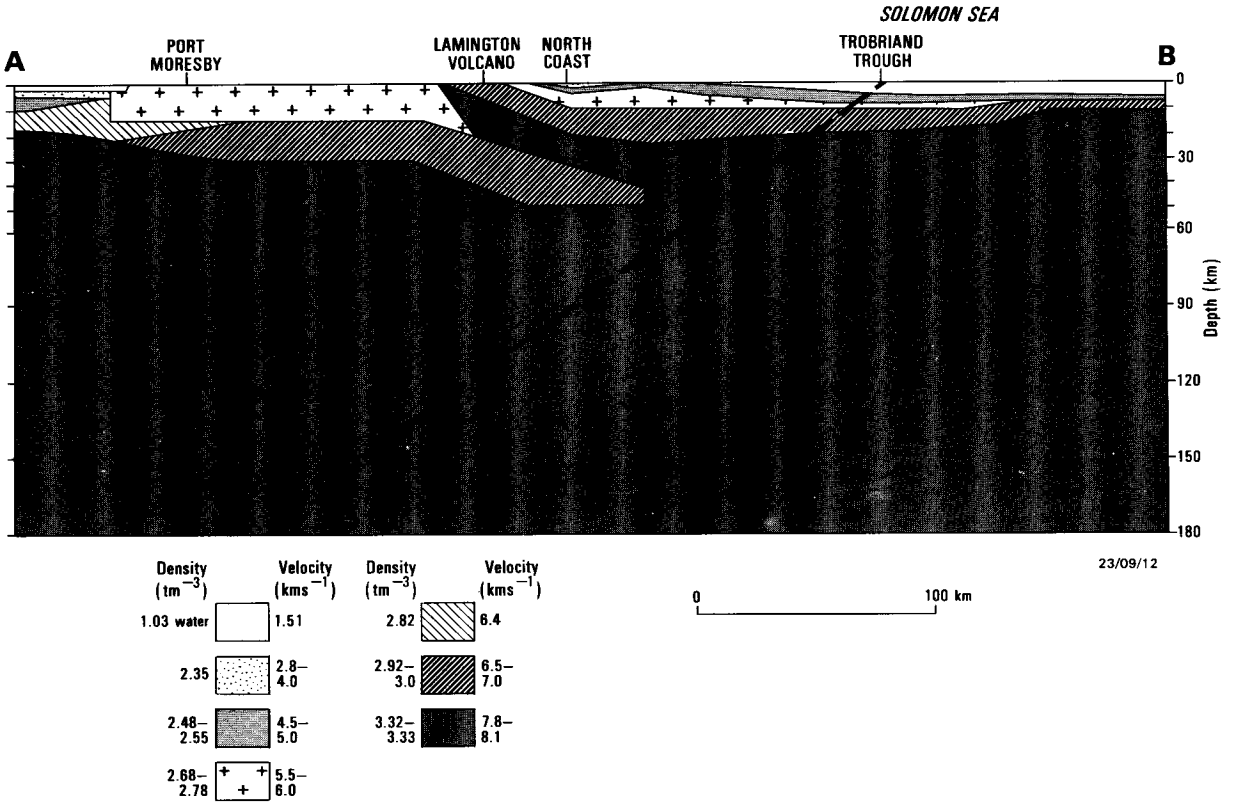

Figure 7. Crustal section across Papuan peninsula and Trobriand Platform.
Shows deep crustal structure deduced from seismic refraction and gravity studies, after Finlayson & others (1977). Broken line indicates approximate position of supposed subducted slab of Solomon Sea Basin lithosphere (this paper). Location shown in Figure 2.

Trist, where the trend of the Owen Stanley Fault changes to north-northeast (Davies & Smith, 1974; Dow & Davies, 1964). Given the present stress regime (see under **Seismicity**), these are probably steep reverse faults.

Other prominent structural features, which are marginal to our area of special interest, are the Ramu-Markham fault system, a valley-forming system that aligns with the Huon Gulf chasm; the major northwesterly trending left-lateral strike-slip faults that cut across southern New Ireland and central Bougainville Island; and the northwesterly-trending normal faults that define the Wide Bay–Open Bay depression in northeastern New Britain (Fig. 3, and see maps: Bain & others, 1972; D'Addario & others, 1976).

Offshore structure

Offshore structural features are illustrated in Figure 3, and the main features have been briefly discussed under **Regional setting** and **Geology.** In the following section we present additional information, drawn partly from previously unpublished seismic reflection profiles. The main observations we draw from these profiles are, firstly, that the Trobriand Trough is a sediment-filled active or recently active trench; secondly, that the floor of the Solomon Sea Basin is arched and faulted in response to north–south (and probably northeast–southwest) horizontal compressive stress, with effects that are more extreme in the west, where the basin is narrower, and, thirdly, that the Trobriand Basin extends further east than previously mapped and is bounded southeastward by rifts associated with the Woodlark Basin spreading system. Although the available seismic data provide incomplete coverage of the Solomon Sea, they are sufficient, particularly when combined with other data, to define significant changes in structural style along the southern margin of the Solomon Sea (structural provinces I, II, III, Fig. 3).

Structural features on a smaller scale are the rifted small rhomboidal Goodenough Basin between the D'Entrecasteaux Islands and the mainland (Fig. 3; Milsom, 1973b; Smith & Davies, 1973b) and the graben that forms Milne Bay (Fig. 2; Jongsma, 1972), features almost certainly related to rifting associated with the Woodlark Basin spreading system (e.g., Weissel & others, 1982). Other extensional basins flank the Huon Peninsula (Huon Gulf chasm, Finsch Deep) and southern New Ireland (St George's Channel, Feni Deep; Fig. 3).

Seismic reflection profiles

The three profiles illustrated here (Figs. 8, 9, 10) are drawn from reconnaissance seismic reflection surveys by Gulf Research and Development (Gulf, 1973) and BMR (CGG, 1974; Tilbury, 1975). We also examined photographically reduced copies of profiles collected by the research vessels *Conrad* and *Vema* and kindly provided by Lamont-Doherty Geological Observatory of Columbia University. We did not have access to profiles collected recently by the Geological Survey of Japan vessel *Natsushima* (Honza & others 1984). Part of the *Vema* profile and one of the BMR profiles have been published previously by Hamilton (1979).

Figure 8. Interpretation of Gulf seismic profile across the central Solomon Sea Basin.
Location shown as profile A in Figure 2. Shows the New Britain Trench and Trobriand Trough, and the deformation front (DF) and slope basin, which are characteristic of subduction systems. I in 8a marks a minor intrusive body beneath the Trobriand Platform. Note overlap between 8a and 8b. 8c is a single-channel, deconvolved seismic section recorded using an Aquapulse energy source. The black dots define the top of oceanic basement, which dips to over 9 seconds of reflection time beneath the slope basin. Arrows mark reflector terminations at major seismic sequence boundaries. Note deformation front is exposed at the sea floor and is not onlapped by the trough-fill sediments, implying that the system is active, or was so until very recently.

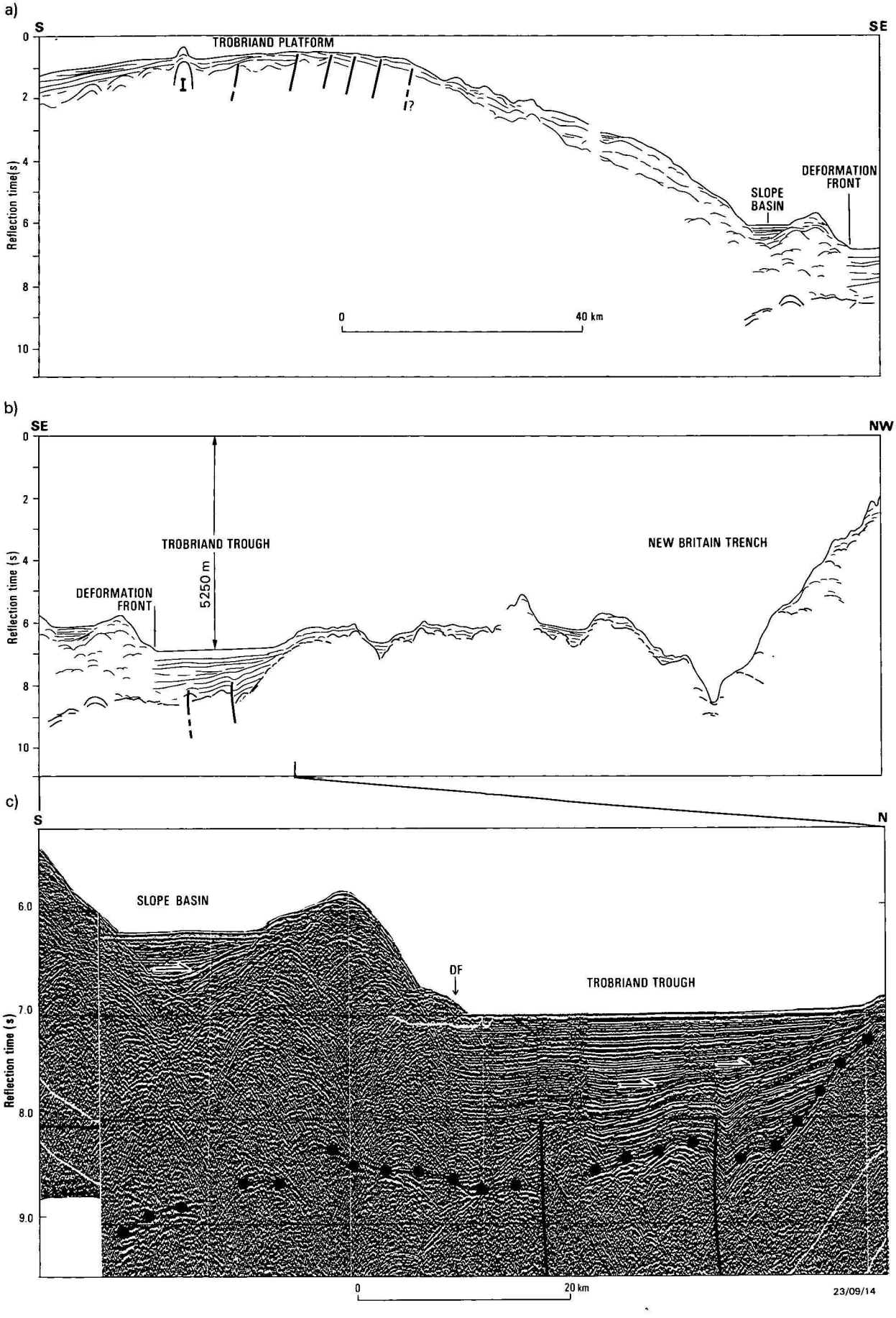
a)
S
SE
TROBRIAND PLATFORM
DEFORMATION FRONT
SLOPE BASIN
Reflection time(s)
0
2
4
6
8
10
0
40 km
b)
SE
NW
TROBRIAND TROUGH
5250 m
NEW BRITAIN TRENCH
DEFORMATION FRONT
Reflection time (s)
c)
S
N
SLOPE BASIN
DF
TROBRIAND TROUGH
Reflection time (s)
6.0
7.0
8.0
9.0
0
20 km
23/09/14

The Gulf profile (Fig. 8; profile A in Fig. 2) crosses the central Solomon Sea Basin in structural province I, and shows a narrow, sediment-free New Britain Trench and the irregular arch-like form of the Solomon Sea Basin basement, which is generally overlain by about 300–400 m of sediment (Fig. 8b). There is at least 1500 m of sediment beneath the Trobriand Trough, made up of two main sequences – a basal southward-dipping sequence that onlaps basement, and an upper flat-lying, ponded sequence (Fig. 8b, c). Basement beneath the Trobriand Trough dips southwards to at least 9 seconds of reflection time beneath an uplifted and deformed sedimentary pile (Fig. 8a, b, c). On this profile, the Trobriand Platform is a broad arch composed of folded and faulted rocks, and minor intrusive bodies (Fig. 8a). We interpret this profile as showing that the southern margin of the Solomon Sea Basin is a convergent margin with subduction of oceanic lithosphere beneath the Trobriand Platform. Characteristic features are the deformation front and the small slope basin (Fig. 8c). Because the deformation front crops out at the sea floor, and apparently is not onlapped or buried by trough-fill sediments, we conclude that subduction is active or has only recently ceased.

Further west, in structural province II, a BMR profile (Fig. 9; profile B in Fig. 2) crosses a sediment-free extension of the Finsch Deep, which is separated from the deep flat floor of the southwestern New Britain Trench by a narrow ridge (the Vitiaz slice of Johnson, 1977). Sediments in this part of the New Britain Trench are about 1500 m thick and gently folded. Further south, the sediment thickness increases to more than 2500 m at the foot of the Trobriand Platform slope. The most remarkable feature of the profile is the series of faults that intersect acoustic basement beneath the 149° Embayment. We interpret the faults as south-dipping thrusts, and note that their dip increases southwards to near-vertical beneath the lower slope of the Trobriand Platform. Near the New Britain Trench the faults impinge upon the sea floor (Fig. 9b), which implies that the deformation is continuing or has only recently ceased. The imbricated stack of acoustic basement blocks formed by the thrust faults is overlain by faulted and gently folded sediments. There is no Trobriand Trough bathymetric feature on this profile, but the structural equivalent of the Trough may lie beneath the zone of thick sediment just north of the slope basin in Figure 9a. The profile indicates that, within structural province II, crustal shortening has been

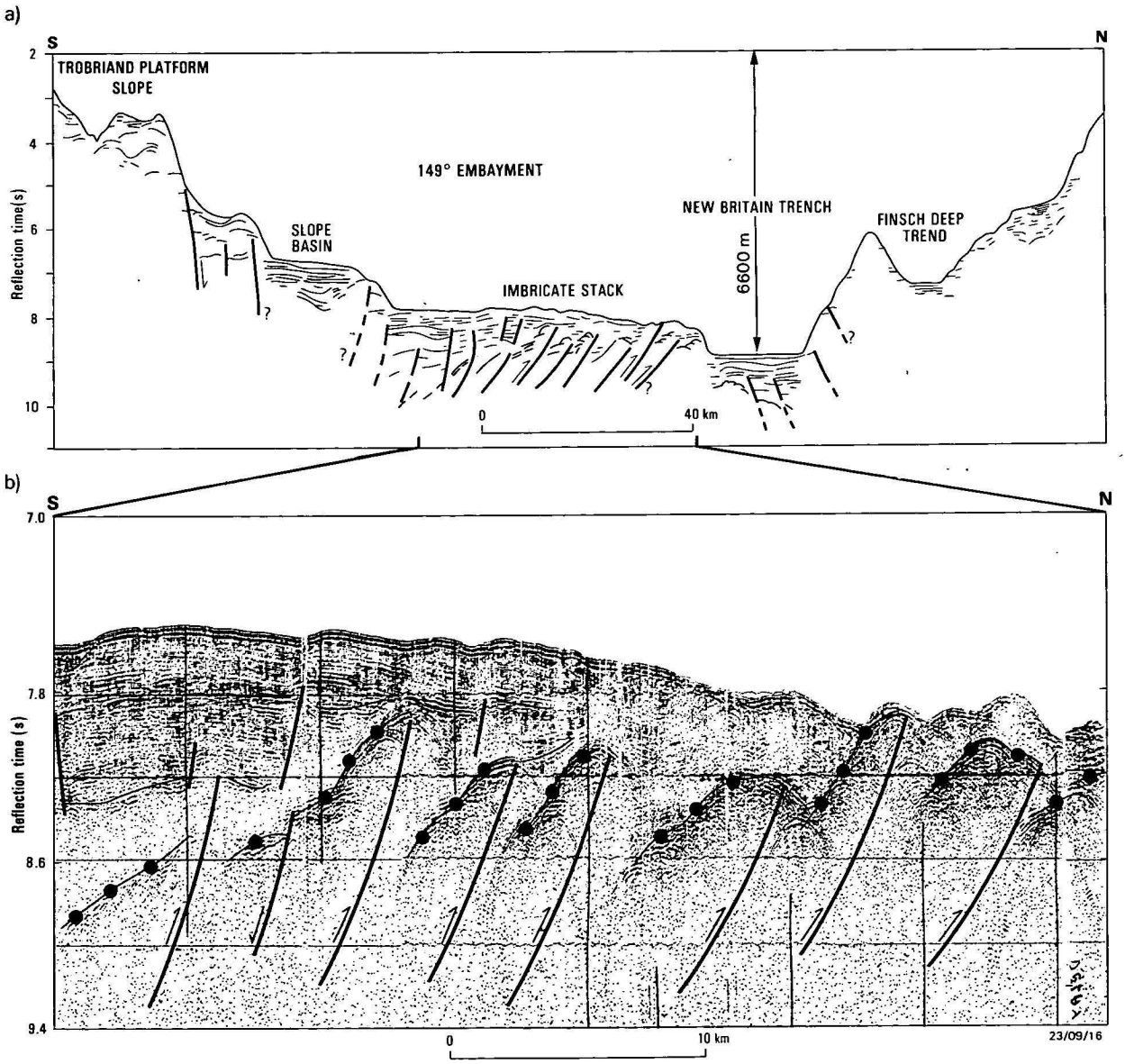

Figure 9. Interpretation of BMR seismic profile across the western Solomon Sea basin.
Location shown as profile B in Figure 2. Shows the Finsch Deep trend, New Britain Trench and the imbricate stack of acoustic basement blocks beneath the 149° Embayment. 9b is a single-channel onboard-monitor seismic section, recorded using a 120 kJ sparker energy source. It shows thrust faults affecting acoustic basement (black dots) beneath the 149° Embayment. Note that the faults impinge upon the sea floor of the northern end of the section.

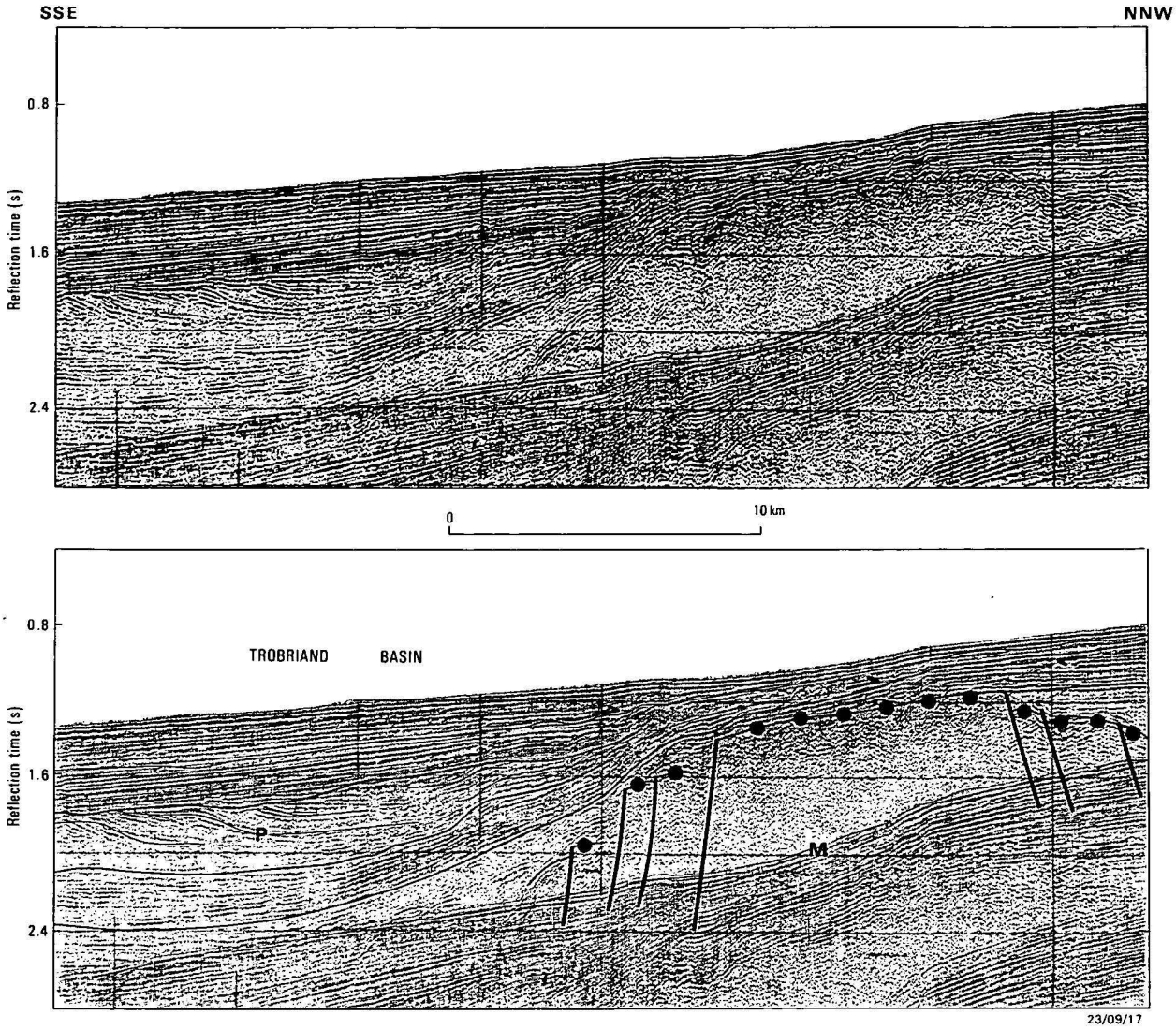

Figure 10. BMR seismic section across the eastern Trobriand Basin.

Location shown as profile C in Figure 2. Single-channel onboard-monitor section recorded using a 120 kJ sparker energy source. Black dots define the top of a faulted basement block. P marks the progradational facies that lies just below a major seismic sequence boundary. Arrows show reflector terminations at seismic sequence boundaries. M is the first water-bottom multiple.

accommodated by imbrication and thrusting of ?oceanic crust, in addition to or after failure of southward subduction. Tectonic thickening of the oceanic crust by thrusting would explain the anomalously thick crust interpreted in this region from seismic refraction, gravity, and magnetic data (Finlayson & others, 1977). Similar imbricate deformation of oceanic crust has been recognised at the Caroline/Pacific Plate boundary, along strike from the Mussau Trench, and is there attributed to a relatively slow rate of plate convergence (Hegarty & others, 1983).

Further west, in structural province III, other unpublished BMR profiles define a series of west-northwesterly trending highs and fault-bounded troughs. These profiles are not reproduced here. The major trough is the Huon Gulf chasm (Fig. 3), the floor and flanks of which are composed of deformed and faulted sediments that generally dip north or northeast; this structural style is similar to that observed on the adjacent Huon Peninsula (Jaques & Robinson, 1977). The dominant structural control here may be wrench faulting associated with movement on the Ramu-Markham fault system, which lies along strike to the west-northwest.

The seismic reflection profiles, taken together with bathymetry, show that the base of the submarine slope that bounds the Papuan peninsula and the Trobriand Platform steps progressively southward from the line of the Trobriand Trough in the east, to the southern margin of the 149° Embayment, and then to the southern wall of the Huon Gulf chasm in the west (Fig. 3). The points of southward inflexion coincide approximately with the boundaries between structural provinces I, II, and III. The primary control on the changes in structural style, and the nature of the boundaries (e.g., whether sharp or gradational) are not known.

Another BMR seismic profile, southeast of the Trobriand Islands (Fig. 10; profile C in Fig. 2) illustrates the eastward extension of the Trobriand Basin. The southern end of this profile (not illustrated) shows large-throw normal faulting, which we associate with rifting related to the actively spreading Woodlark Basin further to the southeast (Fig. 3). On this profile, the eastern Trobriand Basin appears as a fault-bounded structure containing at least 2000 m of sediment, which can be subdivided into two sequences. The basal sequence consists of gently folded and faulted sediments, and

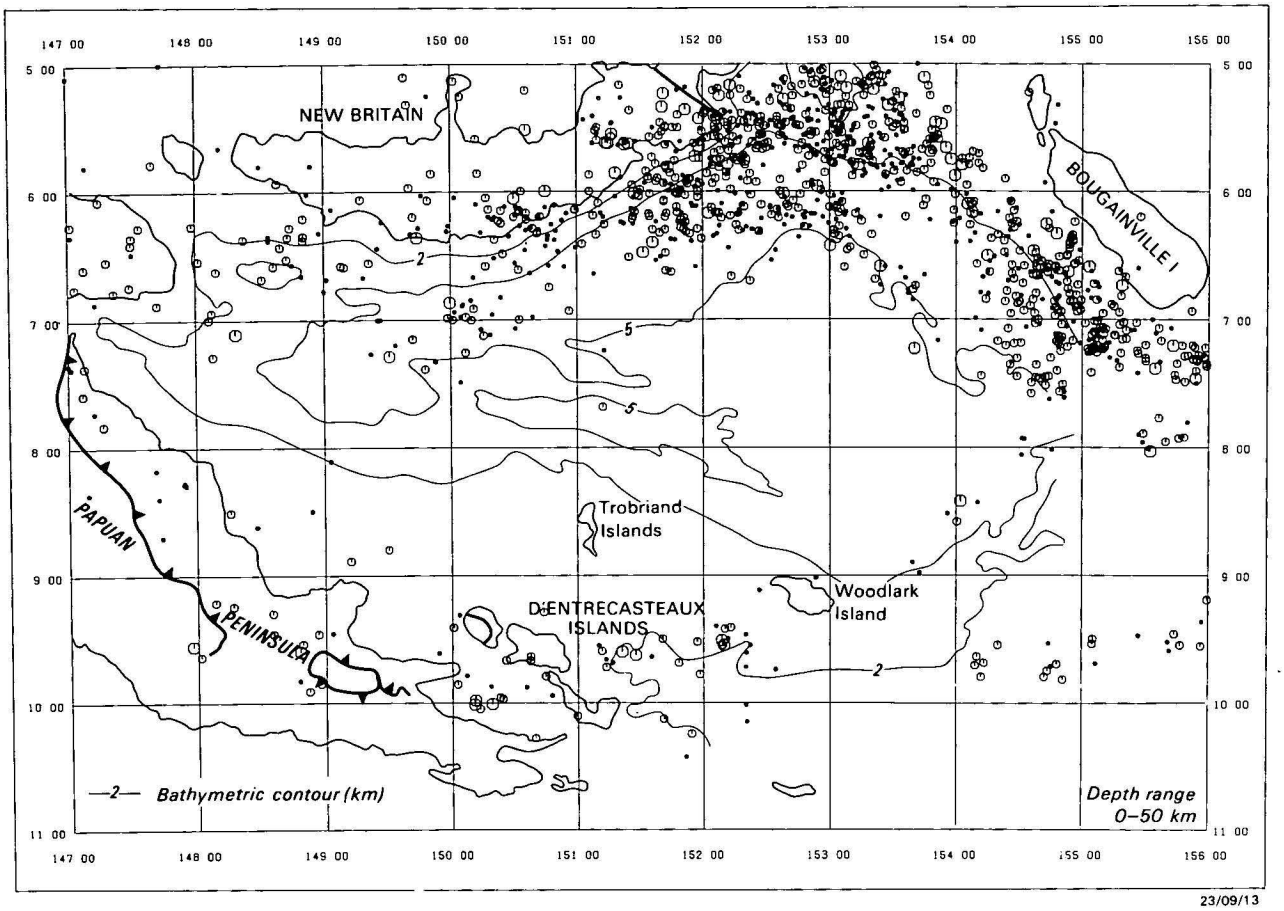
147 00
148 00
149 00
150 00
151 00
152 00
153 00
154 00
155 00
156 00
5 00
6 00
7 00
8 00
9 00
10 00
11 00
NEW BRITAIN
BOUGAINVILLE I
PAPUAN
PENINSULA
Trobriand Islands
D'ENTRECASTEAUX ISLANDS
Woodlark Island
2
5
—2— Bathymetric contour (km)
Depth range 0–50 km
23/09/13

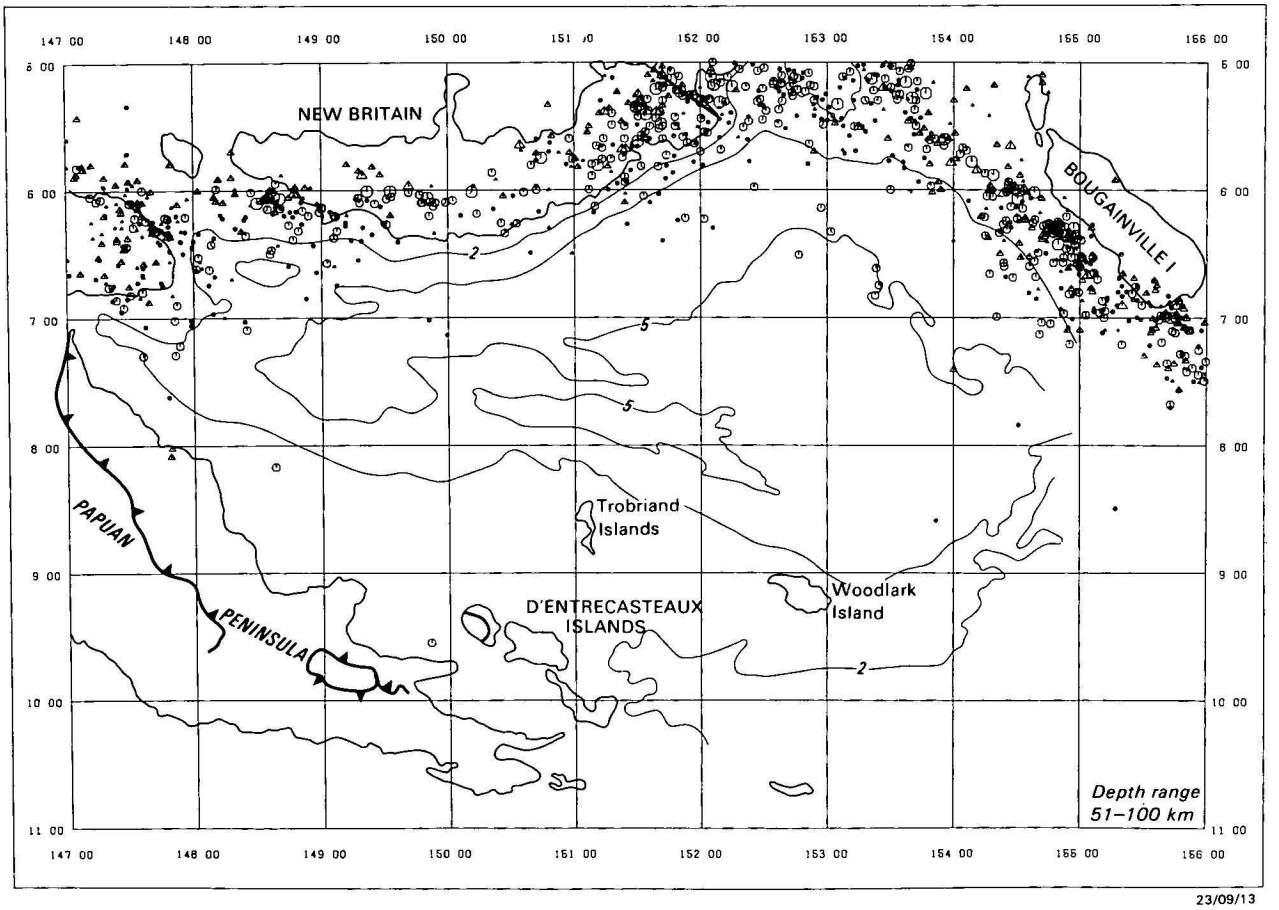
147 00
148 00
149 00
150 00
151 00
152 00
153 00
154 00
155 00
156 00
5 00
6 00
7 00
8 00
9 00
10 00
11 00
NEW BRITAIN
BOUGAINVILLE I
PAPUAN
PENINSULA
Trobriand Islands
D'ENTRECASTEAUX ISLANDS
Woodlark Island
2
5
Depth range 51–100 km
23/09/13

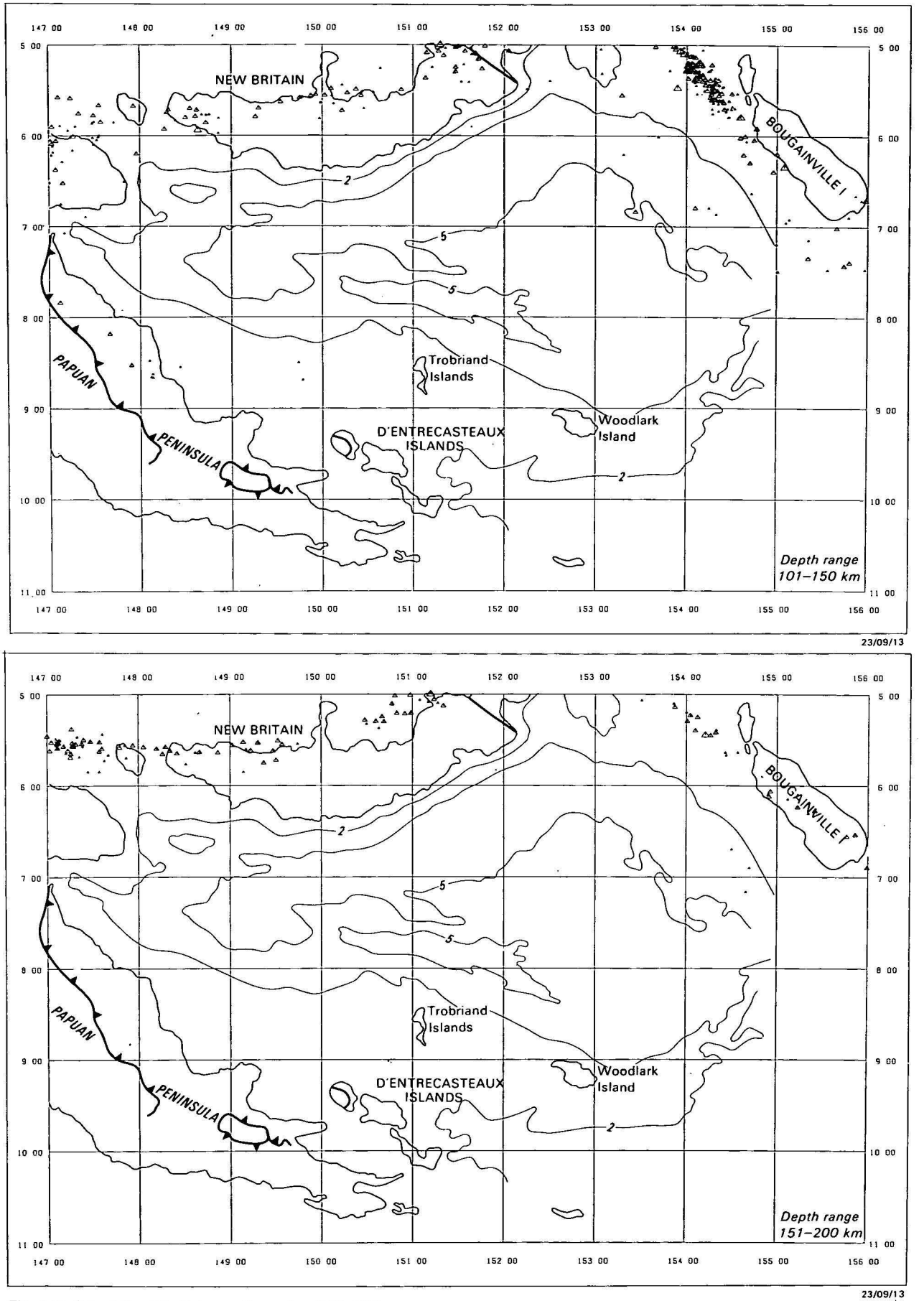

Figure 11. Seismicity of the Solomon Sea region, 1964–1982.

Shows earthquakes in four depth ranges – 0 to 50 km, 51 to 100 km, 101 to 150 km, 151 to 200 km. On the Papuan peninsula, the Owen Stanley Fault is also shown. The various sized circles, triangles and asterisks were produced by the automatic plotting of the earthquake data file and convey information that is not relevant to this study.

its upper part contains possible progradational facies, which may correspond to the Pliocene fluvio-deltaic sediments intersected in the Goodenough and Nubiam wells (Fig. 5; Tjhin, 1976). The sediment source for the progradational facies appears to have been to the south as is the case in the western Trobriand Basin (Tjhin, 1976).

This sequence is unconformably overlain by an onlapping sequence with a high amplitude, parallel reflection configuration. It has a maximum thickness of about 800 m in the south and thins rapidly across the northern flank of the Trobriand Basin, to be almost absent over the northern part of the Trobriand Platform east of the Trobriand Islands. It is probably mainly a Quaternary shallow marine carbonate sequence, such as was intersected in the Goodenough and Nubiam wells. However, without a seismic tie to the Australian Oil and Gas Corporation Ltd seismic data further west (Tjhin, 1976), this interpretation remains speculative.

Seismicity

Earthquakes recorded at more than 10 stations are displayed in 50 km vertical intercepts for 0–200 km depth in Figure 11. Earthquakes deeper than 200 km have been recorded beneath and north of New Britain (to 600 km depth) and beneath Bougainville Island (to 520 km depth; Ripper, 1970, 1982a; Ripper & McCue, 1982; Denham, 1969, 1973; Johnson & Molnar, 1972; R.W. Johnson, 1976a, 1976 b, 1977, 1979). Focal mechanism solutions have been determined by Johnson & Molnar (1972), Ripper (1975, 1977, 1982b) and Taylor (Weissel & others, 1982).

The earthquakes define a highly active Wadati-Benioff zone that dips steeply beneath New Britain and Bougainville Island. In this zone, shallow earthquakes occur over several hundred kilometres across strike, and include earthquakes with extensional solutions along the axis of plate flexure south and southwest of the New Britain Trench, and with thrust solutions down-dip from the trench (Johnson & Molnar, 1972; Ripper, 1982b; Weissel & others, 1982).

Elsewhere, shallow earthquakes define a weakly seismic linear zone along the northern flank of the Woodlark Rise, a broader zone that extends from Woodlark Island westward through the D'Entrecasteaux Islands and along the northern flank of the Papuan peninsula, and a zone that coincides approximately with the Woodlark Basin spreading ridge-transform system.

Shallow earthquakes along the line of the Woodlark Rise include one with a right-lateral northeasterly strike-slip solution (Weissel & others, 1982), and others with extensional and thrust solutions (Ripper, 1982b). Those between Woodlark Island and the Papuan mainland mostly have extensional north-south solutions (Ripper, 1982b; Weissel & others, 1982), presumably related to rifting associated with westward propagation of the Woodlark spreading system, whereas those further west and northwest on the Papuan peninsula mostly have strike-slip or thrust solutions with maximum compression east-west (Ripper, 1982b).

There is no zone of shallow seismicity coincident with the Trobriand Trough and no Wadati-Benioff zone associated with the postulated southwesterly dipping slab of Solomon Sea Basin lithosphere in this area (Ripper, 1982b). However, there are intermediate-depth earthquakes beneath the Papuan peninsula north and northwest of Mount Lamington, which may indicate the presence of such a slab. Ripper (1982b) suggested that southward subduction of the slab has probably ceased, owing to collision of the Trobriand and New Britain subduction systems in the Ramu-Markham region. The intermediate-depth earthquakes, which are aligned approximately beneath the surface trace of the Gira Fault, may reflect wrench faulting of the subducted slab on the line of the Gira Fault as the slab is dragged to the northwest.

Two isolated intermediate-depth earthquakes have been recorded from beneath the Trobriand Platform, 130 km west of the Trobriand Islands, but any relation to the Trobriand subduction system is unclear.

Age of Solomon Sea Basin lithosphere

Most of the marginal seas and small ocean basins of the New Guinea region opened by sea-floor spreading in the Tertiary. For example, the Coral Sea Basin opened in the Palaeocene or latest Cretaceous (Weissel & Watts, 1979; Symonds & others, 1984), and the eastern Bismarck Sea and Woodlark Basins in the Pliocene (Taylor, 1979; Milsom, 1970; Luyendyk & others 1973; Weissel & others, 1982).

Similarly, the Solomon Sea Basin probably opened by sea-floor spreading in the Tertiary, but there are insufficient magnetic data over it to define any magnetic lineation pattern, and there is a complete lack of direct evidence from drilling and other sampling. Karig (1972) compared age, heat flow, and water-depth relationships with those of other basins and concluded that the Solomon Sea Basin opened in the mid-Tertiary. Falvey & Pritchard (in press) have found palaeomagnetic evidence for clockwise rotation of New Britain in the interval 45–30 Ma ago, and concluded that the Solomon Sea Basin may have opened by back-arc spreading at that time.

A Cretaceous age was preferred by Davies (1971, 1980a; Davies & Smith, 1971), who considered the Solomon Sea lithosphere an offshore extension of the ?Cretaceous PUB ophiolite. He proposed that the Solomon Sea and PUB lithosphere were together a remnant of proto-Pacific Cretaceous crust that became isolated from the Pacific by younger arc–trench systems. This is similar to the model proposed by Jacob & others (1977) for the origin of the Aleutian Basin.

We have reviewed various lines of evidence, none of them definitive, and conclude that the most likely age of the Solomon Sea Basin lithosphere is late Palaeocene or Eocene, 60–40 Ma. A Cretaceous age is unlikely.

The approximate age of oceanic lithosphere may be determined from heat flow and water depth, using the relationships of Parsons & Sclater (1977). Heat flow in the Solomon Sea Basin is moderately high, and varies from 99 mW/m^2 in the north to 71 mW/m^2 in the south (Sclater & others, 1972; Halunen & von Herzen, 1973). The average of six values is 84 mW/m^2 and indicates an age of about 45 Ma. Average water depth is about 4500 m, which indicates a minimum age of 33 Ma. However, the water depth may be anomalous because of flexure of the Solomon Sea Basin lithosphere induced by subduction on three sides.

Another means of estimating the age of oceanic lithosphere is to determine its flexural response to stress; this is based on the principle that flexural rigidity increases with age for oceanic lithosphere (Watts, 1978), and with age following a major thermal event for continental lithosphere (Karner & others, 1983). From a preliminary study of the flexure of Solomon Sea Basin lithosphere, G.D. Karner (personal communication, 1984) determined an effective elastic rigidity of 10^{30} dyne cm, and thus a minimum age of 65 Ma.

There is also an approximate empirical relationship between age of subducted lithosphere, down-dip length of the Wadati-Benioff zone, and convergence rate, as follows: Age (Ma) = down-dip length (km) x 10/convergence rate (mm/yr) (Molnar & others, 1979). For the New Britain Trench in the New New Britain area, down-dip length is about 620 km and convergence rate is in the range 9.2–12.5/cm.yr (Johnson, 1979), giving an age for Solomon Sea Basin lithosphere of 70–50 Ma.

If the age of Solomon Sea Basin lithosphere is 60–40 Ma, as we suggest, then sedimentation rates must have been anomalously low. Our profiles show that in the centre of the basin the total thickness of sediments is only 300–400 m, which is equivalent to a sedimentation rate of 10 m/Ma or less, one of the lowest rates recorded in this region even assuming solely pelagic sedimentation (cf., van der Lingen & others, 1973). By way of comparison, other small enclosed basins near the Solomon Sea have recorded much higher rates; e.g., the latest Cretaceous or Palaeocene Coral Sea Basin has 2000 m of sediment, and the Pliocene East Bismarck or Manus Basin, somewhat less than 300 m, thickening to 1000 m just north of New Britain (Tilbury, 1975). Perhaps the apparent low sedimentation rate is due to long periods of non-deposition or to significant erosion by bottom currents, but there is no evidence for this, such as major unconformities or changes in reflection character, in the Gulf seismic profile (Fig. 8).

Geological history

Our interpretation of the evolution of the southern Solomon Sea region is outlined in Figure 4 and summarised below:

1. The Papuan peninsula and nearby islands are probably founded upon thick low-density crust that was rifted from the Australian craton in the late Mesozoic and transported northeastwards with the opening of the Coral Sea Basin in the Palaeocene or latest Cretaceous (Davies, 1980a; Weissel & Watts, 1979; Mutter & Karner, 1980; Symonds & others, 1984).

2. The thick crust and associated sediments collided with a south-facing volcanic arc in the Palaeocene–Eocene. The volcanic arc was founded upon Cretaceous oceanic crust, now preserved as the PUB ophiolite.

3a. If the Solomon Sea Basin lithosphere existed at the time of collison, then subduction jumped northwards to beyond the present boundary of the Solomon Sea, and there started to form the volcanics that now are the basement of New Britain.

3b. If, as seems more likely, the Solomon Sea Basin lithosphere did not exist at this time, then we may postulate that subduction flipped after collision to form a north-facing arc–trench system immediately north of the south-facing Palaeocene–Eocene volcanic arc. The Solomon Sea Basin lithosphere then developed by back-arc spreading behind this arc (Falvey & Pritchard, in press).

4. A north-facing arc–trench system developed on the southern margin of the Solomon Sea Basin in the late Oligocene or early Miocene (on the line of the Trobriand Trough), resulting in subduction-related volcanism and the development of a fore-arc or intra-arc basin (Trobriand Basin).

5. Subduction about New Britain was perhaps inactive in the early and middle Miocene, a period of limestone development, and flipped in the Pliocene to form the present south-facing arc. (Falvey & Pritchard postulate late Oligocene rather than Pliocene reversal. We follow Kroenke, 1972, in linking development of the New Britain Trench with the collison of the Ontong Java Plateau and Solomon Islands volcanic arc in the Miocene.)

6. During the Pliocene, both the eastern Bismarck Sea and the Woodlark Basin started to open by sea-floor spreading (Taylor, 1979; Milsom, 1970; Luyendyk & others, 1973; Weissel & others, 1982). The resulting change in plate boundary configuration may have caused the Trobriand Trough to become inactive or decreased the rate of subduction.

7. The opening of the Woodlark Basin was accompanied by rifting, and rift-related volcanism and rapid uplift in the D'Entrecasteaux Islands, and resultant high-energy clastic sedimentation in the Trobriand Basin.

8. As subduction of Solomon Sea Basin lithosphere continued through the Pliocene and Quaternary, the active northern trench and the possibly inactive southern trench converged in the west, causting imbrication of basin floor in the west (structural province II) and arching and rupturing further east (structural province I).

9. Plio-Quaternary arching of the Solomon Plate caused matching uplift in the upper plate, ie. uplift of the Huon Peninsula above the west-plunging anticlinal axis of the Solomon Plate (Robinson, 1973; Chappell, 1974, 1983;) and uplift of southern New Ireland above the north-plunging anticlinal axis of the Solomon Plate (Fig. 3), Complementary grabens formed on the flanks of the upper plate horsts: Huon Gulf chasm and Finsch Deep in the west, St George's Channel chasm and Feni Deep in the east. In each of the four small extensional basins, and notably in the Huon Gulf chasm, strike-slip movement also contributed to basin formation.

In this scheme of geological history, we postulate that the older sub-basins of the Cape Vogel Basin, such as the Trobriand Basin, developed by fore-arc growth or intra-arc extension in the late Oligocene or early Miocene. Specifically, the Trobriand Basin may have developed as an intra-arc basin, for the sedimentary section within this basin includes middle Miocene volcanics of possible arc–trenchorigin. From the late Miocene onwards, the Trobriand Basin had a form more typical of a residual fore-arc basin (Seely & Dickinson, 1977). Younger sub-basins of the Cape Vogel Basin (e.g. Goodenough Basin) developed by rifting associated with the opening of the Woodlark Basin in the Pliocene.

Southern boundary of the Solomon Plate

Neither the southeastern nor the southwestern boundary of the Solomon Plate is clearly defined. The southeastern boundary may coincide with the Woodlark Basin spreading ridge–transform system (Luyendyk & others, 1973; Curtis, 1973). But this plate configuration fails to account for the moderate level of shallow seismic activity along the northern flank of the Woodlark Rise (Fig. 11). Weissel & others (1982) have suggested that the northern Woodlark Rise may coincide with a line of transcurrent faulting that permits differential rates of subduction of older Solomon Sea lithosphere and younger Woodlark Basin lithosphere where they enter the New Britain Trench subduction system, a model supported by a single right-lateral strike-slip fault-plane solution from a Woodlark Rise earthquake. Following on from Weissel & others, we suggest that the Woodlark Rise may mark the trace of a transform fault that is the southern boundary of the Solomon Plate and the northern boundary of a 'Woodlark Plate'

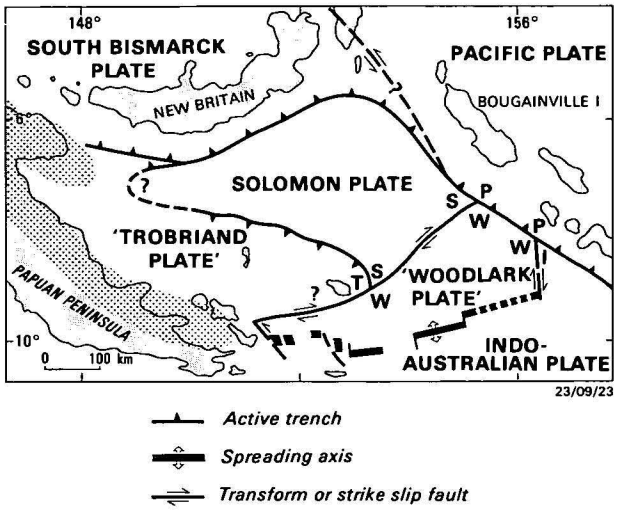

Figure 12. Speculative present-day plate boundary configuration in the Solomon Sea region.

Stipple indicates a zone of deformation that could be considered as a 'transitional' plate boundary. The names of new minor plates arising from this configuration are shown in quotation marks (see text), and resulting triple junctions are shown as TSW,SPW and WPI.

(Fig 12). The existence of this transform remains to be verified by detailed survey. The supposed transform may extend west-southwest from a trench-transform-transform (TFF) triple junction just east of Woodlark Island, to intersect the Woodlark Basin spreading ridge-transform system (Fig. 12); this extension coincides with a linear zone of shallow earthquakes (Fig. 11) and is on the line of a fault mapped (Fig. 3) from seismic reflection profiles. Ripper (1982b) shows a right-lateral strike-slip solution for an earthquake towards the western end of this lineation.

The southwestern boundary of the Solomon Plate is more problematical. Most previous workers show a plate boundary on or near the Papuan peninsula (e.g., Johnson & Molnar, 1972; Krause, 1973; Curtis, 1973; Taylor, 1975; as reviewed by R.W. Johnson, 1979). But no boundary in this area is easily reconciled with surface geology, and none coincides with any linear zone of shallow seismicity. In fact, shallow earthquakes in this region are widely dispersed (Fig. 11) and represent several different styles of seismic activity: earthquakes in the southeast have mainly tensional focal mechanisms related to the Woodlark Basin rift system, whereas those to the northwest generally have strike-slip and thrust mechanisms with maximum east-west compression (Ripper, 1982b). Perhaps, as the distribution of earthquakes would suggest, the plate boundary is a diffuse zone broadly coincident with the Papuan peninsula. Such a boundary might develop during a transition from convergence at the Trobriand Trough to divergence or transform motion, linked with the opening of the Woodlark Basin. This transition is reflected by the change from island arc-type volcanism to intra-plate alkaline volcanism (Smith, 1982).

Trobriand Trough: active or inactive?

Alternatively, the southwestern boundary of the Solomon Plate may coincide with the Trobriand Trough, thus delineating a 'Trobriand Plate' to the south (Fig. 12). However, the evidence for continued convergence at the Trobriand Trough is equivocal. Only a few significant shallow earthquakes have been detected on the line of the Trough in the past 18 years (Fig. 11), and the distribution of deeper earthquakes does not define a clear south-dipping Wadati-Benioff zone. However, there are scattered earthquakes at 51-100 km depth offshore from the Papuan peninsula, and at 101-150 km depth beneath the peninsula (Fig. 11).

The best evidence for continued convergence is in the seismic reflection profile (Fig. 8), which shows the absence of sediment cover over the deformation front, and the adjoining profile (Fig. 9), which shows apparently active faulting along strike from the Trough.

Perhaps subduction is proceeding at a slow rate, and is virtually aseismic. This possibility has been suggested for the Cascades volcanic field of North America (Atwater, 1970; Silver, 1971; McKenzie & Julian, 1971; Crosson, 1972; Riddihough, 1977; Rodgers, 1979), and for southern Chile (Herron & others, 1977) and the Lesser Antilles (Stein & others, 1983). Aseismic subduction has also been discussed by Kanamori (1977) and Kanamori & Ruff (1980).

The continuing andesitic volcanism on the Papuan peninsula may be evidence of continuing convergence or merely a residual effect from earlier subduction (cf. residual volcanism in the South Shetland arc; Gill, 1981).

Like Hamilton (1979), Ripper (1982), and Ripper & McCue (1983), we envisage the Solomon Plate as being a doubly subducted piece of oceanic lithosphere that has the form of a westward-plunging arch. This is similar to the present-day situation in the Molucca Sea (Silver & Moore, 1978). Ripper & McCue (1983, fig. 6) presented a model illustrating the collision of the Indo-Australian and South Bismarck Plates in three stages, from the late Miocene to the present. Their temporal model also illustrates our concept of the spatial change in the form of the Solomon Sea Basin from east to west: subduction of the Solomon Plate at both the New Britain Trench and Trobriand Trough, accompanied by broad arching and rupturing of the basin floor (structural province I), corresponds to their late Miocene stage; crustal shortening by both thrusting and subduction of the tightly arched Solomon Plate beneath the 149° Embayment (structural province II) corresponds to their late Miocene–early Pliocene stage; and transcurrent movement associated with the Huon Gulf chasm (structural province III) and the Ramu-Markham fault system corresponds to their present-day stage, in which the Indo-Australian and South Bismarck Plates have collided, leaving the Solomon Plate as a suspended arch beneath the collison zone.

Tectonic origin of regional unconformities?

The major unconformity recorded in the rocks of the southern Solomon Sea region is in the late Eocene to early and middle Oligocene. No sediments of this age are known, and the hiatus coincides with a change from a predominantly marine environment to an environment in which landmasses emerged and volcano-sedimentary basins developed. The unconformity coincides approximately with a latest Eocene-early Oligocene unconformity recognised throughout much of the southwest Pacific, both onshore (e.g., Australasian Petroleum Company, 1961) and in the adjacent ocean basins (e.g., DSDP 210 and 287 in the Coral Sea Basin, Burns & others, 1973; Andrews & others, 1975b; Edwards, 1973, 1975b). It is the commonly held view that this is an erosional unconformity caused by changes in direction and velocity of ocean currents, and that the changes may be associated with the development of a circum-Antarctic current (e.g., Kennett & others, 1972; Edwards, 1973, 1975b) or other current-related causes (e.g., Taylor & Falvey, 1977). We note the coincidence of timing of this unconformity and of major tectonic events in southern Solomon Sea region, and elsewhere in Papua New Guinea, and suggest that the two may be

connected. In other words, the latest Eocene-early Oligocene regional unconformity may have been caused, in some way, by tectonic events that were part of a significant reorganisation of plate-boundary geometry at the Indo-Australian/ Pacific Plate margin, and possibly elsewhere in the world (cf., Schwan, 1980; Bally, 1980; Richardson & Rona, 1980).

Kutu volcanics

Other regional unconformities in the Palaeocene and early Eocene are recorded in deep-sea cores (Andrews & others, 1975a; Edwards, 1975a). The lack of Palaeocene and early Eocene fossil record in the MORB-type basalts of the Kutu volcanics (KTv in fig. 2; Smith & Davies, 1976) may be simply a reflection of these regional unconformities. Alternatively, the Late Cretaceous and middle Eocene parts of the Kutu volcanics may be unrelated. In the latter case, the Late Cretaceous basalts may be part of the PUB ophiolite and the middle Eocene basalts may have formed by sea-floor spreading in the Solomon or Coral Seas, following the opening of the Coral Sea Basin (Smith, 1976a, p. 43). The Cretaceous and Eocene basalts may, then, have been juxtaposed by convergent tectonism (e.g., see T.L. Johnson, 1979, and Davies, 1980b, fig. 6).

Acknowledgements

We thank Gulf Research and Development for permission to publish the 'Gulfrex' profile across the Solomon Sea, Lamont-Doherty Geological Observatory of Columbia University and J. Weissel for provision of copies of *Vema* and *Conrad* profiles, Jo Lock for assistance with BMR profiles, G.D. Karner, R.W. Johnson, P. Molnar, and I.E.M. Smith for helpful discussion, R.W. Johnson and D.E. Mackenzie for reading preliminary drafts of the manuscript, and B.J. Drummond and D.A. Falvey for constructive criticism of the final draft. I.D. Ripper publishes with the permission of the Secretary for Minerals and Energy, Port Morseby.

References

Andrews, J.S., Packham, G., & others, 1975a - Site 289. *Initial Reports of the Deep Sea Drilling Project*, 30, 231-398.

Andrews, J.E., Packham, G., & others, 1975b - Site 287. *Initial Reports of the Deep Sea Drilling Project*, 30, 133-174.

Arculus, R.J., Johnson, R.W., Chappell, B.W., McKee, C.O., & Sakai, H., 1983 - Ophiolite-contaminated andesites, trachybasalts, and cognate inclusions of Mount Lamington, Papua New Guinea: anhydrite-amphibole bearing lavas and the 1951 cumulodome. *Journal of Volcanology and Geothermal Research*, 18, 215-247.

Ashley, P.M. & Flood, R.H., 1981 - Low-K tholeiites and high-K igneous rocks from Woodlark Island, Papua New Guinea. *Journal of the Geological Society of Australia*, 28, 227-240.

Atwater, T., 1970 - Implications of plate tectonics for the Cenozoic tectonic evolution of western North America. *Geological Society of America Bulletin*, 81, 3513-3536.

Australasian Petroleum Company, 1961 - Geological results of petroleum exploration in western Papua, 1937-1961, by The Australasian Petroleum Company Proprietary.. *Journal of the Geological Society of Australia*, 8(1), 1-133.

Bain, J.H.C., 1973 - A summary of the main structural elements of Papua New Guinea. *In* Coleman, P.J. (editor), The Western Pacific, island arcs, marginal seas, geochemistry. *University of Western Australia Press, Perth*, 147-161.

Bain, J.H.C., Davies, H.L., Hohnen, P.D., Ryburn, R.J., Smith, I.E., Grainger, R., Tingey, R.J., & Moffat, M.R., 1972 - Geology of Papua New Guinea, 1:1 000 000-scale map. *Bureau of Mineral Resources, Canberra.*

Bally, 1980 - Basins and subsidence - a summary. In Bally, A.W., & others (editors), Dynamics of plate interiors. *American Geophysical Union, Geodynamic Series*, 1, 5-20.

Bickel, R.S., 1976 - Cape Vogel Basin. *In* Leslie, R.B., Evans, H.J., & Knight, C.L. (Editors), Economic geology of Australia and Papua New Guinea. Volume 3 - Petroleum. *Australasian Institute of Mining and Metallurgy, Monograph* 7, 506-513.

Blake, D.H., & Miezitis, Y., 1967 - Geology of Bougainville and Buka Islands, New Guinea. *Bureau of Mineral Resources, Australia, Bulletin* 93.

Burns, R.E., Andrews, J.E., & others, 1973 - Initial Reports of the Deep Sea Drilling Project, Volume 21. *U.S. Government Printing Office, Washington*, 369-440.

CGG, (Compagnie Generale de Geophysique) 1969 - Papuan Basin and basic belt aeromagnetic survey, TPNG, 1967, Compagnie Generale de Geophysique. *Bureau of Mineral Resources, Australia, Record* 1969/58.

CGG, (Compagnie Generale de Geophysique), 1974 - Geophysical surveys of the continental margins of Australia, Gulf of Papua and Bismarck Sea, 1970 - 1973. *Bureau of Mineral Resources, Australia, Record* 1974/111.

Chappell, J., 1974 - Geology of coral terraces, Huon Peninsula, New Guinea: A study of Quaternary tectonic movements and sea-level changes. *Geological Society of America Bulletin*, 85, 553-570.

Chappell, J., 1983 - A revised sea-level record for the last 300 000 years from Papua New Guinea. *Search*, 14, 99-101.

Crosson, R.S., 1972 - Small earthquakes, structure and tectonics of the Puget Sound region. *Seismological Society of America Bulletin*, 62, 1133-1171.

Curtis, J.W., 1973 - Plate tectonics and the Papua New Guinea-Solomon Islands region. *Journal of the Geological Society of Australia*, 20, 21-35.

D'Addario, G.W., Dow, D.B., & Swoboda, R., 1976 - Geological map of Papua New Guinea, 1:2 500 000. *Bureau of Mineral Resources, Canberra.*

Davies, H.L., 1968 - Papuan ultramafic belt. *23rd International Geological Congress, Prague*, 1, 209-230.

Davies, H.L., 1971 - Peridotite-gabbro-basalt complex in eastern Papua: an overthrust plate of oceanic mantle and crust. *Bureau of Mineral Resources, Australia, Bulletin* 128.

Davies, H.L., 1973 - Fergusson Island, Papua New Guinea - 1:250 000 geological series. *Bureau of Mineral Resources, Australia, Explanatory Notes* SC/56-5.

Davies, H.L., 1978 - Geology and mineral resources of Papua New Guinea. Proceedings of GEOSEA Conference, *Asian Institute of Technology, Bangkok*, 686-699.

Davies, H.L., 1980a - Crustal structure and emplacement of ophiolite in southeastern Papua New Guinea. Proceedings of conference on mafic- ultramafic rocks in orogenic belts, *Centre National de la Recherche Scientifique, Paris, Colloques Internationaux*, 272, 17-33.

Davies, H.L., 1980b - Folded thrust fault and associated metamorphism in the Suckling-Dayman massif, Papua New Guinea. *American Journal of Science*, 280-A, 171-191.

Davies, H.L., in prep. - Buna — 1:250 000 geological series. *Geological Survey of Papua New Guinea, Explanatory Notes* SC/55-3.

Davies, H.L., & Ives, D.J., 1965 - The geology of Fergusson and Goodenough Islands, Papua. *Bureau of Mineral Resources, Australia, Report* 65.

Davies, H.L. & Jaques, A.L., in press - Emplacement of ophiolite in Papua New Guinea. *Geological Society of London, Special Publication.*

Davies, H.L., & Smith, I.E., 1971 - Geology of eastern Papua. *Geological Society of America Bulletin*, 82, 3299-3312.

Davies, H.L., & Smith, I.E., 1974 - Tufi-Cape Nelson - 1:250 000 Geological Series. *Bureau of Mineral Resources, Australia, Explanatory Notes* SC/55- 8.

Davies, H.L., & Warren, R.G., 1983 - Kyanite eclogite in Cenozoic domed layered metamorphics in S.E. Papua New Guinea (abstract). *Geological Society of America, Abstracts with Programs*, 15, 554.

de Keyser, F., 1961 - Misima Island - Geology and gold mineralization. *Bureau of Mineral Resources, Australia, Report* 57.

Denham, D., 1969 - Distribution of earthquakes in the New Guinea-Solomon Islands Region. *Journal of Geophysical Research*, 74, 4290-4299.

Denham, D., 1973 - Seismicity, focal mechanisms and the boundaries of the Indian-Australian Plate. *In* Coleman, P.J. (editor), The Western Pacific, island arcs, marginal seas, geochemistry. *University of Western Australia Press, Perth*, 35-53.

Dow, D.B., 1977 - A geological synthesis of Papua New Guinea. *Bureau of Mineral Resources, Australia, Bulletin* 201.

Dow, D.B., & Davies, H.L., 1964 - Geology of the Bowutu Mountains, New Guinea. *Bureau of Mineral Resources, Australia, Report* 75.

Dow, D.B., Smit, J.A.J., Bain, J.H.C., & Ryburn, R.J., 1972 - Geology of the south Sepik region, New Guinea. *Bureau of Mineral Resources, Australia, Bulletin* 133.

Edwards, A.R., 1973 - Southwest Pacific regional unconformities encountered during Leg 21. *Initial Reports of the Deep Sea Drilling Project*, 21, 701-220.

Edwards, A.R., 1975a - Further comments on the southwest Pacific Paleogene regional unconformities. *Initial Reports of the Deep Sea Drilling Project*, 30, 663-666.

Edwards, A.R., 1975b - Southwest Pacific Cenozoic paleogeography and an integrated Neogene paleocirculation and an integrated Meogene paleocirculation model. *Initial Reports of the Deep Sea Drilling Project*, 30, 667-684.

Falvey, D.A., & Pritchard, T., in press - Preliminary palaeomagnetic results from northern Papua New Guinea: evidence for large microplate rotations. *American Association of Petroleum Geologists, Studies in Geology.*

Finlayson, D.M., & Cull, J.P., 1973 - Structural profiles in the New Britain - New Ireland region. *Journal of the Geological Society of Australia*, 29, 245-253.

Finlayson, D.M., Cull, J.P., Weibenga, W.A., Furumoto, A.S., & Webb, J.P., 1972 - New Britain - New Ireland crustal seismic refraction investigations 1967 and 1969. *Geophysical Journal of the Royal Astronomical Society*, 29, 245-- 253.

Finlayson, D.M., Muirhead, K.J., Webb, J.B., Gibson, G., Furumoto, A.S., Cooke, R.J.S., & Russel, A.J., 1976a - Seismic investigation of the Papuan Ultramafic Belt. *Geophysical Journal of the Royal Astronomical Society*, 44, 45-60.

Finlayson, D.M., Drummond, B.J., Collins, C.D.N., & Connelly, J.B., 1976b - Crustal structure under the Mount Lamington region of Papua New Guinea. *In* R.W. Johnson (editor) Volcanism in Australasia, *Elsevier, Amsterdam*, 259-274.

Finlayson, D.M., Drummond, B.J., Collins, C.D.N., & Connelly, J.B., 1977 - Crustal structures in the region of the Papuan Ultramafic Belt, *Physics of the Earth and Planetary Interiors*, 14, 13-29.

Furumoto, A.S., Hussong, D.M., Campbell, J.F., Sutton, G.H., Malahoff, A., Rose, J.C., & Woollard, G.P., 1970 - Crustal and upper mantle structure of the Solomon Islands as revealed by seismic refraction survey of November - December 1966. *Pacific Science*, 24, 315-332.

Furumoto, A.S., Wiebenga, W.A., Webb, J.P., & Sutton, G.H., 1973 - Crustal structure of the Hawaiian archipelago, northern Melanesia and the central Pacific Basin by seismic refraction methods. *Tectonophysics*, 20, 153-164.

Furumoto, A.S., Webb, J.P., Odegaard, M.E., & Hussong, D.M., 1976 - Seismic studies of the Ontong Java Plateau, 1970. *Tectonophysics*, 34, 71-90.

Garside, I.E., & Stoen, J.D., 1973 - Goodenough No. 1 well completion report Amoco Australian Exploration Company. *Bureau of Mineral Resources, Australia, Petroleum Search Subsidy Acts Report* 73/228 (unpublished).

Gill, J., 1981, - Orogenic andesites and plate tectonics. *Springer Verlag, New York.*

Gulf, 1973 - Regional marine reconnaissance of Papua New Guinea. *Gulf Research and Development Company and Australian Gulf Oil Company* (unpublished).

Halunen, A.J., & Von Herzen, R.P., 1973 - Heat flow in the western equational Pacific Ocean. *Journal of the Geophysical Research* 78 (23), 5195-5208.

Hamilton, P.J., Johnson, R.W., Mackenzie, D.E., & O'Nions, R.K., 1983 - Pleistocene volcanic rocks from the Fly-Highlands province of western Papua New Guinea: a note on new Sr and Nd isotopic data and their petrogenic implications. *Journal of Volcanology and Geothermal Research*, 18, 449-459.

Hamilton, W., 1979 - Tectonics of the Indonesian Region. *United States Geological Survey, Professional Paper*, 1078, 293-304.

Hegarty, K.A., Weissel, J.K., & Hayes, D.E., 1983 - Convergence at the Caroline-Pacific plate boundary. *In* Hayes, D.E. (editor), The tectonic and geologic evolution of southeast Asian seas and islands, Part 2. *American Geophysical Union, Geophysical Monograph* 27, 326-348.

Herron, E.M., Bruhn, R., Winslow, M., & Chaqui, L., 1977 - Post-Miocene tectonics of the margin of southern Chile. *American Geophysical Union, Maurice Ewing Series* 1, 273-284.

Hohnen, P.D., 1978 - Geology of New Ireland, Papua New Guinea. *Bureau of Mineral Resources, Australia, Bulletin* 194.

Honza, E., Keene, J.B., & others, 1984 - Initial report of the Solomon Sea survey by r.v. Natsushima, December 1983 - January 1984. *Geological Survey of Papua New Guinea, Report.*

Jacob, K.H., Nakamura, Kazuaki, & Davies, J.N., 1977 - Trench-volcano gap along the Alaska-Aleutian arc: Facts and speculations on the role of terrigenous sediments for subduction. *American Geophysical Union, Maurice Ewing Series* 1, 243-258.

Jaques, A.L., & Robinson, G.P., 1977 - The continent/island-arc collision in northern Papua New Guinea. *BMR Journal of Australian Geology & Geophysics*, 2, 289-303.

Jakes, P., & Smith, I.E., 1970 - High potassium calc-alkaline rocks from Cape Nelson, eastern Papua. *Contributions to Mineralogy and Petrology*, 28, 259- 271.

Johnson, R.W., 1976a - Potassium variation across the New Britain volcanic arc. *Earth & Planetary Science Letters*, 31, 184-191.

Johnson, R.W., 1976b - Late Cainozoic volcanism and plate tectonics at the southern margin of the Bismarck Sea, Papua New Guinea. *In* Johnson, R.W. (editor), Volcanism in Australasia, *Elsevier, Amsterdam*, 101-116.

Johnson, R.W., 1977 - Distribution and major element chemistry of late Cainozoic volcanoes at the southern margin of the Bismarck Sea, Papua New Guinea. *Bureau of Mineral Resources, Australia, Report* 188.

Johnson, R.W., 1979 - Geotectonics and volcanism in Papua New Guinea: a review of the late Cainozoic. *BMR Journal of Australian Geology & Geophysics*, 4, 181-207.

Johnson, R.W., 1982 - Papua New Guinea. *In* Thorpe, R.S. (editor), Andesites, *John Wiley and Sons, Chichester*, 225-244.

Johnson, R.W., Mackenzie, D.E., & Smith, I.E.M., 1978a - Volcanic rock associations at convergent plate boundaries: re-appraisal of the concept using case histories from Papua New Guinea. *Geological Society of America, Bulletin*, 89, 96-106.

Johnson, R.W., Mackenzie, D.E., & Smith, I.E.M., 1978b - Delayed partial melting of subduction-modified mantle in Papua New Guinea. *Tectonophysics*, 46, 197-216.

Johnson, T.L., 1979 - Alternative model for emplacement of the Papuan ophiolite, Papua New Guinea. *Geology*, 7, 495-498.

Johnson, T., & Molnar, P., 1972 - Focal mechanisms and the plate tectonics of the southwest Pacific. *Journal of Geophysical Research*, 77, 5000-5032.

Jongsma, D., 1972 - Marine geology of Milne Bay, eastern Papua. *Bureau of Mineral Resources, Australia, Bulletin* 125.

Kanamori, H., 1977 - Seismic and aseismic slip along subduction zones and their tectonic implications. *American Geophysical Union, Maurice Ewing Series*, 1, 163-174.

Karig, D.E., 1971 - Origin and development of marginal basins in the western Pacific. *Journal of Geophysical Research* 76(11), 2542-2561.

Karig, D.E., 1972 - Remnant arcs. *Geological Society of America Bulletin* 83, 1057-1068.

Karner, S.D., Steckler, M.S., & Thorne, J.A., 1983 - Long term thermo- mechanical properties of the continental lithosphere. *Nature*, 304, 250- 253.

Kennett, J.P., & others, 1972 - Australian-Antarctic continental drift, paleocirculation changes and Oligocene deep-sea erosion. *Nature Physical Sciences*, 239, 51-55.

Kesson, S.E., & Smith, I.E., 1972 - TiO_2 content and the shoshonite and alkaline associations. *Nature Physical Sciences*, 236, 110-111.

Krause, D.C., 1973 - Crustal plates of the Bismark and Solomon Seas. *In* Fraser, R. (compiler), Oceanography of the south Pacific 1972. *New Zealand National Commission for UNESCO, Wellington*, 271-280.

Kroenke, L.W., 1972 - Geology of the Ontong Java Plateau. *Ph.D. Thesis, Hawaii Institute of Geophysics, Moana.*

Kroenke, L.W., in press - Cainozoic tectonic development of the southwest Pacific. *CCOP/SOPAC Technical Bulletin* No. 6.

Le Pichon, X., 1970 - Correction to paper by Xavier Le Pichon 'Sea floor spreading and continental drift'. *Journal of Geophysical Research*, 75, 2793.

Luyendyk, B.P., MacDonald, K.C., & Bryan, W.B., 1973 - Rifting history of the Woodlark Basin in the southwest Pacific. *Geological Society of America Bulletin*, 84, 1125-1134.

McGee, W.A., 1978a - Contributions to the geology of Woodlark Island. *Geological Survey of Papua New Guinea, Report* 78/10.

McGee, W.A., 1978b - Stratigraphic nomenclature for the Murua 1:250 000 geological map. *Geological Survey of Papua New Guinea, Report* 78/15.

McKenzie, D., & Julian, B., 1971 - Puget Sound, Washington, earthquake and the mantle structure beneath the northwestern United States. *Geological Society of America Bulletin*, 82, 3519-3524.

Milsom, J.S., 1970 - Woodlark Basin, a minor centre of sea-floor spreading in Melanesia. *Journal of Geophysical Research*, 75, 7335-7339.

Milsom, J.S., 1973a - Papuan Ultramafic Belt: gravity anomalies and the emplacement of ophiolites. *Geological Society of America Bulletin*, 84, 2243-2258.

Milsom, J.S., 1973b - Gravity field of the Papuan peninsula. *Geologie en Mijnbouw*, 52, 13-20.

Molnar, P., Freedman, D., & Shih, J.S.F., 1979 - Lengths of intermediate and deep seismic zones and temperatures in downgoing slabs of lithosphere. *Geophysical Journal of the Royal Astronomical Society*, 56, 41-54.

Morgan, W.R., 1966 - A note on the petrology of some lava types from east New Guinea. *Journal of the Geological Society of Australia*, 13, 583-591.

Mutter, J.C., & Karner, G.D., 1980 - The continental margin off northeastern Australia. *In* Henderson, R.A., & Stephenson, P.J., (editors), The geology and geophysics of northeastern Australia. *Geological Society of Australia Queensland Division, Brisbane*, 47-69.

Page, R.W., & Johnson, R.W., 1974 - Strontium isotope ratios of Quaternary volcanic rocks from Papua and New Guinea. *Lithos*, 7, 91-100.

Page, R.W., & Ryburn, R.J., 1977 - K-Ar ages and geological relations of intrusive rocks in New Britain. *Pacific Geology*, 12, 99-105.

Parsons, B., & Sclater, J.S., 1977 - An analysis of the variation of ocean floor heat flow and bathymetry with age. *Journal of Geophysical Research*, 82, 803-827.

Paterson, S.J., & Kicinski, F.M., 1956 - An account of the geology and petroleum prospects of the Cape Vogel Basin. *In* Papers on Tertiary micropalaeontology. *Bureau of Mineral Resources, Australia, Report* 52, 47- 70.

Richardson, E.S., & Rona, P.A., 1980 - Global Eocene plate reorganisation: implications for petroleum exploration. *United Nations ESCAP, CCOP/SOPAC Technical Bulletin*, 3, 25-36.

Riddihough, R.P., 1977 - A model for recent plate interactions off Canada's west coast. *Canadian Journal of Earth Science*, 14, 384-396.

Ripper, I.D., 1970 - Global tectonics and the New Solomon Islands region *Search*, 1, 226-232.

Ripper, I.D., 1975 - Earthquake focal mechanism solutions in the New Guinea/ Solomon Island region, 1963-1968. *Bureau of Mineral Resources, Australia, Report* 178.

Ripper, I.D., 1977 - Some earthquake focal mechanisms in the New Guinea/Solomon Islands region 1969-1971. *Bureau of Mineral Resources, Australia, Report* 192.

Ripper, I.D., 1982a - Atlas of the seismicity of the New Guinea region in depth zones. *Geological Survey of Papua New Guinea, Report* 1982/12.

Ripper, I.D., 1982b - Seismicity of the Indo-Australia/Solomon Sea Plate boundary in the Southeast Papua region. *Tectonophysics*, 87, 355-369.

Ripper, I.D., & McCue, K.F., 1982 - Seismicity of the New Guinea region, computer plots. *Geological Survey of Papua New Guinea, Report* 1982/10.

Ripper, I.D., & McCue, K.F., 1983 - The seismic zone of the Papuan fold belt. *BMR Journal of Australian Geology & Geophysics*, 8, 147-156.

Robinson, G.P., 1973 - Huon-Sag Sag, Papua New Guinea - 1:250 000 Geological Series. *Bureau of Mineral Resources, Australia, Explanatory Notes* SB/55- 11.

Rogers, G.C., 1979 - Earthquake fault plane solutions near Vancouver Island. *Canadian Journal of Earth Science*, 16, 523-531.

Rose, J.C., Woollard, G.P., & Malahoff, A., 1968 - Marine gravity and magnetic studies in the Solomon Islands. *In* Knopoff, L., Drake, C.L., & Hart, P.J. (editors), The crust and upper mantle of the Pacific area. *American Geophysical Union, Geophysical Monograph* 12, 379-410

Ruff, L., & Kanamori, H., 1980 - Seismicity and subduction process. *Physics of the Earth and Planetary Interiors*, 23, 240-252.

Ruxton, B.P., 1966 - A late Pleistocene to Recent rhyodacite-trachybasalt- basaltic latite volcanic association in north-east Papua. *Bulletin Volcanologique*, 29, 347-374.

Ruxton, B.P., & McDougall, I., 1967 - Denudation rates in northeast Papua from potassium-argon dating of lavas. *American Journal of Science*, 265, 545-561.

St John, V.P., 1967 - The gravity field in New Guinea. *Ph.D. Thesis, University of Tasmania, Hobart.*

St John, V.P., 1970 - The gravity field and structure of Papua and New Guinea. *APEA Journal*, 10(2), 41-55.

Schwan, W., 1980 - Geodynamic peaks in alpine-type orogenies and changes in ocean-floor spreading during late Jurassic - late Tertiary time. *American Association of Petroleum Geologists Bulletin*, 64, 359-373.

Sclater, J.G., Ritter, U.G., & Dixon, F.S., 1972 - Heat flow in the southwestern Pacific. *Journal of Geophysical Research*, 77, 5697-5704.

Seely, D.R., & Dickinson, W.R., 1977 - Structure and stratigraphy of fore-arc regions. *In* Geology of continental margins. *American Association of Petroleum Geologists Continuing Education Course Note Series*, 5.

Silver, E.A., 1971 - Transitional tectonics and late Cenozoic structure of the continental margin off northernmost California. *Geological Society of America Bulletin*, 82, 1-22.

Silver, E.A., & Moore, J.C., 1978 - The Molucca Sea collision zone, Indonesia. *Journal of Geophysical Research*, 83, 1681-1691.

Smith, I.E., 1972 - High-potassium intrusives from southeastern Papua. *Contributions to Mineralogy and Petrology*, 34, 167-176.

Smith, I.E., 1973 - The geology of the Calvados Chain, southeastern Papua. *In* Geological Papers 1970-71. *Bureau of Mineral Resources, Australia, Bulletin* 139, 59-66.

Smith, I.E.M., 1976a - Volcanic rocks from southeastern Papua. The evolution of volcanism at a plate boundary. *Ph.D. Thesis, Australian National University Canberra.*

Smith, I.E.M., 1976b - Peralkaline rhyolites from the D'Entrecasteaux Islands, Papua New Guinea. *In* Johnson, R.W. (editor), Volcanism in Australasia. *Amsterdam, Elsevier*, 275-286.

Smith, I.E., 1982 - Volcanic evolution in eastern Papua. *Tectonophysics*, 87, 315-333.

Smith, I.E.M., & Compston, W. 1982 - Strontium isotopes in Cenozoic volcanic rocks from southeastern Papua New Guinea. *Lithos*, 15, 199-206.

Smith, I.E., & Davies, H.L., 1973a - Abau, Papua New Guinea - 1:250 000 Geological Series. *Bureau of Mineral Resources, Australia, Explanatory Notes* SC/55-12.

Smith, I.E., & Davies, H.L., 1973b - Samarai, Papua New Guinea - 1:250 000 geological series. *Bureau of Mineral Resources, Australia, Explanatory Notes* SC/56-9.

Smith, I.E. & Davies, H.L., 1976 - Geology of the southeast Papuan mainland. *Bureau of Mineral Resources, Australia, Bulletin* 165.

Smith, I.E.M. & Johnson, R.W., 1981 - Contrasting rhyolite suites in the late Cainozoic of Papua New Guinea. *Journal of Geophysical Research*, 86, 10257-10272.

Smith, I.E.M., Taylor, S.R. & Johnson, R.W., 1979 - REE-fractionated trachytes and dacites from Papua New Guinea and their relationship to andesite petrogenesis. *Contributions to Mineralogy and Petrology*, 69, 227-233.

Smith, I.E.M., Chappell, B.W., Ward, G.K., & Freeman, R.S., 1977 - Peralkaline rhyolites associated with andesitic arcs of the southwest Pacific. *Earth and Planetary Science Letters*, 37, 230-236.

Stein, S., Engeln, J.F., Wiens, D.A., Speed, R.C., & Fujita, K., 1983 - Slow subduction of old lithosphere in the Lesser Antilles. *Tectonophysics*, 99, 139-148.

Stoen, J.D., & Garside, I.E., 1973 - Nubiam No. 1 well completion report. Amoco Australia Exploration Company. *Bureau of Mineral Resources, Australian Petroleum Search Subsidy Acts Report* 73/238 (unpublished).

Symonds, P.A., Fritsch, J., & Schluter, H.U., 1984 - Continental margin around the western Coral Sea Basin: structural elements, seismic sequences and petroleum geological aspects. *American Association of Petroleum Geologists, Studies in Geology.*

Taylor, B., 1975 - The tectonics of the Bismarck Sea region. *B.Sc. (Hons) Thesis, University of Sydney.*

Taylor, B., 1979 - Bismarck Sea: evolution of a back-arc basin. *Geology*, 7, 171-174.

Taylor, L., & Falvey, D., 1977 - Queensland Plateau and Coral Sea Basin: Stratigraphy, structure and tectonics. *APEA Journal* 17, 1-17.

Terpstra, G.R.J., 1964 - Age determination of limestone samples of Woodlark Island, Papua. *Bureau of Mineral Resources, Australia, Record* 1964/6.

Tilbury, L.A., 1975 - Geophysical results from the Gulf of Papua and the Bismarck Sea. *Bureau of Mineral Resources, Australia, Record* 1975/115.

Tjhin, K.T., 1976 - Trobriand Basin exploration, Papua New Guinea. *APEA Journal*, 16(1), 81-90.

Trail, D.S., 1967 - Geology of Woodlark Island, Papua. *Bureau of Mineral Resources, Australia, Report* 115.

Van der Lingen, G.J., Andrews, J.E., & others, 1973 - Lithostratigraphy of eight drill sites in the south-west Pacific - preliminary results of Leg 21 of the Deep Sea Drilling Project. *In* Fraser, R. (compiler), Oceanography of the south Pacific 1972. *New Zealand National Commission for UNESCO, Wellington*, 299–313.

Walker, D.A., & McDougall, I., 1982 - $^{40}Ar/^{39}Ar$ and K-Ar dating of altered glassy volcanic rocks: the Dabi Volcanics, P.N.G. *Geochimica et Cosmochimica Acta*, 46, 2181–2190.

Watts, A.B., 1978 - An analysis of isostacy in the world's oceans: 1. Hawaiian-Emperor seamount chain. *Journal of Geophysical Research*, 83, 5989–6004.

Weissel, J.K., & Watts, A.B., 1979 - Tectonic evolution of the Coral Sea Basin. *Journal of Geophysical Research*, 84, 4572–4582.

Weissel, J.K., Taylor, B., & Karner, G.D., 1982 - The opening of the Woodlark Basin, subduction of the Woodlark spreading system, and the evolution of northern Melanesia since Pliocene time. *Tectonophysics*, 87, 253–277.

CONTENTS

Front cover: Mount North, an intrusion of lamproite in the West Kimberley region of Western Australia. New age determinations on this and other similar intrusions, including diamond-bearing pipes, are presented in this issue in a paper by A. L. Jaques & others.

R83/614(1) Cat. No. 84 0488 5